THE CD151-α3β1 AXIS AND ITS ROLE IN BREAST CANCER PROGRESSION

By

GOURI SEETHARAMAN BALDWIN

A thesis submitted to

The College of Medical and Dental Sciences

The University of Birmingham

for the degree of

DOCTOR OF PHILOSOPHY

School of Cancer Sciences

College of Medical and Dental Sciences

The University of Birmingham

November 2011

ABSTRACT

The work described in this thesis has studied the role of CD151 in modulating the form and function of its integrin partners, α3β1 and α6β1/β4. Stable depletion of CD151 in MDA-MB-231 (MDA-231), a metastatic breast cancer cell line, changed the glycosylation profile of the α3β1 integrin but did not affect modification of α6 integrins. Further analysis showed that CD151 influences α3β1 integrin's glycosylation as early as the very first mannose trimming within the ER. Generation and analyses of MDA-231 cell lines expressing various CD151 mutants indicated that tight interaction, recruitment into TERM and glycosylation of CD151 are all required for CD151 to influence the glycosylation of α3β1 integrin. Depletion of CD151 reduced the level of α1,2-linked fucose and β1-4 branching of GlcNAc presented on the integrin, as detected by lectin blot assay.

Sucrose density gradient (SDG) experiments showed that glycosylation-, palmitoylation- and QRD (mutation introduced to CD151 which inhibits tight association between CD151 and α3β1 integrin) mutants of CD151 were all capable of recruiting α3β1 integrin into the light fractions. These data demonstrate that CD151's role in glycosylation of α3β1 integrin is independent from its ability to recruit the integrins into the light fractions of the SDG. Contrary to the published data, we found that CD151 was able to recruit α3β1 integrin into the light fractions as part of a microdomain (QRD mutant) as well as a separate entity (palmitoylation mutant).

Other tetraspanins, such as CD9, CD63 and CD81 showed similar yet distinct roles played by these tetraspanins during glycosylation. For example, CD9 depletion altered the glycosylation of α3 integrin subunit and increase the general level of cell surface α2,6-linked sialic acid presentation by 100%. All four tetraspanins altered the cell surface glycotope profile upon depletion.

Analysis of α6 integrin subunit, showed no difference to its glycosylation profile upon CD151 depletion. In fact, during the course of our investigation, we demonstrated a hierarchical preference for CD151 to form tight associations with α3β1 over α6β1 and α6β4 integrins in MDA-231 cell line. Analysis of α6 integrin subunits from all four tetraspanin depleted cell lines revealed a difference in another type of post translation modification of the α6 integrin subunit which resulted cleavage of the integrin; whereby the head region of the α6 subunit is proteolytically cleaved at the cell surface by urokinase plasminogen activator resulting in a ligand binding deficient variant, α6p (Davis et al., 2001). Depletion of CD151 increased the level of α6p while depletion of CD9 and CD81 decrease its level in MDA-231 cells.

Functionally, depletion of CD151 in MDA-231 decreased their ability to migrate towards Lm332 in Boyden chamber migration assays by ~90%. Reconstitution of MDA-231 CD151(-) cells with wild type CD151, but not glycosylation-deficient CD151 restored their migration potential. During 30 minute adhesion assay, no difference was observed in their ability to adhere to Lm332 or

fibronectin. Finally, their interaction with endothelial cells was compared by performing transendothelial migration assays and transient attachment assays. Depletion of CD151 had no effect on their ability to migrate across the endothelial monolayer. However, transient adhesion assay showed a batch specific influence. MDA-231 CD151(+) attached more readily than CD151(-) cells in some HUVEC batches while the opposite, or no difference was observed in others. These results are discussed from the point of CD151 mediated α3β1 glycosylation and α6β1/β4 cleavage.

Characterisation of tetraspanins by EndoH and PNGase digestion suggested mono-N-glycosylated CD9 and CD151 to be modified by phosphomannosylation and complex N-glycan respectively. Tri-N-glycosylated CD63 and CD82 molecules showed some resistance to both glycosidases, suggesting that they may carry both phosphomannosyl and complex glycan modification. Castanospermine inhibition of the glycosylation pathway markedly reduced the level of several integrins including α3β1 and α6β1/β4 which suggests a novel use for this compound for therapeutic purposes.

God does not play dice.

Albert Einstein

… not only that God does play dice,

..He sometimes confuses us by throwing them where they can't be seen.

Stephen Hawking

Nothing in glycobiology makes sense, except in the light of evolution.

Ajit Varki

DEDICATION

Kayena vacha manasendriyairva
Buddhyatmana va prakrite swabhavath
Karoomi yadyad sakalam parasmai
Narayanayeti samarpayami Narayaniyeti samarpayami

To my family…

My husband Tim, my brother Chandra, my parents (amma & appa), Jeg & Basu, mum & dad (Bob and Eve), Vasu sitti, Anna and Aishah…

Thank you for your love and support

To patti, sittapa and anni…

whom we lost to cancer

To Max…you are always in my heart

With all my love

To Barbara and Gregor…. thank you for the inspiration

ACKNOWLEDGEMENT

First and foremost, I want to thank my husband Tim who first taught me how to do research and for his inspiring guidance ever since. I could not possibly have done this project without the scientific foundation he instilled in me when I first started my research career.

I would also like to thank my supervisor, Dr Fedor Berditchevski, for all his help and advice throughout this project. In addition, I would like to extend my gratitude to him, the School of Cancer Sciences and CRUK for giving me the opportunity to do my PhD here and for funding my research. I would also like to thank Prof Gerard Nash, Mr Phillip Stone and Prof Johannes Eble for kindly providing various resources for my experiments.

My heartfelt gratitude goes to Dr Phillip Taniere for his generosity of spirit and kindness in allowing me the time to write up my thesis, whilst working in his laboratory. I would also like to thank Mr Brendan O'Sullivan for his moral support.

I would like to thank Dr Terry Butters (Glycobiology Institute, Oxford) and Professor Eric Rubinstein (INSERM, Paris) for kindly agreeing to examine my dissertation and for making my PhD viva a wonderful and enriching experience for me.

I am grateful to my previous supervisors, Prof Henri-Jacques Delecluse, Dr Regina Feederle and Prof Alan Rickinson for all their help and advice since my arrival at the

University of Birmingham. I would also like to thank Dr Mike Tomlinson and Dr Neil Hotchin for their constructive advice during my studies.

I am especially grateful to Prof David Blackbourne for his timely support and advice.

My gratitude also goes to various other members of staff, for their help throughout my project, especially Mr David Lloyd, Ms Sue Rookes, Ms Laura Billington, Mr Kevin Hardware and the 'wash up' team.

Last but not least, I would like to thank various members of tetraspanin research group for their help and advice, especially Nadya, Gairat, Rafal, Vera, Dale, and Eva. I would also like to thank Sven and Michael for their help with the software programmes and Dr Rose Tierney for all her help.

ABBREVIATIONS

α	Alpha
AAL	Aleuria Aurantia Lectin
ABO	ABO blood group antigen
ALG	Asparagine Linked Glycosylation
APES	3-aminopropyl)triethoxysilane
Arg	Arginine
Asp	Asparagine Linked Glycosylation
β	Beta
BCECF	2,7-bis-(2-carboxyethyl)-5-(and-6)carboxyfluorescein
BMP	Bone morphogenetic protein
BSA	Bovine Serum albumin
CD	Cluster of differentiation
CMP	Cytidine monophosphate
CNBr	Cyanogen Bromide
CNX	Calnexin
ConA	Concanavalin A

CRT	Calreticulin
Cst	Castanospermine
DBA	Dolichos Biflorus Agglutinin
DMEM	Dulbecco's Modified Eagle Medium
DMSO	Dimethyl sulfoxide
DNA	Deoxyribonucleic acid
EC	Extracellular
ECM	Extracellular Matrix
EDEM	ER degradation enhancing a mannosidase
EDTA	Ethylene Diamine Tetraacetic Acid
EndoH	Endiglycosidase H
ER	Endoplasmic reticulum
ERGIC	ER-Golgi intermediate compartment
ERManI	ER mannosidase 1
FBS	Foetal Bovine Serum
FITC	fluorescein isothiocyanate
GD6	peptide (KQNCLSSRASFRGCVRNLRLSR) based on Laminin111
GDP	Guanosine diphosphate
GFFKR	Glycine-Phenylalanine-Phenylalanine-Lysine-Arginine
GluNAc	N-acetyl-glucosamine

GNT	N-acetyl glucosamine transferase
HBSS	Hank's Balanced Salt Solution
HRP	Horseradish peroxidase
LDV	Leucine-Aspartic acid-Valine motif
LEL	Large extracellular loop
mAb	monoclonal antibody
MFI	Mean fluorescence intensity
MMP	Matrix metalloproteinases
Mn	Manganese
NaCl	Sodium Chloride
$NaHCO_3$	Sodium bicarbonate
pAb	polyclonal antibody
PAGE	Polyacrylamide gel electrophoresis
PBS	Phosphate buffered Saline
PFA	Paraformaldehyde
PHA-E	Phaseolus vulgaris Erythroagglutinin
PHA-L	Phaseolus vulgaris Leucoagglutinin
PNA	Peanut Agglutinin
PNGaseF	Peptide: N-Glycosidase F
RCA I	Ricinus Communis Agglutinin I
RER	Rough endoplasmic reticulum

RGD	Arginin-Glycine-Aspartic acid motif
RNA	ribonucleic acid
rpm	rotation per minute
SBA	Soybean Agglutinin
SDS	Sodium dodecyl sulphate
SEL	Small extracellular loop
shRNA	short hairpin RNA
siRNA	short interfering RNA
SNA	Sambucus Nigra Agglutinin
TERM	Tetraspanin enriched microdomain
Tris	tris(hydroxymethyl)aminomethane
UDP	Uridine diphosphate
UEA I	Ulex Europeus Agglutinin
VLA	Very late antigen
WB	Western Blot
WGA	Wheat Germ Agglutinin

TABLE OF CONTENTS

FIGURES

CHAPTER 1

CHAPTER 2

CHAPTER 3

TABLES

1. INTRODUCTION

1.1 Tetraspanin Superfamily

Tetraspanins are type III transmembrane proteins found in all metazoans. To date, a total of 33 mammalian tetraspanins genes have been characterised. Members of this family have distinguishing characteristics which set them apart from other proteins with four transmembrane regions and tetraspanin-like proteins found in fungi and plants (Huang et al., 2005; Garcia-Espana et al., 2008). Meandering across the membrane 4 times, they consist of a short cytoplasmic amino-terminal tail, followed by a small extracellular loop (SEL), a small intracellular loop, a large extracellular loop (LEL) and finally ending with a cytoplasmic carboxy-terminal tail. These diminutive proteins range in length from 204 to 355 amino acids and protrude 3.5 to 5 nm from the membrane. The SEL and LEL consist of a stretch of 13-30 and 69-150 amino acids respectively. The LEL is subdivided into two domains, consisting of a conserved and a hypervariable region (Figure 1.1). Members of this family also carry an obligatory cysteine-cysteine-glycine (CCG) motif on the LEL and an additional two to eight cysteine residues in the LEL. Disulphide bond formation between the cysteines within the CCG motif and other cysteine residues in the LEL confers a structural heterogeneity to these proteins (Charrin et al., 2009).

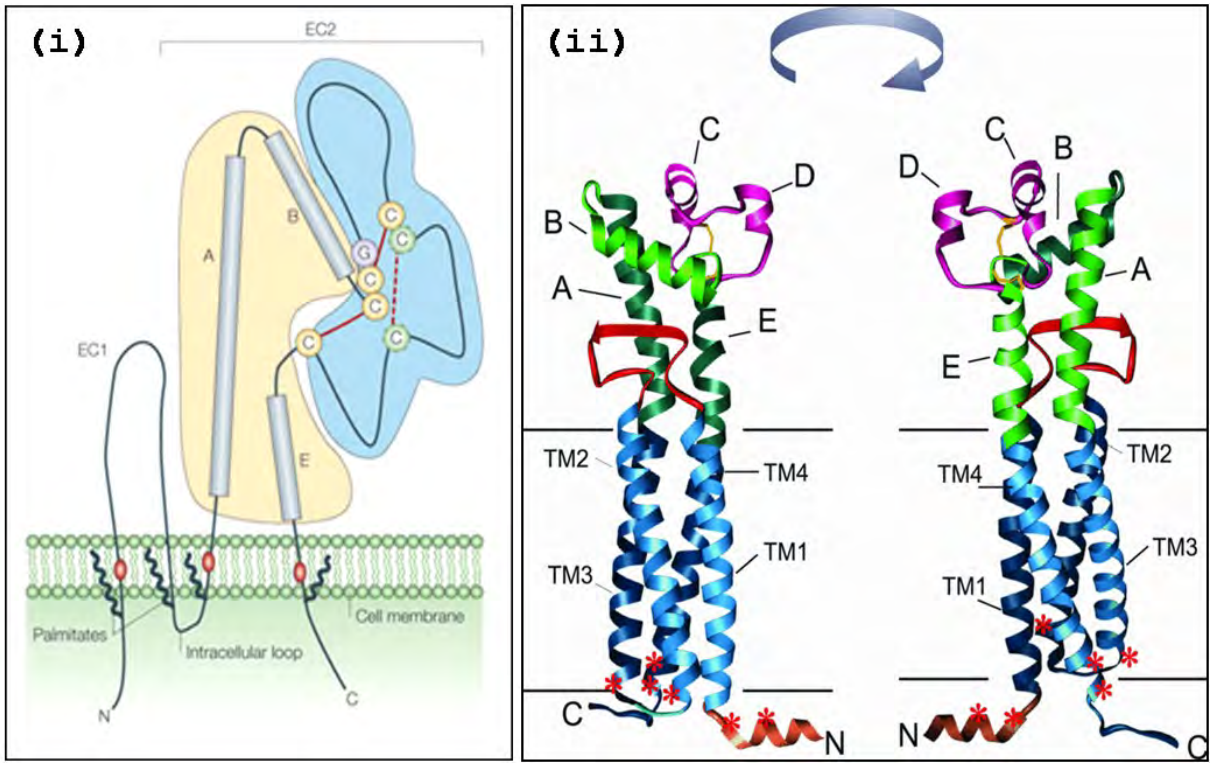

Figure 1.1: A cartoon and 3D structure depicting the structural features of tetraspanin.

(i) Cytoplasmic amino terminal (N), short extracellular loop (EC1), intracellular loop, large extracellular loop (EC2) and cytoplasmic carboxy terminal (C). EC2 is divided into constant region (beige shade) containing a helix stretches (A,B and E) and hypervariable region (blue shade) containing conserved 'CCG' motif and cysteine (C) residues (yellow shade). Many tetraspanins carry additional cysteine (C) residues (green) in EC2. Membrane proximal cysteine residues are usually palmitoylated (image taken from Hemler, 2005). (ii) A predicted 3D structure of tetraspanin CD81 as described by (Seigneuret, 2006) viewed at opposing angles. The blue and red ribbon represents transmembrane domains and small extracytoplasmic loop. The green ribbon labelled A, B and E represents the conserved regions while the pink region (C and D) represents hypervariable region within the LEL. The yellow bridges in the LEL and red asterisk in the cytoplasmic face represent disulphide bonds and palmitoylation sites (image taken from Charrin et al., 2009).

The majority of animal cells contain several different tetraspanins and their distribution varies from cell to cell. For example, CD81 is widely expressed while

CD151 has a more restricted distribution; being expressed on nearly all epithelial, endothelial, fibroblastic and neuronal cells. A select few exhibit a very limited expression. Peripherin/RDS, for example, is only expressed in the rod outer segments in the retina (Kohl et al., 1998; Hemler, 2005).

Glycosylation and palmitoylation are the two most common post-translational modifications of these molecules. Most tetraspanins are glycosylated on their large extracellular loop, except for CD9 which carries a potential glycosylation motif on its small extracellular loop. Palmitoylation, on the other hand, occurs at the membrane proximal cysteine residue of the cytoplasmic leaflet, and contributes to the most important characteristic of the tetraspanin proteins - the ability to form lateral interactions with each other as well as other membrane proteins. In fact, only CD82, CD81, CD9 and UPKIA have so far been identified to have ligand binding capacity (Pileri et al., 1998; Ellerman et al., 2003; Bandyopadhyay et al., 2006). Site-directed mutagenesis of all membrane proximal cysteine residues on CD9 and CD151 disrupted their palmitoylation which adversely affected their ability to form secondary lateral interaction (Charrin et al., 2002; Yang et al., 2002; Berditchevski et al., 2002). Through their lateral interactions, tetraspanins facilitate molecular crowding and the formation of large multimeric complexes on the plasma membrane. This enriched platform of tetraspanins and their interacting partners on the membrane is known as the tetraspanin enriched microdomain (TERM) (Figure

1.2). The formation of TERMs coordinates various cellular functions such as cell adhesion, migration, membrane fusion, inter- and intracellular signaling as well as endocytosis. Composition of the TERM varies according to cell type and the associated function. Within TERM, the interaction amongst component molecules can be characterised as primary, secondary and tertiary interactions. These multiple layers of interactions are categorised by their resistance to dissociation when extracted with various detergents at different stringency.

Detergents are amphiphatic molecules with polar 'head' and non-polar 'tail' structure. Their unique characteristic is usually employed to manipulate the hydrophobic-hydrophilic interactions which exist in the biological systems such as the lipid bilayer organisation of cell membranes. The ability of various detergents to disrupt protein-protein, lipid-lipid and protein-lipid interactions is determined by the composition of its hydrophobic component. Triton X-100, for example, has short bulky hydrophobic chain capable of penetrating through the lipid bilayer and depletes the inner leaflet of the bilayer. However, they are unable to penetrate into the water-soluble components of the membrane and as a result, are unable to disrupt hydrophilic protein-protein interaction. Accordingly, resistance to disruption under 1% TritonX-100 conditions usually denotes a primary (or a direct protein-protein) interaction. The long monolayer spanning hydrophobic tail of Brij 96 on the other hand, is less disruptive on the lipid bilayer. Membrane solubilisation under 1% Brij

96 or 1% Brij 97 has been shown to discriminate tetraspanin-tetraspanin interactions which are lost in 1% Triton X-100 condition (Chen et al., 2009; Charrin et al., 2009). Resistance to the milder detergent, which has been attributed to the presence of gangliosides (Ono et al., 2001) and a partial lipid raft like property observed within these domains (Yashiro-Ohtani et al., 2000; Claas et al., 2001), usually reflects a secondary or tertiary partnership within a TERM (Figure 1.2).

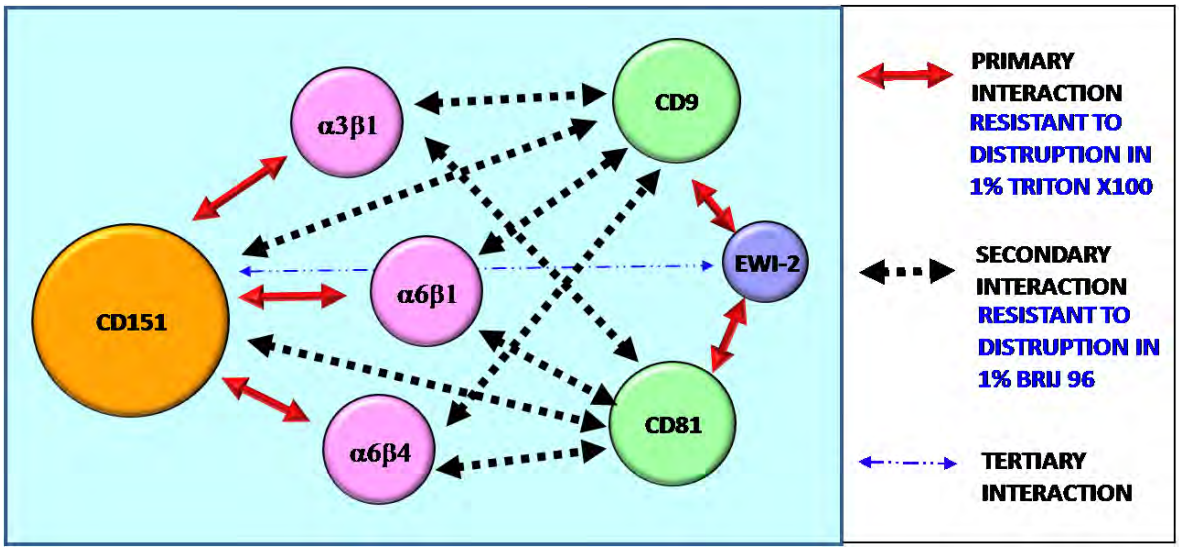

Figure 1.2: Diagram representing different levels of interaction within the tetraspanin enriched microdomain.

CD151 forms primary interaction with integrins α3β1, α6β1 and α6β4; secondary interaction with CD9 and CD81 and tertiary interaction with EWI-2 protein.

[Adapted from (Yauch et al., 1998; Sterk et al., 2002a; Charrin et al., 2003a)]

Stoichiometric primary interactions have been identified between several tetraspanins and their partners which has functional repercussions. For instance, the partnering of uroplakin IA with uroplakinII (UPII) and uroplakin IB with

uroplakinIII (UPIII) are fundamental for urothelial plaque formation (Kong et al., 2004). CD9's association with membrane-anchored heparin-binding EGF-like growth factor precursor (proHB-EGF) has been shown to increase the effectiveness of proHB-EGF's juxtacrine growth factor activity (Iwamoto et al., 1994; Higashiyama et al., 1995). Primary interaction between CD81 and another membrane protein, CD19, is important for lowering the threshold for receptor activation in B cells (Maecker and Levy, 1997; Miyazaki et al., 1997; Tsitsikov et al., 1997). Alliance of CD63 with H,K-ATPase beta-subunit proton pumps have been reported to facilitate its internalisation and trafficking to late endosome-lysosmal compartment by sequential association with adaptor proteins μ2 and μ3 in gastric parietal cells (Duffield et al., 2003).

Furthermore, CD9 and CD81 partner with members of the Ig domain containing cell surface protein, EWI-2 and EWI-F (Stipp et al., 2001a; Stipp et al., 2001b). In a study to understand the implication of EWI-F (CD9P-1) association with CD9 and CD81, CD9P-1 was overexpressed in a model cell line, HEK293. Overexpression of CD9P-1 increased β1 integrin mediated motility of HEK293 cells on collagen I, while their motility on fibronectin was decreased. The opposite was observed upon CD9 or CD81 overexpression. Based on these findings it was proposed that CD9 and/or CD81 ratio to CD9P-1 determines the cellular response to collagen and fibronectin associated motility (Chambrion and Le, 2010).

Among all the known 'tetraspanin-partner' associations, CD151's stoichiometric association with α3β1 integrin is possibly one of the most widely

studied interactions on account of its physiological and pathological significance (Yauch et al., 1998). Tight association between CD151 and laminin binding integrins play an important role in proper hemidesmosome and basement membrane assembly, wound healing, leukocyte cell extravasation and tumour cell metastasis, among others (Sterk et al., 2000; Kazarov et al., 2002; Kohno et al., 2002; Sawada et al., 2003; Barreiro et al., 2005; Chometon et al., 2006; Cowin et al., 2006; Sachs et al., 2006; Caplan et al., 2007; Baleato et al., 2008; Chien et al., 2008; Geary et al., 2008; Sadej et al., 2009; Ang et al., 2010; Novitskaya et al., 2010; Shi et al., 2010).

1.1.1 Tetraspanin CD151

The tetraspanin CD151 is also known as GP27, MER2, PETA-3, RAPH, SFA1, and TSPAN24. The topology and defining characteristics of CD151 are illustrated in Figure 1.3. CD151 was first described as a novel 27kDa platelet surface glycoprotein by Leonie K. Ashman and collegues. A monoclonal antibody (14A2.H1) recognising this protein bound to platelets and other haematopoetic cells such as megakaryocytes, monocytes, epithelial cells in the tonsillar crypts and endothelial cells. However, lymphocytes, lymphoid cell lines, neutrophils and haematopoetic progenitor cells tested negative against this antibody (Ashman et al., 1991). A subsequent molecular study categorised this protein as a member of the tetraspanin family (Fitter et al., 1995). Pretreating endothelial cells with antibodies directed

against CD151, CD81 or α3 integrin, retarded migration of individual cells in wound healing assay. Fluorescence microscopy analysis of these cells revealed localisation of CD151 at cell-cell junction where other members of the tetraspanin family such as, CD9 and CD81 and integrin α3β1 localised (Yanez-Mo et al., 1998). Around the same time, the presence of a stoichiometric association between CD151 and α3β1 was reported and this association was proposed to regulate neutrophil cell migration by recruiting a distinct family of membrane associated phosphatidylinositol 4-kinase into their fold (Yauch et al., 1998). It was later shown that CD151 form a highly stoichiometric association with α3β1 integrin both *in vivo* and *in vitro* while CD9 and CD81 are recruited into the TERM as secondary partners (Charrin et al., 2002). Mutational analysis narrowed down a triamino sequence, glutamine-arginine-aspartic acid or QRD sequence in the large extracellular loop of CD151 as the crucial site for both α3β1 and α6β1 to form tight interaction with CD151(Kazarov et al., 2002). Subsequent studies have identified several roles for CD151 in potentiating α3β1 mediated cell migration; CD151 was shown to stabilise the active conformation of the integrin (Nishiuchi et al., 2005), facilitate its endocytosis(Winterwood et al., 2006) as well as alter the glycosylation profile of the integrin (Baldwin et al., 2008).

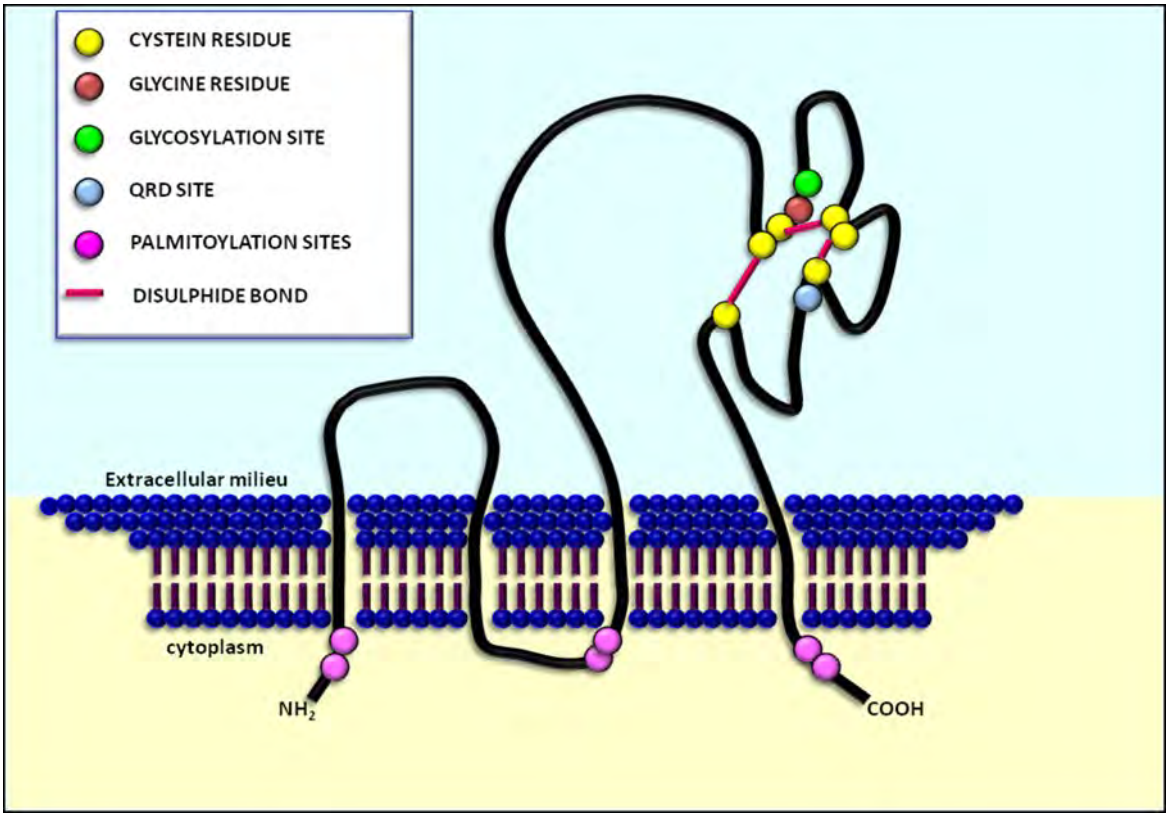

Figure 1.3: A diagram representing the tetraspanin CD151.
The defining characteristics of CD151 are described in the legend.

In contradiction, ablation of CD151 has been reported to have a pro-migratory effect (Johnson et al., 2009). In an elegantly composed study, Johnson et al. showed that silencing of CD151 in A431, an epidermal carcinoma cell line, enhanced collective migration of tumour cells during wound healing assay. E-cadherin mediated cell-cell junction formation was destabilised in these CD151 silenced cells. However, no difference was observed in the level of E-cadherin associated components (β-catenin, α-catenin, p120ctn, α-actinin and plakoglobin) that co-precipitated with E-cadherin in CD151(+) and CD151(-) cells. Junction formation was

restored upon re-expression of wildtype CD151, but not by a CD151 variable region chimera. Further analysis, to explain the increased collective migration revealed that this was not due to E-cadherin dislocation, but was a result of actin displacement from cell-cell junctions that was triggered by excessive RhoA activation. This study highlighted the opposing influences of CD151 on α3β1 integrin function and the need to interpret α3β1 role during metastasis in collective association with CD151.

1.2 Integrin Superfamily

The term 'integrin' was first coined by R.O.Hynes to describe a family of structurally related dimer molecules that 'integrated' the extracellular matrix to the intracellular cytoskeleton and coordinate various cellular functions (Hynes, 1987). This family of functionally conserved adhesion receptors is expressed in all metazoan. They consist of non-covalently paired α and β subunit dimers (Figure 1.4). There are 24 known mammalian integrin heterodimers from a limited combination of 18 α subunits and 8 β subunits. Some β subunits, for example β4, pair with only one α subunit, α6, to form α6β4. The β1 subunit on the other hand, associates with several α subunits to form several paired combinations such as α1β1, α2β1, α3β1, α4β1, α5β1, α6β1, α7β1, α8β1, α9β1, α10β1, α11β1 and αvβ1. The subunits consist of large N-terminal extracellular domains (~800 amino acids), ~ 20 amino acid transmembrane alpha helix and a short cytoplasmic tail of around 13-70 amino acids

with the exception of β4 which has a large cytoplasmic tail (~1000 amino acids). The first three dimensional structure of the integrin extracellular domain was described for αvβ3 integrin (Xiong et al., 2001).

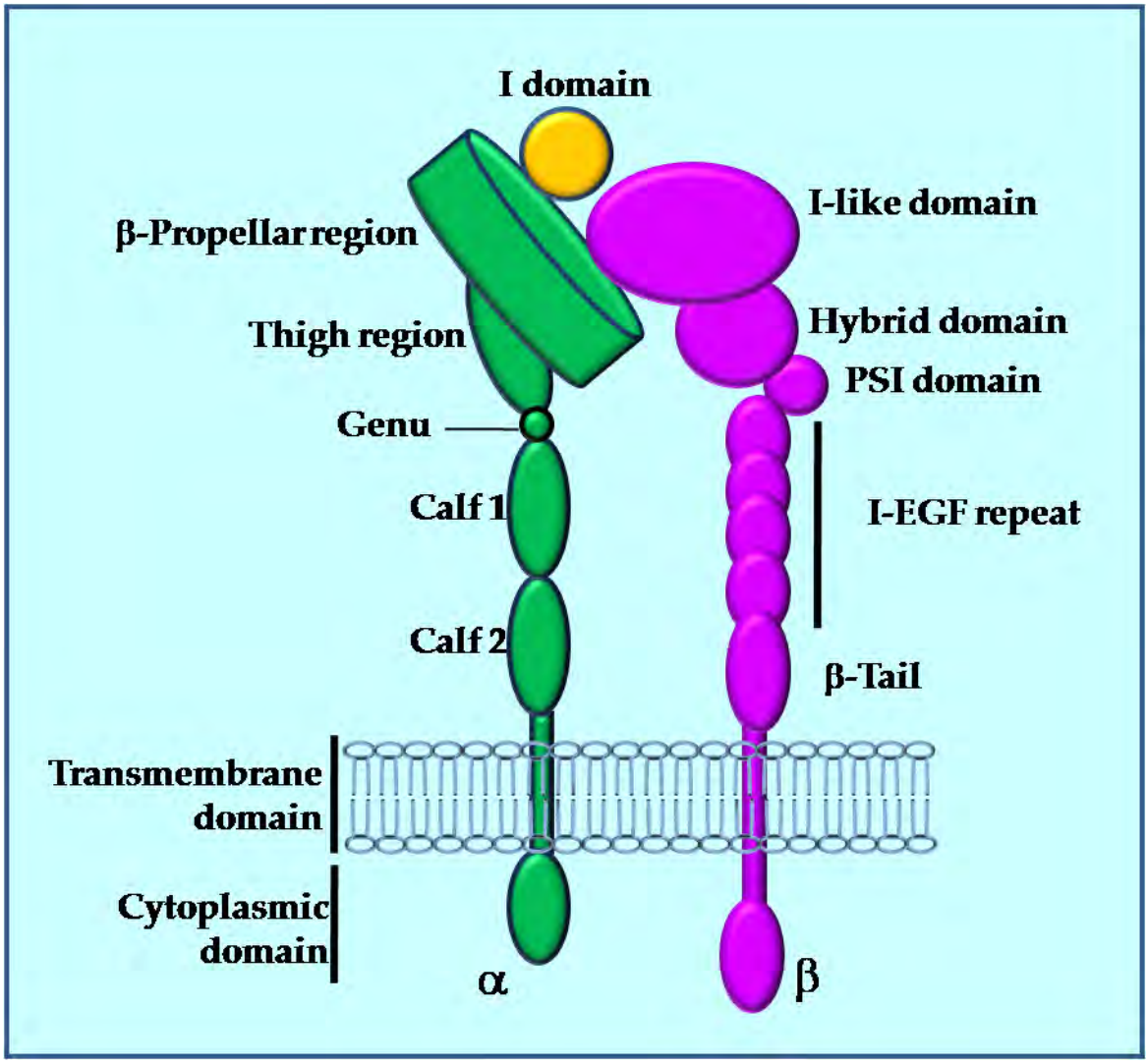

Figure 1.4: Integrin architecture.

A general representation of α (shaded green) and β (shaded magenta) integrin subunit in open conformation. Fifty percent of α subunits contain α I domain (shaded yellow)

The general structure of integrin's extracellular region depicts a large head on two legs. The 'head' of the α subunit contains a conserved FG-GAP repeats that form a seven-bladed β propeller structure and three tandem repeats of calcium binding domain. While the β subunit contains a von-Willebrand factor A-domain, also known as βA-domain. Studies on αIIβ showed that the proper conformation of the calcium binding domain is important for maturation and cell surface expression of αIIbβ3 complex (Gidwitz et al., 2004). The α subunit 'leg' consists of a 'thigh' and two 'calf' domains with a highly flexible knee or 'genu' region between the thigh and the calf. In αv and some other α subunits, the membrane proximal calf region has a furin cleavage site and is post-translationally cleaved, resulting in heavy and light chain fragments which are held together by a disulphide bridge. Through what's possibly an early evolutionary bifurcation, half of the known α subunits, α1, α2,α10, α11, αM, αL, αX, αD and αE, carry a 200aa inserted domain (I-domain) which is homologus to von-Willebrand factor A-domain (Hughes, 1992) within the FG-GAP repeats. The β subunit 'leg' consists of the hybrid domain, the plexin–semaphorin–integrin (PSI) domain, four epidermal growth factor-like repeats and a membrane flanking cystatin-like fold.

The transmembrane regions of both the subunits span across the membrane at different angles. Structural and mutational studies on αIIbβ3 predicted the α subunit transmembrane domain to consist of a short α helix perpendicular to the lipid bilayer

while the β subunit's α helix tilts at a 25^{O} angle. At this angle, the subunits are maintained at the low affinity state by electrostatic interaction between Arg995 (in αIIb) and Asp723 (in β3) and clasp formation at the inner and outer membrane border. Disruption to the tilt/length of the transmembrane angle results in integrin activation (Armulik et al., 1999; Partridge et al., 2005; Shattil et al., 2010).

The cytoplasmic region of the α subunit carries a conserved GFFKR motif that's partially embedded into the membrane. This motif is important for the inner membrane clasp formation that maintains the resting state of the integrin. The cytoplasmic region of β subunits contain two conserved NPXY motif. Binding of cytoskeletal/cytoplasmic proteins talin (Tadokoro et al., 2003) or kindlin (Montanez et al., 2008; Ma et al., 2008; Moser et al., 2008) to the first and second NPXY motif, respectively, is a prerequisite for integrin activation. Integrin activation can be further modulated by competitive binding of filamin (Garcia-Alvarez et al., 2003; Kiema et al., 2006), Dok1 (Wegener et al., 2007) and ICAP1 (Millon-Fremillon et al., 2008) which blocks talin binding as well as strategic phosphorylation of threonine and tyrosine residues (Takala et al., 2008; Oxley et al., 2008). Devoid of a kinase domain, these allosteric molecules go through conformational changes in response to environmental cues and subsequently, orchestrate bidirectional signaling across the membrane (Hynes 1987; Arnaout et al., 2005; Humphries et al., 2006). While cell surface expression and clustering contributes to it, conformational change remains the crucial factor in regulating integrin function.

Integrins exist in three functional states: high, intermediate and low affinity. Structural studies on these receptors attribute the low affinity form to the bent state and the high affinity form to extended state of the extracellular domain (Figure 1.5) (Takagi and Springer, 2002; Takagi et al., 2002; Beglova et al., 2002).

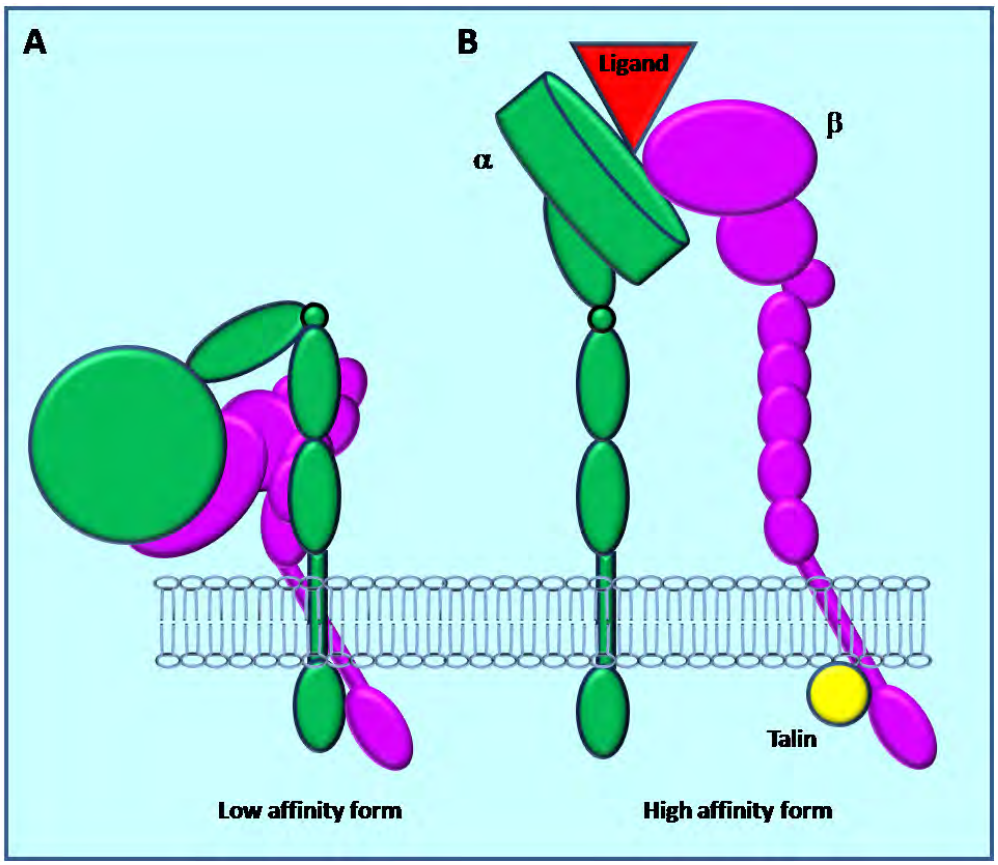

Figure 1.5 Low affinity and high affinity conformation of integrin subunits.

(A) Inactive integrin dimer adopts a compact and bent conformation. (B) The extended conformation is assumed upon activation by talin (yellow) binding of at the cytoplasmic tail (inside out signalling) or ligation of molecule (red) at the ligand binding site at the extracellular domain (outside in signalling)

The mechanism of how integrins change from a low to a high affinity state is not fully understood, however, two models have been proposed. Both models agree that a conformational change in the head domain is required for ligand binding. However, the 'switchblade' model proposes that ligand binding occurs only in the extended form (Luo et al., 2007) while the 'deadbolt' model maintains that the integrin extension occurs upon ligand binding (Xiong et al., 2003). While the 'switchblade' model is more widely accepted, there is also ample evidence from crystallised and transmission electron microscope images of αvβ3 integrin to confirm ligand binding in the bent conformation (Xiong et al., 2001; Adair et al., 2005).

Integrins set the 'cellular mood' by constantly interrogating and responding to environmental cues (Miranti and Brugge, 2002; Berrier and Yamada, 2007). In fact, a cell's survival depends on the integrins' ability to interact with the extracellular matrix (ECM). Presence of unligated integrins on adherent cells, can induce apoptosis through caspase 8 activation (Stupack et al., 2001). Initial ligation of integrins to their ligands is thought to be of foremost importance in inducing clustering. The number, size and distribution of integrin complexes are determined by the physical and chemical properties of the ECM and are especially sensitive to ligand spacing (Arnold et al., 2004; Cavalcanti-Adam et al., 2007) and to rigidity of the matrix (Pelham, Jr. and Wang, 1997; Paszek et al., 2005).

Classification of integrins is rather complicated since they are capable of binding multiple ligands with different affinities. Furthermore, most extracellular matrices have more than one type of ligand binding domain (Plow et al., 2000). Initially, integrins were broadly divided into two subfamilies based on the presence of a 200 amino acid I element in the α subunit which shares a sequence homology to von-Willebrand factor A-domain. A more representative classification was later introduced based on their preferred ligand: the RGD motif, LDV motif, laminin/collagen binding A-domain β1 integrins and laminin binding non A-domain integrins (Humphries et al., 2006) and is summarised in Figure 1.6.

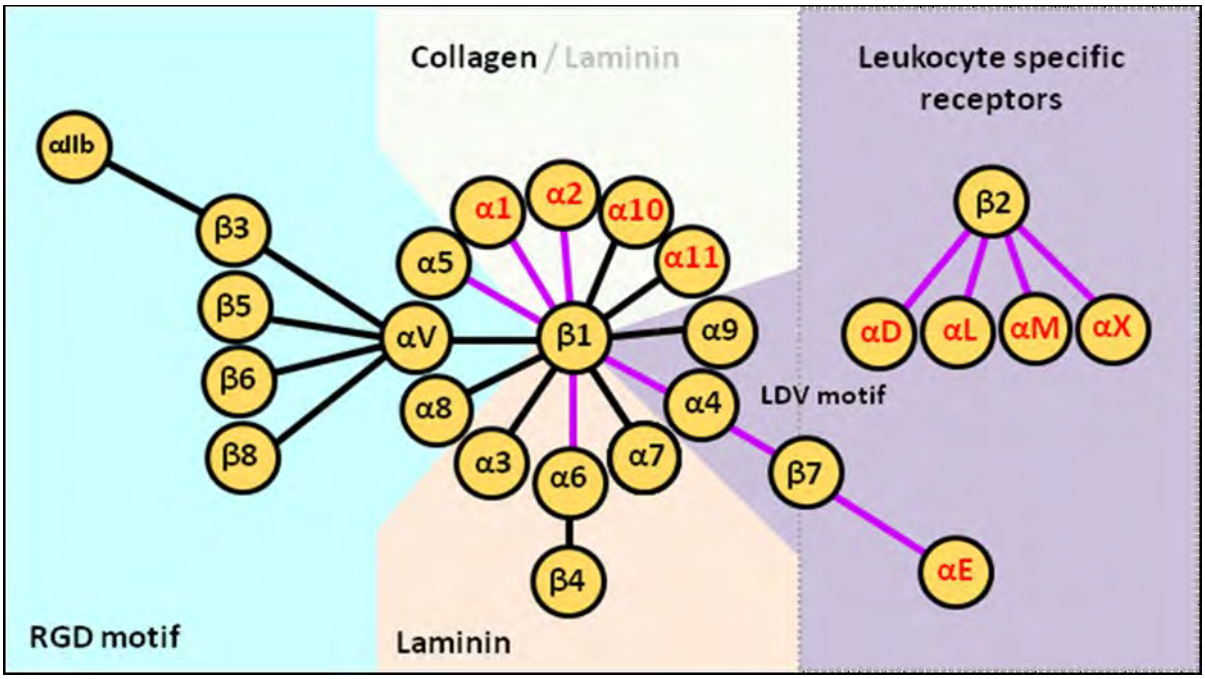

Figure 1.6 Integrin-ligand classification.

Integrins are classified from their best known ligands: RGD motif, LDV motif, non-I domain containing laminin receptors and I-domain containing collagen/laminin receptors. I domain containing α subunits are in red. Purple line represents integrins dimers found in immune cells are. (Humphries et al., 2006; Luo et al., 2007)

1.2.1 Integrin α3β1

A polypeptide corresponding to human α3 integrin subunit was first described while screening for monoclonal antibodies raised against human bladder cancer cell surface antigen. It was also shown to be highly expressed in many tumor cell lines (Fradet et al., 1984). This cell surface glycoprotein was initially assigned to the very late antigen (VLA) group of proteins and named as VLA-3. Similar to the previously described VLA-1 and VLA-2, VLA-3 formed a heterodimer with the VLA-4 β subunit which later came to be known as β1 integrin subunit (Hemler et al., 1987). The two variants that have been reported for α3 subunit, namely isomer 3A and isomer 3B, differ in the splicing of the light chain and have distinct tissue distribution (de Melker et al., 1997). Within the extracellular region, there are 14 potential N-linked glycosylation sites, 11 in the heavy chain and 3 within the light chain (data from www.uniprot.org). At least 7 disulphide bonding patterns have been mapped to this region. Three furin cleavage sites are mapped within the disulphide bridge between amino acids 846 to 890 (Figure 1.7) (Krokhin et al., 2003).

During heterodimer assembly which occurs in the rough endoplasmic reticulum, α3 integrin only pairs with β1 integrin subunit for integrin dimer formation. The β1 subunit has 14 potential glycosylation sites and 28 putative disulphide bonding motifs (data from www.uniprot.org). There are 5 known splice variants of the β1 subunit, all of which occurs at the cytoplasmic tail. The difference

in splice variance does not have any effect on the ligand binding which occurs in the extracellular domain, but triggers different signaling pathways in the cytoplasmic end which leads to different cellular responses (Armulik, 2002). Structural analysis predicts the head region of the dimer forming a ligand binding pocket that interacts with Laminin332 in a divalent ion (Mn^{2+}) dependent manner.

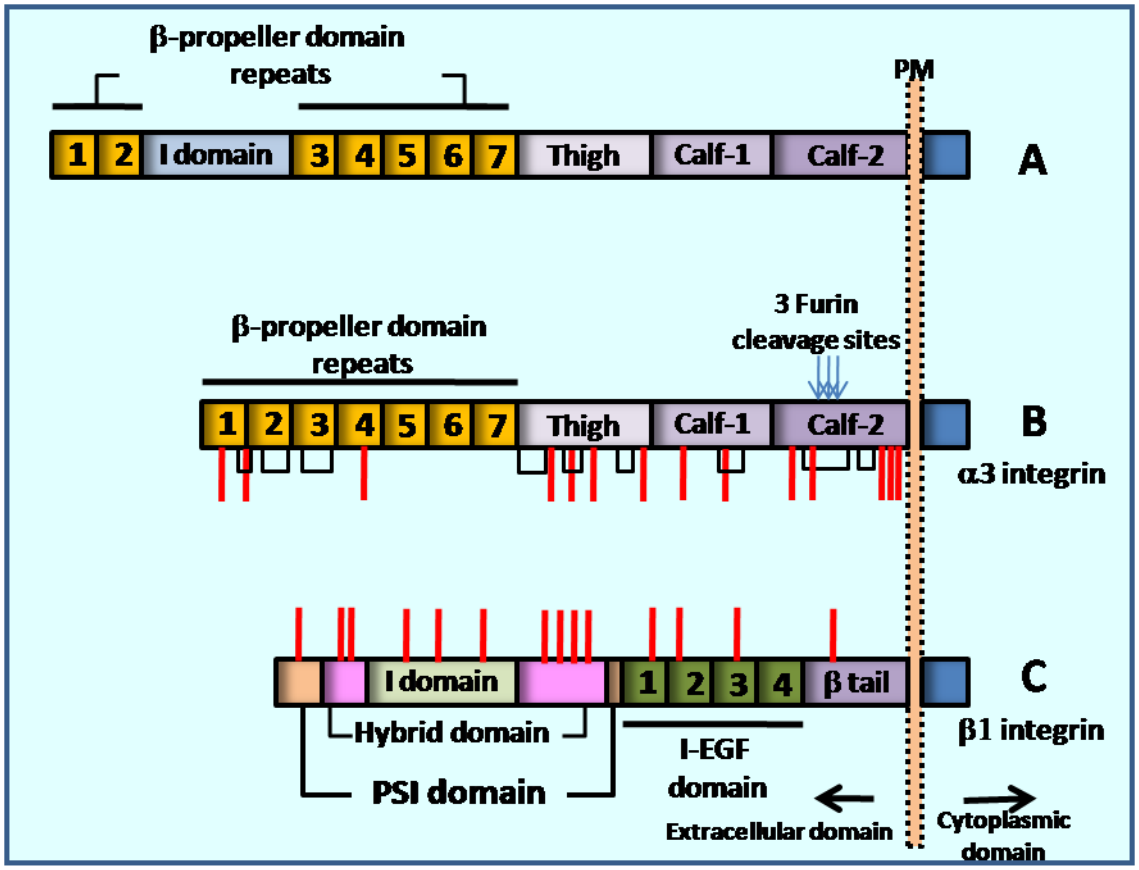

Figure 1.7 Diagram showing a linear model for integrin subunits.

(A) Representation of I-domain containing α subunit. (B) The non I-domain containing α3 integrin subunit domains. Putative post translation modification sites on the extracellular domain are highlighted: glycosylation (red bars), disulphide bond (black connectors) and furin cleavage site (blue arrows). (C) β1 integrin subunit domains. Glycosylation sites are marked with red bars. Disulphide bonds are not shown.PM: plasma membrane. The domains are not drawn to scale and the glycosylation sites are an approximation.

1.3 Laminin 332

The basement membrane that lines the epithelial layer is a crucial component in maintaining the integrity of this tissue. It provides a platform for epithelial cells to anchor to while going through cell division, differentiation and during migration. It also influences cell behaviour by signaling for specific cellular responses such as proliferation and apoptosis.

The basement membrane consists of a mix of several biologically active components including laminins, collagenIV, heparan sulphate proteoglycans and nidogen. Laminins are the most abundant glycoproteins in the basement membrane and are also where they are most widely found. Laminins consist of heterotrimer α, β and γ chains and their nomenclature reflects their chain designation: ie., Laminin111 consist of α1β1γ1 chains while Laminin211 is composed of α2β1γ1 chains (Aumailley et al., 2005). They are composed of a central 400 kD α chain which contains varying numbers of globular regions, and 200 kD β and γ subunits that wrap around the α chain to form a crucifix shape. This large molecule contains many domains that interact with various cell surfaces and secreted molecules as depicted in Figure 1.8. The α3β1 integrin is a laminin binding receptor with clear preference towards Laminin 332 and Laminin 511 (Nishiuchi et al., 2003; Nishiuchi et al., 2006). Using

recombinant proteins, the α3β1 integrin binding site in Laminin332 has been located to the large globular domain 3 (LG3) on the α chain (Shang et al., 2001).

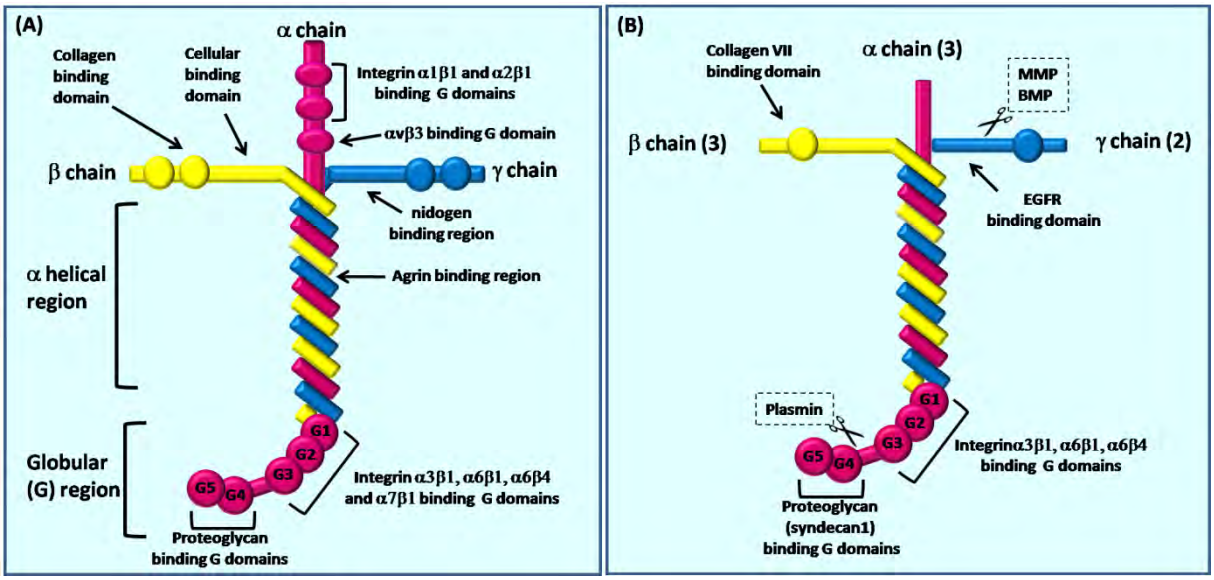

Figure 1.8: The structure of laminin trimer.

(A) Laminins form a crucifix structure consisting of α, β and γ subunit with an average length of 100nm. The α chain (red) has three globular domains in the head region and five globular domains consisting of epidermal growth factor (EGF) repeats in the tail. The β (yellow) and γ (blue) chains coil around the α chain and form the 'trunk'. (B) Laminin 332 is a truncated form of the typical laminin structure. It is devoid of the globular domain in the head region, and has single globular domain on the β and γ chains. Laminin 332 can be cleaved by various proteases (MMP,BMP and plasmin) exposing this region for potential ligand binding.

The basement membrane was initially thought to play an important role in restraining *in situ* carcinomas from spreading to the surrounding area. A breach of this border, attributed to the proteolytic degradation by enzymes secreted by tumour cells, defines invasive carcinoma (Liotta et al., 1977; Jones and DeClerck, 1980; Hu et al., 2008). While this observation is a widely accepted model, later studies have also

shown that carcinomas secrete their own brand of basement membranes which is utilised as a substrate in promoting proliferation and metastasis (Frenette et al., 1988; Frenette et al., 1989; Hao et al., 1996; Katayama et al., 2003). Transition from a benign to a metastatic tumour is preceded by several events. One of the major changes that mark this transition is altered glycosylation of cell surface receptors and the secreted extracellular matrix components. Coupled with the tumour-associated proteolytic enzymes secreted by carcinomas, this alteration has a profound effect on invasion and metastasis (Oz et al., 1989; Singh et al., 2004).

1.4 Glycosylation

The majority of proteins go through at least one or more post-translational modifications in their lifetime. These modifications include covalent attachment of small molecules (phosphorylation and sulphation) or larger preassembled structures (palmitoylation, glycosylation and ubiquitination) to specific amino acid or motifs on the protein backbone. Among membrane associated proteins, glycosylation represents the most common type of modification. Glycosylation is a co- and post-translational modification event which is controlled both genetically and epigenetically. Protein glycosylation itself exists in various forms depending on the nature of the preassembled oligosaccharide structure and the amino acid residue it is attached to on the polypeptide backbone. Following these prerequisites, glycol-

peptide linkages consist of 5 types of N-glycosyl, 27 O-glycosyl, 4 Phospho-glycosyl, one C-mannosyl and one glypiation type of linkages. Of all the different types of sugar-amino acid bond, the β-glucosylamine linkage of N-acetylglucosamine (GlcNAc) to asparagine (N) is the most common type of oligosaccharide modification. During this type of glycosylation, a homogeneous preassembled high mannose oligosaccharide structure is attached to the asparagine residue of a triamino motif, Asn-X-Ser/Thr, where X represents any amino acid except proline. Consequently, this type of glycosylation is also known as asparagine-linked glycosylation (ALG) or N-linked glycosylation (NLG). Approximately, ~70% of all glycosylated proteins are asparagine-linked glycosylated (Spiro, 2002). Since ALG occurs within the ER and the Golgi apparatus, the glycosylated portion of glycoproteins are found either within the secretory pathway or exposed to the extracellular face of the cell. However, some Ser/Thr linked O-linked glycoproteins have been reported to have nuclear and cytoplasmic distribution (Hart, 1997). Due to the inherent variation accrued in glycan structures during maturation, glycosylation proves the simplest way for diversification to modify cellular behaviour.

1.4.1 The N-linked Glycosylation (NLG) Pathway

1.4.1.1 Assembly of dolichol oligosaccharide precursor

While the NLG pathway itself starts in the lumen of ER, the components required for this process are synthesised and transported from the cytosol into the lumen. Monosaccharides, obtained as nutrients or as a degradation product, are activated to form UDP-monosaccharides, GDP-monosaccharides or CMP-sialyl sugars and transported across the ER and Golgi membranes via specific barrel shaped sugar nucleotide transporters (SNT). Most SNTs are localised to the Golgi but some are also found in the ER. The assembly of triantennary tetradecasaccharide dolichol biphosphate glycolipid, $Glc_3Man_9GlcNAc_2$-PP-dolichol, which is a universal precursor for eukaryote ALG is also initialised at the cytoplasmic face and flipped across to mature in the lumenal compartment of the ER as illustrated in Figure 1.9.

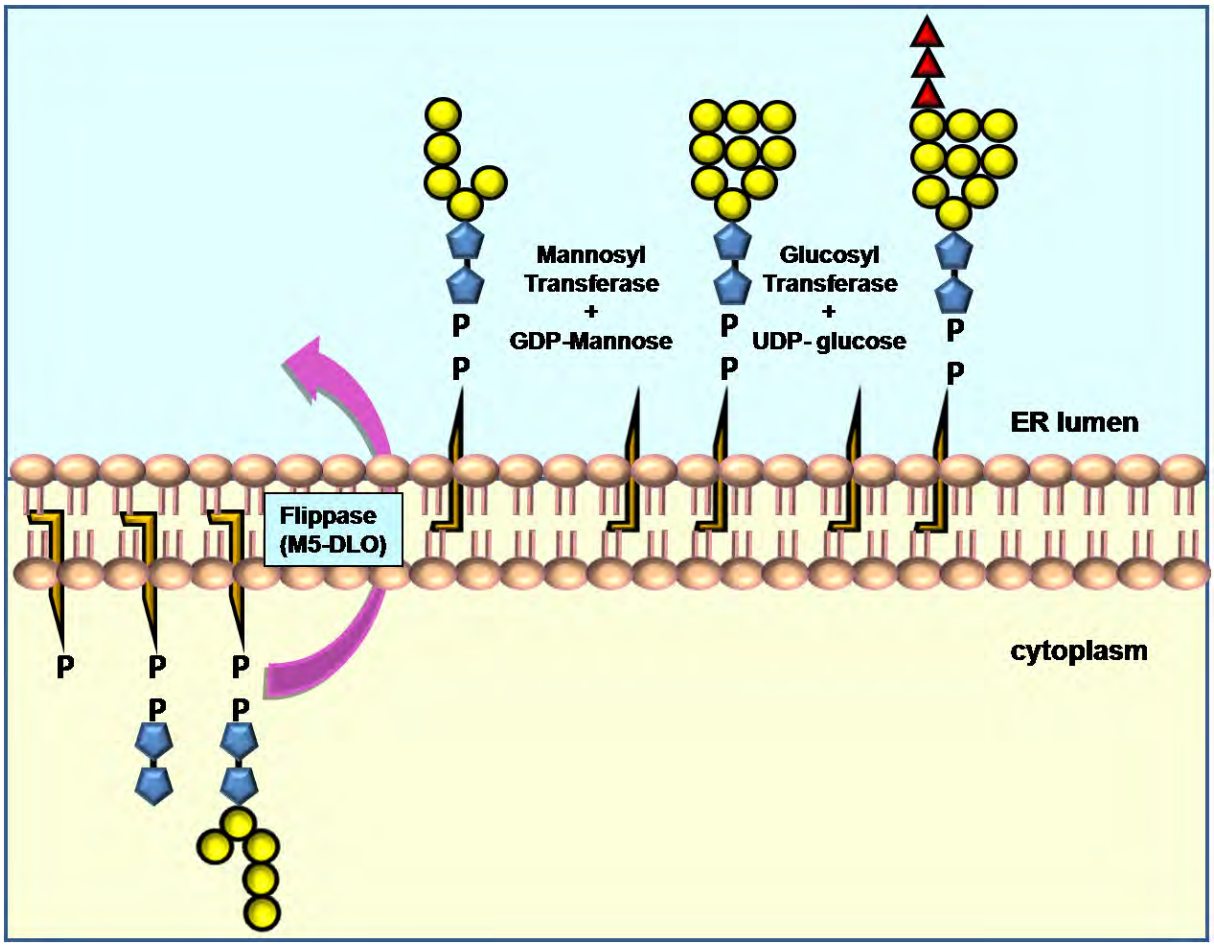

Figure 1.9 Assembly of dolichol oligosaccharide precursor at the cytoplasmic and lumenal surface of the ER membrane.

Two N-Acetylglucosamine residues (pentagon shaded blue) are attached to the membrane embedded dolichol biphosphate chain followed by the addition of five mannose residues (circles shaded yellow) at the cytoplasmic face of the ER. M5-DLO flippase then flicks to re-orientate this structure into the ER lumen where four more mannose residues are added to form a high mannose structure. Eventually, three glucose residues are added to the first branch and the glucosylated high mannose precursor is now ready to be transferred to a peptide backbone by the oligosaccharyl transfer complex.

The enzyme M5-DLO (5 mannose containing dolichol oligosaccharide) flippase has been identified to be responsible for this function after comparing the

flipping potential of several glycolipids ranging from M3-DLO to M9-DLO (Sanyal et al., 2008; Sanyal and Menon, 2009). The name M5-DLO flippase was selected to reflect the glycolipid candidate that flipped across the membrane most rapidly, $Man_5GlcNAc_2$-PP-dolichol or M5-DLO. The maturation of the precursor continues within the ER lumen in the presence of Man-P-dolichol, Glc-P-dolichol and glycosyltransferases until the final precursor, $Glc_3Man_9GlcNAc_2$-PP-dolichol, is assembled and is ready to be transferred onto a polypeptide. A representation of the final oligosaccharide assembly and the type of linkages between the monosaccharides is detailed in Figure 1.10(A-E).

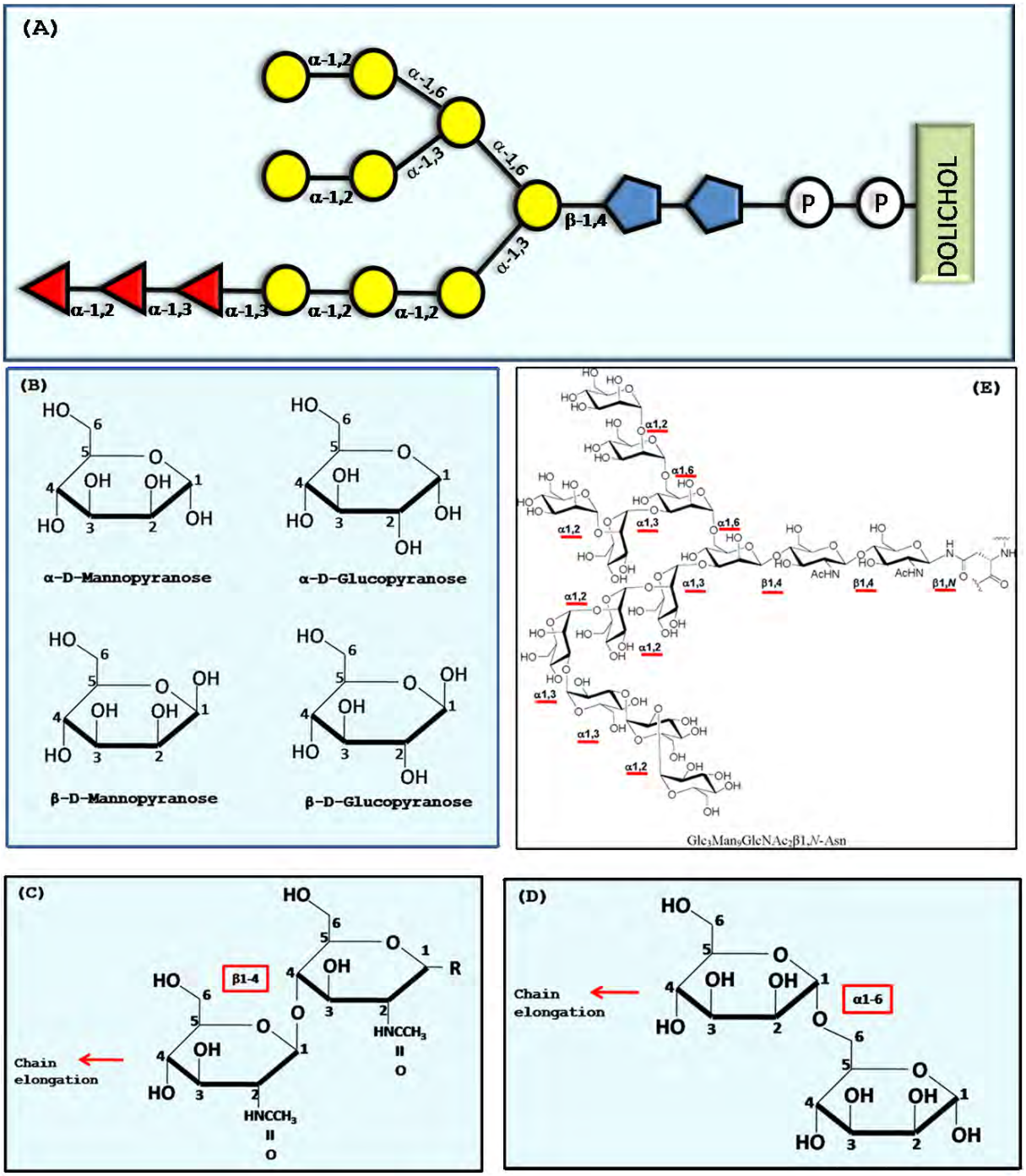

Figure 1.10 Structure of N-linked oligosaccharide.

(A) The high mannose precursor consists of three glucose residues (triangles shaded red), nine mannose residues (circles shaded yellow) and two N-Acetylglucosamine (GlcNAc) residues (pentagon shaded blue) linked to the dolichol lipid via two phosphate residues (P). **(B)** A Haworth projection represents a 3D structure of cyclic monosaccharides where thicker lines indicate atoms closer to the observer. Numbers

1-6 represent the six carbon atoms of the hexose molecule. The 'α' designation indicates the hydroxyl group on the first carbon (C-1) and hydroxymethyl group attached to the fifth carbon (C-5) are on the opposite sides of the ring's plane, while 'β' is designated when they are on the same side of the plane. **(C)** The example of a β1-4 linkage depicted here represents the glycosidic linkage between two GlcNAc residues, linking C-1 of a newly attached monosaccharide to the C-4 of the GlcNAc on the growing chain. **(D)** A representation of the α1-6 linkage where a glycosidic bond is formed between C-1 of the donor (left) and C-6 of the acceptor (right) mannose residue. **(E)** A chemical structure representing the mature precursor ($Glc_3Man_9GlcNAc_2$) covalently attached to the asparagine residue of protein backbone. The various linkages are underlined in red. This image was reproduced from (Weerapana and Imperiali, 2006) with slight modifications.

1.4.1.2 Glycoprotein synthesis – chaperones and checkpoints

Nascent proteins destined for the secretory pathway are tagged with a signaling peptide sequence at the amino terminal end. This model, suggesting that the attachment of ribosome to the ER is directed by a signal at the amino terminus end of the polypeptide, was first proposed by David Sabatini and Gunter Blobel in 1971. Their hypothesis was based on the difference they found in the protein size when secreted proteins such as immunoglobulin were translated *in vitro* in the presence or absence of microsomes (Sabatini and Blobel, 1970; Blobel and Sabatini, 1970). A RNA-multiprotein complex called signal recognition particle (SRP) recognises and binds to both the signal peptide sequence and the ribosome in the cytosol, temporarily halting the translation process. In the mammalian system, SRP guides the whole complex toward the rough endoplasmic reticulum (RER)

membrane where it anchors to SRP receptor protein. Binding of SRP to its receptor releases both the ribosome and the signal peptide from this complex, immediately restoring the translation process. The signal peptide from the growing polypeptide sequence is directed into the RER membrane through a multiprotein complex that forms a channel through the membrane called SEC61. The signal peptide is then cleaved by signal peptides located within the RER lumen. Once the translation is completed, the protein is released into the RER lumen. However, not all polypeptides are cleaved to remove the signal peptide sequence. And depending on where the signal peptide(s) and hydrophobic stretches are located, various types of transmembrane proteins are generated, ie.type 1, type 2 and multipass (Figure 1.11).

ER chaperone proteins recognise and bind to the nascent polypeptide as it emerges through the SEC61 translocon. If an ALG site is detected within the first 50 amino acid sequence, the emerging polypeptide associates with calnexin, a membrane bound ER lectin that recognises oligosaccharides or bulky hydrophilic patches. Otherwise, it associates with a chaperone from the Hsp70 family called BiP, which associates directly to the polypeptide. Crowding of calnexin, BiP and another soluble ER lectin called calreticulin towards the nascently synthesised polypeptide protects it by inhibiting aggregation and allowing the time required for proper folding of N-linked glycoproteins (Molinari and Helenius, 2000).

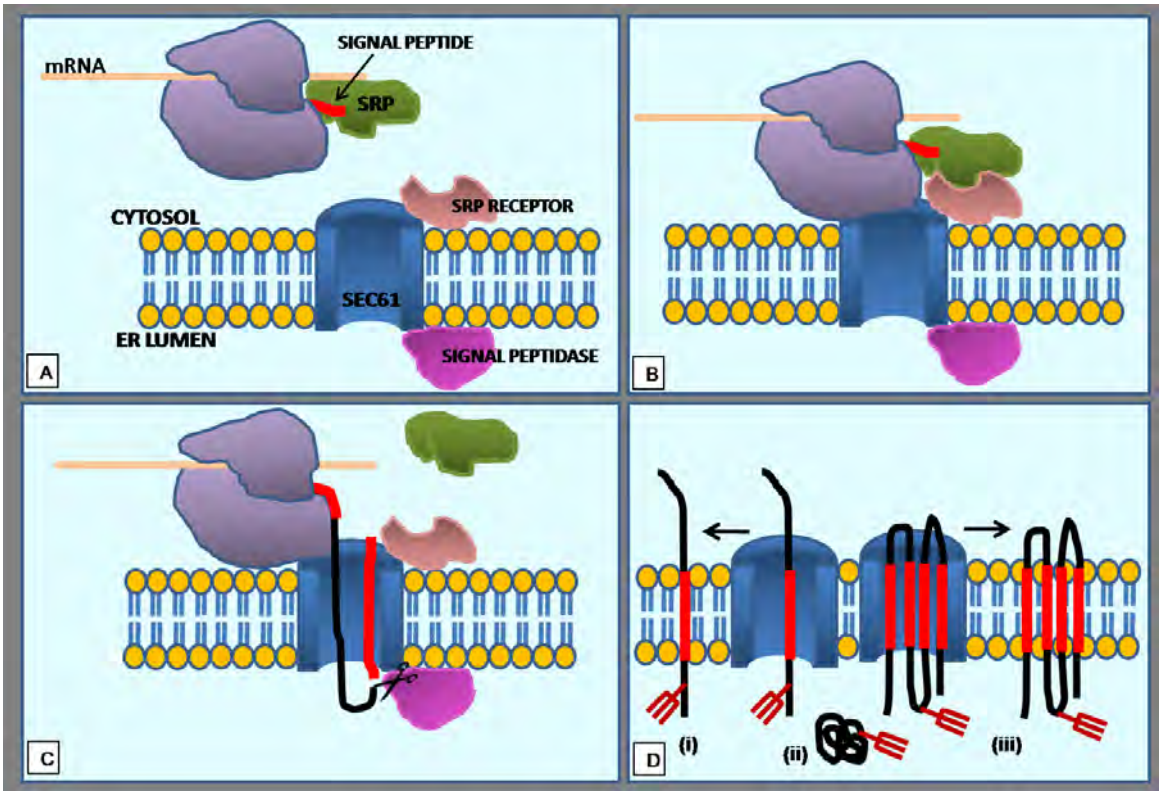

Figure 1.11 Assembly of proteins/glycoproteins destined for the secretory pathway. (A) Nascent polypeptides are guided to the Sec61 translocon by SRP molecule that recognises the signal peptide sequence. (B) Binding of SRP to its receptor engages the ribosome to the translocon. (C) The nascent polypeptide chain is injected into the ER lumen co-translationally and signal peptide sequence is cleaved by signal peptidase. (D) Single transmembrane glycoproteins (i), multipass glycoproteins (iii) and secreted glycoproteins (ii) generated based on the number of hydrophobic stretches present. Red line represents hydrophobic site, red fork represents oligosaccharides.

Glycosylation of the emerging nascent polypeptide is catalyzed by the oligosaccharyltransferase (OST) complex. The OST complex is an integral membrane protein complex consisting of seven (mammal) or eight (yeast) subunits which facilitates co-translational and post-translational *en bloc* transfer of the preassembled high mannose oligosaccharide onto a polypeptide chain. The mammalian OST complex consists of ribophorin I, ribophorinII, DAD1, OST4, N33 or IAP, STT3A or

STT3B, and Ost48 and is located adjacent to each active translocon. siRNA mediated depletion of ribophorin I and *in vitro* cross-linking analyses indicated selective presentation of substrates by the subunits to the catalytic domain of the OST complex and led to the hypothesis that the elaborate OST subunits exist because each subunit present a different group of substrates to a catalytic core (Wilson et al., 2008). The active site of eukaryotic OST is attributed to the STT3 subunit (Yan and Lennarz, 2002; Nilsson et al., 2003). Two types of STT3 catalytic subunit have been identified; STT3A and STT3B, both of which are involved in the transfer of OS-PP-DOL to the acceptor site. These isomers have been shown to have an overlapping, as well as complimentary role in oligosaccharyl transfer. STT3A which is located adjacent to SEC61 requires a distance of 65-75 amino acid residues from the large ribosomal subunit to access the acceptor site (Nilsson and von, 1993; Whitley et al., 1996). Should an N-X-S/T sequon exist within this region, STT3B which is located further from the SEC61 is able to access this site at later stages. While STT3A functions co-translationally, STT3B has a co- and post-translation role in oligosaccharyl transfer (Ruiz-Canada et al., 2009).

Trimming of the appended oligosaccharide ($Glu_3Man_9GluNAc_2$) starts as soon as they are attached to the asparagine residue within the triamino sequon. This indicates that in most cases, processing of the newly added glycan to a polypeptide may be initiated before the polypeptide is completely glycosylated and folded. In

fact, glycosylation has been shown to play an important role in glycoprotein folding. Upon covalent attachment of oligosaccharide to the polypeptide, the outermost α1,2 linked glucose residue is trimmed by a membrane bound ER enzyme glucosidase I (Shailubhai et al., 1991). This is followed by the trimming of the second α1,3 linked glucose residue by the soluble ER enzyme, glucosidase II. Glucosidase II is composed of α subunit which harbours the catalytic domain while the β subunit bears a KDEL-like ER retention motif (Trombetta et al., 1996) and a sequence homologous to the mannose binding domain of Mannose-6-phosphate (Man-6-P) receptor (Munro, 2001). The resultant monoglucosylated structure is then recognised by two resident ER lectins, calnexin (CNX) or calreticulin (CRT). This is an important juncture in the glycoprotein's life cycle. If a glycoprotein is misfolded, the ER glucosyltransferase acts as a conformation sensor that recognises non-native structure and utilises UDP-glucose to reglucosylate the glycoprotein, prompting reassociation with CNX or CRT. Association with the ER lectins retains misfolded proteins as well as folding intermediates within the ER, allowing time for proper folding. Achieving a native structure may take several rounds of reglucosylation and deglucosylation. Parodi's group was the first to characterise the abundantly expressed ER glucosyltransferases (Parodi et al., 1984) but its significance was only understood much later (Hammond et al., 1994; Trombetta and Helenius, 1998; Trombetta and Helenius, 1999; Trombetta and Helenius, 2000; Keith et al., 2005). If the deglucosylated glycoprotein has a native tertiary structure, it will continue to the next stage of maturation. This is

followed by the removal of the final glucose residue, simultaneously releasing the non-glucosylated structure from the lectin's clutch.

Another crucial process at this stage that ensures correct protein folding is disulfide bond formation. This step is critical for the maturation of many proteins that transit the secretory pathway. Disulfide bond formation is catalyzed by oxidoreductases from the protein disulphide-isomerase (PDI) family which carry CXXC motif in thioredoxin domain. Besides formation of disulphide bonds, these enzymes also function as isomerases that change non-native disulfide linkages to native linkages (Ellgaard et al., 1999; Ellgaard and Frickel, 2003; Ellgaard and Ruddock, 2005) and as chaperones to inhibit aggregation of misfolded proteins (Cai et al., 1994). The role of calnexin and calreticulin in disulphide bridging is more selective. Disulphide bond formation in CD1d heavy chain is dependent on the presence of the ER lectin (Kang and Cresswell, 2002) but not in MHC I folding (Zhang et al., 1995; Tector et al., 1997).

Following deglucosylation, glycoproteins exit the ER for either further glycan processing in the Golgi or to the cytosol for degradation. In both cases, prior to ER exit, they are earmarked for demannosylation which is performed by two of the three subfamilies of glycosylhydrolase family 47. This includes the ER α1-2mannosidase I (ERManI) and three EDEMs (ER degradation enhancing mannosidase like protein) comprising of EDEM1, EDEM2 and EDEM3 (Hosokawa et al., 2001; Mast et al.,

2005; Olivari et al., 2005). A possible evolutionary divergence occurs at this point. In *S. cerevisiae*, the ERManI homologue MnsI, removes the mannose residue from the middle branch to form isomer B, and this has been shown to initiate retrotranslocation and degradation of the misfolded protein in (Jakob et al., 1998b). The corresponding mammalian ERManI which trims mannose to isomer B conformation does not have the same effect. The CNX/CRT binding offer protection from degradation and is important for cellular energy conservation. In fact, it is the isomer A formation which abolishes reglucosylation and recruitment into the CNX/CRT cycle and subsequently, removal of the misfolded glycoproteins (Ermonval et al., 2001). Various theories have been proposed as to how isomer A is generated in the ER. One that's gaining momentum describes the role played by EDEMs in demannosylation prior to degradation.Upon exiting the ER, the misfolded protein is ubiquitinated by SCF E3 ligase complex (Yoshida et al., 2005; Yoshida, 2005) and in some cases, deglycosylated by cytosolic peptide:N-glycanase PNGase1 (Hirsch et al., 2003; Misaghi et al., 2004; Yoshida and Tanaka, 2010; Hosomi et al., 2010). Demannosylation of misfolded proteins ensures these proteins are not recruited into Golgi by ERGIC53/VIP36 cargo receptors which requires branch A mannose residue for recognition.

However, if a glycoprotein is properly folded, it is sent on a different pathway. Firstly, the high mannose oligosaccharides are trimmed by various ER mannosidases. There are at least three known ER mannosidases based on their

sensitivity to inhibitor *in vivo*. Within the RER, ER mannosidase I (kifunensine sensitive) and ER mannosidase II (kifunensine insensitive) have been identified. ER mannosidase I hydrolyzes α-1,2-linked to form isomer B while ER mannosidase II activity results in isomer A or isomer C though it is a less common occurance (Weng and Spiro, 1993a; Trombetta, 2003). However, it is important to note that only a third of the glycoproteins that exit the ER are processed by ER mannosidases (Bischoff et al., 1986). A summary of this early glycosylation stage is illustrated in Figure 1.12 below.

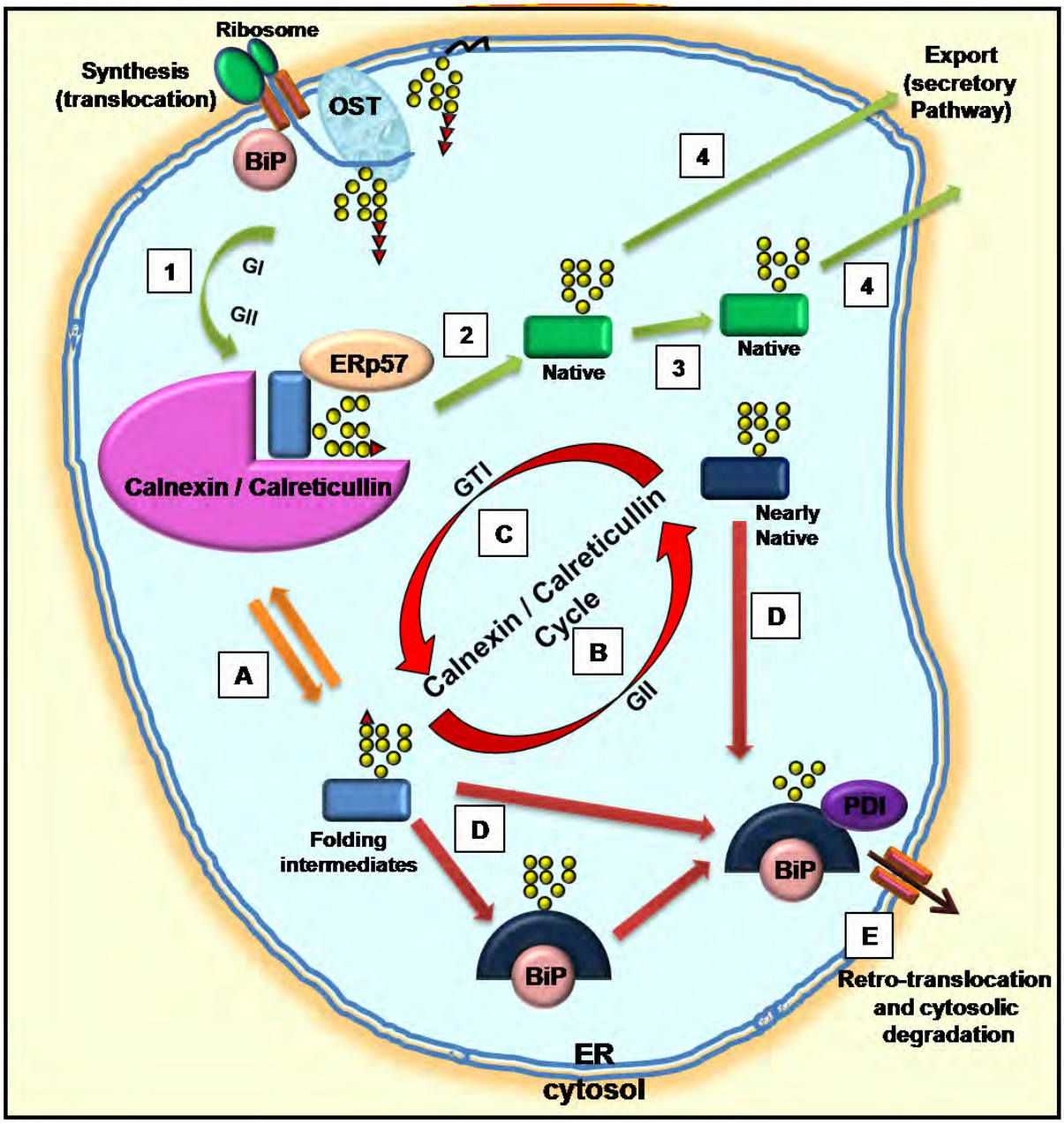

Figure 1.12 Processing of newly synthesised glycoprotein in the ER. OST complex transfers the triglucosylated high mannose precursor onto the nascent polypeptide upon reconizing the Asn-X-Ser/Thr seqoun. [1] Immediately after oligosaccharyl transfer, the first and second glucose residue is removed by glucosidase I (GI) and glucosidase II (GII) respectively. [2] The monoglucosylated glycoprotein associates with ER lectin, calnexin/calreticullin and oxidoreductase ERp57 to ensure it is properly folded. Natively folded glycoproteins are deglucosylated by glucosidase II. [4] Deglucosylated glycoproteins are either immediately transported out of ER by ERGIC53, ERGL or VIP36 chaperones, or [3] & [4] demannosylated by ERManI before being escorted out by the chaperones. [A] A proportion of nearly native glycoproteins initially released by the lectin are also deglucosylated by GII [B], but

further progress is stopped by glucosyltransferase I (GTI) which reglucosylated the glycoprotein [C]. This step is repeated until a native conformation is achieved. [D] Non native glycoproteins and glycoproteins that fail to achieve the native conformation after several rounds of calnexin/calreticullin cycle are attracted to BiP. These glycoproteins are extensively demannosylated by ERManI and EDEMs before removal from ER for proteosomal degradation [E].

[Figure modified from: (Hebert and Molinari, 2007)]

Beyond this stage, processing of the high mannose ensemble differs between yeast and mammalian system. In yeast, trimming of mannose in the ER is followed by addition of mannose residues in the Golgi by Golgi mannosyltransferases, forming extended mannan structures. In the mammalian system, both $Man_9GlcNAc_2$ and $Man_8GlcNAc_2$ oligosaccharides are recruited by ER cargo receptors ERGIC53/VIP36 to the Golgi, where they are trimmed down to $Man_5GlcNAc_2$ sugars by Golgi mannosidase I which specifically targets α-1,2-linked mannose. Three different isoforms of Golgi mannosidase I have been identified (GolgiManIA, IB and IC) distributed in the cis and medial Golgi (Herscovics et al., 1994; Lal et al., 1998; Tremblay and Herscovics, 2000). The resulting $Man_5GlcNAc_2$ glycan is a specific substrate for N-Acetylglucosaminyltransferase I (GNTI/MGAT1) in medial Golgi cisternae which adds a GlcNAc residue to the α-1,3-linked mannose on the A branch. Next, Golgi α-mannosidase II cleaves the remaining two α3 and α6 linked mannose and commit to the biosynthesis of complex N-linked oligosaccharides by addition of GlcNAc by GNTII, GNTIII, GNTIV and GNTV. All the GlcNAc addition occurs in a sequential manner except for addition by GNTIII which, upon addition, inhibits

GNTII, GNTIV and GNTV activity. The synthesis of complex N-linked glycans starts with the attachment of GlcNAc residue by GlcNAc transferase II (GnTII). Beyond this stage, the glycans are modified by various glycosyltransferases in median and trans Golgi where terminal galactosyl, fucosyl or sialyl residues are added. The resulting diverse oligosaccharides will eventually be presented at the cell surface. Glycosyltransferases are classified based on the monosaccharide they add (for example, fucosyltransferases add fucose to the N-linked glycan) and the linkages they initiate (for example α1-2, α2-3 or α2-6). The choice of sugar and the linkages is determined by multiple factors which include the repertoire of glycosyltransferases expressed by the cell as well as the level of donor and acceptor molecules present at any given time (Kornfeld and Kornfeld, 1985; Dennis et al., 2009).

Besides the conventional pathway which involves removal of all three glucose residues before progressing on the glycosylation pathway, selected monoglucosylated high mannose structures are also subverted within the ER to different pathways. One such pathway involves addition of phospho N-Acetylglucosamine residues to the mannose residues on the peripheral chains. This particular modification allows for recognition by the mannose-6-phosphate receptors and eventual trafficking of the tagged glycoprotein and its associated partners to the late endosomal and lysosomal compartments. In the second alternative pathway (or the endomannosidase I pathway), instead of removal of mannose residues by ER mannosidase I, the glycoprotein containing the monoglucosylated structure is

recruited to the Golgi apparatus where it serves as a substrate for endomannosidase. The various branches of the asparagine-linked glycosylation pathway is summarised in Figure 1.13.

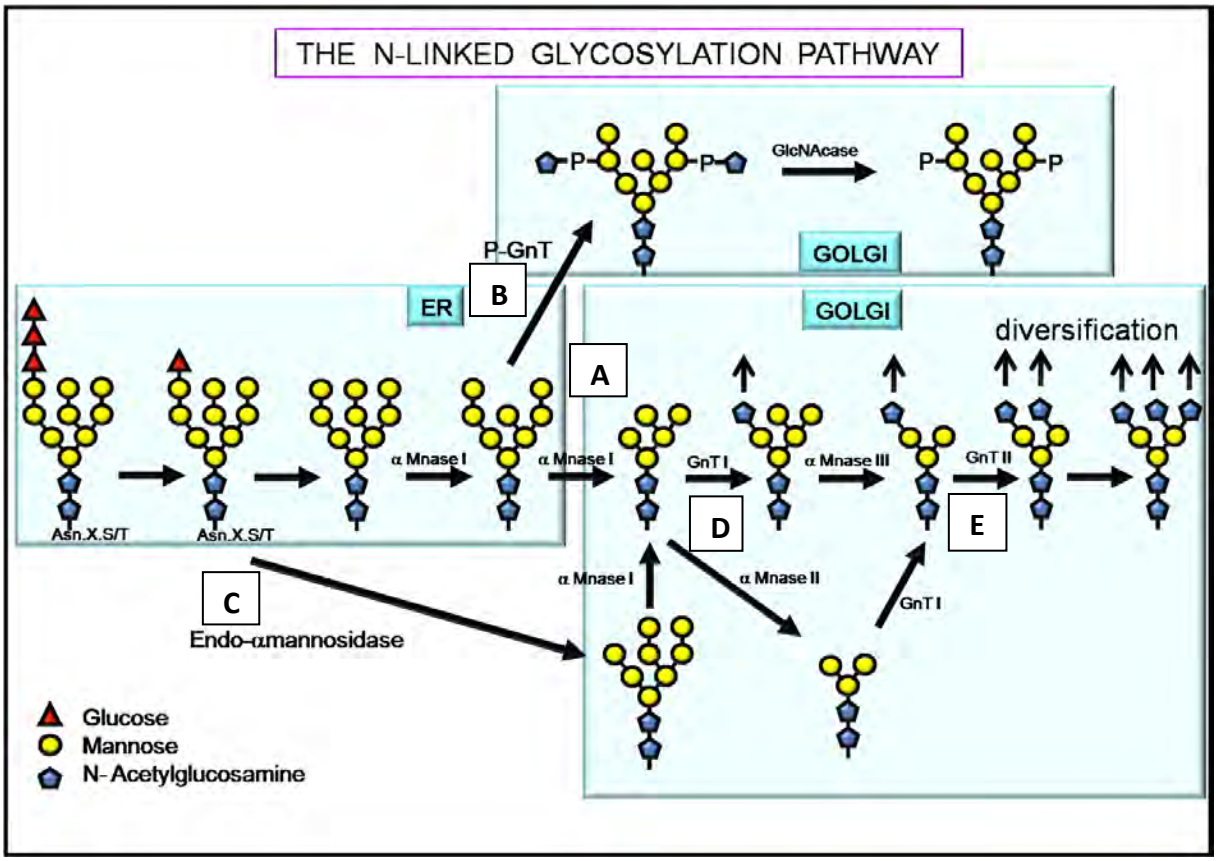

Figure 1.13 The various branching of asparagine-linked glycosylation pathway.

During glycan processing in the ER, deglucosylation precedes trimming of mannose residues. At this stage, the mannose residues are trimmed in the ER prior to diversification [A], or phosphorylated for lysosomal targeting [B]. Alternatively, monoglucosylated structures can be recruited into the endo-mannosidase pathway where the final deglucosylation and subsequent demannosylation occurs within the Golgi apparatus [C]. During their transit in the Golgi, addition of a third N-Acetylglucosamine residue by GnT I produces the hybrid glycan species [D]. Further mannose trimming and addition of the forth N-Acetylglucosamine residue marks the beginning of complex glycan formation [E] and diversification of the glycan structure. (continued…)

α Mnase I – α mannosidase I; α Mnase II - α mannosidase II; α Mnase III - α mannosidase III; GnT I - N-Acetylglucosamine transferase I; P-GnT – Phospho N-Acetylglucosamine transferase; GlcNAc ase – N-Acetylglucosaminidase

Figure modified from: (Stanley et al., 2009)

1.5 Glycosylation and Cancer

Interest in glycobiology accelerated when antibodies raised against tumour cell surface antigens were found to specifically recognise sugar epitopes on both tumour cells and developing embryos (Feizi, 1985). Abnormal expression of fetal glycans in adults is detected during metastatic cancer progression. Altered glycosylation of functionally important membrane proteins such as integrins, cadherins and growth factor receptors change the signaling capacity of these receptors and profoundly affect the proliferation, differentiation and migration potential of the cell (Mendelsohn et al., 2007; Lau et al., 2007; Pinho et al., 2009a; Pinho et al., 2009b). Glycosylation has also been shown to play an important role in homing of lymphocytes and metastatic cells (Mitoma et al., 2007; Bos et al., 2009). Several oligosaccharide structures found on both proteins and lipids have been identified and associated with human cancer. Cancer associated glycans commonly involve terminal residues such as sialic acid, fucose and galactose probably due to the fact that they are readily accessible to their environment.

1.5.1 Sialylation

The role of sialylation in cancer has been reported in two different types of linkages of this sugar. Firstly, the expression of the linear poly sialic acid polymer have been shown to play an important role in controlling the strength of cell-cell and cell-matrix interaction by modulating the number of α2,8-linked sialic acid added (Figure 1.14[A]). These structures which are usually expressed in fetal tissues are re-expressed during tumour progression (Livingston et al., 1988; Moolenaar et al., 1990). Another type of sialic acid addition, α 2,6-linkage to galactose was commonly observed in histological sections of colon cancer specimens (Figure 1.14[B]) (Dall'Olio et al., 1989). Increased expression of α 2,6-linked sialic acid has also been shown to home metastatic human breast cancer cells, MDA-MB-231 to the brain in mouse models (Bos et al., 2009). Furthermore, rampant liver colonizing variants of murine colon cancer cell lines have been shown to express fourfold higher levels of α2,6 sialyl transferase mRNA compared to the low liver colonizing population (Piscatelli et al., 1995).

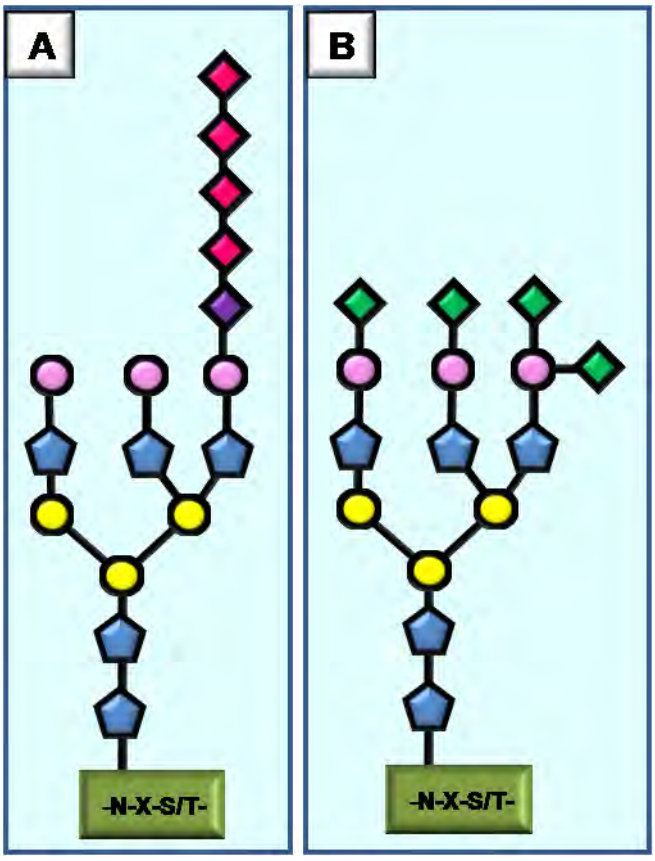

Figure 1.14 Tumour associated sialyl modification. [A] Polysialylation of cell adhesion molecules (N-CAM) during cancer progression consist of terminal α2-8 linked sialic acid repeats (squares shaded red) linked to galactose residue (pink circle) via α2-3 linked sialic acid (purple square). [B] Another cancer associated sialyl modification involves addition of terminal α2-6 linked sialic acid (green squares). An increase in this type of glycosylation during cancer progression changes how tumour cells interact with their environment.

1.5.2 Fucosylation

Blood group antigens (H, h, ABO and Lewis) are glycan structures found on glycoproteins and glycolipids that carry α1,2, α1,3 and α1,4-linked fucose (Figure 1.15).

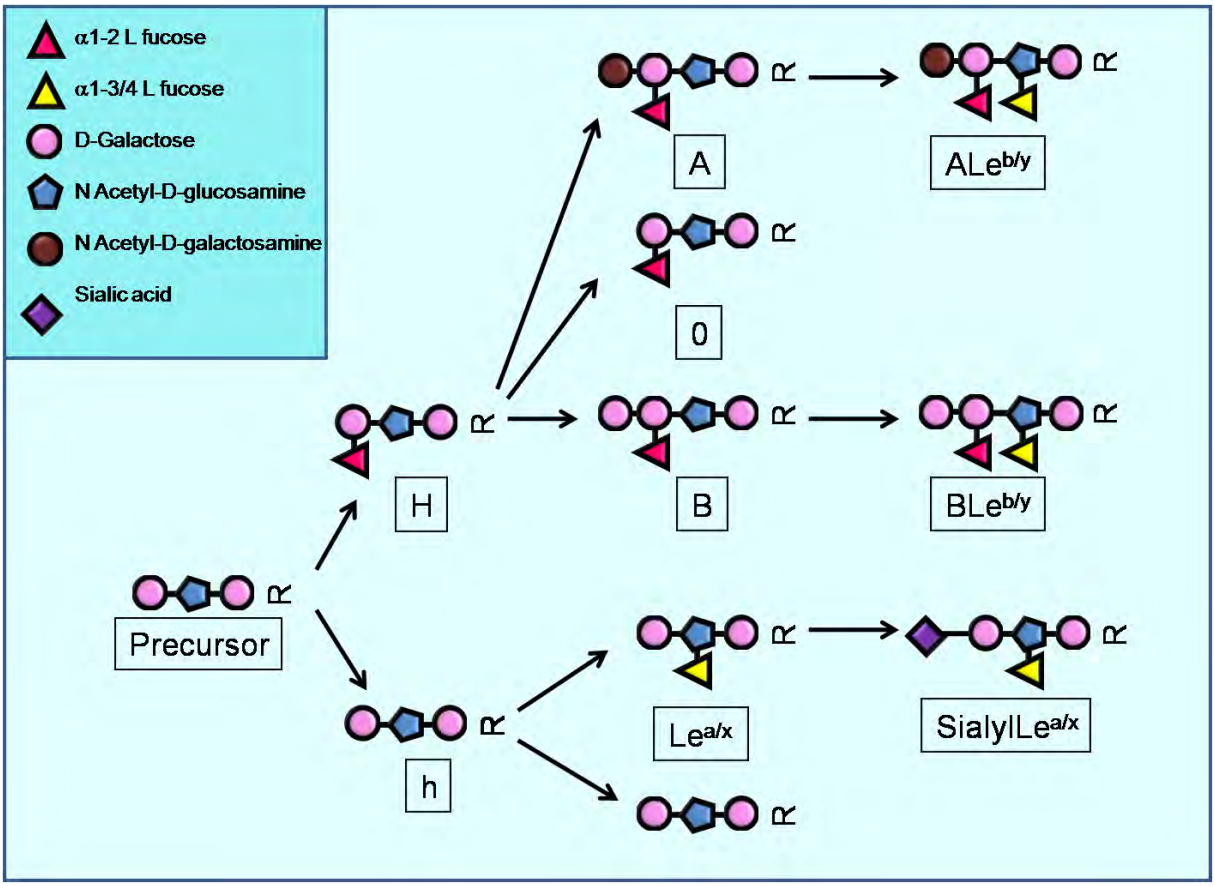

Figure 1.15 Diagram showing the glycan structure of various blood group antigens. Stepwise modification of these terminal structures on N-glycan, O-glycan or glycolipid (R) enriches the pool of oligosaccharide repertoire. Alteration in their expression profile due to pathological stress changes their binding property to various selectins.

Under normal physiological conditions, these sugars have a spatially and temporally restricted expression. Abnormal or increased expression of these structures has been reported in pancreatic cancer (Yuan et al., 1985) and hepatocellular carcinoma (Okada et al., 1987; Zhang et al., 2002). These structures can be further modified with the addition of terminal sialic acid, forming the corresponding sialyl Lewis antigens. The functional implication of Lewis antigen

over-expression in tumour cells was realised when it was found that sialyl Lewis X acts as a ligand for E-Selectin, a lectin like cell adhesion molecule expressed on activated endothelial cells. These molecules mediate leukocyte extravasation from the circulatory system by arresting them on endothelial cell surface prior to anchoring by a stronger receptor ligand interaction (Phillips et al., 1990). Accordingly, the expression of Lewis antigens on tumour cell surface may play a key role during extravasation.

In order to answer the question whether glycosylation is one of the factor that determine the secondary metastasis location, B16 mice were subcutaneously injected with liver and lung metastasizing variants of lewis lung carcinoma. Subsequent histochemical analysis of: 9 primary murine tumors recovered from the injection site, 9 liver metastases and 13 lung metastases showed high levels of UEA I lectin binding property for the lung colonizing variant compared to the primary site and liver colonies (Kahn et al., 1988). UEA I lectin which selectively binds to α1,2-linked fucose, point to a possible role played by α1,2-fucose in homing the tumor cells to lung as a secondary site. A definitive role played by fucosylation in homing was later shown in murine cord blood hematopoietic stem and progenitor cells (CB-HSPCs). Poor homing of murine CB-HSPC to the bone marrow of immune deficient mice correlated with the expression levels of sialyl Lewis X. Pretreating the HSPC enriched cord blood cells with α1-3 fucosyltransferase in the presence of high energy fucose

donor (UDP-fucose) increased the cell surface level of sLe^x and consequently, increased cell rolling on P an E-Selectin and the engraftment of these cells to the bone marrow (Xia et al., 2004).

Fucosylation and sialylation have also been shown to change how cancer cells interact with their environment. Exogenous expression of α(1-2)-Fucosyltransferase-1 in hepatocarcinoma cells HepG2, inhibited sialyl-Lewis X expression and switched their preferred affinity from E-Selectin to P-Selectin (Mathieu et al., 2004). In another study, enzymatic removal of either cell surface sialyl or fucosyl residues in H7721 cells altered their preference to extracellular matrix components, fibronectin and laminin (Zhang et al., 2002).

1.5.3 β1-6 Poly-N-Acetyllactosamine and β1-4 bisecting N-Acetylglucosamine

An increase in β1-6 branching of poly-N-Acetyllactosamine from increased GNT-V activity is considered one of the most significant cancer associated glycan structures which displays typical 'oncogenic' characteristic (Dennis et al., 1987; Laferte and Dennis, 1989). The increase in the resulting chain is controlled at the transcriptional level of GNT-V by viral activation or carcinogenic transformation.

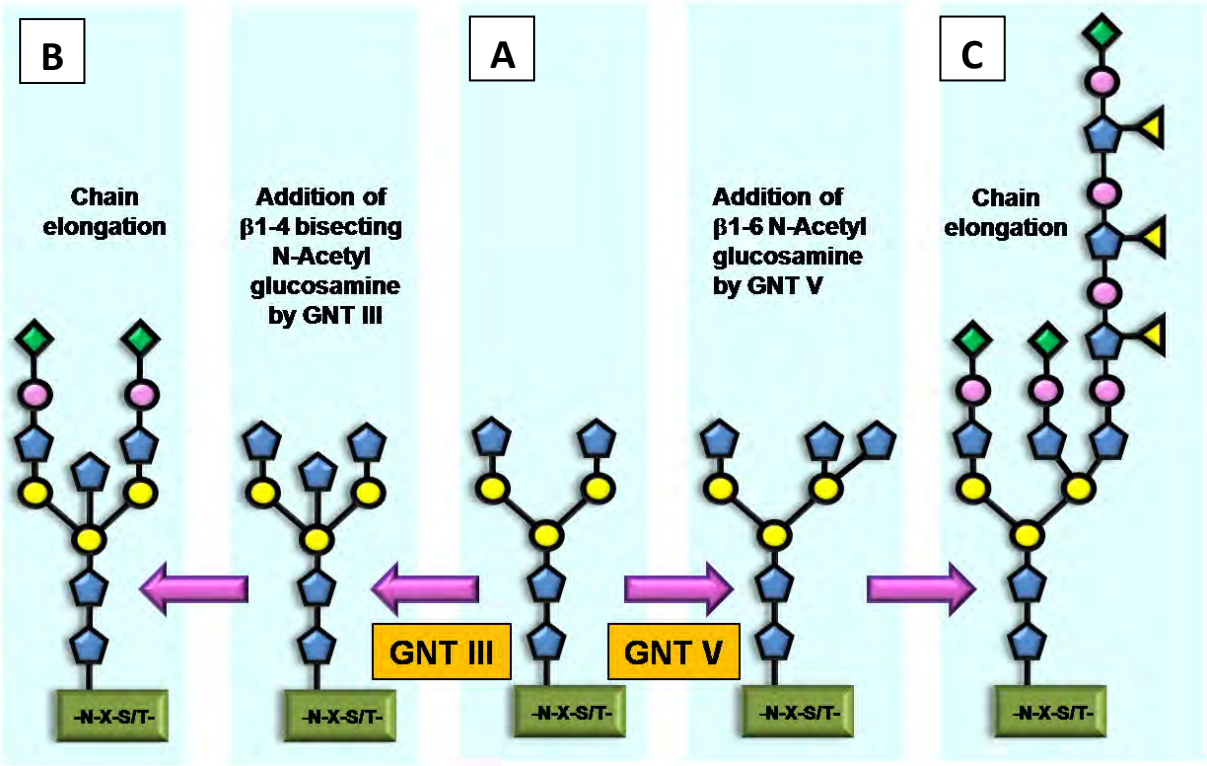

Figure 1.16 Diagram illustrating complex glycan biosynthesis by GNT III and GNT V. The precursor for complex glycan [A] is modified by various glycosyltransferase in the Golgi. GNT III mediated addition of β1-4 linked N-acetylglucosamine generates a bisecting structure and terminates glycan chain elongation upon addition of terminal galactose (circle shaded pink) and sialic acid (green square)[B]. GNT V on the other hand introduces β1-6 linked N-Acetylglucosamine which elongates through the formation of poly N-Acetyllactosamine chain [C]. This broken wing formation further serves as a backbone for fucosylation and sialylation, giving it a definitive metastasis promoting characteristic.

Even though it is not clearly understood how this glycan structure can increase the metastatic potential of tumour cells, a few theories have been proposed. The β1-6 branching involves elongation of this specific GlcNAc branch, resulting in a different type of structure termed as a 'broken wing' conformation (Figure 1.16). Such structures are speculated to increase direct association with neighbouring

proteins and thereby enhance the cell's metastatic potential. Presence of this glycan on cell surface receptors may affect the physical characteristics and functional behaviour of these molecules. Another possibility is that the long antenna-like chain provides a backbone for the addition of multiple sialyl and fucosyl residues providing a platform for polyfucosylation, or sialyl Lewis production and selectin interaction (Varki et al., 2009). Poly-N-acetyllactosamines are also recognised by galectins on the cell surface. Galectin mediated lattice formation can alter the turnover rate of cell surface receptors and growth factors, duly affecting cell proliferation and differentiation (Partridge et al., 2004; Lajoie et al., 2009).

Enhanced expression of another GlcNAc transferase known as GNT-III has also been implicated in increased metastatic potential. GNT-III catalyzes the addition of β1-4 linked bisecting GlcNAc branch (Figure 1.16). However, this type of branching did not always represent an unequivocal oncogenic characteristic as observed in β1-6 branching. While overexpression of GNT-III is observed in rat hepatomas (Miyoshi et al., 1993), mouse hepatomas did not show a similar phenotype. However, GNT-III deficient mice showed retarded liver tumor progression (Stanley, 2002). Exogenous expression of GNT-III in highly metastatic mouse melanoma B16-hm cells on the other hand, suppressed metastasis (Yoshimura et al., 1995). Further investigation of this initial observation showed that increased addition of bisecting sugar on E-cadherin molecules in these cells delayed turnover

of this protein compared to wild type E-cadherin. Accumulation of E-cadherin at cell-cell border resulted in cell-cell aggregation and metastasis suppression (Yoshimura et al., 1996). In conclusion, GNT-III mediated glycosylation can either enhance or suppress tumorigenesis depending on secondary factors.

Aberrant glycosylation remains one of the key events in initiation of invasion and metastasis. Much progress has been made since the 1970s when the role played by glycosylation in cancer was first realised. However, the complexity of the subject makes it less attractive compared to popular subjects such as cell surface receptor and oncogenes even though glycosylation has been shown to have direct and indirect effect on the functional aspect these molecules (Hakomori, 2002). A better understanding of cancer glycobiology will not only provide a clearer understanding of the pathology of this disease, but could also be utilised as a tool for diagnosis, prognosis and treatment.

1.6 Objectives of thesis

In earlier investigations, a novel role played by CD151 in influencing the glycosylation of α3β1 integrin was observed. Based on these data, using MDA-231 cells as a model system, the current study was designed to investigate (a) when, where and how CD151 regulates α3β1 integrin's glycosylation, (b) the type of glycomodification induced by CD151 and (c) the consequences of the glycomodification, using various molecular, biochemical and cell culture techniques. For this purpose:

1) Cell lines expressing various mutations of CD151 will be generated. The influence of CD151 on another of its partners, α6β1/β4 integrin will also be studied. In addition, the contribution of other tetraspanins on glycosylation of α3β1 and their influence on α6β1/β4 integrins will be analysed. The functional implications of CD151 mediated changes to α3- and α6- integrins will be compared by performing Boyden chamber migration, adhesion, transendothelial migration and endothelial rolling assays.

2) The extent to which tetraspanins CD9, CD151, CD63 and CD81 influence glycosylation of α3β1 integrin and cell surface glycotope presentation will be investigated using biochemical and lectin binding/flow cytometry assays on tetraspanin depleted cell lines.

3) The mode of glycomodification and the influence it may have on the tetraspanin's function will be determined by Western blotting after enzymatic digestion of glycans on these molecules and glycosylation inhibitor treatments.

2. MATERIALS AND METHODS

2.1 Cell culture

The cell lines used in this study were maintained in DMEM media (Invitrogen) containing 10% final concentration of heat inactivated FBS (Invitrogen) and 50U/ml final concentration of Penicillin and Streptomycin (Invitrogen). The various cell lines used throughout this study are listed in Table 2.1 below:

Table 2.1 Summary of cell lines used in this study

Cell line	Origin	Description	Source	Reference
MDA-MB-231 (MDA-231)	Human breast adenocarcinoma	Invasive, pleural effusion	CRUK	(Cailleau et al., 1978)
MCF7	Human breast adenocarcinoma	Non-invasive, pleural effusion	CRUK	(Soule et al., 1973)
BT474	Human breast ductal carcinoma	Invasive, solid ductal carcinoma	CRUK	(Lasfargues et al., 1978)
HeLa	Human cervical adenocarcinoma	Malignant solid tumour	CRUK	(Scherer et al., 1953)
U87MG	Human glioblastoma	Astrocytoma	CRUK	(Ponten and Macintyre, 1968)

2.1.1 Maintenance of cell lines

Cells were grown in 10cm gamma radiated tissue culture petri dish (Corning) in 10ml complete DMEM medium (except for BT474 cell line which was maintained in RPMI 1640 (Invitrogen) medium containing 10% FBS) at 37^0C in a humidified chamber permeated with 5% CO_2. Cells were maintained by removing the media and washing them twice in 5ml sterile phosphate buffer before detaching them in 0.25% Trypsin(1X) (Invitrogen). Detached cells were further resuspended in an appropriate volume of DMEM medium containing 10% Foetal Calf Serum (10% DMEM) and transferred to 15ml tubes (Corning). Cells were centrifuged for 3 min at 800rpm in Beckmann tabletop centrifuge. Upon removal of media, 20% of the resuspended cell pellet was plated onto a fresh petri dish and passaged every 2-3 days or when they reached 70-80% confluency.

2.1.2 Cryo storage and recovery of cell lines

Cells (~$3X10^6$) were detached and washed in 10ml of 10% DMEM once by centrifugation. The cell pellet was resuspended in 1ml cryo-medium (10% DMSO in 10% DMEM) and frozen in a CryoTube™(Nunc) at -80^0C for 24 hours before transferring to liquid nitrogen for long term storage.

Cells were recovered by thawing in a waterbath at 37^0C. Cells were transferred to 15ml tube containing 10ml prewarmed media and washed by pelleting the cells at 800rpm for 3 min. Cell pellet was resuspended in 10ml fresh media and transferred to a petri dish. Freshly recovered cells were incubated for at least 48 hours before further manipulation.

2.1.3 Mycoplasma testing

Cell lines were regularly tested to ensure they were mycoplasma free using Mycoalert® Mycoplasma Detection Kit (Lonza) as per manufacturer's recommendation. Reaction catalysed by the mycoplasma enzyme in the presence of the substrate provided with the kit leads to ADP —> ATP conversion. The level of converted ATP is then detected by bioluminescent reaction which converts Luciferin in the presence of Luciferase.

2.2 Generation of various plasmid constructs

2.2.1 Generation of short hairpin constructs for tetraspanin knock-down

pSUPERIORpuro (OligoEngine) based plasmids expressing short hairpin RNA (shRNA) targeting tetraspanins CD151 and CD81 were generated by Dr Fedor

Berditchevski based on published sequences (Winterwood et al., 2006; Mazzocca et al., 2005). The final sequence for CD63 shRNA construct was selected from a panel of CD63 siRNA by Dr Berditchevski. The pSUPERIORpuro constructs were generated by inserting double stranded short hairpin oligonucleotide containing BglII and HindIII restricted overhangs (SigmaGenosys) into the pSUPERIORpuro vector linearised with the same restriction enzymes. The shRNA cassette generated for tetraspanin CD151 is as follows:

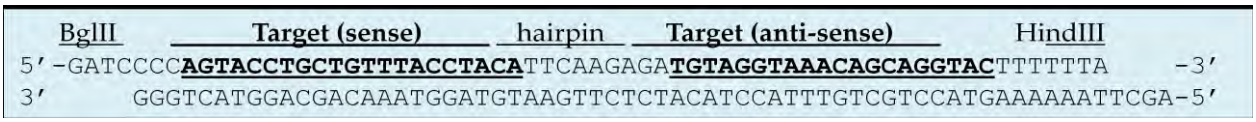

The target oligonucleotide sequences for all the tetraspanin short hairpin constructs are listed in Table 2.2

Table 2.2 Target shRNA sequence for various tetraspanins

Target protein	Target sequence
CD151	5′-AGTACCTGCTGTTTACCTACA
CD81	5′-ATCTGGAGCTGGGAGACAA
CD63	5′-GGTTTTTCAATTAAACGGA
CD9	5′-ACCTTCACCGTGAAGTCCT

pSuper-shCD9 construct was a kind gift from Prof E. Rubinstein (Inserm 1004, Villejuif, France).

2.2.2 – Generation of various sh resistant CD151 mutant constructs

MDA-231 cells lines expressing various permutation of CD151 were generated by reintroducing the pZeoSV based CD151 mutant constructs into MDA-231 CD151 (-) cells. A point mutation was introduced to these constructs to confer resistance to CD151 shRNA by standard PCR protocol using QuikChange® Multi Site-Directed Mutagenesis as described in section 2.2.5. The silent sh resistant point mutation introduced is highlighted in red below:

	shCD151 resistant primer sequence
Forward	**5′ CAACAGCCGGCACCGTTGCCCTCAAGTACCTGCTC**
Reverse	**5′ GAGCAGGTACTTGAGGGCAACGGTGCCGGCTGTTG**

Previously published CD151 mutant construct used in this experiment are CD151 palmitoylation mutant (Berditchevski et al., 2002), CD151 cytoplasmic C terminal substitution (Sawada et al., 2003), CD151SW6 mutant (Berditchevski et al., 2001). Two new constructs, CD151 glycosylation mutant (by Dr Berditchevski) and CD151 QRD (194 →196) INF substitution (jointly constructed with Dr Berditchevski) were also generated for this study. The glycosylation mutant of CD151 was generated by substituting the asparagine residue at position 159 with glutamine while the QRD mutant of CD151 was generated by swapping glutamine-arginine-aspartic acid (QRD) triamino sequence with isoleucine-asparagine-phenylalanine (INF) residues as described by Kazarov et al. (2002) using standard PCR protocol.

The CD151 construct carrying a CD63 N-terminal region substitution (dN) was a kind gift from Dr L.Ashman. A schematic representation of all the CD151 variants used in this study is presented in Figure 2.1

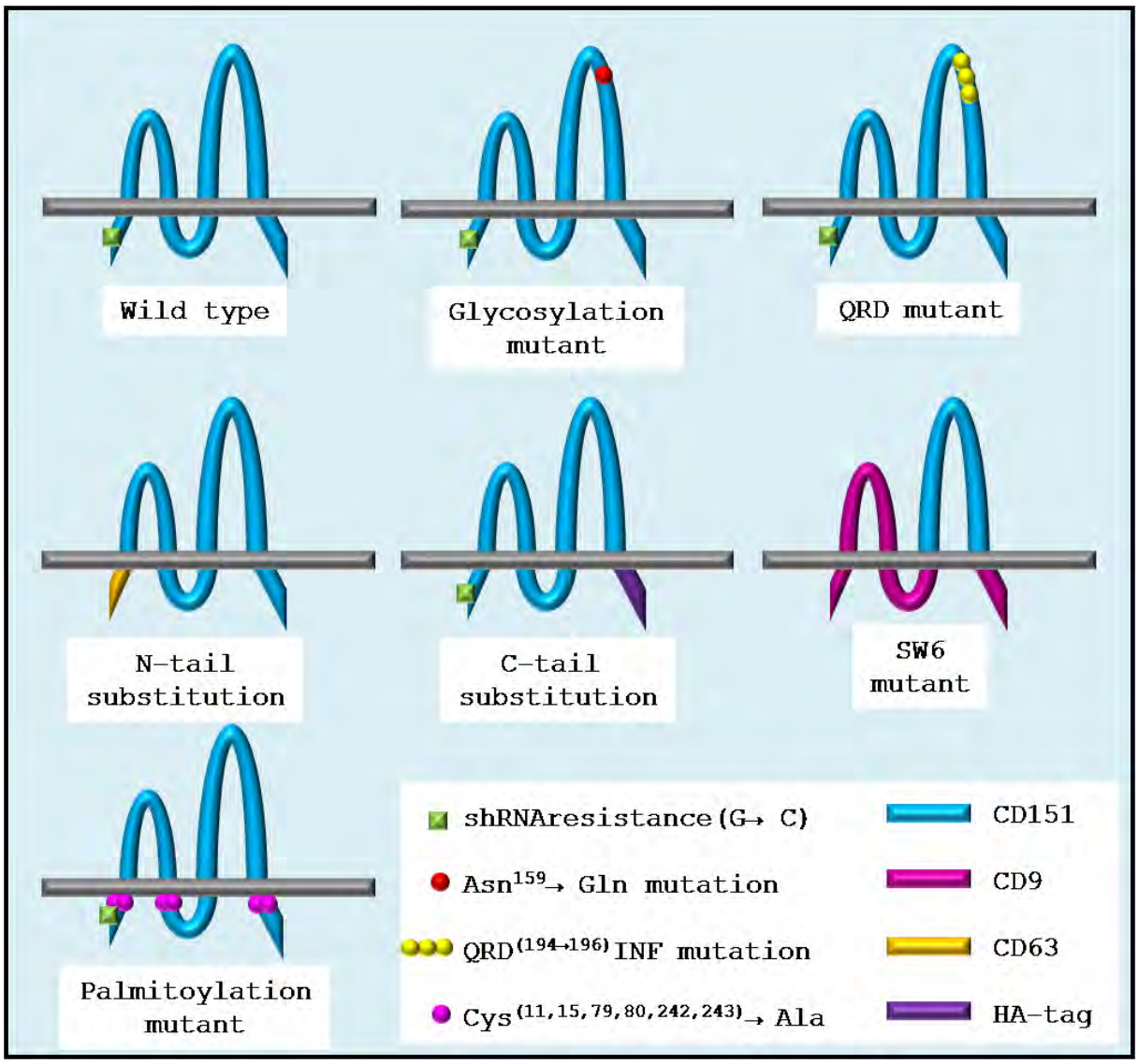

Figure 2.1 Cartoon representing the shCD151 resistant wild type and CD151 mutants generated for reintroduction into MDA-231 CD151(-) cells.

A point mutation was introduced to the N-terminal region where required (CTG → CTC). Glycosylation mutant CD151 was generated by substituting (AAC → CAG) while in QRD mutant, the following mutation was introduced (CAG-CGA-GAC →

ATC-AAC-TTC). In N- and C-tail mutants, N-tail of CD151 was swapped with the same region from CD63 while C-tail was substituted with a HA-tag. SW6 mutant comprised of CD151 LEL on a CD9 backbone. In the CD151 palmitoylation mutant construct, all six membrane proximal cysteine residues were swapped with alanine.

2.2.3 Generation pLVTHMshα3 integrin construct

The shα3 integrin construct was generated to target the following sequence: **5′ GCTACATGATTCAGCGCAA**. The α3 integrin targeting sh oligonucleotide was first ligated into the BglII/HindIII cleaved pSuperiorPuro plasmid as previously described. The cloned product was confirmed by resolving EcoRI and ClaI digested plasmid on 2% agarose gel as well as sequencing. The successfully cloned product was then cleaved with EcoRI and ClaI and religated into the pLVTHM vector linearised with the same restriction enzymes. The final cloned product was transformed into competent bacterial cells and following plasmid purification, the presence of the cloned insert was confirmed by agarose gel electrophoresis and sequencing.

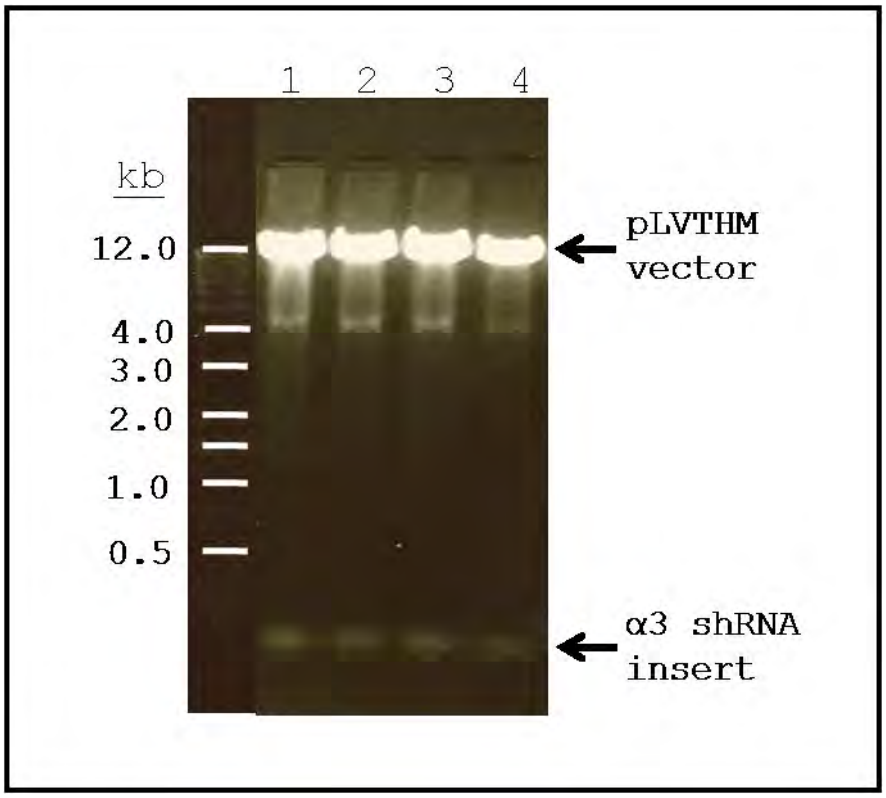

Figure 2.2 DNA digest profile of pLVTHM based α3 shRNA

Successful cloning of α3 shRNA cassette in pLVTHM plasmid was confirmed on a 2% agarose gel after restriction digest of the plasmid with EcoRI and ClaI. All four bacterial clones tested showed successful cloning.

2.2.4 Ligation of various shRNA constructs

All shRNA oligonucleotides inserts were purchased (SIGMAGenosys). To prepare the inserts for cloning (annealing of the two strands), an Eppendorf tube containing 25 µl of 4ng/µl DNA resuspended in TE buffer was incubated on a heat block (100^0C)

for 10 minutes and left to cool down to room temperature. A ligation mix was then prepared as follows and incubated overnight at 16^0C:

pSuperiorPuro	50ng
insert	10ng
T4 DNA ligase (40,000 Units/ml)	0.5 µl
10X Ligase buffer	1.0 µl
H_2O	to 10 µl

2.2.5 Site directed mutagenesis

The introduction of point mutation to plasmid DNA was performed using QuikChange® Multi Site-Directed Mutagenesis kit (Stratagene) as per manufacturer's recommendation.

2.2.6 Bacterial transformation

An aliquot (12.5µl) of *E. coli* DH5α competent cells (New England Biolabs) was mixed with 2µl of chilled ligation product and incubated for a 30 min on ice.

Transformation of bacterial cells was performed at 42^0C for 30 seconds in a heated waterbath and chilled immediately on ice for 2 min. The bacterial cells were rescued with 200µl LB medium and shaken in an incubator set at 37^0C for 30 min at 120rpm. Transformed cells were selected on LB agar plate supplemented with 100µg/ml ampicillin.

2.2.7 Small and large scale plasmid preparation

Individual clones were transferred to Eppendorf tubes containing 1ml LB medium and 100 µg/ml ampicillin. The culture was incubated in a shaking incubator for 18-24 hours at 37^0C, 120rpm. Cells were harvested by centrifuging at 13,000 rpm for 10 seconds and the supernatant was discarded. Plasmid purification was performed with the Qiagen Plasmid Miniprep Kit® as per manufacturer's instructions. Bacterial clones containing the desired plasmid constructs (verified by gel electrophoresis and sequencing) were grown in 250ml LB broth containing ampicillin and plasmid purification was performed with Qiagen Plasmid Maxiprep Kit® according to manufacturer's protocol.

2.2.8 DNA sequencing

Various plasmid constructs generated were confirmed by sequencing. Briefly, 100-200ng plasmid DNA, 3.2 pmol of an appropriate primer and dH_2O was premixed to a final volume 10µl in an Eppendorf tube and sent for sequencing analysis at the Functional Genomics Unit, University of Birmingham. The plasmids generated and their corresponding sequencing primers are is listed below:

Vector	Sequencing primer
pSuperiorPuro based shCD151, shCD9, shCD63 and sh CD81	Forward: T7 5′ TAATACGACTCACTATAGGG
pLVTHM based shα3	Forward: 5′ GTGAAAGTCGGGGCTGCAGGAATTC Reverse: 5′ CGATTTAGGTGACACTATAGAATACACGG
pZeoSV based CD151 mutants	Forward: T7 5′ TAATACGACTCACTATAGGG or PZeoF 5′ TTCCAGAAGTAGTGAGGAGG Reverse: SP6 5′ ATTTAGGTGACACTATAG

2.2.9 Agarose gel electrophoresis

The DNA restriction digest was mixed with 6 X gel loading buffer (0.25% w/v xylenecyanol, 0.25% w/v bromophenol blue, 30% v/v glycerol) and subjected to electrophoresis through 2% w/v agarose gel containing 0.5 μg/ml ethidium bromide in 0.5 X TBE buffer [made up of 45mM Tris Base, 45mM Boric acid and 2mM EDTA (pH 8.0)]. After electrophoresis, the resolved products were visualised and recorded in a UV gel documentation system (InGenius® Syngene).

2.3 Establishing various cell lines

2.3.1 Establishing tetraspanin knock-down cell line

The MDA-231 CD151(-) and MCF7 CD151(-) cells were generated by Dr Vera Novitskaya while MDA-231 CD63(-) cells was generated by Dr Berditchevski. Other tetraspanin knock down cell lines generated for this study includes HeLa CD151(-), MDA-231 CD9(-) and MDA-231 CD81(-). Transfection of MDA-231 cells was performed with GeneJammer (Stratagene) while MCF7 and HeLa cells were transfected using Fugene (Roche). The transfection mix was prepared as follows: 18μl of transfection reagent, Fugene or GeneJammer was added to 582μl of serum- and antibiotic-free DMEM medium in an Eppendorf tube, mixed and incubated for 10 min at room temperature (RT). 6μg DNA of plasmid encoding the shRNA was then

added, mixed thoroughly and incubated at RT for a further 30-45 min. The transfection mix was added dropwise onto the adherent cells, swirled gently to mix and incubated overnight as previously described in section 2.1.1. After 24 hours, the transfection medium was removed and 10ml fresh DMEM medium containing 10% FBS, Pen/Strep and 1μg/ml puromycin (Sigma) was added. After another 24 hour incubation, the selection medium was replaced with fresh 10% DMEM medium containing 0.5μg/ml puromycin. The selection medium was changed every 2-3 days until resistant colonies started to grow. The colonies were detached and transferred to a fresh plate until it reached 80-90% confluency. The mixed population comprising of depleted, moderately depleted and undepleted tetraspanin was surface labelled with appropriate antibodies and sorted to select for tetraspanin-depleted cells (-ve population) and undepleted cells (+ve population). The level of knock-down achieved for various tetraspanins after cell sorting was determined by flow cytometry and Western blotting.

2.3.2 Establishing of lentivirus based shα3 integrin knock-down cell line

Lentivirus encoding shRNA which target α3 integrin subunit was produced as follows: 293T cells were grown for 18-24hrs to ~60% confluency on a 10 cm petridish. Transfection reagent was prepared by mixing 18μl of Fugene to 582μl of serum- and

antibiotic-free DMEM in an Eppendorf tube and incubated at RT for 10min. In a separate tube, a plasmid mix was prepared as listed in Table 2.2 below:

Table 2.3- Ratio of plasmid mix for lentivirus production

	Plasmid	µg/10cm petridish
shRNA vector	pLVTHM shα3 integrin	2.4
Packaging construct	pSPAX (TronoLab)	2.3
Envelope construct	pMD2G-VSVG (TronoLab)	1.3

The plasmid combination was then added to the transfection reagent, mixed well and incubated for a further 30-45 min at RT before adding dropwise to the 293T cells. The transfection mix was evenly distributed by gently swirling the petri dish and incubated for 5-18 hours. The transfection medium was then exchanged with fresh medium and incubated for 72 hours. The lentivirus containing supernatant was harvested and centrifuged at 1000 rpm for 5 min and filtered through a sterile 0.45µm filter (Millipore) to remove cell debris. The viral supernatant was either used immediately for infection or 1ml aliquots were stored at -80^{0}C.

MDA-231 cells were prepared for infection by growing them for 24 hours in a 10 cm petridish till they reached ~30-40% confluency. The medium was removed and 10ml filtered viral supernatant was added and incubated for 24 hours. The

supernatant was then removed and 10ml fresh medium was added and incubated with cells for further 48 hours. Cells were detached and a small aliquot (~5%) of the cells was analysed by flow cytometry to detect for the presence of the GFP positive population. The presence of GFP positive cells signified successful viral infection. The mixed population containing GFP(+) and GFP(-) cells was surfaced labelled for α3 integrin (anti-α3 A3-IVA5 and PE conjugated secondary antibody) and sorted for GFP-positive / PE-negative population. GFP-positive control cells (i.e. cells expressing α3β1 integrin) were obtained by infecting MDA-231 cells with lentivirus generated from pLVTHM vector devoid of shRNA insert.

2.3.3 Establishing various CD151 wild type and mutant cell lines

MDA-231 CD151 (-)ve cell lines reconstituted with various CD151 mutants were generated by transfecting appropriate plasmids using GeneJammer transfection reagent as described in section 2.3.1. Selection of transfected cells was performed in the presence of 300μg/ml Zeocin and resistant colonies were maintained in 10% DMEM Pen/Strep supplemented with 100μg/ml Zeocin until they reach confluency in a 10 cm petri dish. The cells were then sorted to obtain a population expressing the mutant CD151 at a level comparable to that of the wild type CD151 by presetting the sorting gate. Selected population was grown in 10% DMEM medium containing 100μg/ml Zeocin and 0.5μg/ml puromycin. The level of reconstituted CD151

expressed was confirmed by Western blotting and flow cytometry analysis. Cryo stocks of the cell lines were made before proceeding with various experiments.

2.3.4 Flow cytometry

Flow cytometry analysis was performed to quantitatively analyse cell surface epitope presentation. Prior to flow cytometry analysis, cells were passaged and grown in a 10 cm tissue culture dish for 18-24 hours in a tissue culture incubator. 2-3x10^6cells were washed twice in sterile Dulbecco buffer and detaching with 2mls of Cell dissociation buffer® (Invitrogen) at 37^0C for 10 - 15min. The detaching cell clumps were loosened to form single cell suspension by pipetteing and transferred to a sterile 15ml centrifuge tube containing 10mls of cold 10% DMEM medium. The following steps were performed on ice and in prechilled centrifuge. Cells were washed by centrifuging them at 800rpm for 5 min at 4^0C in ice-cold 10% DMEM medium before resuspending in 1ml of 10% DMEM medium. Cells were counted and 2x10^4 aliquots were taken for each antibody tested. The primary antibodies used for flow cytometry analysis are listed in Table 2.4.

Antibody binding was performed in 96 well round bottom plates (Iwaki) placed on ice. 100µl of neat hybridoma supernatant or 100µl of 1µg/ml of purified antibody was aliquoted into labelled wells. Cells were then added to appropriate

wells, mixed and incubated for 1hr on ice. Cells were then washed twice in 10% DMEM by centrifuging at 800 rpm for 5 minutes and incubated in secondary antibody conjugated with fluoresceinisothiocyanate (FITC) or phycoerytherin (PE) (Dako) on ice for 30 min in the dark (100µl of 1:300 antibody/DMEM dilution). Cells were washed twice in 10% DMEM, resuspended 100µl Dulbecco buffer and transferred to FACS tubes containing 400µl of 2% paraformaldehyde (PFA). Mean fluorescence intensity was measured on EPICS XL Flow cytometry (Coulter) using System II software (Coulter).

2.3.5 Cell sorting

Cells for sorting were prepared in a similar way as cell prepared for flow cytometry with a few modifications. Every step of the experiment was carried out in the tissue culture hood under sterile conditions. Primary and secondary antibodies used were azide free and filtered with 0.22µm filter prior to use. In the final step, instead of fixing in PFA, cells were resuspended in prechilled 10% DMEM medium. Cells were then gated and sorted by Mr David Lloyd from the Cancer Studies, University of Birmingham. The primary antibodies used in this study is listed in Table 2.4

Table 2.4 List of primary antibodies used for flow cytometry and cell sorting

Epitope	Antibody	Source
CD151	5C11 11B1G4	Hybridoma (Berditchevski et al., 1997) Ascites (Fitter et al., 1995)
CD9	C9BB BU16	Hybridoma (Tachibana et al., 1997) Purified mAb (The Binding Site, Birmingham)
CD81	M38	Hybridoma (Fukudome et al., 1992)
CD82	M104	Hybridoma (Fukudome et al., 1992)
CD63	6H1	Hybridoma (Berditchevski et al., 1995)
α3 integrin	A3-IVA5	Hybridoma (Weitzman et al., 1993)
α6 integrin	A6ELE	Hybridoma (Lee et al., 1995)
β1 integrin	TS2/16	Hybridoma (Hemler et al., 1984)

2.4 Biochemical analysis

2.4.1 Cell lysis

Cell lysis was performed in either 1% Triton X-100, 1% Brij 96 or 1% Brij 98 according to the lysis stringency required. Brij 96 and Brij98 were melted in a water bath at 50^0C prior to use. The 1% (v/v) detergent solution was prepared in PBS buffer by dissolving 1 PBS tablet (Oxoid) in 100ml dH_2O supplemented with 1mM $MgCl_2$ and 0.5mM $CaCl_2$ and adjusted to pH 7.4. Protease inhibitors (2mM

phenylmethylsulfonyl fluoride, 20µg/ml aprotinin and 20µg/ml leupeptine) and phosphatase inhibitors (2mM NaF, 0.5mM Na_3VO_4, 5mM $Na_4P_2O_7$) were added to the lysis buffer immediately before use. Cells were lysed overnight on a rotating wheel in the cold room and the lysates were harvested by centrifugation in a chilled tabletop centrifuge at 13,000 rpm for 10 min. The clarified cell lysates were transferred to a fresh Eppendorf tube and their concentration was normalised.

2.4.2 Normalisation of protein concentration

DC protein assay kit (Biorad) was used to normalise protein concentration. Briefly, reagent S was diluted in reagent A at 1:50 dilution. 25µl of the mix was aliquoted into a required number of well in a microplate. 5µl of cell lysate was added to each well containing the reagent mix followed by 200µl of reagent C. After 15 min incubation at room temperature, colorimetric reading was performed at 630nm absorbance. Appropriate dilutions were performed for each lysate based on the read out to normalise their concentration.

2.4.3 SDS-Polyacrylamide gel electrophoresis

Cell lysates were diluted 1:3 with 4 X Laemmli buffer (0.5M Tris pH6.8, 4.4ml glycerol, 2.2ml 20% SDS, 1ml dH_2O and 0.05g bromophenol blue). If required,

protein samples were reduced by adding β-mercaptoethanol at 1:20 dilution. Protein samples were denatured by boiling at 100^{0}C for 5 min, except for the detection of CD151 with CD151 polyclonal antibody which requires 'native proteins' for detection. Proteins were resolved by SDS-PAGE using the MiniPROTEANIII system (Biorad). Table 2.5 represents the recipe for preparation of SDS-PAGE at various concentrations:

Table 2.5 Recipe for two SDS polyacrylamide gels

	5% Stacking gel	8% resolving gel	10% resolving gel	12% resolving gel
30% Acrylamide:Bis	1.6 ml	2.6 ml	3.3 ml	4 ml
1.5 M Tris-HCl pH 8.8	-	1.25 ml	1.25 ml	1.25 ml
1 M Tris-HCl pH 6.8	1.3 ml	-	-	-
20% SDS	50 µl	50 µl	50 µl	50 µl
dH2O	7.6 ml	4.7 ml	4.0 ml	3.3 ml
10% Ammonium Persulphate	50 µl	50 µl	50 µl	50 µl
TEMED	20 µl	40 µl	40 µl	40 µl

The electrophoresis was performed at 18mA per gel in 1X running buffer (14.4g glycine, 3g Tris-HCl, 1g SDS dissolved in dH2O to a final volumn of 1 L)

2.4.4 Western Blotting

Proteins resolved by SDS-PAGE were transferred to a nitrocellulose membrane (Gelman Science) in Mini Transblot® system (Biorad) overnight at 40V in Tris-Glycine buffer (3.03g Tris base, 14.4g glycine and dH_2O to a final volumn of 1 L). The membrane was rinsed and blocked with 5% non-fat dry milk in PBS-T (0.5% Tween-80 in PBS) for 1hr at room temperature. Incubation with primary antibody was performed overnight on an orbital shaker at 4^0C. The membranes were washed four times for 15 mins in PBS-T and incubated with horseradish peroxidase-conjugated secondary antibody diluted 1:20,000 in 5% milk PBS-T for 1 hr at room temperature. The membranes were washed again 4 X 15 min and proteins were detected with chemiluminescence kit (Western Lighting™, PerkinElmer Life Sciences). Signal was visualised on HyperFilm® (Amersham) in the dark room.

2.4.5 Immunoprecipitation

Immunoprecipitation (IP) or co-IP was performed to analyse protein complex formation within the cell. All steps were performed on ice. Cells were scraped from 10cm plate and lysed in 500µl of lysis buffer as described above (2.4.1). 20-50µl of total lysates was put aside to be used as positive controls. The lysates were

precleared with 20µl goat anti-mouse IgG conjugated agarose beads (Sigma) at 4^0C on a rotating wheel for 2 hrs. Beads for protein capture were prepared by incubating 20µl beads with 1ml hybridoma supernatant under the same conditions. As a negative control, beads were incubated in 500µl of wash buffer (lysis buffer without aprotinin and leupeptin). The beads were washed once in washing buffer and the buffer was removed by aspiration after centrifuging at 3,000 rpm for 1 minute. The precleared lysate was centrifuged for 30 seconds at full speed and then transferred into a fresh tube. The precleared lysate was then distributed equally to tubes containing antibody bound and unbound beads and incubated overnight on a rotator in the cold room. The beads were washed 5 times in washing buffer by centrifugation and co-IP complexes were eluted twice by incubating in 20µl 1 X Laemmli buffer for 5 minutes at room temperature. The elution was boiled, resolved by SDS-PAGE and analysed by Western blotting.

2.4.6 Preparation of 5:35:45 discontinuous sucrose density gradient

Cells from two confluent 10cm plates were scraped and washed once with ice-cold PBS. Cell lysate preparation and centrifugation was performed at 0-4^0C. Scraped cells were lysed in 950µl lysis buffer containing either 1% Triton X-100, 1% Brij96 or 1% Brij98 made up in 25mM MES [2-(N-Morpholino) ethanesulfonic acid hemisodium salt] buffer, pH 6.5 (Sigma-Aldrich) for 3 hrs in the cold room. Lysates

were homogenised by passing through a 25G needle 10 times and centrifuged for 1 min at 13,000 rpm to remove bubbles and cell debris. The supernatant was carefully transferred to a fresh Eppendorf tube and their concentration was normalised with appropriate lysis buffer solution. For sucrose density gradient assay, 90%, 35% and 5% sucrose solutions were prepared in 25mM MES buffer supplemented with 1:500 dilution of 10mg/ml aprotinin and leupeptin. The sucrose solutions were chilled before use. 850µl of cell lysate was mixed with 850µl of 90% sucrose and transferred to a prechilled 12ml Beckman ultracentrifuge tube. A second layer consisting of 1.7ml 35% sucrose was carefully laid followed by 850µl of 5% sucrose layer on the top. Care was taken to maintain separate density layers. The tube was then secured in a bucket, clasped to a prechilled SW-40 rotor and centrifuged at 38,000 rpm for 16 hrs at 4^0C in a prechilled Beckman Ultracentrifuge. 400µl aliquots of the centrifuged assay was carefully transferred to Eppendorf tubes containing 130µl of 4 X Laemmli buffer while the pellet was resuspened in 400µl of 1 X Laemmli buffer. The fractions were analysed by SDS-PAGE and Western blotting.

2.5 Glycan analysis

2.5.1 Deglycosylation (PNGaseF/EndoH)

Cell lysates prepared in 1% Triton X-100 lysis buffer was denatured by boiling for 10 min in the presence of 0.5% SDS. The boiling step was omitted for CD151 Western blot detection. Deglycosylation assays to remove all N-linked glycan (PNGaseF) and non-complex N-linked glycans (EndoH) (from New England Biolabs) was set up as follows:

	EndoH	PNGaseF
10X G5 Buffer	5 µl	-
10X G7 buffer	-	5 µl
10% NP-40	-	5 µl
Cell lysate	43 µl	38 µl
Deglycosylation enzyme	2 µl	2 µl

The reaction mix was incubated at 37^0C for 18 hrs after which, 16µl 4X Laemmli was added and boiled at 100^0C for 3 min to terminate the reaction. The deglcosylated product was analysed by SDS-PAGE and Western blotting.

2.5.2 Inhibition of N-linked glycosylation pathway

Cells were grown in the presence of various inhibitors for 48 -72 hours. Upon harvesting, cells were washed in cold PBS and lysed in 1% Triton X-100 lysis buffer for 18 hrs in a rotator in the cold room. Cell debris was removed by centrifuging at 13,000 rpm for 10 min and cleared lysate was collected into a fresh Eppendorf tube. Protein concentration was normalised using DC protein assay kit (Biorad) and analysed for the changes in the glycosylation profile of various glycoproteins by SDS-PAGE and Western blot analysis. The concentration of the various glycosylation pathway inhibitors used is listed below:

Inhibitor	Concentration	Reference
Castanospermine	1 mg/ml	(Saul et al., 1984)
Kifunensine	2 μg/ml	(Elbein et al., 1990)
Deoxymannojirimycin	2 mM	(Bischoff and Kornfeld, 1984)
Swainsonine	2 μg/ml	(Elbein, 1987)

(chemical structures of the inhibitors are presented as supplementary data)

2.5.3 Flow cytometry (glycan epitope)

Cells were grown in a 10 cm plate overnight, washed in PBS and detached with 1X trypsin (Invitrogen). Detached cells were washed once in PBS and resuspended in 1ml of chilled 1% BSA in PBS. Cells were counted and ~$1X10^5$ cells

was incubated in 200µl of 2µg/ml of biotinylated lectin (Vector Laboratories) for 30 min on ice. The list of lectins used and the glycan epitopes they recognise is presented in Table 2.6. Lectin bound cells were washed once in 1% BSA/PBS by centrifugation and resuspended in 200µl 1:500 dilution of FITC conjugated Avidin (Sigma) in 1% BSA/PBS for 30 min on ice. Cells were washed again twice in BSA/PBS buffer and finally resuspended in 100µl of cold PBS. Labelled cells were fixed in 2% PFA and analysed on EPICS XL Flow cytometry (Coulter) using System II software (Coulter).

Table 2.6 List of biotinylated lectins used for flow cytometry analysis

[from www.VectorLabs.com; (Goldstein, 2002)]

Biotinylated Lectin	Glycan epitope
ConcanavalinA	α-linked mannose
Aleuria aurantia Lectin	fucose linked (α -1,6) to N-acetylglucosamine or fucose linked (α -1,3) to N-acetyllactosamine
Dolichos biflorus agglutinin	α-linked N-acetylgalactosamine
Peanut Agglutinin	galactosyl(β-1,3) N-acetylgalactosamine
Phaseolus vulgaris Erythroagglutinin	bisecting complex N-glycan
Phaseolus vulgaris Leucoagglutinin	Tri- and tetra- antennary N-linked glycans containing (β-1,6) linked N-acetylglucosamine
Ricinus communis agglutinin I	Terminal galactose and to a lesser degree, N-acetylgalactosamine.

Sambucus nigra agglutinin	(α-2,6) sialic acid attached to terminal galactose in and to a lesser degree, (α-2,3) linkage
Soybean Agglutinin	Terminal α- or β-linked N-acetylgalactosamine and to a lesser extent, galactose residues.
Ulex europaeus Agglutinin I	glycoproteins and glycolipids containing (α-1,2) linked fucose residues
Wheat Germ Agglutinin	N-acetylglucosamine and sialic acid

2.5.4 Lectin blotting

Glycoproteins were resolved by SDS-PAGE and transferred onto nitrocellulose membrane. For lectin blotting, membranes were blocked with 1% BSA in PBS-T for 1 hr at room temperature and incubated in 1µg/ml lectin prepared in 1% BSA/PBS-T supplemented with 2mM $CaCl_2$. Blots were washed 4 times, 15 min each wash and incubated in 1:2000 dilution of neutravidin conjugated with HRP (Sigma) in 1% BSA/PBS-T for 1 hr at room temperature. The blots were washed again 4x15 min and glycans were detected with chemiluminescence kit (Western Lighting™, PerkinElmer Life Sciences). Western blots were exposed to HyperFilm® (Amersham) in the dark for various times before development.

2.6 α3β1 integrin purification

In order to perform a large scale α3β1 integrin purification, monoclonal antibody to α3 integrin subunit (A3-IVA5) was purified from hybridoma culture supernatant and coupled to cyanogen bromide activated CNBr) Sepharose beads. The antibody coupled beads was used to purify α3β1 integrin from total cell lysate. α3β1 integrin was also prepared in a smaller scale using GD6 peptide. Both protocols are presented below.

2.6.1 Antibody purification

Hybridoma cells were grown in T225 tissue culture flasks (IWAKI) in RPMI-1640 medium (Invitrogen) containing 20% FBS (Invitrogen). The supernatant was collected by centrifugation and pH was adjusted to ~8.0 with 10 X PBS solution. The hybridoma supernatant was filtered through a 0.45μm filter and NaCl was added to a final concentration of 2.5M. Antibody was captured with Protein-A conjugated agarose beads (Sigma) on a rotating wheel overnight in the cold room (1ml packed beads was used per 100ml of hybridoma supernatant). Beads were centrifuged at 3,000 rpm for 30 min at 4^0C and washed twice with 50 ml PBS containing 2.5M NaCl at pH 8.0. Beads were then packed into a 2 ml syringe plugged with glass wool. Stepwise elution of monoclonal antibody was performed by sequentially adding 1ml

aliquots with 100mM sodium citrate, pH 4.5 and each fraction was collected into separate tubes containing 100µl Tris-HCl, pH 8.8. Concentration of the eluted antibody was determined by measuring the optical density (OD) at 280nm using the NanoDrop 1000. The fraction(s) containing the highest antibody concentration was pooled together and dialysed overnight against 5L 0.1 M $NaHCO_3$ buffer containing 0.5M NaCl, pH 8.3-8.5 at 4^0C by constant stirring. The dialysed antibody was used for coupling.

2.6.2 Antibody based α3β1 integrin purification

Coupling of monoclonal antibody to CNBr beads

1 gram of activated CNBr beads (Sigma) were swelled in 10 ml cold 1mM HCl for at least 1 hr (1ml of swelled resin is required to couple 5-10 mg protein). Swelled resin was washed by gentle suction in a Buchner funnel with 10 ml of cold dH_2O followed by 10 ml coupling buffer (0.1M $NaHCO_3$ buffer containing 0.5M NaCl) and immediately mixed with the monoclonal antibody dialysed in coupling buffer. The coupling of antibody or BSA (control) with resin was performed by rotating the mix in a 15ml tube overnight in a cold room. The beads were sedimented by centrifuging at 3000 rpm for 15 minute. Absorbance of the supernatant was measured at 280nm before and after the coupling step to determine coupling efficiency. Post coupling

absorbance reading at around zero indicates efficient coupling. The beads were washed twice in coupling buffer and unreacted groups on the beads were blocked by incubating overnight in 0.1M Tris/0.5M NaCl, pH 8.3-8.5 by rotating in a cold room. Coupled beads were washed extensively first with coupling buffer followed by acetate buffer (0.1M NaAc/0.5M NaCl, pH 4) and the cycle of washes was repeated five times. Finally, the beads were washed in PBS and used immediately or stored at 4-8^{0}C in the presence of 0.1% sodium azide.

Purification of α3β1 integrin

MDA-231 CD151(+) and CD151(-) cells were grown in three 15 cm tissue culture plates for large scale α3β1 integrin purification. Cells were scraped into ice-cold PBS and washed by centrifuging at 800rpm for 3 min at 4^{0}C. Washed cells were lysed in 3 ml 1% Triton X-100 lysis buffer overnight and non-solubilised cell debris was removed by centrifuging at 13,000 rpm for 10 min at 4^{0}C. Cell lysates were collected into fresh tubes and assayed with DC protein assay kit (Biorad) to standardise their concentration. A small aliquot of the lysate (~40 μl) was collected as total lysate and the rest was precleared on a rotator in the cold room with BSA coupled CNBr beads for 2 hr. Precleared lysate was collected by centrifuging at 3000 rpm for 10 min and incubated with anti-α3 antibody (A3-IVA5) coupled Sepharose beads on a rotator in the cold room overnight. Beads were washed five times with

lysis buffer and captured α3β1 integrin was eluted twice by incubating the beads with 100 µl of 0.1 M glycine (pH 2.6) for 5 min on ice. The eluate was collected after centrifuging the beads at 13,000 rpm for 1 min and immediately mixed with 20 µl 1 M Tris-HCl (pH 8.8). The eluate was boiled in the presence of 1 X Laemmli for 3 min, resolved by either 8% or 12% SDS PAGE and analysed by Western and lectin blotting.

2.6.3 GD6 peptide based α3β1 integrin purification

Coupling GD6 peptide to CH-Sepharosebeads

Activated CH-Sepharose® 4B (Sigma) beads were swelled overnight in 1mM cold HCl at 1:200 (w/v). Swelled resin was washed twice in cold HCl (1mM). 2mg GD6 peptide was dissolved in 1ml coupling buffer (0.1 M $NaHCO_3$, 0.5 M NaCl, pH 8.0) and mixed with 100 µl of swelled resin in a cold room on a rotator for at least 4 hours. Absorbance of the supernatant was measured at 280nm before and after the coupling step to determine coupling efficiency. Excess active groups were blocked by incubating in 0.1 M Tris-HCl, pH 8.0 for 1 hour. Beads were then washed sequentially in 1.5 ml coupling buffer, followed by 1.5 ml Tris buffer (0.1 M Tris-HCl, 0.5 M NaCl, pH 8.0), 1.5 ml Acetate buffer (0.05 M NaAc, 0.5 M NaCl, pH 4.0) and

finally in PBS (pH 7.2). Coupled beads were either used immediately or stored in the cold room in the presence of 0.01% sodium azide.

α3β1 integrin purification.

MDA-231 CD151(+) and CD151(-) cells were grown in a 10 cm tissue culture plates for α3β1 integrin purification. Cells were scraped into cold PBS and washed by centrifuging at 800rpm for 3 min at 4^0C. Washed cells were lysed in 500 μl 1% Triton X-100 lysis buffer overnight and non-solubilised cell debris was removed by centrifuging at 13,000 rpm for 10 min at 4^0C. Cell lysates were collected into fresh tubes and assayed with DC protein assay kit (Biorad) to standardise their concentration. A small aliquot of the lysate (~40 μl) was collected as total lysate and the rest was precleared on a rotator in the cold room with BSA coupled CNBr beads for 2 hr. Precleared lysate was collected by centrifuging at 3000 rpm for 10 min and incubated with 50 μl packed volume of GD6 peptide coupled CH-Sepharose beads on a rotator in the cold room overnight. Beads were washed five times in lysis buffer and captured α3β1 integrin was eluted by boiling in 50 μl of 1 X Laemmli for 5 min. The eluate was resolve in 12% SDS-PAGE and analysed by Western blotting.

2.7 Migration assay

Comparison of the migration potential of various MDA-231 cell lines was performed using a standard Boyden chamber assay method. The day before the assay was performed, the underside of tissue culture inserts with 8 μm pore polycarbonate membrane (Nunc) were coated with 100 μl of extracellular matrix components [10 μg/ml fibronectin (Sigma) or 2 μg/ml Laminin332 (a kind gift from Prof Johannes Eble)] and incubated overnight in the cold room. Cell lines were grown overnight to ~60% confluency in 10 cm tissue culture plates and detached with Cell Dissociation Solution (Invitrogen). Cells were washed once and resuspended in serum free DMEM medium. ~5 X 10^4 cells were resuspended in 500 μl serum free DMEM medium and added into the tissue culture inserts. The inserts were then placed in a 24 well plate (Iwaki) containing serum free DMEM supplemented with 10ng/ml epidermal growth factor (EGF). Cells were allowed to migrate for 8 hours, after which, non-migrated cells were wiped off and the migrated cells were fixed in 2% PFA/PBS. Fixed cells were permeabilised and stained with 0.1% Triton X-100/0.1μg/ml Hoechst 33342 Fluorescent dye/PBS solution for 30 seconds and the inserts were rinsed twice with PBS. Polycarbonate membranes were peeled from the inserts and mounted on slides with DAKO mounting solution. Migrated cells were visualised with Nikon Eclipse E600 microscope. Up to seven random fields were photographed and scored using ImageJ nuclear/cell counter

software programme. Each combination of migration conditions was repeated up to four times (i.e. up to four tissue culture inserts was used for each condition) and independent assays were performed 2 – 3 times for each cell line.

When required, detached cells were pre-incubated with 10μg/ml monoclonal antibody diluted in 500 μl serum free DMEM on ice for 30 min. A fresh aliquot of 10μg/ml of antibody was added immediately before transferring the cells into tissue culture inserts to proceed with the migration assay.

2.8 BCECF cell labeling

Cells were labeled with 2,7-bis-(2-carboxyethyl)-5-(and-6)carboxyfluorescein-acetoxylmethyl (BCECF-AM) for quantitative detection. Briefly, 1:100 dilution of BCECF-AM (from 1 mg/ml stock) was mixed with prewarmed DMEM medium containing 1 x 10^6 / ml viable cells. Cells were incubated at 37^0C for 15 minutes and washed twice with fresh medium. The stained cells are ready to be used in functional assays.

2.9 Cell Adhesion assay

Wells in a 96 flat bottom plate were marked and coated with 200 µl of various extracellular matrix dilutions for 2 hr at 37^0C. Each condition (1 µg/ml Laminin332, 2 µg/ml Laminin332, 10µg/ml fibronectin and 10µg/ml BSA) was loaded in six wells. Coated wells were washed twice in PBS and blocked with 200 µl of 0.1% BSA/PBS for one hour at 37^0C. Blocked wells were rinsed once in PBS and loaded with 200 µl of BCECF-AM stained 2 X 10^4 cells in DMEM medium containing 0.1% BSA. Static adhesion was performed at 37^0C for 20-25 min and input reading was measured in a plate reader (Odyssey 2.1) at 485-538nm absorbance. The wells were washed 3 times in 200 µl of prewarmed DMEM/BSA medium and finally 200 µl of DMEM/BSA was added before reading the output on a plate reader. Percentage of cells which attached to the extracellular matrix was calculated from the ratio of (output reading)/(input reading).

2.10 Transendothelial migration assay

Internal chamber of polycarbonate tissue culture inserts with 8 µm pore size was coated with 10 µg/ml fibronectin at 37^0C for 2 hr. Inserts were rinsed in PBS and 2 X 10^5 human brain microendothelial cells (HBMEC) were loaded to each insert with

500 µl of 10% DMEM medium and the insert was immersed into a 24 well plate containing 500 µl of 10% DMEM medium. Cells were grown overnight in a tissue culture incubation chamber to obtain a confluent monolayer. The number of cell required to form a confluent monolayer overnight was determined by performing permeability assay as previously described (Fiuza et al., 2002). Briefly, 0.036% Trypan blue and 0.8% BSA were dissolved in Hank's Balanced Salt Solution (HBSS) [Invitrogen] and incubated at 37^0C for 10 min to form a stable Trypan blue-protein complex. Tissue culture inserts containing HBMEC monolayer plated at different cell concentration overnight (5×10^4, 1×10^5, 2×10^5 and 4×10^5) were washed in warm HBSS and transferred to 24 well plate containing 1 ml of HBSS. 500 µl Trypan blue complex was added to the inserts and incubated for 5 min in a tissue culture incubator. Cells are considered confluent if the 590 nm absorbance of the Trypan blue complex that diffused into the 24 well plate is < 1% of the absorbance for Trypan blue complex loaded into the tissue culture inserts.

Prior to performing the transendothelial migration assay, the HBMEC monolayer was stimulated by incubating the cells for 3 hr in 500 µl of 20ng/ml tumour necrosis factor α (TNF-α) in a tissue culture incubator. The stimulated endothelial cells were washed in 10% DMEM and 2×10^5 BCECF labelled MDA-231 CD151(+) or CD151(-) cells resuspended in 500 µl of the 10% DMEM medium was added to the inserts. Assays for each cell lines were performed in triplicates for

statistical representation. Transendothelial migration assay was performed for 4 hr, 6 hr and 8 hr. Non-migrated cells within the insert were wiped off with cotton bud and migrated cells were fixed in 2% PFA. Number of migrated BCECF stained MDA-231 cells were visualised and scored with Nikon Eclipse E600 microscope.

2.11 Laminar flow assay

The assay was performed in flat glass capillaries (μ slides) with internal dimension of 0.3mm/3mm/50mm. Clean μ slides were immersed in 4% APES (3-aminopropyl)triethoxysilane (Sigma) solution prepared in anhydrous acetone overnight in the dark and this step was repeated with fresh APES solution. μ slides were washed twice in acetone and finally in distilled water by sucking a few ml through using a vacuum pump. The μ slides were dried on tissue and the internal chambers were coated with P-selectin (10 mg/ml), E-selectin (10 mg/ml) (R&D Systems) or Laminin332 (4 mg/ml) (a kind gift from Prof Johannes Eble). The assembly of various components for the flow assay is described in Figure 2.3.

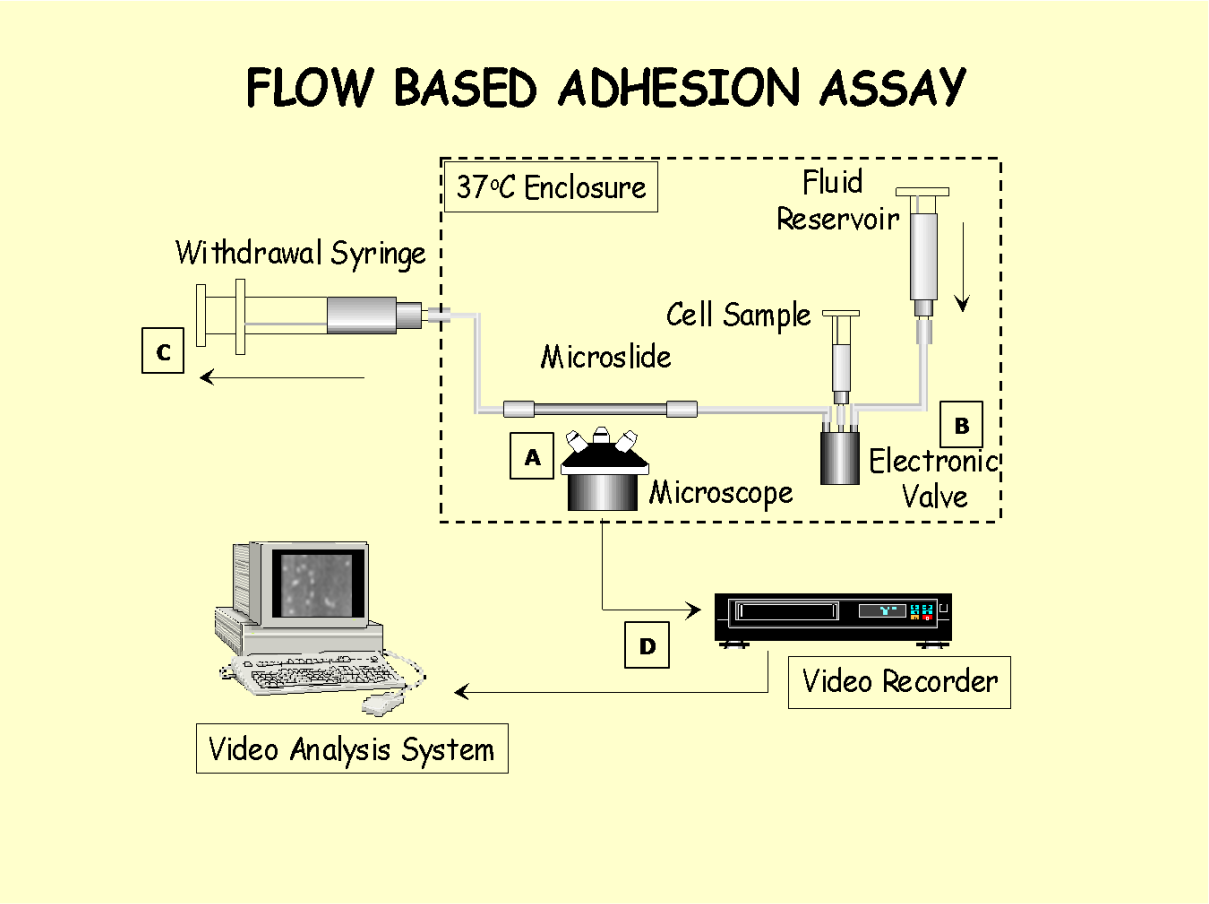

Figure 2.3 Assembly of various components for flow assay.

The laminar flow assay was performed in a heated enclosure at 37^{0}C. The μ slide was secured on the microscope platform (A) A tubing network which allows the flow of cells and wash medium through the μ slide to the withdrawal syringe is controlled by an electronic valve (B). The flow speed is set electronically with a suction pump attached to the withdrawal syringe (C). Cell flow was recorded with a video recorder and analysis system attached to the microscope (D). (The image was kindly provided by Mr Phillip Stone)

The laminar flow assay was performed and documented at three different tumour cell flow rates (0.085 ml/min, 0.175 ml/min and 0.35 ml/min) as well as up to

5 min in static conditions where cell flow was halted and then resumed at the same rate after an interval of 30 sec, 1 min, 2 min and 5 min.

2.12 Endothelial rolling assay

Microslide preparation

The inner chamber of sterile glass μ slides were coated with 1% gelatine (Sigma) for ~30 min and washed with sterile PBS. Freshly prepared HUVEC was obtained from Prof Gerard Nash (IBR, University of Birmingham). HUVECs grown in a T25 flask were detached, washed and resuspended in 400 μl of 20% endothelial medium containing antibiotics and supplements (Medium 199 (Invitrogen), 20% foetal bovine serum (Sigma), 2.5 μg/ml Amphotericin (Invitrogen), 1000 U/ml penicillin (Sigma), 0.1 μg/ml streptomycin (Sigma), 1 mg/ml hydrocortisone (Sigma) and 1ng/ml epidermal growth factor (Sigma). The cells were loaded into 6 gelatine coated μ slides and left to attach to the slides for two hours in a tissue culture incubator. The μ slides were immersed in a petri dish containing 20 ml of endothelial medium and attached to a peristaltic pump set on timer so that fresh medium uptake occurs within the capillary tube every hour, overnight. The following day, the required number of endothelial slides was activated with 100U/ml TNFα (R&D Systems) for 3 hours.

Rolling assay

The ability of MDA-231 cells to roll on activated and non-activated HUVEC was compared by attaching the μ slide to the laminar flow assembly as described in Figure 2.3. The flow assay was performed at 0.085 ml/min, 0.175 ml/min and 0.35 ml/min while shear rate was set at 0.025 Pa, 0.05 Pa and 0.1 Pa. The static adhesion assay on endothelial cells was performed by streaming in the MDA-231 cells at 0.35 ml/min into the μ slides and the flow was stopped for 1 min, 2 min, and 5 min. Unbound cells were washed away by applying 0.1 Pa shear force. Number of cells before and after the wash was recorded and counted.

3. RESULTS AND DISCUSSION

3.1 Generation and analysis of various tetraspanin knock-down cell lines

3.1.1 Generation and analysis of CD151 knock-down cell lines

To study the effect of CD151 depletion in tumour cell lines, endogenous CD151 was ablated by introducing CD151 targeting short hairpin RNA (shRNA) to three different cell lines: MDA-MB-231 (MDA-231), MCF7 and HeLa. The resulting drug resistant colonies were sorted for CD151 positive and CD151 negative populations. The level of endogenous CD151 in the final sorted population was determined by Western blot analysis [Figure 3.1(A)] while and cell surface expression level was determined by flow cytometry analysis [Figure 3.1(B)].

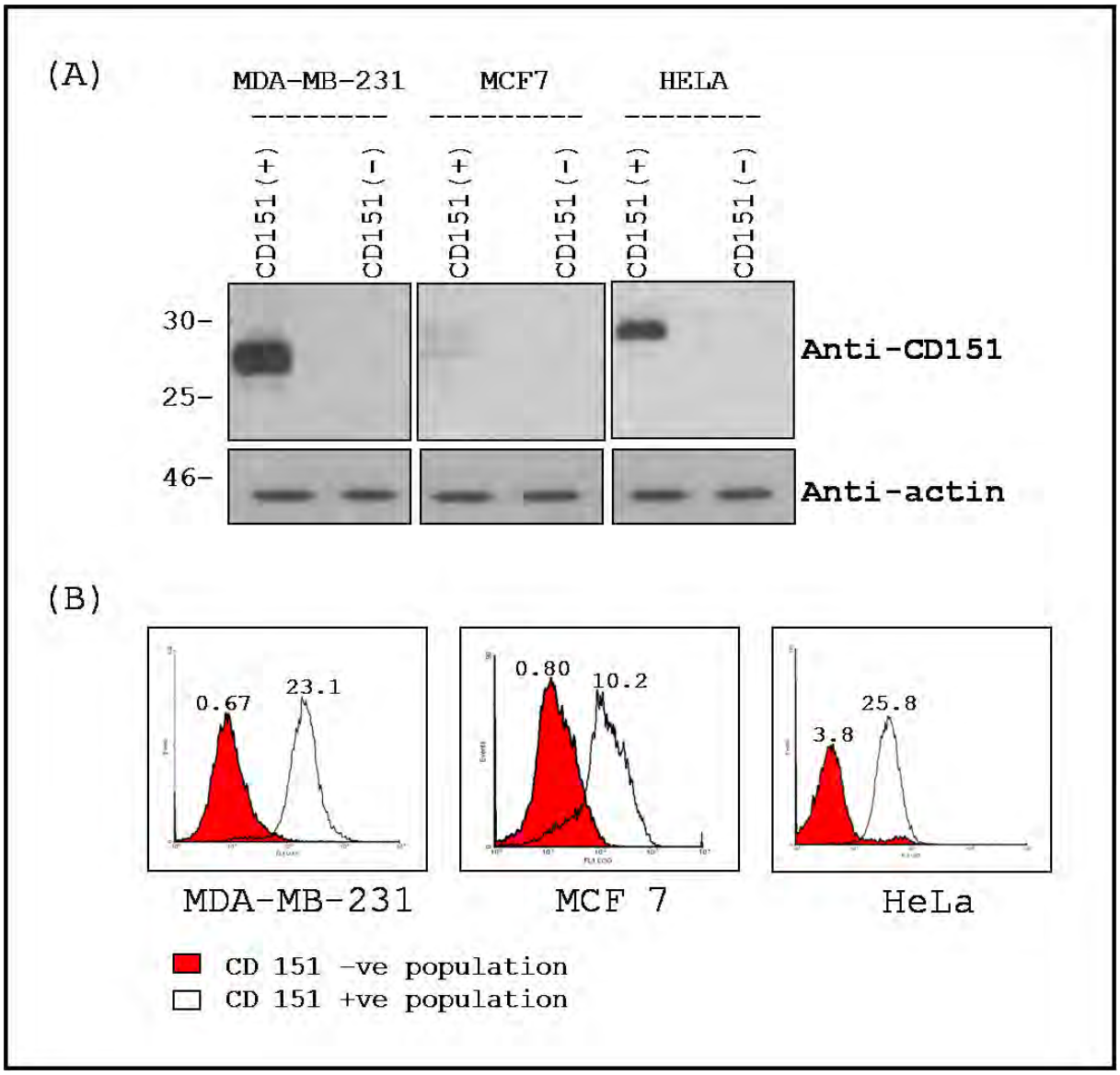

Figure 3.1 Comparison of CD151 levels in in wild type and CD151 ablated MDA-MB-231, MCF7 and HeLa cell lines.

(A) Total lysate was resolved in a 12% SDS polyacrylamide gel and the level of CD151 (anti-CD151 pAb) in each cell line was compared by Western blot analysis (upper panel). Loading calibration was confirmed by detecting for β-actin (lower panel). The level of CD151 expression in parental MCF7 cell line (lane 3) was markedly low compared to MDA-231 (lane 1) or HeLa (lane 5) cell lines. (B) Flow cytometry analysis was performed to determine the cell surface expression levels of CD151. The value accompanying each peak represents the mean fluorescence intensity (MFI).

3.1.1.1 The effect of CD151 depletion in various cell lines

CD151 forms tight stoichiometric complexes with laminin binding integrins and contributes to their function (Serru et al., 1999; Yauch et al., 2000; Sterk et al., 2002b). Increased CD151 level has been associated with poor prognosis in prostate cancer (Ang et al., 2004) and non-small cell lung cancer (Tokuhara et al., 2001). CD151 is also reportedly upregulated during breast cancer progression (Yang et al., 2008). In this study I focused on the contribution made by CD151 in highly metastatic breast cancer cell line, MDA-231. While laminin binding integrins, $\alpha 3\beta 1$,$\alpha 6\beta 1$ and $\alpha 6\beta 4$, are expressed in this cell line, the expression level of $\alpha 3\beta 1$ integrin is markedly higher than $\alpha 6\beta 1$ and $\alpha 6\beta 4$ integrins. Consequently, as a first line of study, I investigated CD151's contribution to the stability and cell surface presentation of $\alpha 3\beta 1$ integrin by flow cytometry and Western blot analysis.

3.1.1.2 Flow cytometry analysis

Flow cytometry analysis was performed to quantify cell surface expression level of $\alpha 3\beta 1$ integrin in MDA-231 CD151(+) and CD151(-) cells. As controls, the cell surface levels of $\alpha 2$, $\alpha 6$ and $\beta 1$ integrin subunits, as well as tetraspanins CD9, CD63, CD81, CD82 and CD151 was determined and summarised in Figure 3.2. The raw data for

this experiment is presented in Appendix 1. Depletion of CD151 did not have any effect on the cell surface expression of tetraspanins CD9, CD63, CD81, CD82 or α2, α3, α6 and β1 integrin subunits. Investigation into the contribution made by cell density on the cell surface expression was made by plating cells to reach 50% and 90% density prior to detachment for flow cytometry analysis. Again, no significant difference was observed in the cell surface expression levels of these proteins upon CD151 depletion at different cell densities. The results are summarised in Figure 3.2.

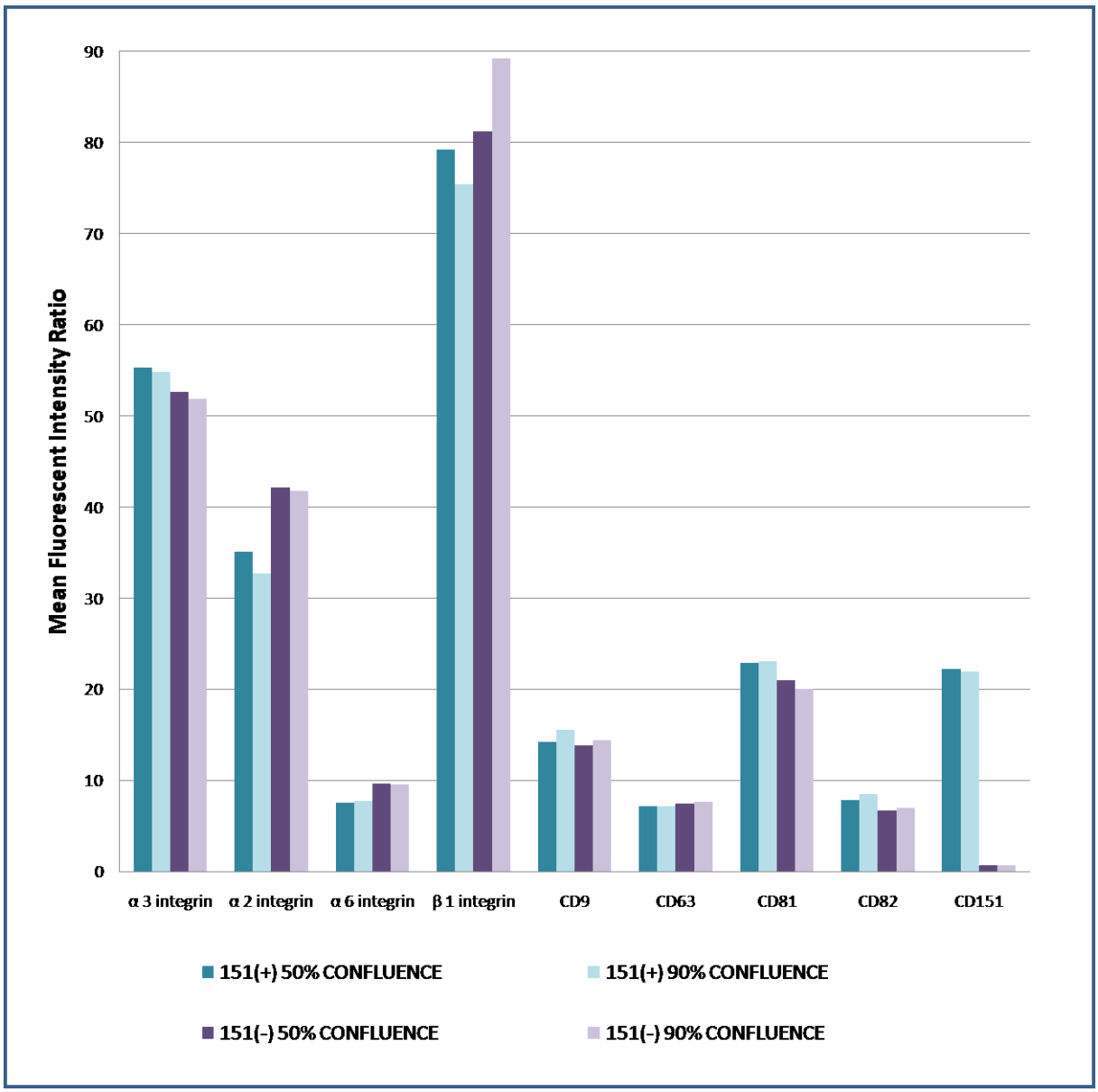

Figure 3.2 Flow cytometry analysis of MDA-231 CD151 (+) / (-) cells

Cells were grown to 50% (blue bars) and 90% (green bars) confluence and analysed for the level of various cell surface proteins by flow cytometry. Monoclonal antibodies used are anti-α3 (A3-IVA5), anti-α2 (HAS3), anti-α6 (A6-ELE), anti-β1 (TS2/16), anti-CD9 (C9BB), anti-CD63 (6H1), anti-CD81 (M38), anti-CD82 (M104) and anti-CD151 (5C11). No significant difference was detected in the surface level of these proteins at either confluence upon CD151 depletion.

3.1.1.3 Western blot analysis of α3β1 integrin in MDA-231 CD151 (+) / (-) cell lines

Total levels of α3β1 integrin in MDA-231 CD151 (+) and CD151 (-) cells were analysed by Western blot under reducing conditions. Interestingly, I noted that while the total levels of the integrin remained comparable between the two cell lines, the mobility and intensity of the three light chain fragments of α3 integrin subunit generated under reducing condition were altered upon CD151 depletion [Figure 3.3(A)]. These differences can be attributed to (1) changes in the proportion of each furin cleavage occurrence, (2) an alteration in the glycosylation of the integrin or (3) a variation in the splicing of the integrin's light chain. To determine if glycosylation plays a role in this difference, glycoproteins in cell lysates were deglycosylated using Peptide: N-Glycosidase F (PNGaseF) and the α3 light chain fragments from MDA-231 CD151 (+) and 151 (-) cell lines were compared by Western blot. Removal of glycan residues effectively negated the difference in the mobility of the integrin fragments between the two cell lines [Figure 3.3(B)].

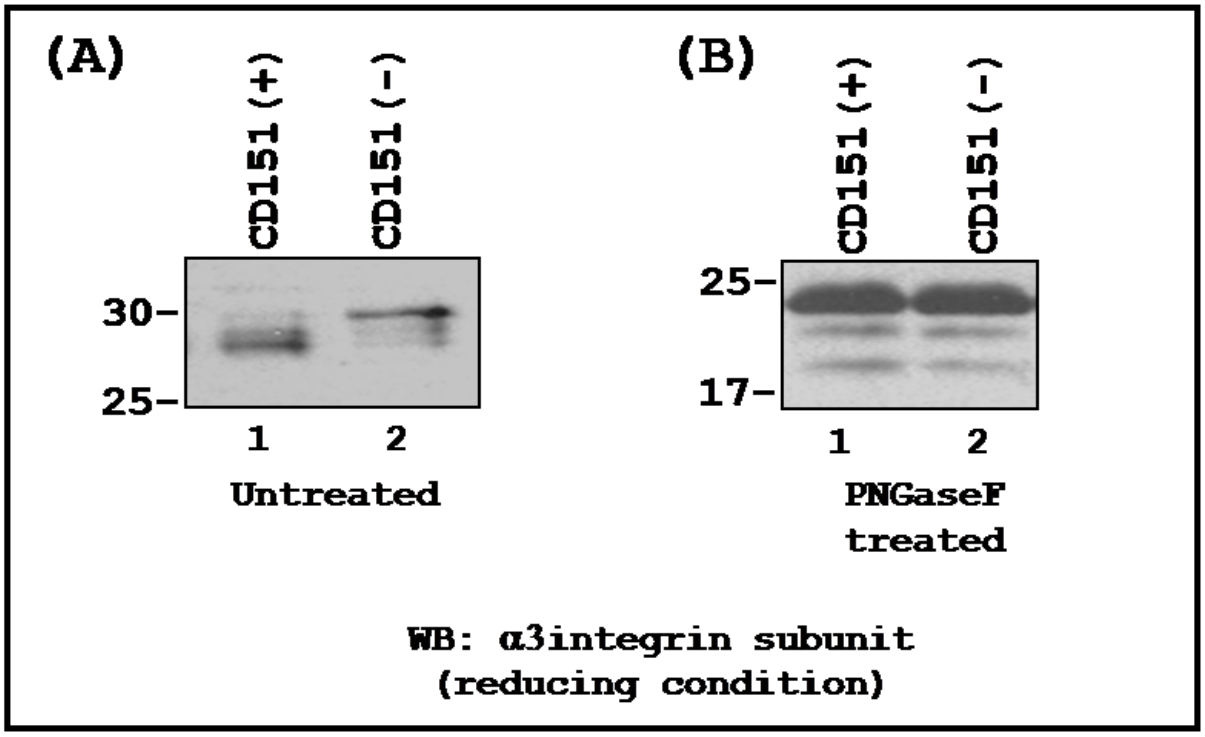

Figure 3.3 Western blot analysis of α3 integrin light chain in MDA-231 CD151(+) and CD151(-) cell lines.

Total cell lysate was resolved by 12% SDS-PAGE before and after PNGaseF treatment and probed for α3 light chain fragments on Western blot using anti-α3 pAb. (A) A difference was observed in the mobility of the α3 light chain fragments between CD151(+) (lane 1) and CD151(-) (lane 2) MDA-231 cells. (B) Pretreating the cell lysates with deglycosylation enzyme, PNGaseF, removed the sugar moieties attached to the integrin and consequently, the difference in the mobility of the α3 integrin light chains between the two cell lines was also eliminated (lanes 1 & 2).

The glycosylation profile of α3 integrin subunit was also analysed by comparing their mobility under non reducing condition. Two different deglycosylation enzymes were used for this purpose; Endoglycosidase H (EndoH) which removes the high mannose and hybrid N-linked oligosaccharides but not the complex N-linked oligosaccharides, and Peptide: N-Glycosidase F (PNGaseF), which eliminates all three types of N-linked oligosaccharides, leaving just the protein backbone. Under non-reducing conditions, EndoH treatment revealed a difference in the mobility of the integrin molecules between the two cell lines [Figure 3.4 (B)] which was not immediately apparent prior to deglycosylation treatment [Figure 3.4(A]. Conversely, complete removal of the sugars from the protein backbone by PNGaseF quenched this difference [Figure 3.4(C)]. These results indicate that the CD151 mediated changes in the mobility of α3 integrin subunit on Western blots are entirely due to its altered glycosylation state.

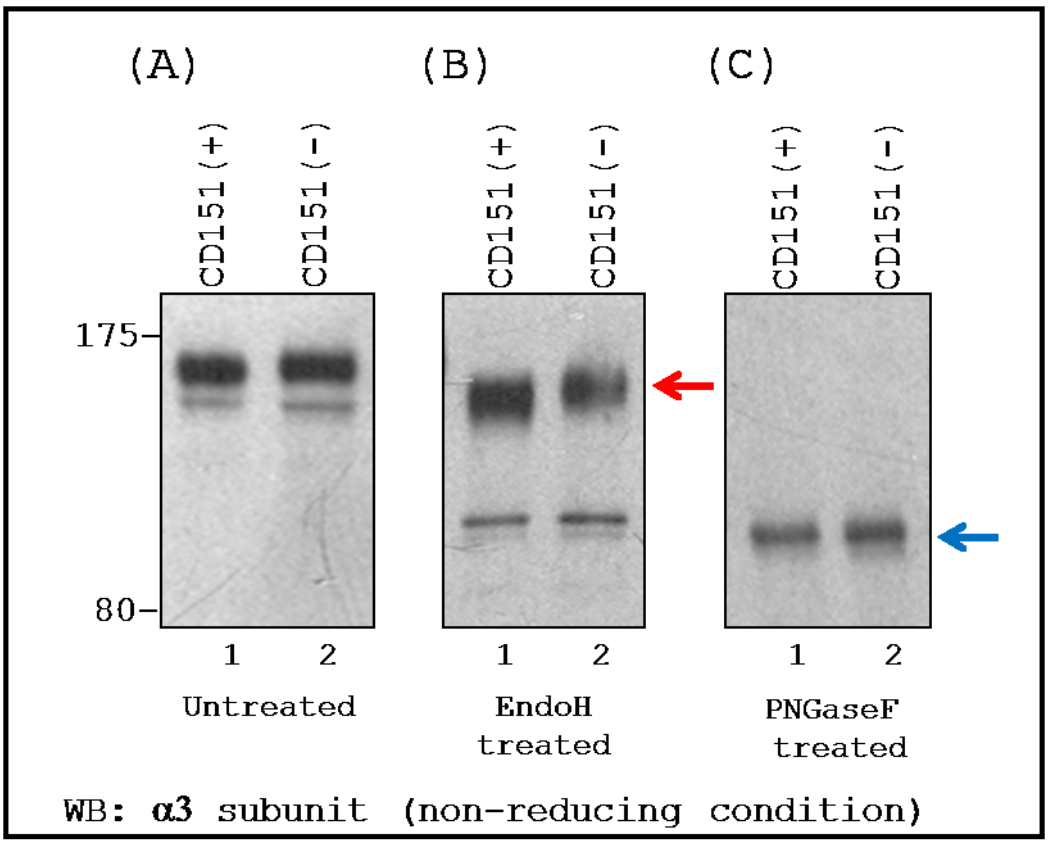

Figure 3.4 Western blot analysis of α3 integrin under non-reducing condition.

Total cell lysates were resolved by 8% SDS-PAGE before and after EndoH or PNGaseF treatment and probed for α3 integrin subunit on Western blot using anti-α3 pAb. (A) A slight difference was observed in the mobility of the α3 integrin subunit in CD151(+) (lane 1) and CD151(-) (lane 2) MDA-231 cells. (B) Removal of high mannose and hybrid glycan by pretreating the cell lysates with deglycosylation enzyme EndoH, enhanced the difference in the mobility of the integrin (red arrow). (C) Complete removal of all the glycan chains with PNGaseF negated the difference in the mobility of the α3 integrin molecule between the two cell lines (blue arrow).

3.1.1.4 Western blot analysis of α3 integrin in CD151 depleted MCF7 and HeLa cell lines

In order to determine the universality of CD151 mediated glycosylation changes to α3 integrin, a comparison of their mobility was made in CD151 depleted MDA-231, HeLa and MCF7 cell lines. The Western blot analysis of EndoH treated lysates showed change in the intensity of the various light chains of α3 integrin subunit in MDA-231 and HeLa cells, but not in MCF7 cells, upon CD151 depletion (Figure 3.5).

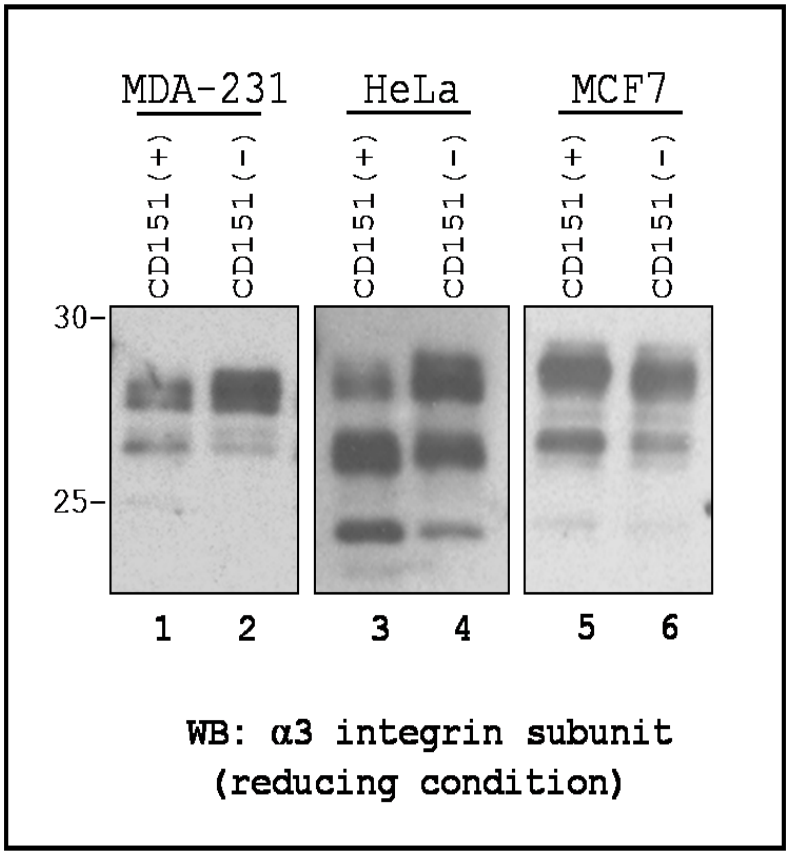

Figure 3.5 Western blot analysis of light chains of α3 integrin subunit in HeLa and MCF7 cell lines

Cell lysates were resolved by 12% SDS-PAGE, after EndoH treatment and probed for the light chain of α3 integrin subunit on Western blot using anti-α3 pAb. CD151 depletion markedly altered the intensity of α3 integrin light chain fragments in MDA-231 (lanes 1 & 2) and HeLa (lane 3 & 4) cell lines but not in MCF 7 cell line (lanes 5 & 6).

3.1.2 Generation of CD9 (-), CD63 (-) and CD81 (-) MDA-231 cell lines

CD151, like all tetraspanins, form microdomains on the plasma membrane through homotypic and heterotypic lateral interactions with other members of the family. A hierarchy of primary, secondary and tertiary partners are then realised. Depending on their proximity, various components that make up a TERM can collectively influence each other's function. To access the extent to which other tetraspanins within the CD151/α3β1 associated TERM may influence α3 integrin glycosylation, a panel of CD9, CD63 and CD81 depleted MDA-231 cell lines were generated as detailed in the Materials and Methods (section 2.2 & 2.3). Depletion of each tetraspanin was confirmed by Western blot analysis (Figure 3.6).

The α3β1 integrin was immunoprecipitated with anti-α3 mAb from total cell lysates of the tetraspanin depleted cell lines and treated with EndoH to remove high mannose and hybrid oligosaccharides. The EndoH untreated and treated immunoprecipitation complex was resolved on 12% SDS PAGE and detected by Western blotting as presented in Figure 3.7.

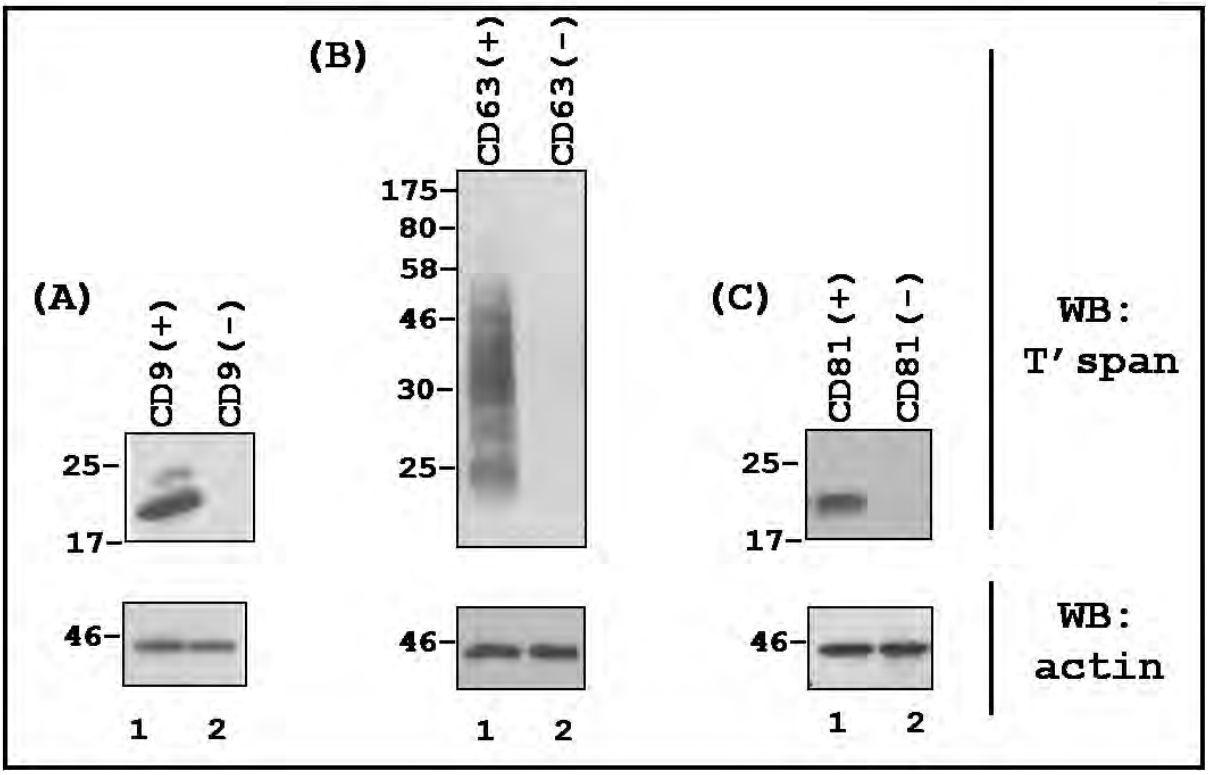

Figure 3.6 Western blot analyses of CD9, CD63 and CD81 depletion in MDA-231 cell lines.

Upon shRNA introduction, antibiotic selected cells were surfaced labelled for CD9 (BU16), CD63 (6H1) or CD81 (M38), gated and sorted for (+)ve and (-)ve populations. Cell lysis of the selected populations were performed in 1% Triton X-100 and resolved by 12% SDS-PAGE. The shRNA knock-down levels for (A) CD9, (B) CD63 and (C) CD81 was confirmed by Western blot analysis using C9BB, 6H1 and M38 monoclonal antibodies respectively.

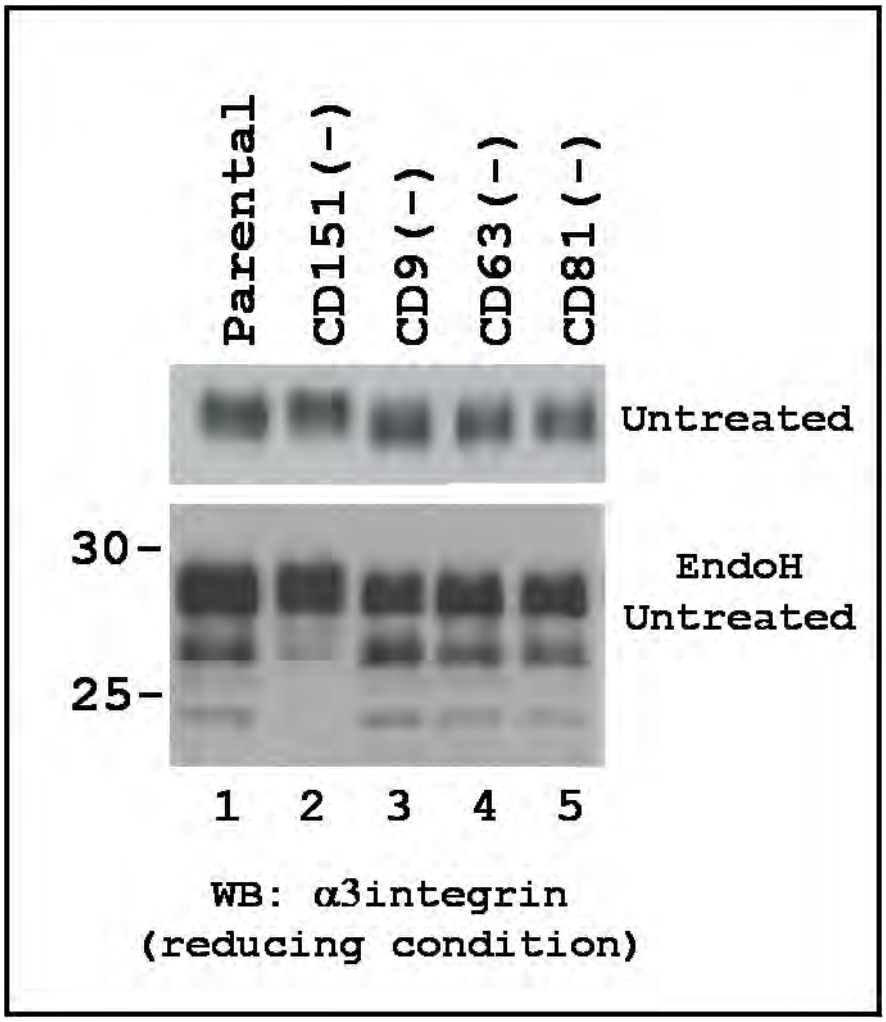

Figure 3.7 Western blot analysis of α3 integrin light chain from various tetraspanin depleted MDA-231 cell lines.

The α3β1 immunoprecipitaion complex (mAb A3-IVA5) from 1% Triton X-100 lysed cells was resolved by 12% SDS-PAGE, before and after EndoH treatment and probed for light chain of α3 integrin subunit on Western blot using anti-α3 pAb. Depletion of CD151 showed a marked difference in the intensity of the three α3 integrin light chain fragments (lane 2) compared to the parental line (lane 1). While depletion of CD9 did not produce a similar shift, a slight change in the intensity of the middle band is detected upon CD9 depletion (lane 3). Depletion of CD63 (lane 4) or CD81 (lane 5) did not produce a noticeable change in the intensity of α3 integrin light chains compared to the parental line.

3.1.3 Comparison of CD9 and CD81 associated α3 integrin pool

The CD151-α3β1 tight association is attested by the fact that they remain associated under a relatively stringent detergent treatment such as 1% Triton X-100. The association of α3β1 with CD9 and CD81 is less robust. Nevertheless, both tetraspanins can be co-precipitated with α3β1 when cells are lysed in 1% Brij96, signifying a secondary interaction between the tetraspanins and α3β1 integrin. Curiously though, CD9 depletion produced a slight difference in the mobility of light chain fragments of α3 integrin subunit on Western blot while CD81 depletion did not have the same effect (Figure 3.7). In order to determine if a difference exist in the α3β1 integrin populations that associates with CD9 or CD81, the α3 integrin subunit that co-immunoprecipitation with CD9 or CD81 under 1% Brij 98 detergent condition was analysed. I also compared the CD151 co-immunoprecipitation complexes under 1% Triton X-100 condition. Comparisons between CD9 and CD81 associated α3 integrin indicated a difference in the ratio of the glycoforms that associate with these tetraspanins as indicated in Figure 3.8. The precipitate was treated with EndoH and their profile was compared by Western blot. As expected, α3 integrin co-precipitated in abundance with CD151 compared to CD9 or CD81.

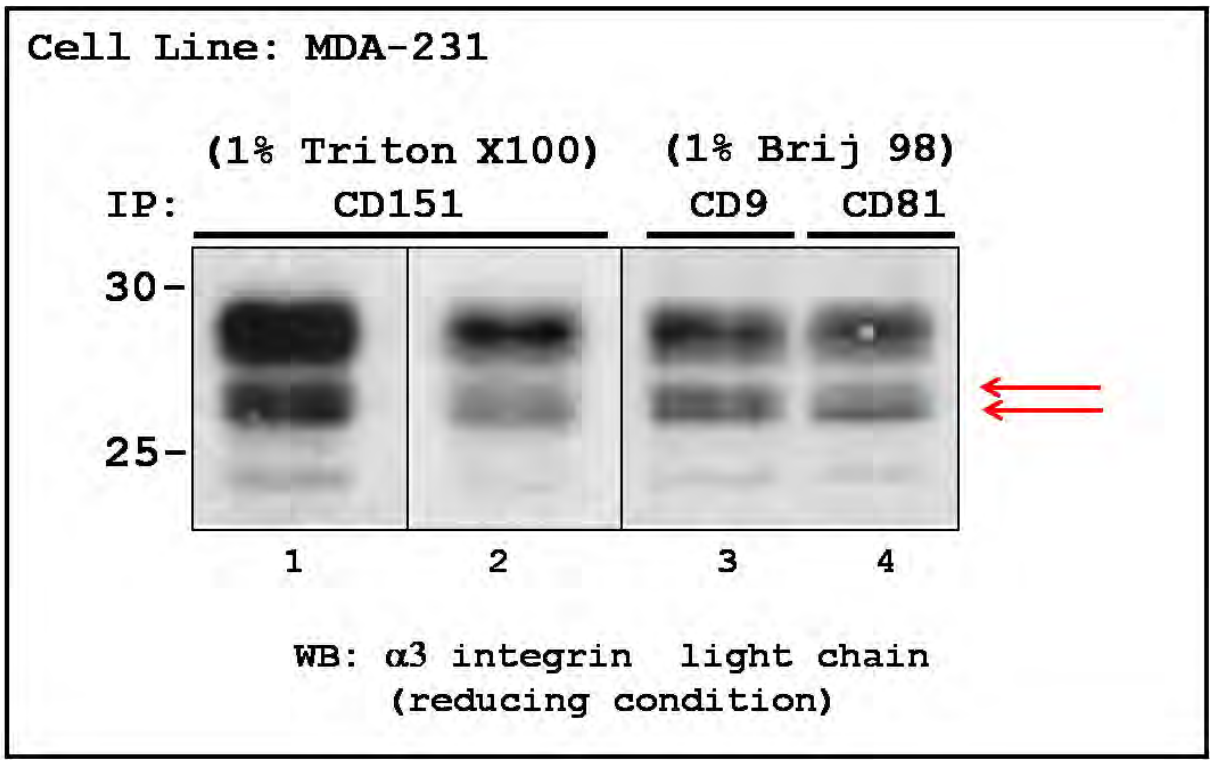

Figure 3.8 Western blot analysis of CD151, CD9 and CD81 associated α3 integrin light chain.

Co-immunoprecipitation (co-IP) of α3β1 integrin from precleared MDA-231 cell lysate was performed with anti-CD151 (5C11), anti-CD9 (C9BB) or anti-CD81 (M38) monoclonal antibodies. Co-IP complexes were deglycosylated with EndoH (NEB) as follows: sample was boiled in 1 X denaturation buffer for 10 minutes and incubated overnight at 370C in 1 X G5 buffer and 1µl of EndoH. The deglycosylated sample was then boiled in 1 X Laemmli buffer, resolved by 12% SDS-PAGE and analysed for the light chain fragments of α3 integrin subunit by Western blotting. A relative difference in the intensity of the doublet in the middle (as indicated by the arrows) from the CD81 co-precipitate (lane 4) was not observed during CD9 co-precipitation (lane 3). Lanes (1), (3) and (4) represents identical exposure time to show the relative abundance of α3 integrin that co-precipitate with each of the tetraspanin. Lane (2) is a shorter exposure of lane (1).

3.1.4 Western blot comparison of various cell surface glycoproteins in MDA-231 CD151(+) and CD151(-) cell lines

The main functional characteristic of tetraspanin is realised through their ability to form lateral interactions with other cell surface proteins. Consequently, the extent of CD151's influence on glycosylation of other cell surface proteins was investigated by comparing the mobility of the light chain fragments of α6 integrin subunit (forms tight association with CD151), CD63 (a highly glycosylated member of the tetraspanin family) and emmprin, an extracellular matrix metalloproteinase inducer membrane protein shown to associate with α3β1 integrin (Berditchevski et al., 1997) Western blot comparison of these proteins in the two cell lines, with and without EndoH treatment, is presented in Figure 3.9.

No difference in migration or intensity was observed for all three proteins upon CD151 depletion. A more stringent assessment was made by pretreating the lysate with EndoH to remove the presence of high mannose and hybrid oligosaccharide that may obscure any slight difference before analysing by Western blot. Again no difference in the mobility of the bands was observed, regardless of their CD151 status.

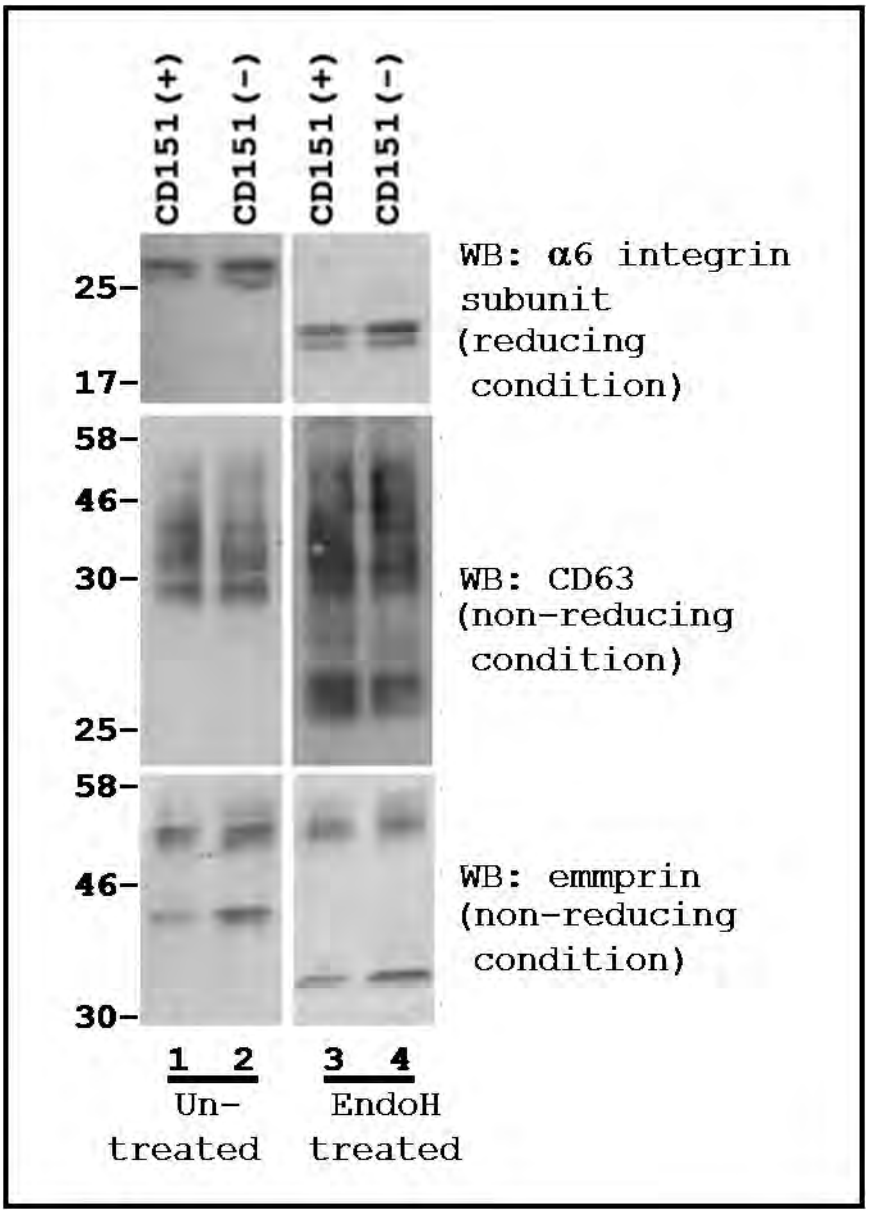

Figure 3.9 Western blot analysis of α6 integrin subunit, CD63 and emmprin in MDA-231 CD151(+) and CD151(-) cells.

The cells were lysed in 1% Triton X-100 and resolved by 12% SDS-PAGE before and after EndoH treatment and analysed by Western blot. The upper panels represent α6 integrin light chain immunoprecipitated with mAb A6-ELE and detected by rabbit polyclonal antibody against α6 integrin light chain; the middle panels represent CD63 detected with mAb (IB5) while the lower panels represent emmprin detected with mAb (8G6). Both EndoH untreated (lanes 1 and 2) and treated (lanes 3 and 4)

samples showed no difference in the migration profile of the glycoproteins upon CD151 depletion.

3.1.5 Analysis of α6 integrin's association with CD151 in MDA-231 cell line

CD151 forms tight interactions with both α3β1 and α6 (β1 / β4) integrins via the QRD tri-amino sequence within the large extracellular loop of CD151 (Kazarov et al., 2002). Loss of the tight interaction between α3β1 integrin and the QRD mutant of CD151 under 1% Triton X-100 condition have also been reported elsewhere (Baldwin et al., 2008; Zevian et al., 2011). Interestingly however, depletion of CD151 only affected the glycosylation of α3 integrin but not α6 integrin. I hypothesised that one of the reason for this observation may be because CD151 preferentially associates with α3 integrin over α6 integrin in MDA-231. To test this hypothesis, α3 and α6 integrins were immunoprecipitated from equal amounts of total cell lysate prepared in 1% Triton X-100 lysis condition, and compared for the level of CD151 that co-precipitated with each of the integrin. Even though CD151 has been widely reported to form primary interaction with laminin binding integrins, the co-immunoprecipitation analysis showed CD151 forming a preferentially or stronger associated with α3β1 integrin over α6 integrins in MDA-231 cells when analysed under 1% Triton X-100 condition [Figure 3.10 (A) & (B)]. In fact, the level of α6 integrins that complexed with CD151 in MDA-231 cells under this condition, compared to α3β1 integrin, was so low that it was almost negligible.

Furthermore, Western blot analysis for α3 and α6 integrin subunits that co-precipitated with CD151 under 1% Triton X-100 condition confirmed the earlier observation on preferential tight interaction between CD151 and α3β1 integrin compared to α6 integrins [Figure 3.10 (C) & (D)]. These results may offer an explanation as to why CD151 depletion altered glycosylation of α3 integrin but not α6 integrin in MDA-231 cells even though they have both been reported to interact at the QRD motif on LEL of CD151 with similar stoichiometry.

In order to determine whether α6(β1/β4) integrins are recruited into the CD151 TERM in MDA-231 cells, I performed the immunoprecipitation assay under 1% Brij96 condition and compared the level of α3β1 and α6β1/β4 that co-precipitated with CD151. Western blot analysis showed that under these experimental conditions, CD151 associated with both α3β1 and α6(β1/β4) integrins at comparable levels. In fact, the level of α6β1/β4 integrins that co-precipitated with CD151 was slightly higher than α3β1 integrin. This result shows that even though CD151 preferentially forms tight association with α3β1 integrin in MDA-231 cells, α6β1/β4 integrins are still recruited into the CD151 associated TERM at high levels.

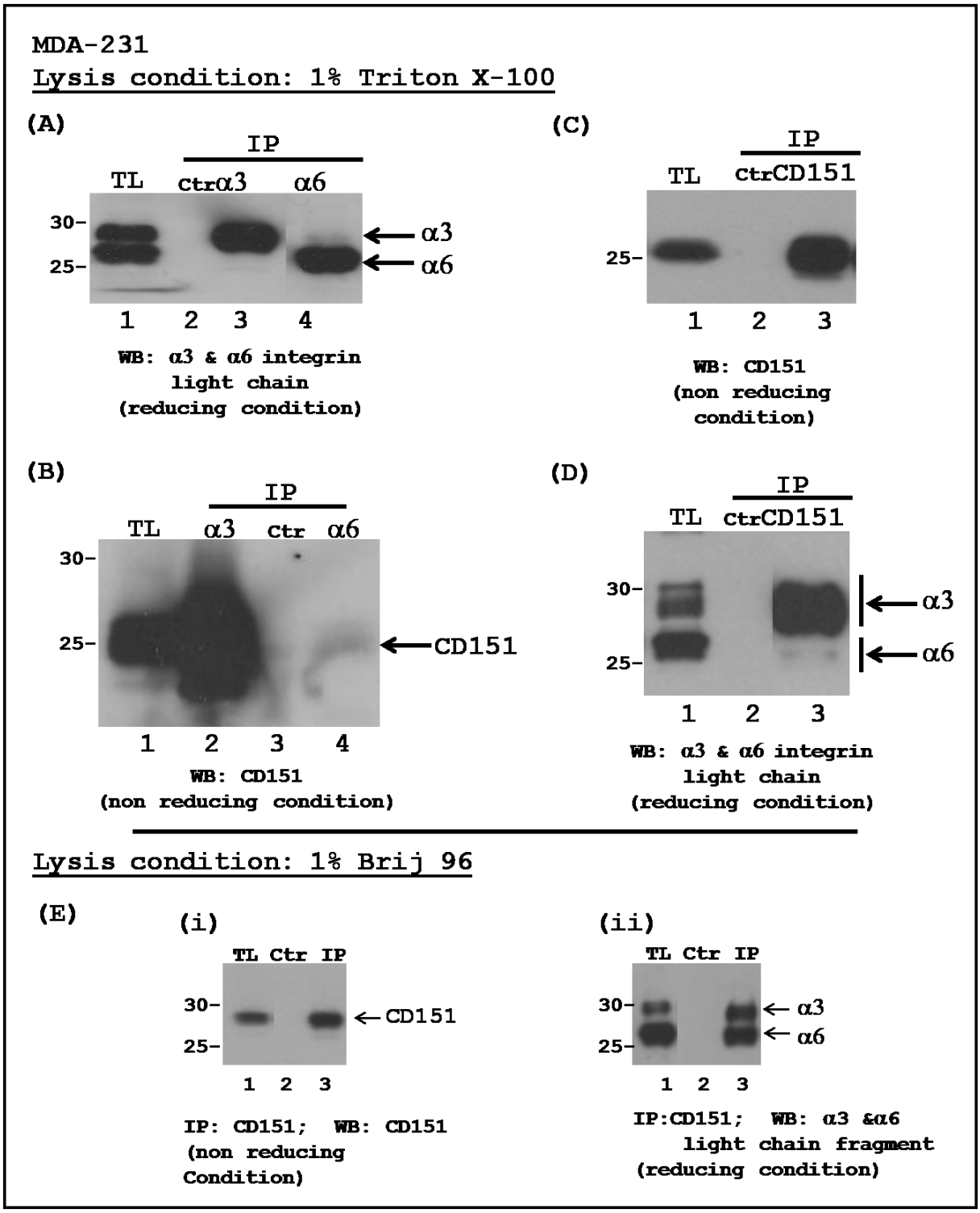

Figure 3.10 Comparison of CD151's association with α3 and α6 integrins. In the first experiment (A & B), α3 integrin and α6 integrin was immunoprecipitated(IP) with mAb A3-IVA5 and A6-ELE respectively, from MDA-231 cell lysate (A) Western blot analysis of the integrins from total cell lysate (TL) (lane 1), 5μl of α3 IP (lane 3)

and 5µl of α6 IP (lane 4) was performed using a polyclonal antibody which recognises both α3 and α6 integrin subunits (AA6A). (B) Equal loads (15µl) of α3 IP and α6 IP was used to detect for the presence of CD151. An abundance of CD151 was detected in the α3 co-IP (lane 2) while only a weak signal was detected for CD151 that co-precipitated with α6 (lane 4). A long exposure was required for this blot in order to detect the low level of CD151 in α6 co-IP. In the second experiment (C & D), CD151 was IP-ed with mAb 5C11. (C) The presence of CD151 in the TL (lane 1) and IP (lane 3) was confirmed using anti-CD151 rabbit polyclonal antibody. (D) The relative abundance of α3 and α6 integrins in TL (lane 1) and in the CD151 IP (lane 3) was detected with anti α3/α6 antibody, AA6A. A large amount of α3 was detected in CD151 co-IP (lane 3, upper band) compared to the weak signal detected for α6 in CD151 co-IP (lane 3, lower band). (E) Secondary association between CD151 and α3β1 / α6(β1/β4) integrins subunits were analysed under 1% Brij 96 lysis condition. IP of CD151 was confirmed by Western blot [E(i), lane 3]. CD151 co-precipitated comparable levels of α3β1 and α6(β1/β4) integrins under this condition [(ii), lane 3]. Control IP (Ctr) in all the experiments consists of IP of lysate with beads without mAb bound to it. IP was performed in 1% TritonX-100 [(A) - (D)] and 1% Brij 96 (E) the immunoprecipitates were resolved by 12% SDS-PAGE for Western blot analysis.

3.1.6 Analysis of α6 integrin subunit in various tetraspanin depleted cell lines

Even though CD151 seems to preferentially associate with α3β1 integrin, α6 integrins are still recruited into the CD151 TERMs. My results so far showed that depletion of CD151 did not have any influence on the mobility of the light chain fragment of α6 integrin subunit when analysed by Western blotting. Besides glycosylation, another post translational modification of α6 integrin subunit which associates with both β1 and β4 integrin subunits has previously been reported in

human prostate and colon cancer cell lines (Davis et al., 2001). Here, a cleaved form of α6 subunit was detected. This cleaved variant of α6 integrin subunit which is missing the extracellular β-propeller region was named the α6p variant. Biochemical and kinectis analysis of this variant showed it was glycosylated as per normal but had a three-fold increase in half life compared to the full length α6 subunit. While endogenous α6p was found associated with β1 or β4 subunit, exogenous expression of this truncated form of α6 integrin subunit was not capable of dimer formation. In DU145 cells, it was found that all α6p variants can be surface biotinylated compared to 50% of the full length subunit. These observations taken together prompted the conclusion that α6p is not a degradation product, but resulted from cleavage that occurred at the cell surface (Davis et al., 2002; Demetriou and Cress, 2004). The α6p variant was later described as a product of ectodomain shedding due to proteolytic cleavage by urokinase-type plasminogen activator (uPA) (Demetriou et al., 2004). In their paper, Demetriou and Cress (2004) hypothesised that the ectodomain shedding only occurred when the α6 subunit is not tightly associated with CD151 (however, whether the proteolitic cleavage led to ectodomain shedding or the head region remained associated with β subunit was not explored in the study).

Consequently, I investigated the role played by CD151 in α6 integrin clipping in MDA-231 cells. Since my results so far seem to indicate that CD151 mainly forms secondary interactions with α6β1/β4 integrins, I also wanted to compare the

influence of other tetraspanins within a TERM on α6 integrin subunit's clevage. For this purpose, Western blot analysis for the integrin was performed on total lysates and immunoprecipitation of α6β1/β4 integrin from MDA-231, CD9-, CD63-, CD81- and CD151-knock-down cell lines. The predicted molecular weight of the α6p variant consisting of 497 amino acid residues is ~56.5 kD (www.bioinformatics.org/sms/index.html). However, owing to glycosylation, it resolves at a slighty higher position at ~65 kD.

In agreement with findings from the Cress laboratory, I found that depletion of CD151 increased the level of α6p variant in MDA-231 under non-reducing conditions [Figure 3.11(A)]. Additionally, I found that depletion of CD9 and CD81 (to a lesser extent) reduced the level of α6p variant in this cell line under non-reducing conditions. Interestingly, I also found a difference in the level of α6p variant detected under non-reducing [Figure 3.11(A)] and reducing conditions [Figure 3.11(B)]. For example, while some reduction was observed in α6p level in MDA CD9(-) cells under non-reducing condition, it was almost undetectable under reduced conditions. This difference probably reflects the presence of furin cleaved α6p fragments which under reducing conditions, will not be detected as an intact ~65kD fragment as illustrated in [Figure 3.11(C) iv & v].

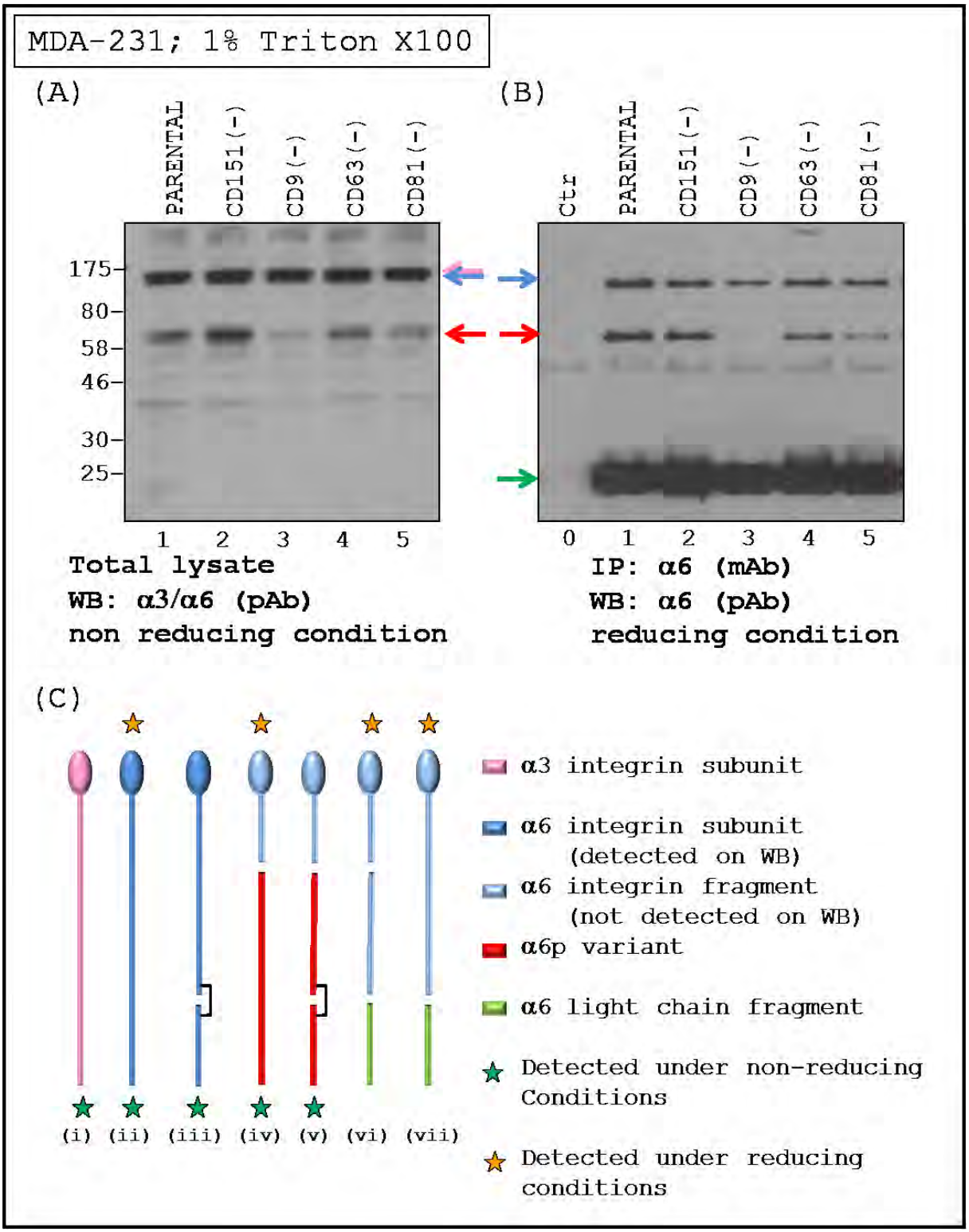

Figure 3.11 Analysis of α6 integrin subunit in various tetraspanin depleted cell lines.

The level of α6p integrin fragment (red arrow) in various tetraspanin depleted cell lines was analysed either from total cell lysate (TL) under non-reducing conditions

(A); or after immunoprecipitation of the α6β1/β4 integrin with mAb A6-ELE under reducing conditions (B). (A) Depletion of CD151 showed an increase in the level of α6p fragment in TL of MDA-231 cells (lane 2) compared to the parental line (lane 1). Depletion of CD9 (lane 3) and CD81 (lane 5) resulted in a decrease in the level of α6p fragment compared to the parental line. Depletion of CD63 did not seem to have any effect on the total level of α6p fragment. (B) A similar pattern was observed in the level of α6p fragment under reducing conditions. However, a general decrease was detected in the level of α6p under this condition. It is especially obvious in CD9 depleted cell line where α6p band was almost absent (lane 3). The proteins were resolved by 12% SDS PAGE and detected by Western blotting using anti-α6 pAb which binds both α3 and α6 light chain subunits. Samples were reduced by adding 1:20 v/v β-mercaptoethanol before denaturation.

3.1.7 DISCUSSION

In this study, I found that depletion of CD151 in metastatic breast cancer cell line, MDA-231, did not have any effect on the total and cell surface levels of its primary partners, α3β1 integrin and α6β1/α6β4 integrins. Flow-cytometry analysis of several other membrane proteins such as CD9, CD63, CD81, CD82 as well as α2 and β1 integrin subunits, revealed no difference in the level of these proteins upon CD151 depletion. Functionally, members of the tetraspanin family are associated with microdomain formation as well as intracellular and extracellular trafficking. The lacklustre effect CD151 depletion had on the cell surface presentation of various membrane proteins, including its primary partners α3β1 and α6β1 integrins, may indicate that CD151 does not regulate these proteins or it may also reflect a compensatory role played by other members of this family following CD151 depletion.

However, a detailed study of the α3 integrin subunit revealed a novel role played by CD151 during post-translation modification of the integrin. Depletion of CD151 altered the glycosylation of this integrin as observed from its mobility and band intensity on Western blots. The loss of this difference upon PNGaseF deglycosylation treatment confirmed CD151's role in glycosylation of α3β1 integrin. Depletion of CD151 in HeLa cell line produced similar, but not identical, changes to the glycosylation of α3β1 integrin demonstrating it to be a general phenomenon

exerted by CD151 on its partner. The differences observed between MDA-231 and HeLa cells may reflect the different repertoire of endogeneous glycosyltransferases expressed in each cell line. However, CD151 depletion in MCF7 cell line did not alter the integrin's mobility on Western blot even though EndoH treatment was performed to remove non-complex sugars that may mask the mature complex glycan (Figure 3.5). A possible explanation for this can be attributed to the fact that the level of endogenous CD151 in the MCF7 cell line is very low compared to MDA-231 and HeLa cell lines (Figure3.1) As such, depletion of CD151 in MCF7 cells, which was already expressing very low level of the tetraspanin, did not elicit the same level of response on the α3β1 integrin glycosylation.

Analysis of α6 integrin, another stoichiometric CD151 partner, in MDA-231 cell line showed no difference to its mobility or intensity on Western blot upon CD151 depletion. Furthermore, EndoH treatment of the lysate, which should accentuate any difference in glycosylation, remained unchanged (Figure 3.9). A possible explanation for this observation is the sensitivity, or lack of it, of Western blot assay in detecting subtle changes. Another possible explanation is that the N-linked glycosylation sites on the folded α6 integrin are located at an angle/site where they are independent from any CD151 influence. Furthermore, this result may also represent a difference in how the CD151/α3β1 complex and CD151/α6(β1/β4) complexes are trafficked during their transit in the ER and Golgi, whereby

glycosylation of α3β1 integrin is determined by CD151 while α6β1/α6β4 integrins are not (Baldwin et al., 2008).

Alternatively, this observation may be due to a difference in the stoichiometry of the association between CD151 and α3β1 over α6β1 or α6β4 in MDA-231 cell line. In order to investigate this possible angle, I compared the level of tight CD151/α3β1 pairing to CD151/α6(β1/β4) by co-immunoprecipitaion assay under 1% Triton X-100 condition. Western blot analysis clearly indicates that CD151 preferentially forms tight association with α3β1 compared to α6β1/α6β4 in MDA-231 cell line (Figure 3.10). Consequently, α3β1 integrin's glycosylation is modulated by CD151 while glycosylation of α6 integrins which do not form tight interaction with CD151 are not. This observation implies that tight association between CD151 and its partner may be a prerequisite for CD151 to exert its influence on their glycosylation profile. The possibility of preferential partnering is of particular interest since both α3β1 integrin and α6 integrins are capable of forming tight interaction with CD151. This observation raises several important questions. Firstly, what are the factors that determine the hierarchy of preferential association? Secondly, when a laminin binding integrin (in this case α6β1 / α6β4) is not tightly associated with CD151, do they have a new partner. And if they do, how does this alternate association affect their function.

CD151's influence in the glycosylation of α3β1 integrin seems to hinge on their direct association. However, although CD9 is considered to be a secondary partner of the integrin, it is still able to exert its influence on the integrin's glycosylation (Figure 3.7). Another secondary partner, CD81, did not have the same influence. One possible explanation for the difference in CD9 and CD81's influence is that CD9 may have a global role within the glycosylation pathway. For example, it may play an important role in trafficking molecules towards or away from compartments that are involved in specific glycomodification such as terminal glycan addition. Consequently, its depletion will affect a whole spectrum of proteins it is associated with including α3β1 integrin (This point will be discussed further in the later sections). Alternatively, the selective influence of secondary partners may also indicate the existence of independent subpopulation of α3β1 integrin within the TERM or different types of TERM complex (ie. [CD151/α3β1/CD9], [CD151/α3β1/CD81] and [CD151/α3β1/CD9/CD81] complexes). Comparison of α3β1 integrin population that co-precipitated with CD9 or CD81 showed a difference in the glyco-population of the integrin. This observation not only accounts for the difference in behaviour of the two tetraspanin towards the integrin, but it also suggests a functional hierarchy within various α3β1/CD151 complexes.

While depletion of CD151 did not have any effect on the glycosylation of α6β1/β4 integrins, it did seem to affect another post translational modification

attributed to α6 integrin subunit, the uPA mediated integrin clipping which resulted in the generation of α6p form. Depletion of CD151 increased the level of α6p while depletion of CD9 and CD81 decreased its level. The clevage of α6 integrin subunit which occurs at or near the cell surface alters the affinity and avidity of receptor – ligand interaction and allows rapid cellular response to changes in its environment. This modification is thought to be developmentally regulated since a dynamic membrane remodelling system is crucial during rapid growth (Peschon et al., 1998; Zhao et al., 2001). The existence of α6p fragment was first identified in DU145 moderately metastatic prostate cancer cell lines. Metastatic progression in prostate cancer has been linked to, among other factors, α6 integrin subunit's class switch from $\alpha6\beta4$ to $\alpha6\beta1$ (Demetriou and Cress 2004), down-regulation of CD9 (Wang et al., 2007) and up-regulation of CD151 (Ang et al., 2004), while RNAi knock-down of uPA and uPAR inhibited prostate cancer cell invasion (Pulukuri et al., 2005). The α6p variant was first characterised in prostate cancer cell line, and was proposed to increase tumour cell migration by limiting its adhesion to Lm511. Depletion of CD151 in MDA-231 cells, which incidentally resulted in increased α6p variant presentation (Figure 3.11) has been shown to reduce its migratory potential towards Lm332 (Baldwin et al., 2008). Furthermore, I found that depletion of CD9 in MDA-231 resulted in decreased α6p expression. Reduced CD9 expression prosate cancer on the other hand, is associated with increased metastatic potential. These contradicting responses may indicate that other factors are also involved in determining the

outcome of α6 integrin cleavage. For instance, difference in the affinity of α6β1/β4 integrins towards different laminins may influence the tumour cell's response. Moreover, how cells respond when they are directly sitting on the laminin may defer from how they respond when they are migrating towards the laminin which is presented as a haptotactic attractant. These observations taken together, paints a complex and dynamic relationship that exists between integrin receptors and their ligands in modulating the invasive process. Accordingly, it underscores the importance of considering not only the level, but also the post-translational modification of cell surface receptors in understanding the metastatic process.

3.2 Generation of various CD151 mutant and wild type reconstituted MDA-231 cell lines

In this study, I uncovered a previously unknown role of CD151 in modulating glycosylation of α3 integrin. In order to identify CD151's characteristic that contributes to this function of the protein, a series of MDA-231 cell lines expressing various CD151 mutants were generated as follows: (1) CD151 glycosylation-deficient mutant (CD151/GLY), (2) CD151 palmitoylation-deficient mutant (CD151/PLM), (3) CD151 C-terminal deletion (CD151/dC), (4) CD151 N-terminal substitution with N-terminal domain of CD63 (CD151/dN), (5) CD151 QRD →INF substitution at position 194-196 in the large extracellular loop (CD151/QRD), and a (6) Chimera consisting of CD151 large extracellular loop on a CD9 backbone (CD151/SW6). These constructs were reintroduced into the MDA-231 CD151 (-) cell line. Besides the panel of CD151 mutants, I also generated a wild type CD151 reconstituted cell line (CD151/REC). Detailed description of the mutant constructs and cell lines generated is presented in the Materials and Methods (Section 2.2.2 and 2.3.3).

3.2.1 Flow cytometry analysis of MDA-231 CD151 mutant cell lines

The mutant CD151 cell lines generated was first analysed by flow cytometry to ensure that the CD151 mutants were expressed at a level comparable to the wild type CD151. Flow cytometry analysis showed the reconstituted cell lines to express similar levels of the tetraspanin as depicted in Figure 3.12. The mean of fluorescence intensity value is accompanied in Table 3.1. However, I also observed that the CD151(PLM) mutant was less stable compared to other mutants in MDA-231 cell line. The expression level of this mutant decreased by 50% within a period of 1 week after fresh cell sorting.

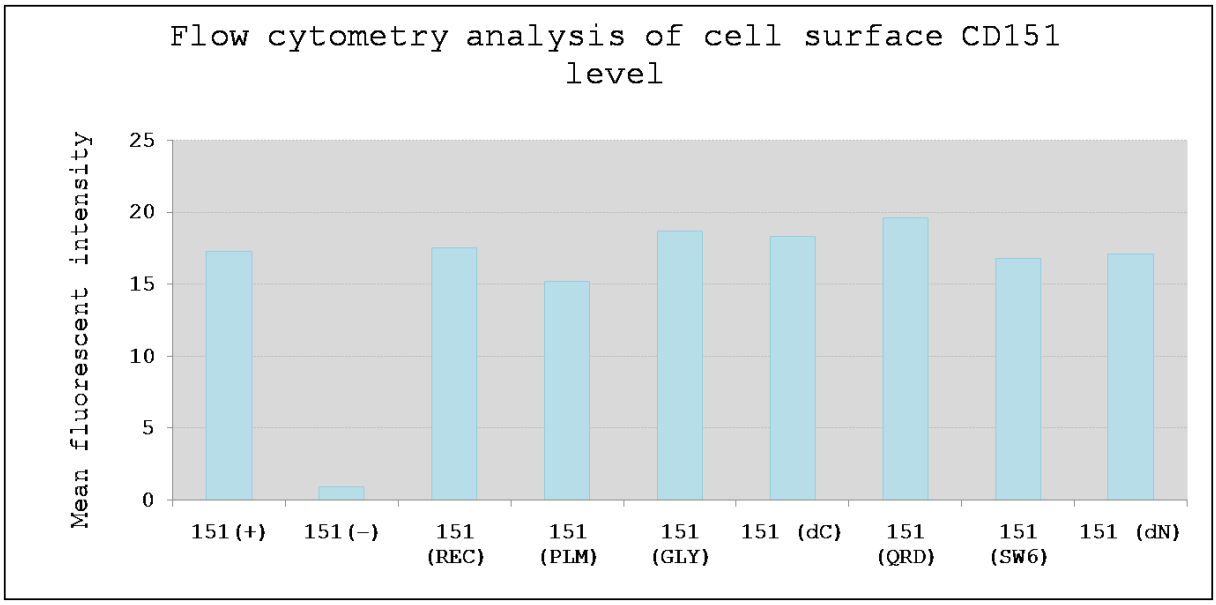

Figure 3.12 Flow cytometry analyses of cell surface CD151 levels on the panel of CD151 mutant cell lines. Cells were incubated in primary anti CD151 mAb (5C11), followed by FITC conjugated goat anti mouse secondary antibody. Cells were washed after each incubation and the level of the CD151 epitope was measured on EPICS XL Flow cytometry (Coulter) using System II software (Coulter).

Table 3.1 Flow cytometry analysis of cell surface level of CD151 detected with anti CD151 (mAb 5C11)

	CD151 (+)	CD151 (-)	CD151 (REC)	CD151 (PLM)	CD151 (GLY)	CD151 (dC)	CD151 (QRD)	CD151 (SW6)	CD151 (dN)
MFI	**17.3**	**0.9**	**17.5**	**15.2**	**18.7**	**18.3**	**19.6**	**16.8**	**17.1**

MFI: Mean fluorescence intensity

3.2.2 Biochemical analyses of the CD151 mutants in MDA-231

The panel of CD151 mutant cell lines generated were analysed biochemically to assess the stoichiometry of their association with their primary partner, α3β1 integrin. This association was examined by lysing the cells in 1% Triton X-100, a condition which only maintains tight primary interactions. Upon lysis, CD151 was immunoprecipitated with anti-CD151 mAb (5C11) bound IgG beads and analysed for CD151 and α3 integrin by Western blotting.

Co-immunoprecipitation analysis shows that the tight association of CD151 with α3β1 integrin was markedly reduced with the introduction of QRD->INF mutation in the LEL (Figure 3.13) as previously described (Kazarov et al., 2002). Furthermore, mutation of the QRD site in LEL of CD151 affected its detection by CD151 mAb, 11B1.G4. This finding is also consistent with a previous study where substitution of glutamine to lysine (Q194K) of the QRD triamino sequence in CD151

reduced their ability to be precipitated by mAb 11B1.G4 by ~60% (Yamada et al., 2008).

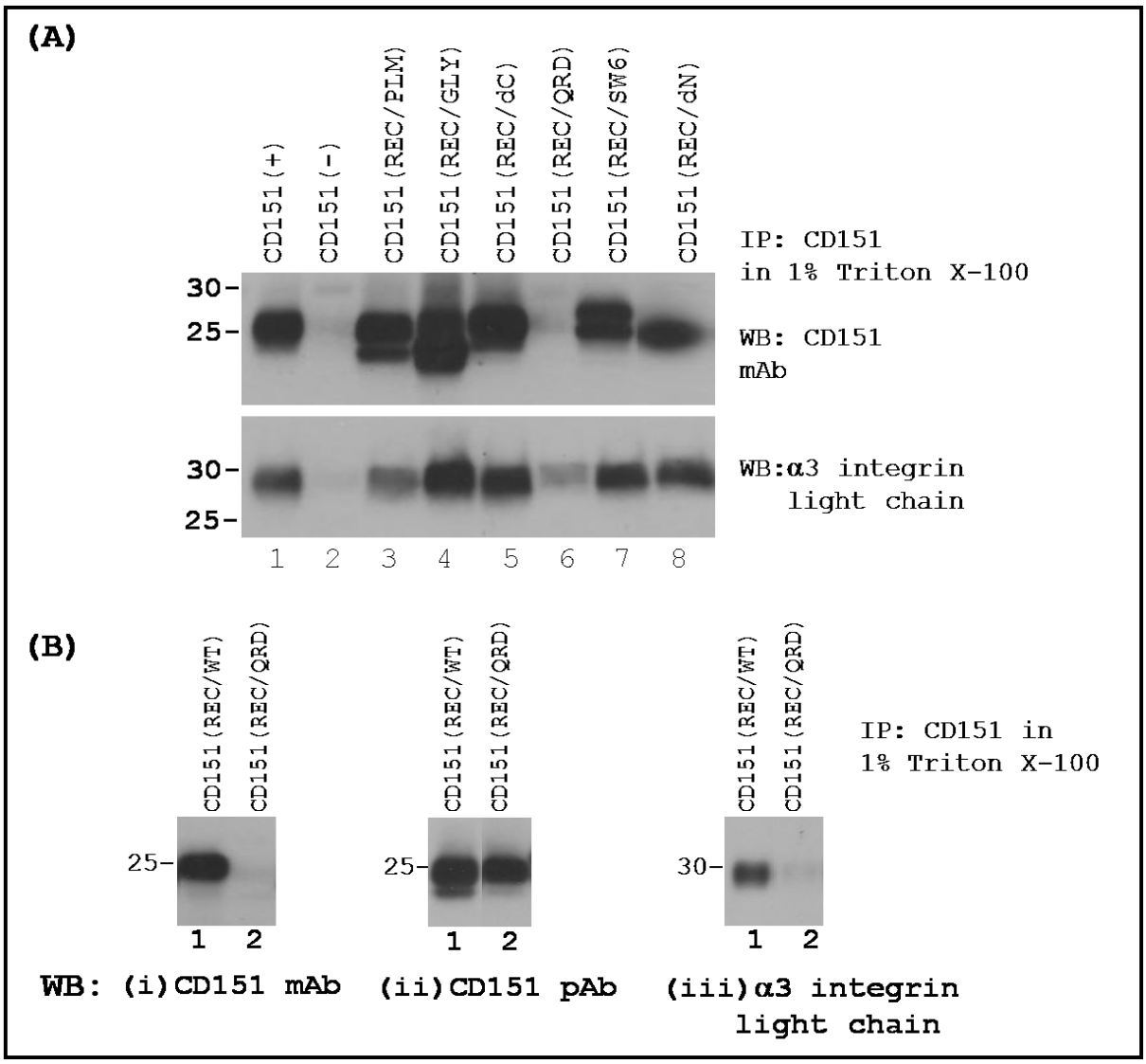

Figure 3.13 Analysis of CD151 and α3 integrin interaction in various CD151 mutant cell lines.

(A) Cells were lysed and immunoprecipitation (IP) of CD151 was performed under 1% Triton X-100 condition. The eluate was resolved by 12% SDS PAGE and analysed by Western blotting for CD151 mAb (11B1.G4) and α3 integrin (rabbit polyclonal). CD151's strong association with α3β1 under this condition (lane 1) is lost upon depletion of the tetraspanin (lane 2). Association of CD151 with α3 integrin in cells

reconstituted with CD151 glycosylation mutant (lane 4), C-tail deletion (lane 5), CD9/CD151 chimera, SW6 (lane 7) and N-tail substitution (lane 8) was comparable to the wild type CD151. However, as expected, α3 integrin's association with CD151 is reduced in cell lines expressing QRD mutant forms of CD151 (lower panel, lane 6) compared to the parental line (lower panel, lane 1). (B) Immunoprecipitation of CD151 was performed in CD151 (-) cell line reconstituted with CD151 (REC) and CD151 (QRD) and the level of CD151 was analysed by Western blot with CD151 monoclonal antibody (11B1G4) [i] and CD151 rabbit polyclonal antibody [ii]. A comparable level of CD151 was detected in co-IP of both cell lines when detected with CD151 pAb [ii] even though the CD151 mAb did not give and signal for QRD (i). This result confirms that the reduced level of α3 that co-precipitated with CD151 in QRD mutant (iii) is due diminished capacity of the integrin to form tight association with CD151 (QRD) mutant.

The panel of CD151 mutant cell lines were also assayed for their ability to recruit α3β1 integrin into the TERM. For this purpose, the cells were lysed in 1% Brij96 lysis buffer and CD9- and CD81- containing complexes were immunoprecipitated. The efficiency of the immunoprecipitation was confirmed by Western blot analysis for CD9 or CD81. The immunoprecipitation complex was then analysed for the presence of α3β1 integrin by Western blotting (Figure 3.14).

The level of α3 integrin that co-precipitated with CD9 or CD81 in CD151 (PLM) mutant cell line was markedly reduced compared to the level of wild type CD151. This result is in accordance with previous observations on the role played by palmitoylation of tetraspanin in lateral interactions (Berditchevski et al., 2002). In

addition, CD151 (dN) and CD151 (SW6) mutants showed reduced level of α3β1 integrin co-precipitation with both CD9 and CD81 IP. However, this reduction was not as drastic as the reduction observed for CD151 (PLM). CD151 (GLY), CD151 (dC) and CD151 (QRD) showed similar levels of co-precipitation with CD9 compared to the wild type CD151. Interestingly, CD151 (QRD) mutant which loses its capacity to associate tightly with α3 integrin subunit is still capable of recruiting α3β1 integrin into the TERM under 1% Brij96 condition. Similar observation have recently been reported on the ability of CD151 (QRD) mutant to form secondary lateral interaction under Brij99:Brij96V (1:1) lysis condition (Zevian et al., 2011).

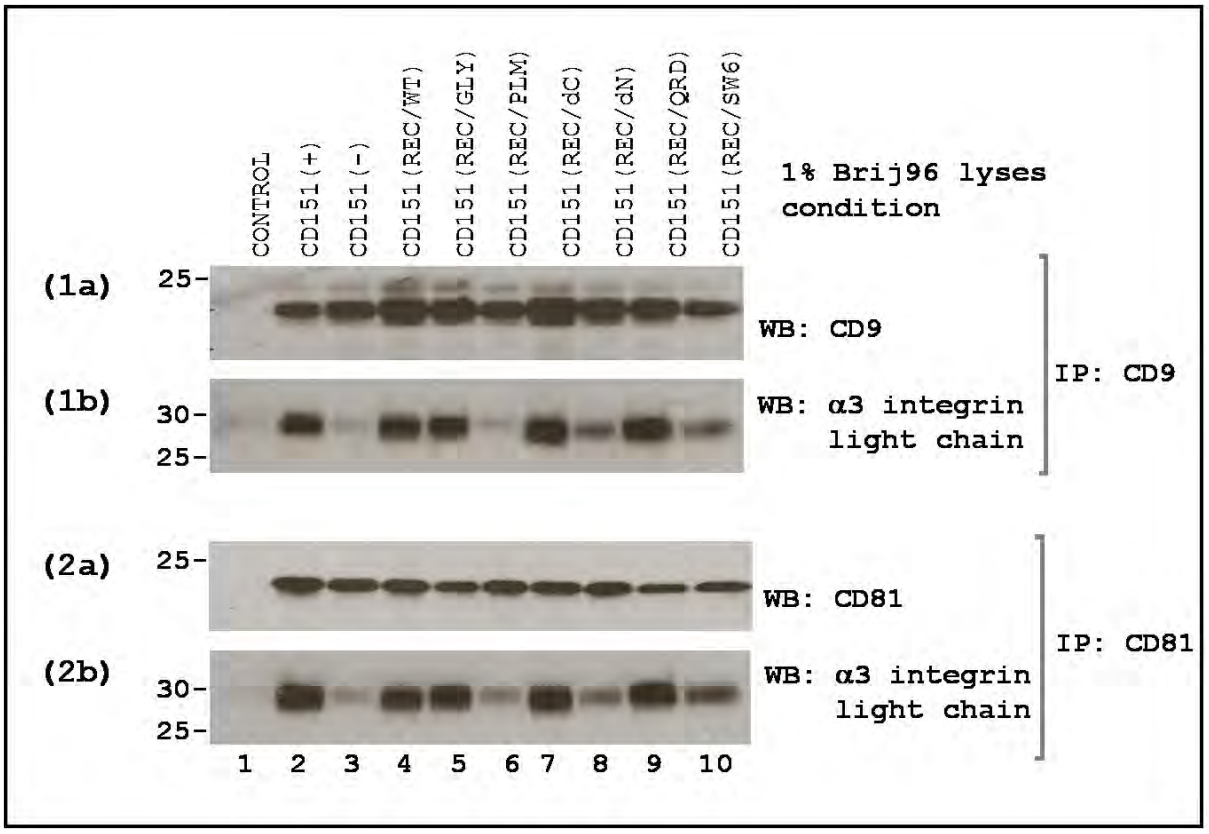

Figure 3.14 Analysis of CD151 mutant panels for potential secondary interaction formation.

CD9 (mAb C9BB) and CD81 (mAb M38) co-immunoprecipitation complex captured in 1% Brij96 lyses buffer condition was resolved in 12% SDS PAGE and analysed by Western blot. The presence of CD9 (1a) in CD9 IP and CD81 (2a) in CD81 IP was confirmed by western blot to ensure the IP was successful. The level of α3β1 integrin that co-precipitated with CD9(1b) and CD81(2b) in each of the MDA-231 CD151 variant cell line was compared. Presence of CD151 enables α3β1 integrin's recruitment into the TERM in both CD9 and CD81 IP (lane 2).The level of α3β1 integrin that co-IPed with CD9 and CD81 was markedly reduced in the absence of CD151 (lane 3) as well as in the CD151 (PLM) mutant (lane 6), however CD81 always coprecipitated slightly higher levels of the α3β1 integrin in these cell lines compared to CD9. CD151 (dN) (lane 8) and CD151 (SW6) (lane 10) demonstrated a less dramatic reduction in the level of α3β1 integrin that co-IPed with CD9 and CD81. Reconstitution of the wild type (lane 4), glycosylation deficient mutant (lane 5), C-tail deletion (lane 7) and QRD mutant (lane 9) co-precipitated similar levels of the

integrin compared to the parental line (lane 2). In the control experiment (lane 1), IP was performed in the absence of mAb.

3.2.3 Analyses of α3 integrin light chain in CD151 mutant cell lines

The glycosylation profile of α3 integrin light chain fragment in the panel of CD151 mutant cell lines was analysed to determine the CD151 characteristics that influences the integrin's glycosylation. Western blot analyses of α3 integrin light chain were performed on total cell lysate extracted with 1% Triton X-100. The various mutant cell lines presented an interesting mix of the α3 integrin light chain fragments glycosylation profile as depicted in Figure 3.15. Only the reconstitution of MDA-231 CD151 (-) cell line with the wild type CD151, C-terminal deleted CD151 (dC) or N terminal substituted CD151 (dN) reverted the glycosylation profile of α3 integrin light chain fragment to a wild type phenotype. Reconstitution of palmitoylation mutant CD151 (PLM), glycosylation mutant CD151 (GLY), QRD →INF substitution CD151 (QRD) and CD9/CD151 chimera CD151 (SW6) were unable to restore the α3 integrin light chain fragment glycoforms.

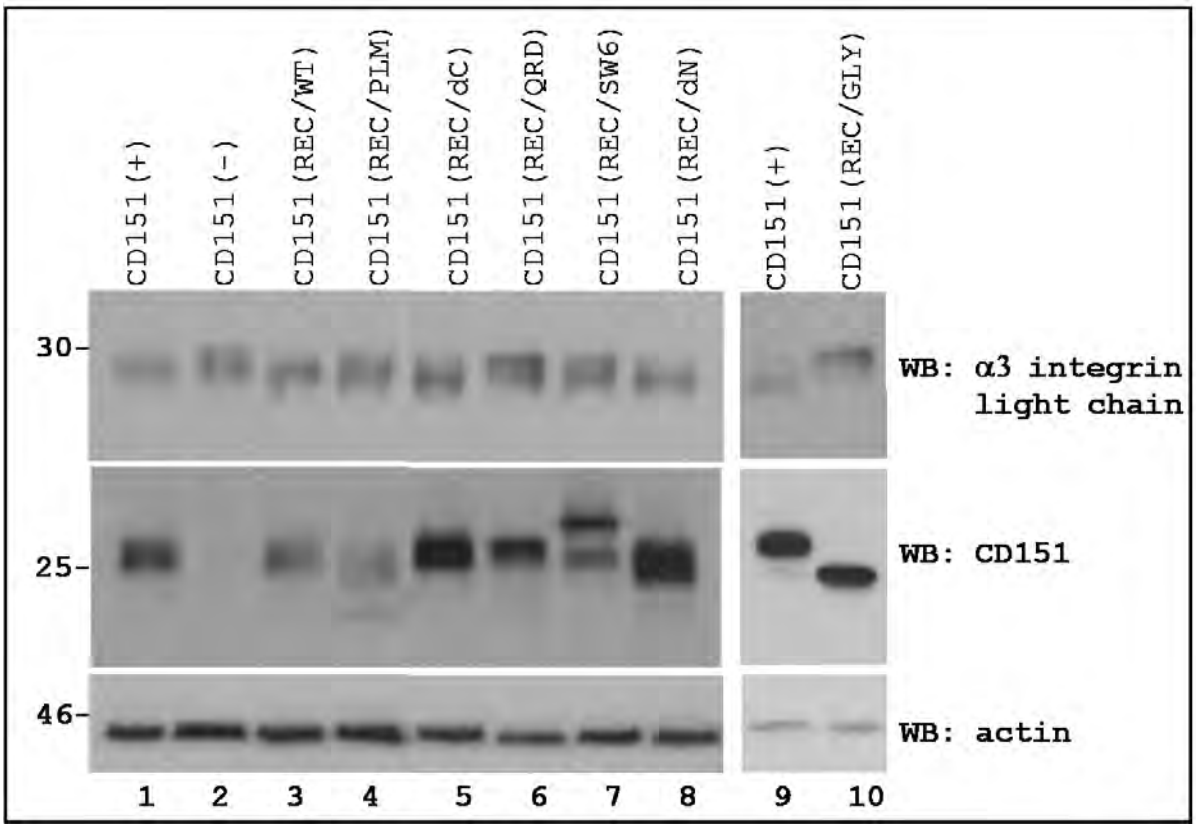

Figure 3.15 Western blot analyses of α3 integrin light chain and CD151 in various CD151 mutant cell lines.

Total lysate of MDA-231 cell lines harbouring various permutations of CD151 were resolved by 12% SDS-PAGE and analysed by Western blot (WB) for α3 interin light chain (upper panel) and CD151 (middle panel). Reconstitution of MDA-231 CD151(-) cell line with the wild type CD151 (lane 3) or CD151 mutants carrying C-terminal deletion (lane 5) or N-terminal substitution (lane 8) were able to revert the glycosylation profile of α3 light chain fragment to the pattern observed in the CD151 (+) cells (lane 1). However, reconstitution with CD151 palmitoylation-deficient mutant (lane 4), QRD mutant (lane 6), SW6 mutant (lane 7) and glycosylation-deficient mutant (lane 10) were unable to do so and a CD151 (-) phenotype for α3 integrin light chain fragment (lane 2) persisted in these cell lines. WB of actin confirms equal loading of the lysates (lower panel).

3.2.4 Sucrose gradient floatation analyses of MDA-231 CD151(+) and CD151(-) cell lines

It has previously been reported that α3β1 integrin transfected in B lymphoid Daudi cell line partitioned into the light fractions of 1% Brij97 sucrose density gradient floatation assay only in the presence of CD151 (Charrin et al., 2003). Brij 96 and Brij 97 lysis conditions have previously been shown to maintain secondary level of interaction and produce discrete and intact TERM complexes which are distrupted under the Triton X-100 condition which only maintains primary interactions. Even though more molecules are detected in tetraspanin complexes precipitated under Brij 96/97 conditions, both primary and secondary interaction represent functional relevence. Tertiary interactions between tetraspanins and other molecules are detected under conditions milder than Brij 96 such as Brij 98, Brij99 and detergent free conditions. Under these conditions, indiscriminate membrane domains are generated comprising of tetraspanin complexes and raft associated components (Class et al., 2001).

In this study, I found that glycosylation and palmitoylation of CD151 as well as tight association of CD151 with α3β1 integrin, are all required for CD151 to modulate glycosylation of α3β1 integrin. Consequently, since the glycosylation profile of α3 integrin in CD151 depleted cell line is similar to that of CD151(GLY), CD151(PLM) and CD151(QRD) mutants, we wanted to determine if recruitment into

the light fractions of 1% Brij96 sucrose density gradient correlated with CD151's characteristics which influences the glycosylation of the integrin. For this purpose, we first performed 5-35-45% discontinuous sucrose density gradient assay (SDG) in 1% Brij98, 1% Brij96 and 1% Triton X-100 to determine the effect of detergent strength on $\alpha 3\beta 1$ integrin partitioning in MDA-231 CD151(+) and CD151(-) cells. The results are presented in Figures 3.16 (Brij98), 3.17 (Brij96) and 3.18 (Triton X-100).

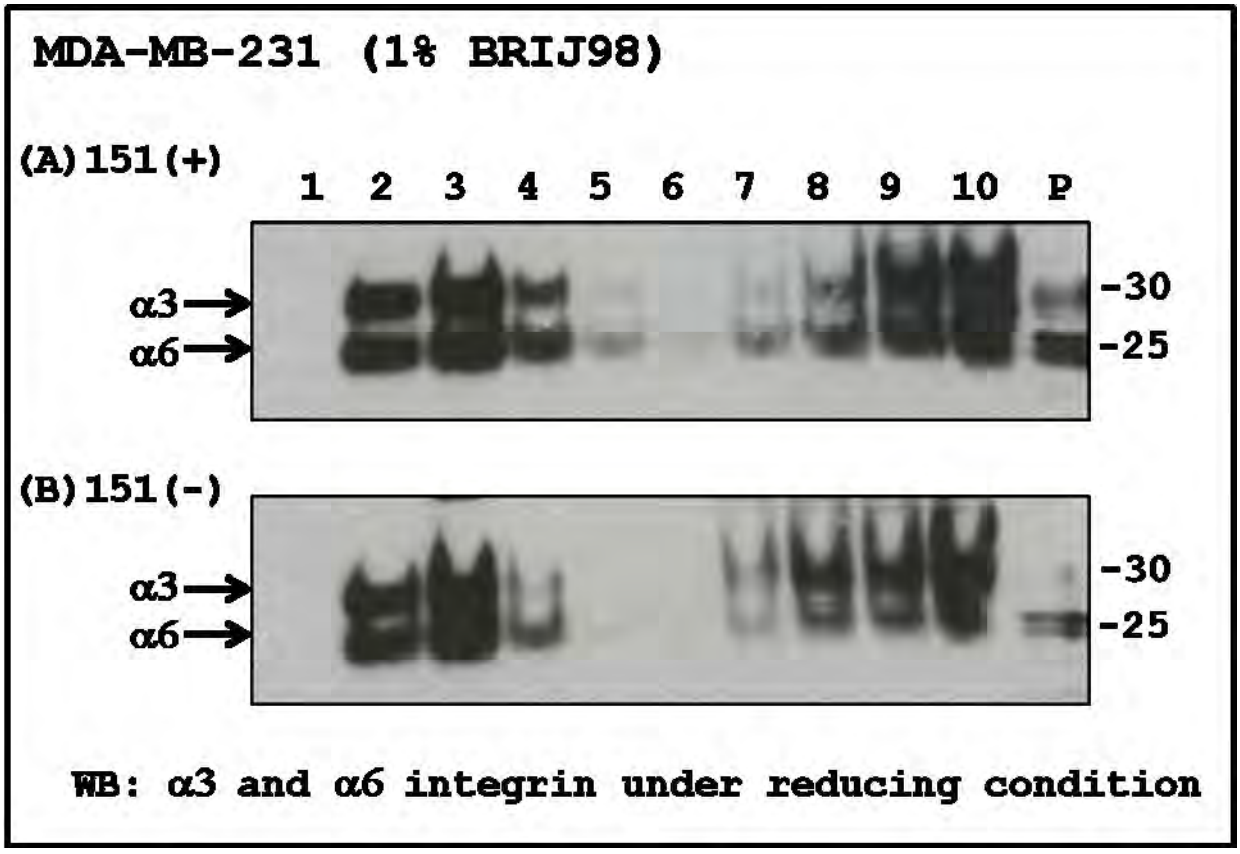

Figure 3.16 Western blot analyses of α3 and α6 integrin distribution in sucrose density gradient fractionation assay in 1% Brij 98.

Sucrose density gradient fractionation assay of cell lysate from (A) MDA-231 CD151 (+) and (B) MDA-231 CD151 (-) cells prepared in 1% Brij 98 was resolved by 12% SDS PAGE and analysed by Western blot for the distribution of α3 and α6 integrin subunits. Under these experimental conditions, the integrins were detected in the heavy fractions (lanes 7-10) and in light fractions (lanes 1-4) of the gradient in both cell lines. (P: cell pellet)

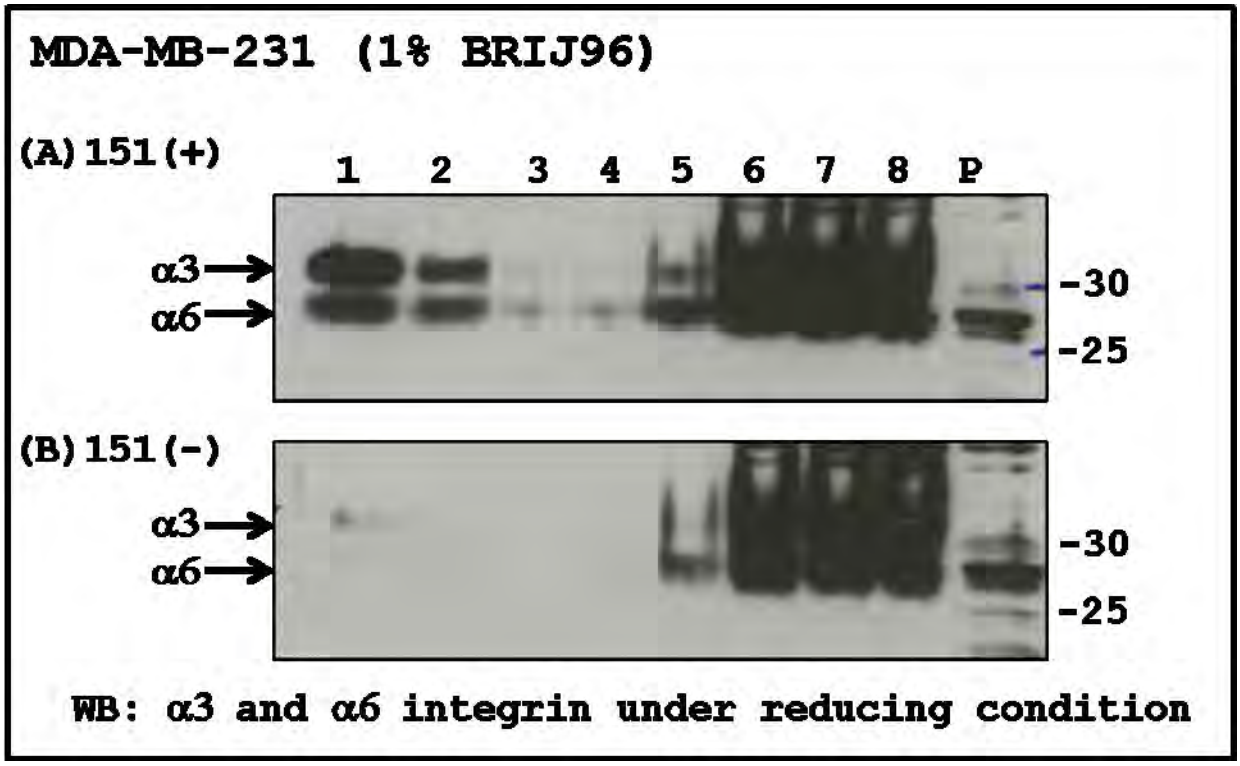

Figure 3.17 Western blot analyses of α3 and α6 integrin distribution in sucrose density gradient fractionation assay in 1% Brij 96.

Sucrose density gradient fractionation assay of cell lysate from (A) MDA-231 CD151 (+) and (B) MDA-231 CD151 (-) cells prepared in 1% Brij 96 was resolved by 12% SDS PAGE and analysed by Western blot for the distribution of α3 and α6 integrin subunits. Under these experimental conditions, the integrins were detected in the heavy (lanes 5-8) and light fractions (lanes 1 & 2) for lysate prepared from MDA-231 CD151(+) (A). However, in the absence of CD151, α3 and α6 integrin subunits failed to localise to the light fractions (B), lane 1&2. (P: cell pellet).

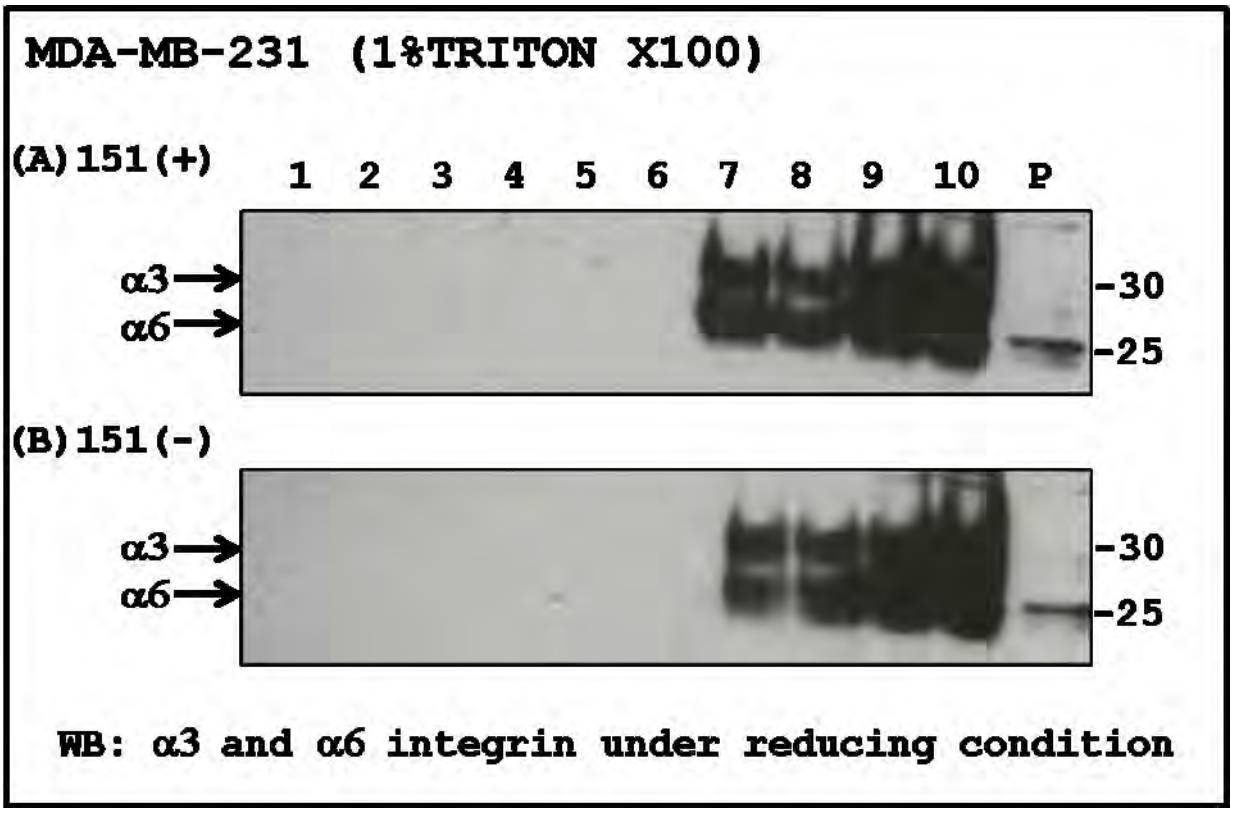

Figure 3.18 Western blot analyses of α3 and α6 integrin distribution in sucrose density gradient fractionation assay in 1% TritonX-100.

Sucrose density gradient fractionation assay of cell lysate from (A) MDA-231 CD151 (+) and (B) MDA-231 CD151 (-) cells prepared in 1% Triton X-100 was resolved by 12% SDS PAGE and analysed by Western blot for α3 and α6 integrin subunit distribution. Under these experimental conditions, the integrins were only detected in the heavy fractions (lanes 7-10), but not in the light fractions (lanes 1-4) of the gradient in both cell lines. (P: cell pellet)

Comparison of α3β1 integrin fractional distribution in MDA-231 CD151 (+) and CD151 (-) cell lines under three different detergent condition showed a difference only when the extraction was performed in 1% Brij 96 buffer. In agreement with previously published work (Charrin et al., 2003), the α3β1 integrin was only recruited into the light fraction of SDG in the presence of CD151. Analysis of α6 integrin subunit showed a similar distribution pattern to α3.

Since a difference was observed in the distribution of α3 integrin subunit during 1% Brij96 SDG between CD151 (+) and CD151 (-) cell lines, we analysed various fractions collected for the presence of several tetraspanin proteins (CD151, CD9, CD63 and CD82) as well as a lipid raft associated protein, Src. Western blot analysis of the various fractions obtained from 1% Brij96 SDG showed no difference in the distribution of any of these proteins upon CD151 depletion (Figure 3.19).

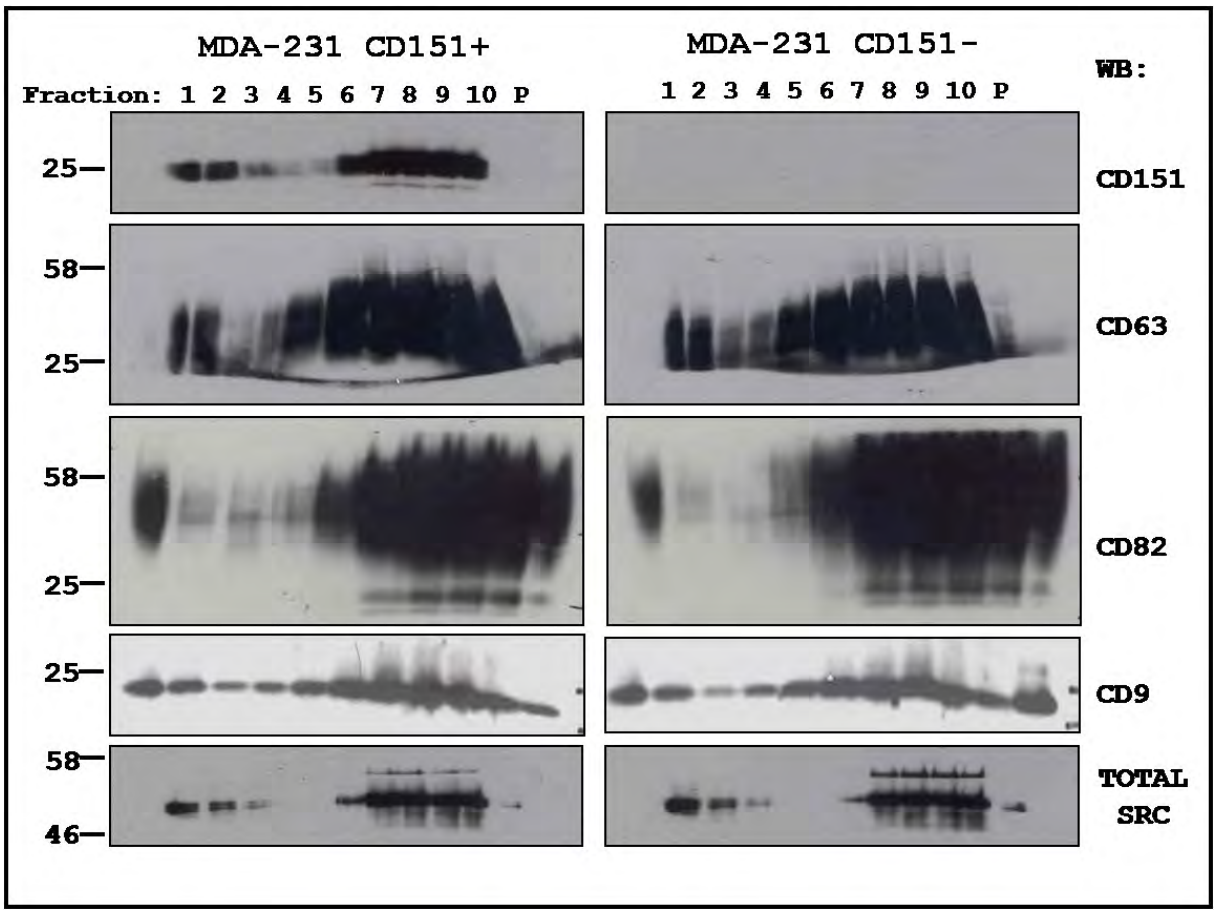

Figure 3.19 Western blot analyses of the distribution of various membrane associated proteins sucrose density gradient fractionation assay in 1% Brij 96.

SDG of cell lysate from MDA-231 CD151 (+) (left panel) and (B) MDA-231 CD151 (-) (right panel) prepared in 1% Brij 96 was resolved by 12% SDS PAGE and analysed by Western blot. Under these experimental conditions, no difference was observed in the distribution of CD9, CD63, CD82 and Src proteins upon CD151 depletion (P: cell pellet).

3.2.5 Sucrose gradient floatation analyses of MDA-231 CD151 (GLY) cell line

Ablation of CD151 in MDA-231 cells inhibited the recruitment of the α3β1 integrin to the light fractions of 1% Brij96 SDG. In order to determine if changes in membrane distribution may somehow affect glycosylation of the integrin, SDG was performed on MDA CD151 (GLY) cells in 1% Brij96 lysis condition. Our result showed glycosylation status of CD151 was irrelevant to its role in modulation the membrane distribution of α3β1 and α6β1/β4 integrins. Under these conditions, CD151 (GLY) was capable of recruiting these integrins to the light fractions of 1% Brij96 SDG (Figure 3.20).

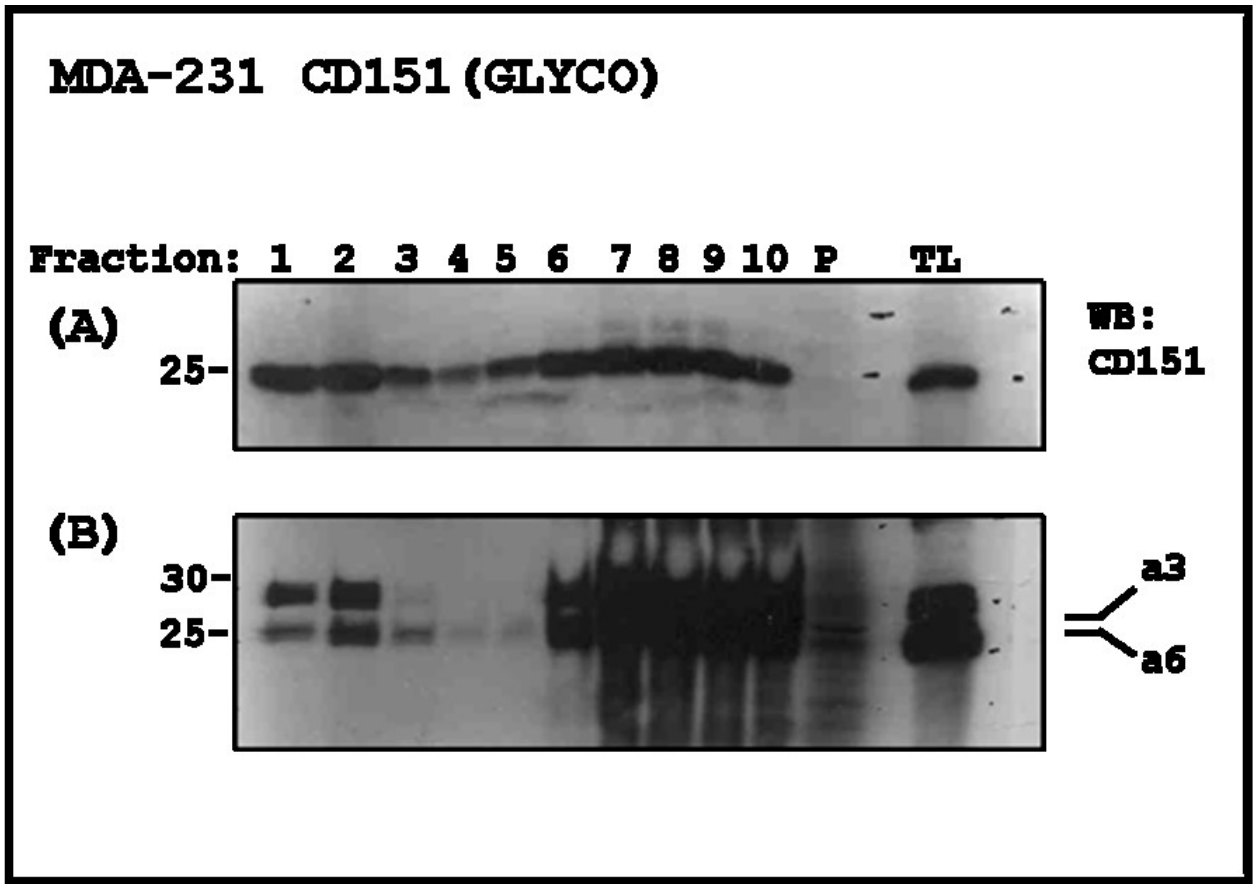

Figure 3.20 Western blot analyses of MDA CD151(GLY) sucrose density gradient fractionation assay in 1% Brij 96

SDG of cell lysate from MDA-231 CD151 glycosylation mutant prepared in 1% Brij 96 was resolved by 12% SDS PAGE and analysed by Western blot. Under these experimental conditions, presence of glycosylation mutant CD151 (A) as well as both α3 and α6 integrins subunits (B) were detected in the light fractions of the sucrose gradient (fractions 1-3), similar to that observed in parental line. (P: pellet; TL: total lysate)

3.2.6 Sucrose gradient floatation analyses of MDA-231 CD151 (PLM) and (QRD) mutant cell lines

It has previously been reported that palmitoylation of CD151 is crucial for its role in recruiting α3β1 integrin to the light fractions of Brij96 SDG (Yang et al., 2002). In order to confirm this observation, and to determine the contribution of CD151's tight association with α3β1 integrin in its ability to recruit the integrin to the light fractions, we also included CD151 (QRD) mutant cell line in this study. For the sake of uniformity, 1% Brij96 SDG was performed with MDA-231 CD151(+), CD151(-), CD151 (PLM) and CD151 (QRD) and detected for α3β1 integrin. Since I consistently found that the expression level of CD151 (PLM) decreased after several passages, I freshly sorted the CD151 (PLM) cell line one day before performing the SDG assay.

Surprisingly, I found that only the CD151 depleted MDA-231 cells were unable to recruit α3β1 integrin into the light fractions (fraction 1-4) of 1% Brij96 SDG (Figure 3.21B). CD151 (PLM) (Figure 3.21C) and CD151 (QRD) (Figure 3.21D) behaved similarly to the parental line (Figure 3.21A) and was able to recruit the integrin to the light fractions of SDG. Apart from its inability to restore the glycosylation of α3 integrin, no other biochemical changes have so far been attributed to CD151 (GLY). Consequently, its ability to recruit α3β1 integrin into the light fractions of the gradient was not unexpected (Figure 3.20). However, palmitoylation-deficient CD151 loses its ability to form lateral interaction with other

membrane proteins and recruit α3β1 integrin into the TERM while QRD mutation affects the tight interaction between α3β1 integrin and CD151. Yet, despite these major changes to their biochemical properties, both mutants were able to recruit α3β1 integrin into the light fractions of 1% Brij96 SDG. The CD151 (PLM) and CD151 (QRD) mutants were also able to recruit α6 integrins to the light fractions of 1% Brij96 SDG in MDA-231 cells (presented as supplementary data).

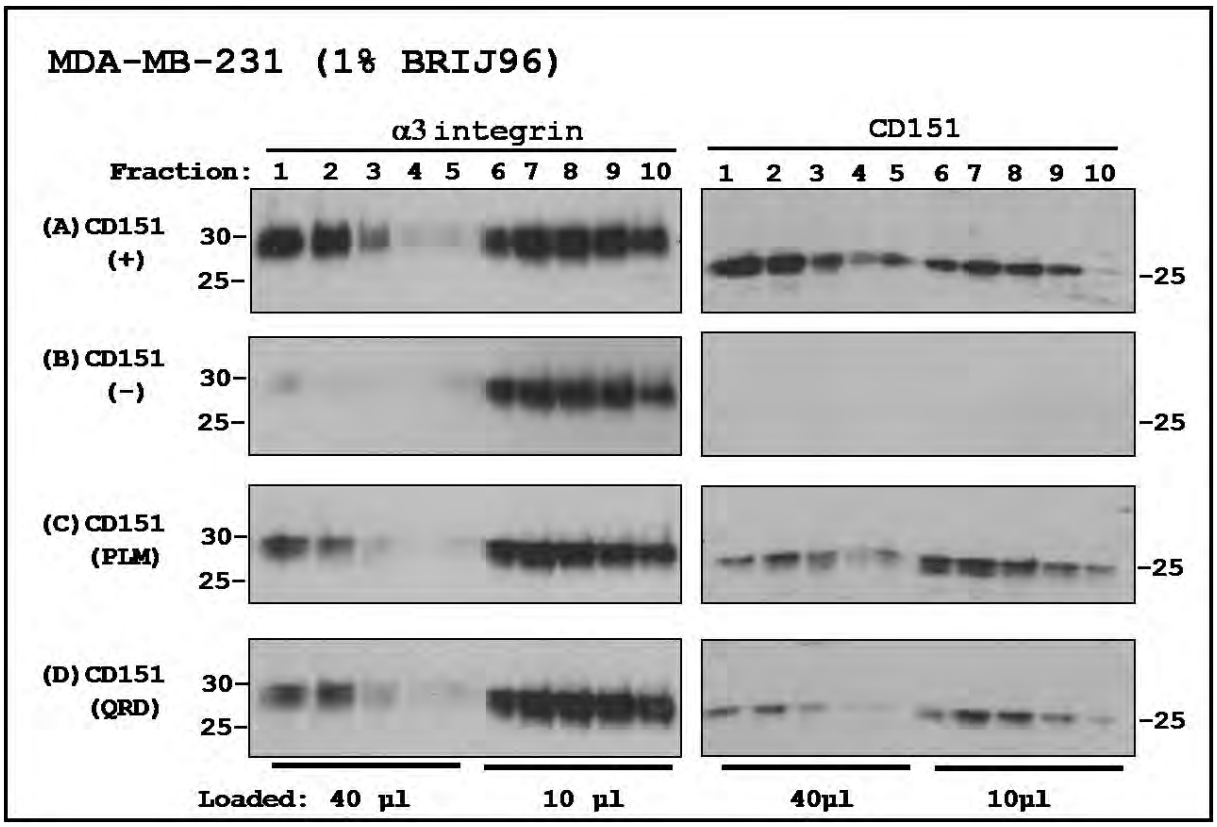

Figure 3.21 Western blot analysis of various MDA-231 sucrose density gradient fractionation assay in 1% Brij 96

SDG of cell lysate from MDA-231 (A) CD151 (+), (B) CD151(-), (C) CD151 (PLM), and (D) CD151 (QRD) prepared in 1% Brij 96 was resolved by 12% SDS PAGE and analysed by Western blot. Under these experimental conditions, presence of the various permutation of CD151 was detected in the light and heavy fractions of sucrose density gradient (right panels). Correspondingly, α3 integrin subunit was detected in the light fractions of the sucrose gradient (fractions 1-3) from MDA-231 (A) CD151(+), (B) CD151(-), (C) CD151(PLM) and (D) CD151 (QRD) cell lines. Only depletion of CD151 failed to recruit the integrin to the light fraction of SDG (B).

3.2.7 DISCUSSION

A panel of MDA-231 cell lines were establishedto determine the characteristics of CD151 that controls the glycosylation of the α3 integrin subunit. Most of these characteristics have previously been described, but the biochemical assays were performed in the presence of endogenous CD151. Consequently, I used an endogeneous CD151 free environment to study the characteristics of various CD151 permutations. Palmitoylation deficiency of CD151 has previously been shown to reduce the capacity of the tetraspanin to recruit α3β1 integrin into the TERM (Berditchevski et al., 2002). Furthermore, even though increased degradation of CD151 due to palmitoylation deficiency has been shown to be compensated by an increase in its synthesis (Berditchevski et al., 2002) altered subcellular localisation of nascently expressed palmitoylation tetra-mutant CD151 has also been suggested to reduce the half life of the protein (Yang et al., 2002). Additionally, knock-down of DHHC2, a CD9 and CD151 palmitoylating enzyme, have been shown to have a destabilizing effect on the tetraspanin but not on the level of the α3 integrin (Sharma et al., 2008). These studies have also reported that CD151 palmitoylation had no effect in its ability to form tight association with α3 integrin.

In agreement to previous findings, CD151 (PLM) showed a marked decrease in its ability to co-precipitate α3β1 integrin with CD9 and CD81 in 1% Brij96 (Figure 3.14). However, I also found that under 1% Triton X-100 condition, co-precipitation

of α3β1 with CD151 (PLM) was reduced compared to parental line (Figure 3.13A). This was unexpected as palmitoylation deficiency has been shown to have no bearing on the tight association of α3β1 integrin with CD151. A possible explanation may lie in the fact that, during the course of the study, I found that the stability of CD151 (PLM) tetraspanin was compromised in MDA-231 cell line. I consistently had to sort this cell line to maintain a comparable level of the mutated tetraspanin to the parental line. I speculate that while total level of α3β1 integrin may not be affected in this cell line, increased degradation rate of CD151 may affect the cellular ratio of α3 associated and α3 non-associated pools of CD151 (i.e. nascent CD151). Thus resulting in a reduced level of α3β1 co-precipitating with CD151 in the CD151 (PLM) cell line. Furthermore, previous studies on palmitoylation mutated CD151 were performed in cells expressing endogenous CD151 which may have masked the true characteristics of this mutant.

The tight association between CD151 and α3β1 integrin have been narrowed down to the QRD tri-amino sequence within the LEL of CD151 (Kazarov et al., 2002). And in agreement with this finding, I too found that the mutation introduced to the QRD site reduced the level of α3β1 integrin co-precipitating with CD151 in 1% Triton X-100 lysis condition (Figure 3.13). Secondary interaction between CD151 (QRD) and other components of TERM are however unaffected under 1% Brij 98 and 1:1 Brij99:Brij96V conditions (Baldwin et al., 2008; Zevian et al., 2011). In this study, we

found that recruitment of α3β1 integrin to the CD9 and CD81 associated TERM by CD151(QRD) was similar to the wild CD151 levels under 1% Brij96 lysis condition. Similar results have also been reported under 1:1 Brij99:Brij96V lysis condition (Zevian et al., 2011).

All other mutants [CD151: (GLY), (dC), (dN) and (SW6)] showed similar stoichiometry in their association with α3 integrin to wild type CD151 when IP of CD151 was performed under 1%Triton X-100 condition (Figure 3.13). Furthermore, CD151(GLY) and CD151(dC) were able to recruit α3 integrin to the CD9 and CD81 associated TERM at similar capacity as the wild type CD151 (Figure 3.14). Interestingly, CD151(dN) and CD151(SW6) recruited α3 integrin into the CD9 and CD81 associated TERM at a reduced capacity even though they both were able to form tight stoichiometric association with the integrin (Figure 3.14). A possible explanation for this observation is that both these constructs carry elements of other tetraspanins within them. CD151(SW6) is basically a CD9 molecule carrying CD151 LEL fragment while CD151(dN) is substituted at the N-terminal region with CD63. In both cases, even though they are capable of tight association with α3 integrin subunit through LEL, their lateral interactions may also be dictated by elements that interact with CD9's transmembrane and cytoplasmic regions or CD63's N-terminal region, respectively. Consequently, which TERM they are recruited into becomes a 'push

and pull' situation within the chimera and may explain why a reduced level of α3 integrin co-precipitated with CD9 and CD81.

My results showed that palmitoylation- and glycosylation- deficient mutants, QRD substitution mutant and SW6 CD9/CD151 chimera are unable to restore the glycosylation profile of the integrin to a wild type phenotype (Figure 3.15). The inability of these CD151 mutants to restore glycosylation profile of α3 integrin suggests a multi- layered influence of CD151 on glycosylation of α3 integrin. Tight association of CD151 with α3β1 integrin, recruitment into the TERM and glycosylation of the CD151 molecule itself all collectively contribute to the integrins glycosylation. Any distruption to this equilibrium alters the glycosylation of the integrin.

Interestingly, while, QRD->INF, SW6 and palmitoylation mutations affect either primary or secondary lateral interactions associated with CD151 and α3β1 integrin, glycosylation mutation which did not affect their tight association or their recruitment into the TERM, was unable to revert the glycosylation of the integrin to a wild type phenotype. Previous studies have shown a distinguishing difference between CD151(+) and CD151(-) cells in the way α3 integrin is distributed when sucrose density gradient is performed under conditions that keep a discrete TERM intact (Charrin et al., 2003b). We confirmed this in our model by performing SDG in 1% Brij98, 1% Brij96 and and 1% Triton X-100 for MDA-231 CD151 (+) and CD151(-)

cell lines. SDG in 1% Brij98 showed α3 integrin's distribution in heavy and light fractions for both cell lines. SDG performed in 1% Triton X-100 on the other hand distributed α3 integrin to only the heavy fractions in both cell lines, distinguishing it from lipid raft component. SDG in 1% Brij96 showed that in the absence of CD151, α3 integrin was not distributed into the light fractions. To determine if a co-relation exists between their ability to float into the light fractions and glycosylation of CD151, I performed SDG in 1% Brij96 with CD151(GLY), CD151(PLM) and CD151(QRD). In all three cell lines, α3β1 integrin was distributed into the light fractions of the SDG. Thus membrane distribution is independent of glycosylation status of α3 integrin subunit. Furthermore, I also found that recruitment into the light fractions was not solely dependent on TERM formation or CD151-α3β1 tight interaction. This was an intriguing observation, especially since it contradicts two previous findings that concluded palmitoylation-defecient CD151 does not localise nor recruit α3 integrin into the light fractions of SDG.

In the first study, SDG was performed on MDA-231 cells with or without 2-Bromopalmitate treatment (a potent inhibitor of protein palmitoylation). No difference was observed in the distribution of CD151 and α3 integrin between these two lysates (Berditchevski et al., 2002). However, the SDG was performed under non-detergent condition which does not discriminate TERM assemblies from 'larger indiscriminate pieces of membrane' that are usually produced under this condition.

This may explain why, in their study, the CD151/α3β1 complexes were not recruited into the light fractions (fractions 1-3) of the SDG. Similarly, in this study, SDG performed under 1% Brij98 condition did not show any difference in the distribution α3β1 integrin even in the absence of CD151 (Figure 3.16). In the second study, introduction of palmitoylation tetramutant of CD151 failed to localise CD151 and α3 integrin into the light fraction of 1% Brij 96 SDG (Yang et al., 2002), a condition that we used in our study. One possible explanation for this discrepancy is that their assay was performed using an N-terminal tagged CD151 palmitoylation tetramutant construct and this may have a bearing on how the protein interacts with its microenviroment. Furthermore, CD151(PLM) used in this study is mutated at all six palmitoylation sites as previously described (Berditchevski et al., 2002).

While the recruitment of α3β1 integrin by CD151(PLM) into the light fractions of SDG would rely on their tight association, the ability of CD151(QRD) mutant to recruit α3 integrin into the light fractions would solely depend on its capacity to form or be recruited into TERM. These two results, taken together, imply that CD151 is distributed into, and recruits α3β1 integrin into the light fraction of 1% Brij 96 SDG as part of [α3β1/CD51/TERM] complex as well as separate entities. And this entity may consist of [α3β1/CD51] complex or [α3β1/CD151/non-TERM] components.

3.3 CD151's role in glycosylation of α3 integrin

The N-linked glycosylation pathway is a multistep process with various factors influencing the glycosylation profile of the end product. Glycosidases and glycosyltransferases present within the endoplasmic reticulum (ER) and Golgi apparatus contributes through enzymatic modification while various chaperones determine when and where these modifications occur. The synergy between the enzymatic components and trafficking machinery determines the final glycosylation product. Tetraspanin function has largely been attributed to membrane associated complex formation and trafficking. Therefore, we hypothesised that CD151 may be influencing the glycosylation of α3β1 integrin by recruiting and channelling it to a specific pathway during the glycosylation process. To determine how or where CD151 exerts it influence along the glycosylation pathway, chemical inhibitors which terminate the glycosylation process at various stages were introduced into the growth medium. Inhibitor treated and untreated MDA-231 CD151 (+) and CD151 (-) cell lines were then harvested and comparison of their α3 integrin light chain fragment mobility on Western blot was made.

The progression of the glycosylation process can be inhibited at various stages using different inhibitors as summarised in Figure 3.22

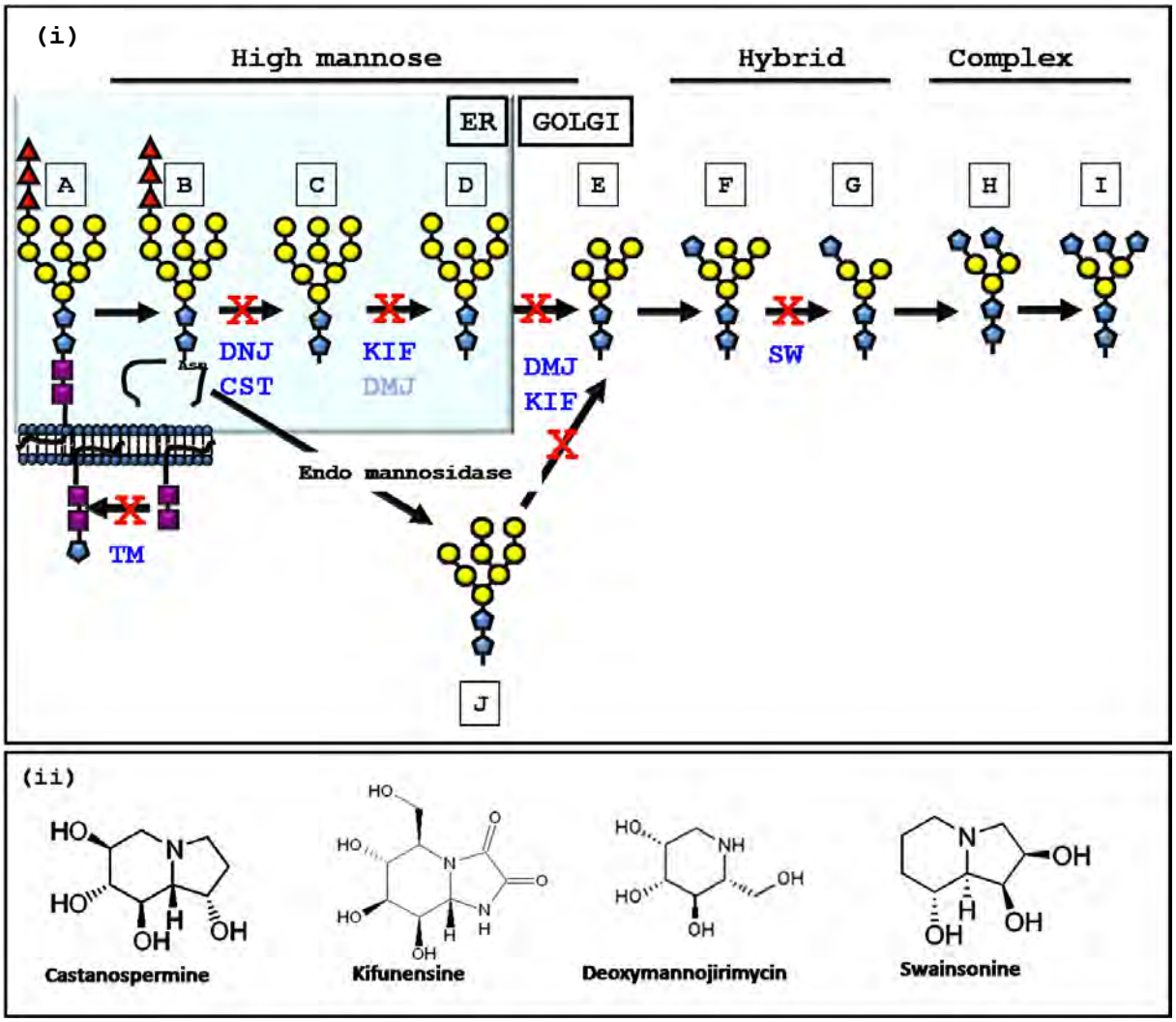

Figure 3.22 Inhibition of the glycosylation pathway with various chemical inhibitors.

(i)Tunicamycin (TM) inhibits the transfer of N-acetylglucosamine-1-phosphate from UDP-N-acetylglucosamine to dolichol phosphate, blocking the synthesis of all N-linked glycan. Deoxynojirimycin (DNJ) and Castanospermine (CST) inhibits glucosidase I and glucosidae II. Kifunensine (KIF) is a strong inhibitor of ER α-1,2-mannosidase I and Golgi mannosidase I while Deoxymannojirimycin (DMJ) mildly and strongly inhibits ER mannosidase I and Golgi mannosidase I respectively. Swansonine (SW) is a strong inhibitor of Golgi α-mannosidase II. The progression of the glycosylation process can be inhibited with these compounds at various stages. Inhibition with CST or DNJ can also be used to distinguish between glycoproteins that commit to the conventional ER mannosidase pathway and the Endo

mannosidase pathway. (ii) Chemical structure of various glycosylation inhibitors used in this study

3.3.1 Inhibition of the glycosylation pathway to determine the site of CD151's influence on α3 integrin glycosylation

CD151 has previously been reported to associate with α3 integrin during the very early stage of secretory pathway transition either in the ER or pre-Golgi compartments. This stable association is suggested to precede even the α3β1 dimer formation (Berditchevski et al., 2001). Consequently, I mapped CD151's influence on glycosylation of α3 integrin by inhibiting the glycosylation pathway progression at the early stages. MDA-231 CD151 (+) and (-) cells were grown in the presence of kifunensine, deoxymannojirimycin and swansonine, and cell lysates were analysed by Western bloting for α3 integrin. The detailed experimental procedure is presented in the Materials and Methods section.

The difference in the mobility of α3 integrin light chain between the two cell lines were maintained when the glycosylation progression is inhibited in cis (Golgi mannnosidase I) and medial Golgi (Golgi mannosidase II) [stage (E) and (G) respectively in Figure 3.22]. However, inhibition of ER mannosidase I with kifunensine revoked this difference [stage (D) in Figure 3.22] (Figure 3.23). Based on

this observation, CD151's influence on glycosylation of α3 integrin can be traced to the trimming of the first mannose residue in the ER.

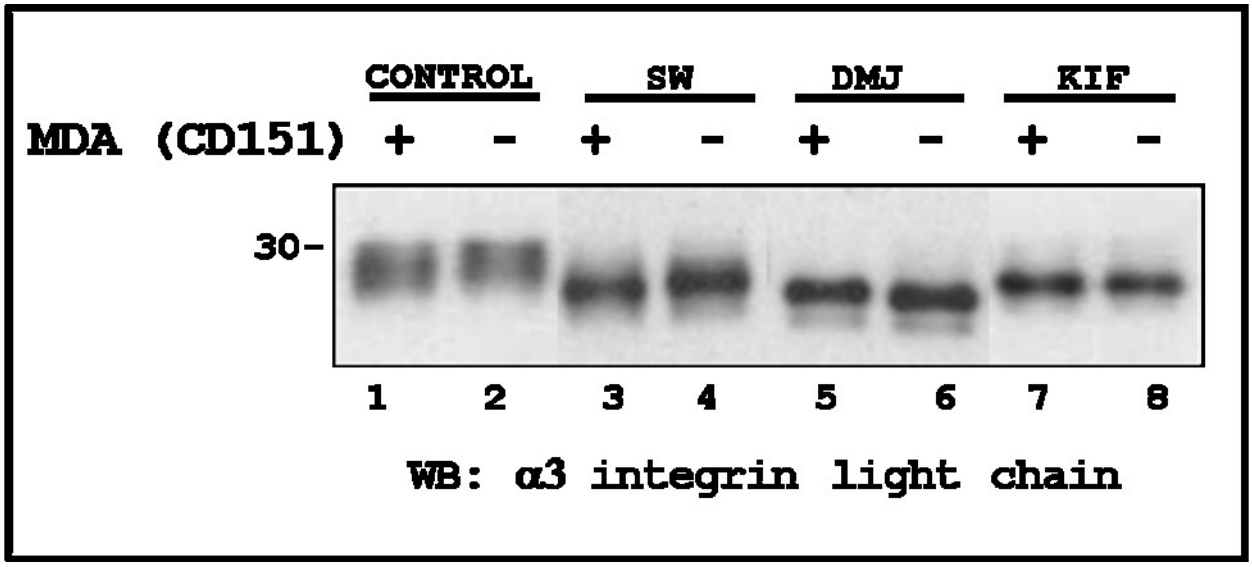

Figure 3.23 Western blot analysis of α3 integrin light chain upon inhibition of the glycosylation pathway.

MDA-231 CD151(+) and CD151 (-) were grown in the absence or presence of various glycosylation pathway inhibitors (Swainsonine, 2μg/ml; Deoxymannojirimycin, 2mM; Kifunensine, 2μg/ml) for 2-3 days, harvested and analysed by Western blotting for α3 integrin light chain. In the absence of inhibitors, difference in mobility is observed between CD151(+) (lane 1) and CD151(-) (lane 2) cells. Inhibition of the Golgi mannosidase II in the medial Golgi with swansonine (SW) maintained this difference (lanes 3 and 4). The difference between the two cell lines was still exhibited when treated with deoxymannojirimycin (DMJ) which predominantly inhibits Golgi α-mannosidase I in cis Golgi (lanes 5 and 6). However, inhibition of ER α-mannosidase I with kifunensine (KIF) abrogated this difference (lanes 7 and 8).

3.3.2 Partial characterisation of glycosyl moieties on α3 integrin purified from MDA-231 CD151(+) and CD151(-) cell lines

I have identified that CD151 influences the glycosylation of α3 integrin from the very first mannose trimming stage. In order to determine how changes in the early stage can affect the final glycosylation status of the integrin, I performed a large scale purification of the integrin from MDA-231 CD151(+) and CD151(-) cells and compared their lectin binding property on Western blot. Large scale purification of α3β1 integrin from MDA-231 CD151(+) and CD151(-) was performed using anti-α3 mAb (A3-IVA5) coupled to CNBr-activated beads. Lectins are protein or glycoproteins capable of binding to specific carbohydrate moieties. Due to their substrate specificity, they are often used to identify the presence of specific glycotopes. Detection with lectins that showed clear results was repeated with a fresh batch of purified integrins to confirm their binding pattern and the result is presented in Figure 3.24.

From the four lectins used in this study, two of them UEA I and PHA-E, showed altered binding capacity towards α3 and β1 integrin subunits. PHA-L and WGA did not show any difference in their binding capacity towards either subunit.

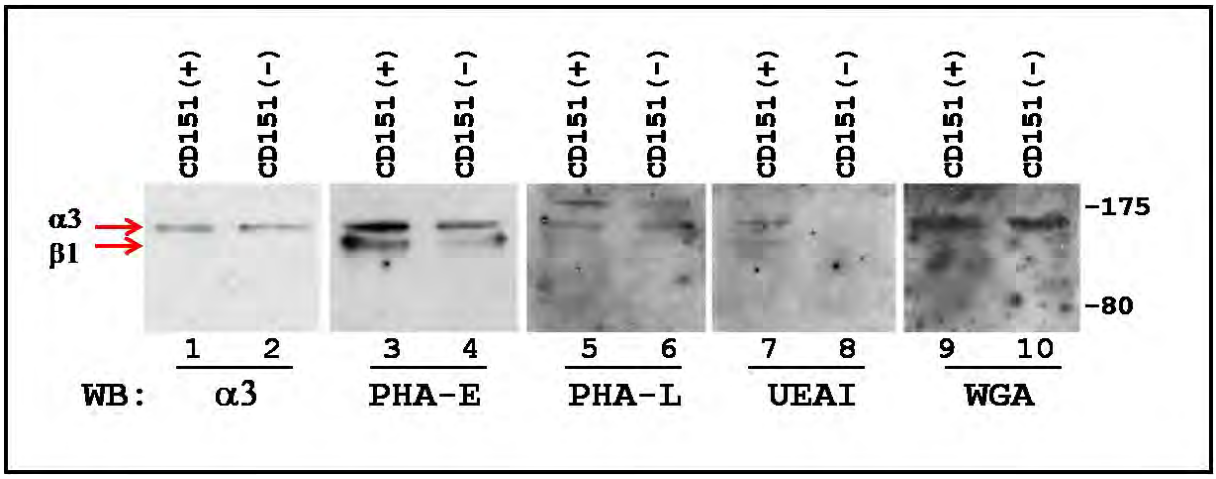

Figure 3.24 Western blot analysis of lectin binding assay on α3β1 integrin purified from MDA-231 CD151(+) and CD151(-) cells.

Purified integrins from MDA 231 CD151(+) [lanes 1, 3, 5, 7 and 9] and CD151(-) [lanes 2, 4, 6, 8 and 10] cells were resolved on a 10% SDS PAGE gel. Equal loading was confirmed by Western blot for α3 integrin (lanes 1 and 2). The red arrows represent positions of the integrin subunits on Western blot. The purified integrins were compared for their lectin binding property with four lectins: PHA-E (β1–4 linked GlcNAc) [lanes 3 and 4], PHA-L (β1–6 linked GlcNAc) [lanes 5 and 6], UEA I (α1–2 linked fucose) [lanes 7 and 8] and WGA (GlcNAc and sialic acid) [lanes 9 and 10]. Depletion of CD151 resulted in marked decreased of β1–4 linked GlcNAc (lanes 3 and 4) and almost complete loss of α1-2 linked fucose (lanes 7 and 8) that adorn the α3 subunit and its associated partner, β1 subunit. The binding of PHA-L and WGA was not affected. [UEA I: Ulex Europaeus Agglutinin I; WGA: Wheat Germ Agglutinin; PHA-E: Phaseolus vulgaris Erythroagglutinin; PHA-L: Phaseolus vulgaris Leucoagglutinin]

3.3.3 The effect of tetraspanin CD151 depletion on cell surface glycotope presentation

So far, my results indicate that depletion of CD151 did not change the cell surface expression levels of any of the proteins analysed (Figure 3.2). However, it did change the glycosylation of α3β1 integrin even though it did not have an apparent effect on the glycosylation of all other cell surface proteins analysed (Figure 3.9). In order to determine if CD151 may change the glycosylation of cell surface proteins other than α3β1 integrin, I analysed the lectin binding property of MDA-231 CD151(+) and CD151(-) cells by flow cytometry. A panel of lectins which recognise various glyco-motifs were used in this analysis and relative abundance of each glycan was compared between parental and CD151 depleted cell line. The panel of lectins used in this study as described previously in Table 2.5 is listed below:

Biotinylated Lectin	Glycan epitope
ConcanavalinA	α-linked mannose
Aleuria aurantia Lectin	fucose linked (α -1,6) to N-acetylglucosamine or fucose linked (α -1,3) to N-acetyllactosamine
Dolichos biflorus agglutinin	α-linked N-acetylgalactosamine
Peanut Agglutinin	galactosyl (β-1,3) N-acetylgalactosamine
Phaseolus vulgaris Erythroagglutinin	bisecting complex N-glycan
Phaseolus vulgaris Leucoagglutinin	Tri- and tetra- antennary N-linked glycans containing (β-1,6) linked N-

	acetylglucosamine
Ricinus communis agglutinin I	Terminal galactose and to a lesser degree, N-acetylgalactosamine.
Sambucus nigra agglutinin	(α-2,6) sialic acid attached to terminal galactose in and to a lesser degree, (α-2,3) linkage
Soybean Agglutinin	Terminal α- or β-linked N-acetylgalactosamine and to a lesser extent, galactose residues.
Ulex europaeus Agglutinin I	glycoproteins and glycolipids containing (α-1,2) linked fucose residues
Wheat Germ Agglutinin	N-acetylglucosamine and sialic acid

Depletion of CD151 reduced the cell surface binding capacity of UEA I by 52% and SBA by 43% (Figure 3.25). These two lectins specifically recognise α1-2 linked Fucose (UEA I) and terminal α or β linked N-acetylgalactosamine or galactose residues (SBA). All other lectins tested did not show significant difference in their binding capacity towards MDA-231 CD151(+) and CD151(-) cells. Interestingly, while the lectin blot assay on α3β1 integrin reflects the cell surface UEA I binding property, the Western blot analysis was not in agreement with flow cytometry data on PHA-E binding property (Figures 3.24 and 3.25).

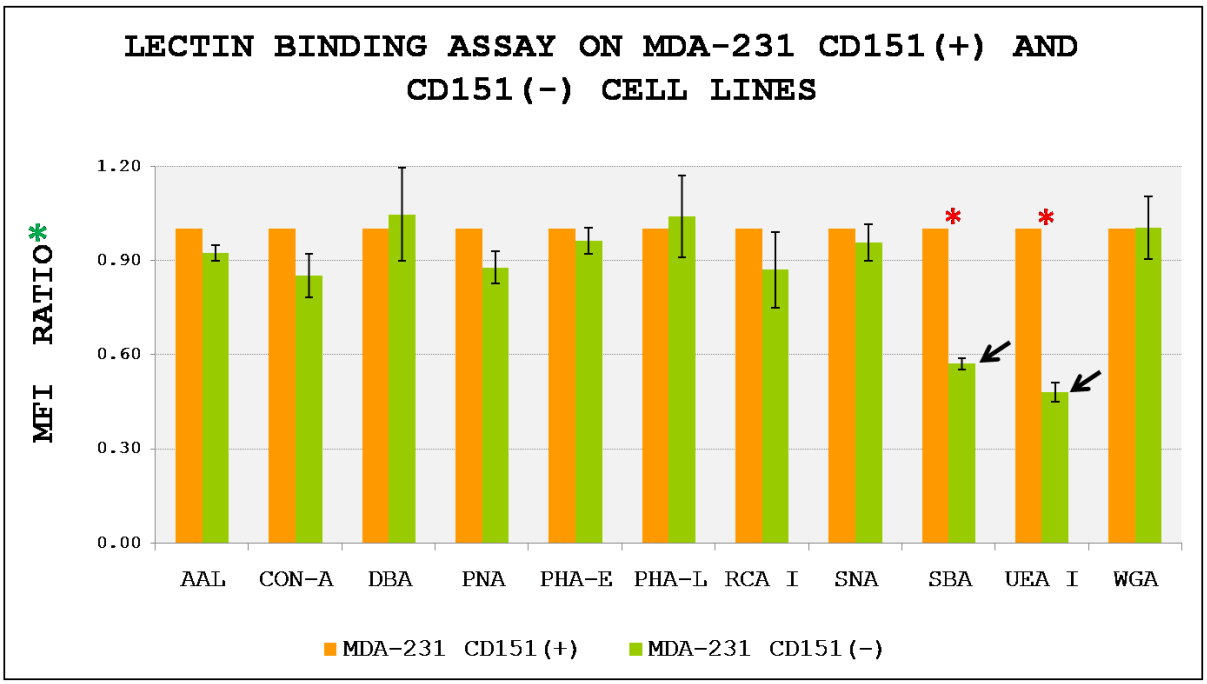

Figure 3.25 Flow cytometry analysis of lectin binding assay performed on MDA-231 CD151(+) and CD151(-) cell lines.

The lectins used for this experiment are Aleuria Aurantia Lectin (AAL), Concanavalin A (CON-A), Dolichol Bifloris Agglutinin (DBA), Peanut Agglutinin (PNA), Phaseolus vulgaris Erythroagglutinin E (PHA-E), Phasoelus vulgaris Leucoagglutinin L (PHA-L), Ricinus Communis Agglutinin I (RCA I), Sambucus Nigra Agglutinin (SNA), Soybean Agglutinin (SBA), Ulex Europeus Agglutinin I (UEA I) and Wheat germ Agglutinin (WGA). Depletion of CD151 in MDA-231 cell line resulted in a striking decrease in UEA and SBA binding capacity on the cell surface (black arrows). These lectins bind α1-2 linked Fucose and terminal α or β linked N-acetylgalactosamine respectively. Data is collated from three separate experiments. Raw data for all three experiments are presented in Appendix (2). (*) indicates significant difference between parental and depleted cell line ($P < 0.05$). (*) MFI ratio is calculated as follows: (MFI detected in depleted cell line/MFI detected in parental line).

3.3.4 The effect of tetraspanin depletion on cell surface glycosylation profile

Western blot comparison of α3 integrin light chain fragments in CD9, CD63 and CD81 depleted MDA-231 cell lines showed a difference in the mobility of the integrin only in the CD9 depleted cell line (Figure 3.7). However, all three tetraspanins are known to associate with other glycosylated protein. In fact, CD81 has been shown to influence the glycosylation of its primary partners, EW1/2 (Stipp et al., 2003) and CD19 (Shoham et al., 2006). Furthermore, glycosylation of H,K, ATPase β subunit, a CD63 partner, is important for lysosomal targeting (Vagin et al., 2004). Therefore, we investigated if depletion of these tetraspanins had any consequences on various glycotope presentation on the surface of MDA-231 cells. Using the same panel of lectins we used previously, cell surface lectin binding assay was performed and analysed by flow cytometry.

Figure 3.26

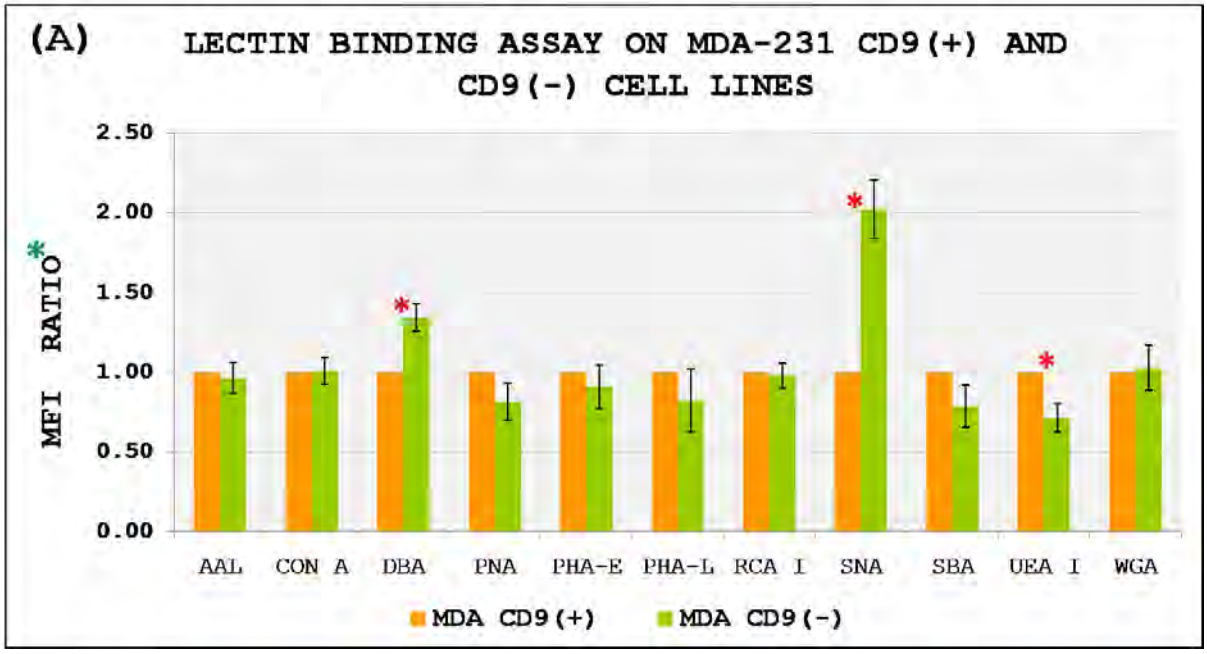
(A)
LECTIN BINDING ASSAY ON MDA-231 CD9(+) AND CD9(-) CELL LINES
MFI RATIO*
2.50
2.00
1.50
1.00
0.50
0.00
AAL
CON A
DBA
PNA
PHA-E
PHA-L
RCA I
SNA
SBA
UEA I
WGA
MDA CD9(+)
MDA CD9(-)

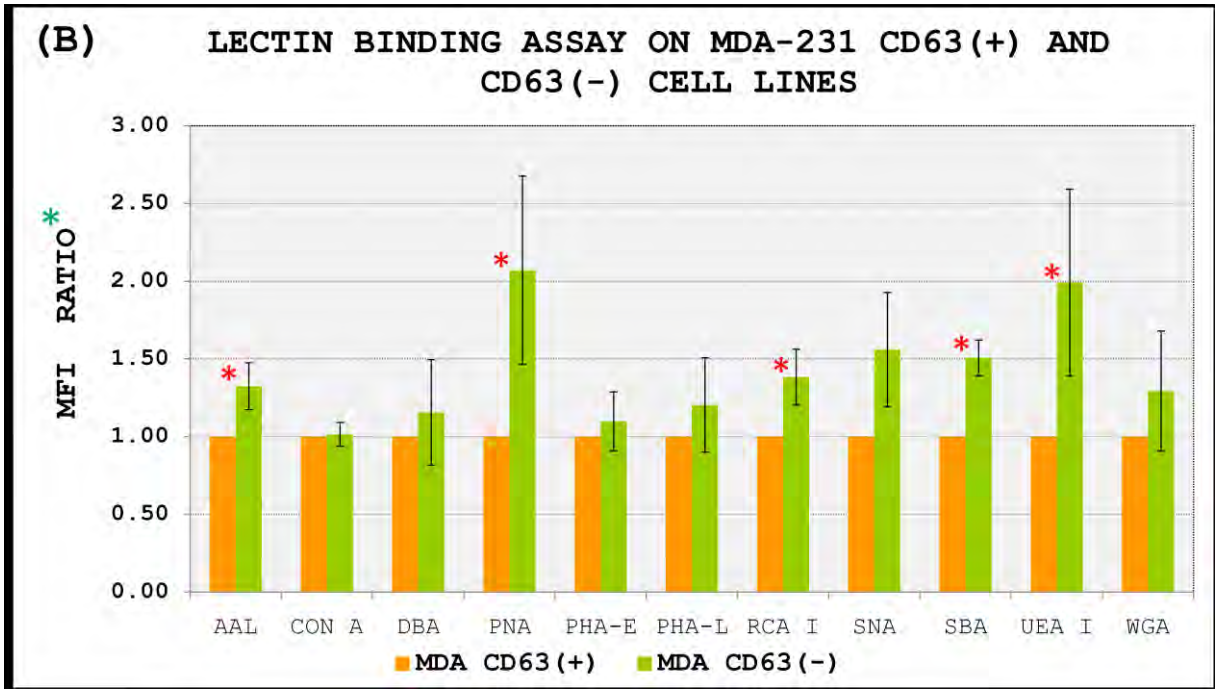
(B)
LECTIN BINDING ASSAY ON MDA-231 CD63(+) AND CD63(-) CELL LINES
MFI RATIO*
3.00
2.50
2.00
1.50
1.00
0.50
0.00
AAL
CON A
DBA
PNA
PHA-E
PHA-L
RCA I
SNA
SBA
UEA I
WGA
MDA CD63(+)
MDA CD63(-)

Figure 3.26….continued

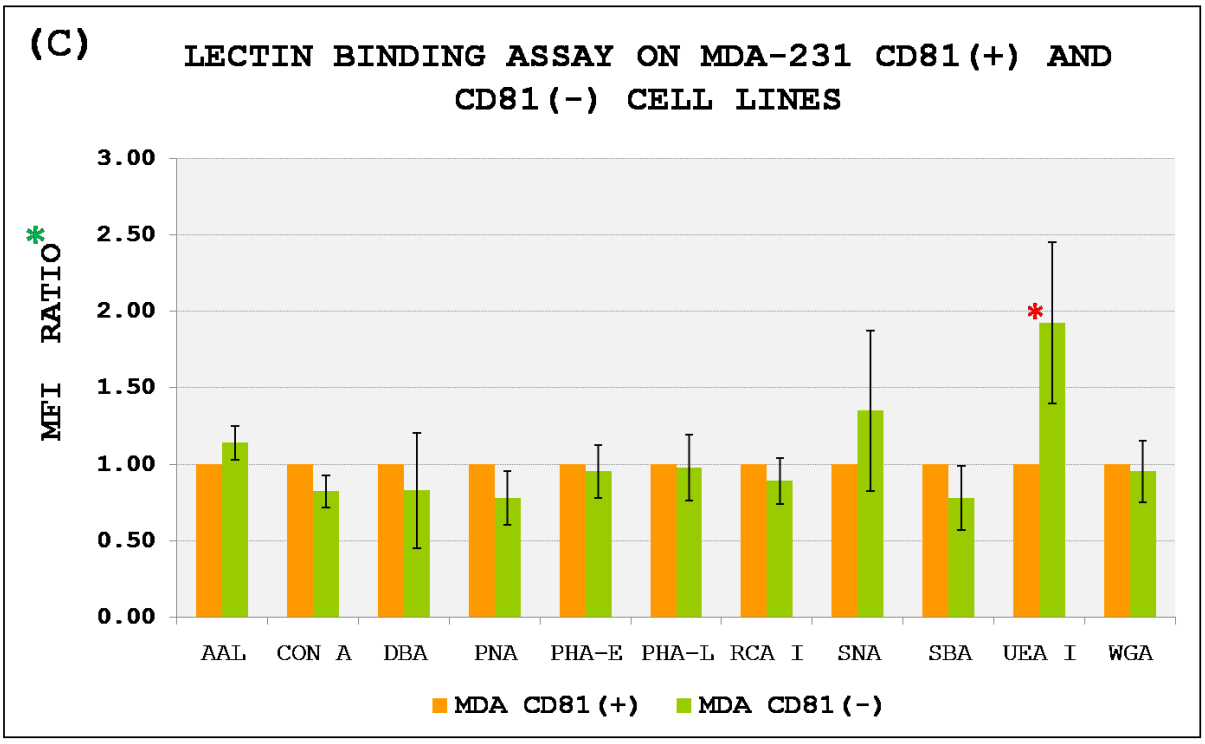

Figure 3.26 Flow cytometry analysis of lectin binding assay performed on MDA-231 parental and tetraspanin depleted cell lines.

Comparison was made between parental and CD9 depleted (A), CD63 depleted (B) and CD81 depleted (C) MDA-231 cell lines for their lectin binding capacity. The graphs represent an averaged result from three independent experiments. The lectins used for this experiment are Aleuria Aurantia Lectin (AAL), Concanavalin A (CON A), Dolichol Bifloris Agglutinin (DBA), Peanut Agglutinin (PNA), Phaseolus vulgaris Erythroagglutinin E (PHA-E), Phasoelus vulgaris Leucoagglutinin L (PHA-L), Ricinus Communis Agglutinin I (RCA I), Sambucus Nigra Agglutinin (SNA), Soybean Agglutinin (SBA), Ulex Europeus Agglutinin I (UEA I) and Wheat germ Agglutinin (WGA). Raw data for all three experiments are presented in Appendix (2). (*) indicates significant difference between parental and depleted cell line ($p < 0.05$). (*) MFI ratio is calculated as follows: (MFI detected in depleted cell line/MFI detected in parental line).

Depletion of CD9 resulted in 100% increase of cell surface level of 2-6 linked sialic acid based on their SNA binding capacity, as well as a 22% decrease in SBA and

29% decrease in UEA binding capacity. Binding of other lectins did not show obvious difference [Figure 3.26 (A)]. Depletion of CD63, on the other hand, resulted in a general increase in the binding capacity of all lectins. Specifically, UEA I and PNA (galactosyl (β-1,3) N-acetylgalactosamine) binding increase by 100% while SNA and SBA binding increase by 56% and 51% respectively [Figure3.26(B)]. And finally, depletion of CD81 resulted in a significant increase (92%) in the level of UEA I (α1–2 linked fucose) binding and a 35% increase in SNA binding capacity [Figure 3.26(C). Interestingly, depletion of all four tetraspanins, CD151, CD9, CD63 and CD81, seems to affect α1–2 linked fucosylation in MDA-231 cells. Depletion of CD151 and CD9 reduced while depletion of CD63 and CD81 significantly increased their cell surface expression.

3.3.5 DISCUSSION

Inhibition of the glycosylation pathway at various stages of glyco-maturation identified the first mannose trimming stage as the starting point of CD151's influence on the glycosylation of α3 integrin. Upon inhibition of ER α-mannosidase I by kifunensine, the mobility of α3 integrin light chain fragment from MDA-231 CD151(+) and CD151(-) cell lines were similar (Figure 3.23, lanes 7 & 8). This observation also indicates that within the ER, the integrin is processed by a kifunensine sensitive ER α-mannosidase I (Weng and Spiro 1993a). However a difference in their mobility was detected when inhibition was performed with 1-Deoxymannojirimycin (DMJ), a specific inhibitor of Golgi α-mannosidase I (Bischoff and Kornfeld, 1984). Migration of α3 light chain fragment from CD151(+) cell line was slower than in CD151 (-) cells when analysed by Western blot (Figure 3.23, lanes 5 & 6). DMJ was initially reported as a potent Golgi α-mannosidase I inhibitor, but was later shown to inhibit ER α-mannosidases as well. However, due to their much lower potency compared to kifunensine, it has been suggested that they may not efficiently inhibit all ER mannosidase I activity (Elbein et al., 1990; Weng and Spiro 1993a).

The best approach to determine how CD151 alters the glycosylation of α3 integrin subunit would be to perform a mass spectrometry analysis of the integrin's glycan structures from the two cell lines, upon various glycosylation inhibition

treatments. However, since those experiments were not performed in this study, we suggest here a few possibilities on how CD151 may influence the glycosylation of α3 integrin. The presence of CD151 may impose a conformational restraint that restricts the mannose-processing in α3 integrin subunit within the ER. Another plausible explanation is that, CD151 which has been trimmed by ER mannosidase I, exits the ER and inadvertently, bring along with it its tightly associated partner, α3β1 integrin, eventhough the integrin has not been trimmed by ER mannosidase I. The tight association between CD151 and α3β1 hastens the integrin's exit from ER, resulting in an unprocessed higher molecular weight form (possibly $Man_9GlcNAc_2$) being presented for trimming by Golgi α-mannosidase I. In the absence of CD151, the α3 integrin subunit is processed by ER α-mannosidase I resulting in the slightly reduced molecular weight form of the $Man_8GlcNAc_2$ isomer (B). This may also explain why the glycosylation deficient CD151 is unable to influence the glycosylation of the integrin. Alternatively, it could be due to a combination of both events, where CD151-α3β1 in its ligated form, due to constrained mannosidase I activity within the ER, takes an early exit. As a result, the α3 integrin's rapid departure from ER in the presence of CD151 will make it a substrate for Golgi α-mannosidase I which is capable of removing all α1,2-manose residues, resulting in a $Man_5GlcNAc_2$ structure.

The mammalian family of α 1,2-mannosidases differ in their kinetics, subcellular localisation and substrate specificity (Moremen et al., 1994). Even though

the slow advancing α3β1 integrin from CD151(-) cells will eventually be trimmed to $Man_5GlcNAc_2$ structure, variation in the high mannose form that reach the Golgi makes them preferred substrates for different isomers of Golgi α-mannosidase I. The Golgi α-mannosidase I isomer have previously been shown exhibit substrate specificity (Lal et al., 1998; Tempel et al., 2004), distinct subcompartmentalisation within the Golgi and cell specificity (Igdoura et al., 1999). Consequently, changes in the kinetics of mannose processing upon CD151 depletion may change the compartmentalisation of the integrin within the ER, resulting in the altered state of α3β1 integrin glycosylation. Furthermore, we found that the glycosylation of CD151 plays an important role in influencing the α3β1 integrin's glycosylation (Section 3.1; also described in Baldwin et al., 2008). These observations, taken together, may indicate that not only the presence of CD151, but glycosylation of CD151 molecule itself may recruit or steer the α3β1 integrin towards a select group of mannosidases and glycosyltransferases which inadvertently influences the glycosylation of the integrin.

While CD151 changes the glycosylation of α3 integrin subunit, the type of glycan that are presented on α3 will depend on the repertoire of glycosyltransferases present in these cells. A good example of this, is how CD151 itself is differently glycosylated in MDA-231, MCF7 and HeLa cell lines as observed from the difference in their mobility by Western blotting (Figure 1). In order to determine the glyco-

modification induced by CD151 in MDA-231, a comparison was made on the lectin binding capacity of α3 integrin purified from CD151(+) and CD151(-) cells. Depletion of CD151 showed a marked decrease in the level of α1,2-linked Fucose and bisecting GlcNAc-β(1-4) linked glycans presented on the α3β1 integrin. Both glycan structures have been shown to play a role in metastasis as described in the Introduction chapter. Fucosylation is especially important to enhance selectin binding and homing of haematopoietic cells. Increased expression of α1,2-linked Fucose which forms Lewis b/y antigen structures is a poor prognosis for lymph node negative breast carcinomas (Madjd et al., 2005). Consequently, it is interesting to note that CD151, identified as a metastasis promoter in breast cancer seem to promote the presentation of these antigens on α3β1 integrin. Furthermore, analysis of the cell surface glycan expression showed a marked decrease in the expression of α1,2-linked Fucose on the cell surface. The bisecting GlcNAc-β(1-4) branching detected with PHA-E has a more ambiguous role in metastasis (as described in the Introduction chapter - 1.5.3). This characteristic reflects the pro-and anti-metastatic stance CD151 molecules assume based on their environment. Incidentally, we observed a decrease in the level of PHA-E binding by α3β1 integrin upon CD151 depletion even though the surface expression of this glycotope was not duly effected.

Analysis of cell surface glycan presentation in MDA-231/ CD9, CD63 and CD81 depleted cells gave an interesting result. Notably, depletion of CD9 doubled the level of 2-6 linked sialic acid, another tumour associated glycan, presented on the

cell surface. Depletion of CD81 on the other hand, doubled the level of cell surface α1,2-linked Fucose. Though the consequences of these changes is still unknown, it is interesting to note that these tetraspanins seem to modulate the cell surface expression of various tumour associated glycans. Depletion of CD63 on the other hand resulted in a general increase of all the cell surface glycans probed for. This result may mean that CD63 plays an important role in glycosylation. On the other hand, CD63 is also known for its role as a major lysosomal targeting glycoprotein with a –GYEVM- lysosome targeting motif on its C-tail (Metzelaar et al., 1991). Consequently the accumulation of cell surface glycotope upon CD63 depletion may be due to sluggish internalisation and degradation rather than changes to the glycosylation process itself. The role that some of these tetraspanins may play in ER-Golgi-lysosome trafficking will be explored further in the later sections.

3.4 Physiological implications of changes in the glycosylation of α3 integrin

CD151 has been shown to either promote or suppress tumour progression in various studies. These opposing influences is usually attributed to the tetraspanin's interaction with various membrane and cytoplasmic proteins [as reviewed in (Stipp, 2010)]. However, no functional data are available on the consequences of CD151 mediated glycosylation changes in α3 integrin. In order to determine the contribution made by α3 integrin glycosylation to its function, I performed a Bowden chamber haptotactic migration assay towards Laminin332 (Lm332), a ligand for α3β1 integrin (Nishiuchi et al., 2003). In this investigation, I first performed the migration assay to confirm the specifity of α3β1-Lm332 interaction in our model cell line, MDA-231. Upon confirmation, we designed a migration assay experiment to address the role of α3 integrin glycosylation in migration towards Lm332.

3.4.1 Establishing the contribution of integrin α3β1 and α6β1/α6β4 in migration of MDA-231 cells towards Lm332

In order to confirm the specificity of the interaction between α3β1 integrin and Lm332, we performed the migration assay of MDA-231 cells in the presence or absence of function blocking antibody to α3 integrin subunit (A3-IVA5). We also used A3-X8 antibody which has been shown to slightly inhibit cell migration

(Hintermann et al., 2001). Integrins α6β1 and α6β4 on the other hand bind to several types of laminins including Lm332. To assess the contribution of the α6 integrins in migration, we blocked the integrin's function with anti-α6 (GOH3) monoclonal antibody. In the control experiment, we used the isotype control mAb to a cytoplasmic protein (PKCα). An 8 hour of migration was performed and the number of cells that migrated toward Lm332 was scored.

A bar chart comparing the migratory potential of MDA-231 cells upon various antibody treatments is presented in Figure 3.27. Pre-incubation of MDA-231 cells with a mildly blocking antibody, A3-X8, reduced the migration potential of these cells towards Lm332 by almost 50% compared to pretreatment with an isotype control, anti PKC. In cells preincubated with α3β1 blocking antibody, A3-IVA5, their migration potential was inhibited by 88% compared to the isotype control. Interestingly, pre-incubating the cells with GOH3 mAb which blocks the function of α6 integrins reduced the migration potential of these cells compared to isotype control by 41%. However, the level of inhibition was not dissimilar to level of inhibition observed upon A3-X8 pretreatment which mildly blocks α3β1 integrin function during cell migration. In both cases, ~50% decrease was observed compared to the isotype control. The drastic decrease in migration potential upon blocking of α3β1 integrin function with A3-IVA5 antibody shows that under these experimental

conditions, migration of MDA-231 cells towards Lm332 is predominantly mediated by α3β1 integrin.

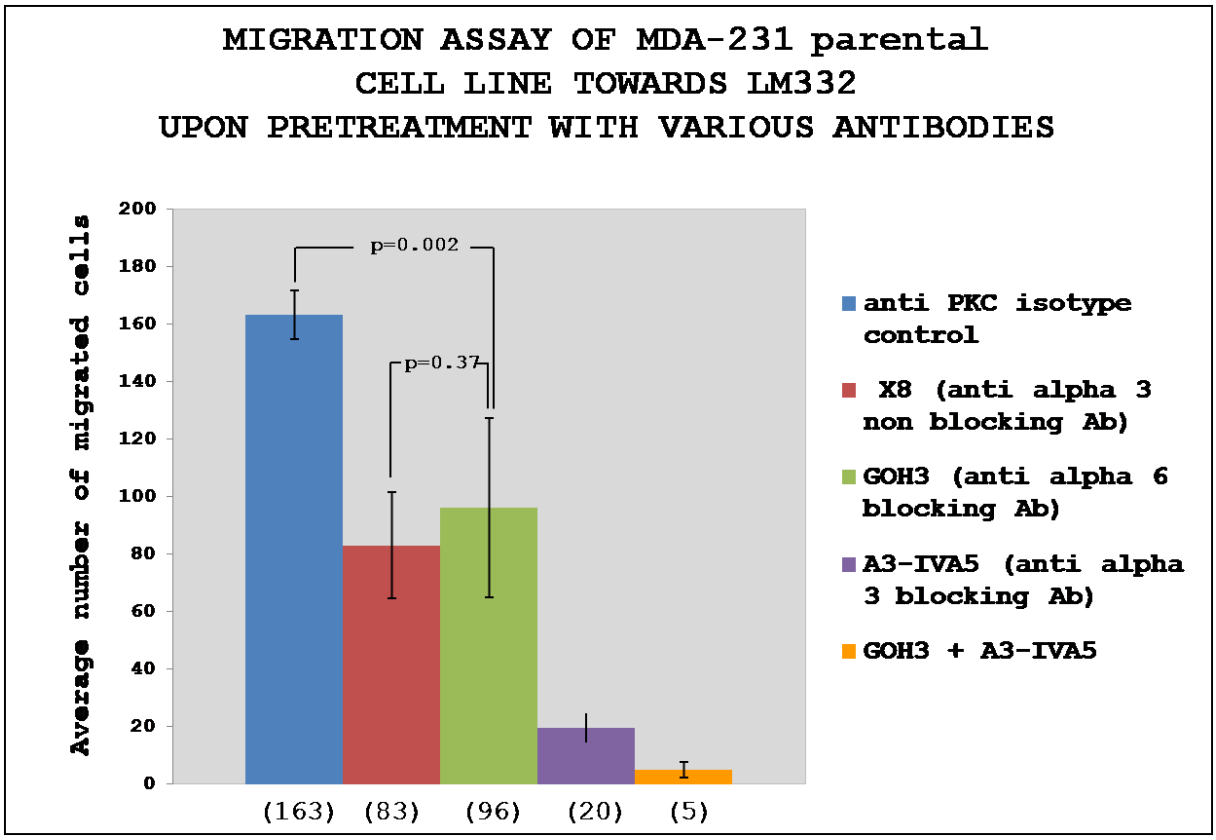

Figure 3.27 Migration potential of MDA-231 cells towards 2μg/ml Lm332 upon various antibody treatment.

Cells were prepared for migration assay by preincubating with mAb (10μg/ml) for 30 min at 4^0C. MAbs used are: A3-IVA5 (anti-α3 integrin subunit), GOH3 (anti-α6 integrin subunit), A3-X8 (anti-α3 integrin subunit) and isotype control, anti-PKC. Cells were allowed to migrate towards Lm332 for 8hrs and migrated cells were fixed and counted. Data are presented as average number of migrated cells per microscopic field (10X objective). Results are shown as mean ± SD calculated from two separate experiments, each performed in duplicates. *p* values are calculated using a two tailed *t* test. The values at the base of the bar represent the average number of cells per viewing field. Raw data for this experiment is presented in Appendix 3.

3.4.2 Establishing the role of α3β1 integrin glycosylation in migration towards Lm332

Having established that α3β1 integrin plays a major role in migration of MDA-231 cells towards Lm332, I then went on to investigate the role played by CD151 and CD151 mediated glycosylation of α3β1 integrin in migration towards the ligand. For this specific purpose, I selected a panel of MDA-231 cell lines: MDA-231 CD151 (+), MDA-231 CD151 (-), MDA-231 CD151 (-) reconstituted with wild type CD151 or glycosylation mutant CD151. I also included a MDA-231 α3 integrin knock down cell line in this experiment. Knock-down of α3 integrin level in the MDA-231 sh(α3) cell line was confirmed by Western blot and flow cytometry analysis (Figure 3.28).

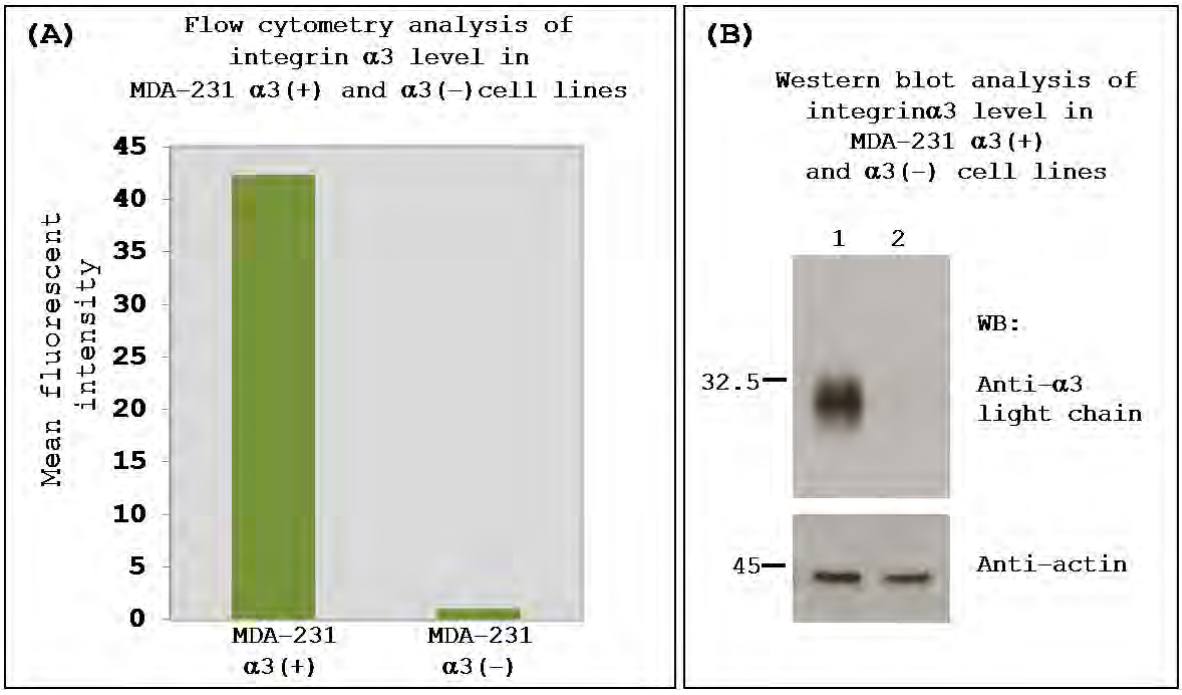

Figure 3.28 Flow cytometry and Western blot analyses of MDA-231 α3 knock down cell line.

(A) Cell surface expression of α3β1 integrin in the parental and α3 knock-down cell lines were analysed by flow cytometry with anti-α3 mAb, A3-IVA5. The mean of fluorescent intensity value for α3 integrin reduced from 42.3 to 1.03 upon depletion of the integrin. (B) MDA-231 (α3+) and (α3-) cell lysate was resolved by 12% SDS-PAGE and analysed by Western blot for α3 integrin and actin levels. The integrin was almost completely depleted in MDA-231 α3(-) (lane 2) cell line while actin levels confirms equal loading.

Migration assay to determine if changes in glycosylation of α3 integrin has any influence on ligand interaction, was performed under the same conditions with MDA-231 CD151(+), CD151(-), CD151 wild type reconstitution [CD151(REC)], CD151 glycosylation mutant reconstitution [CD151(GLY)] and CD151(+)/α3(-). We included MDA-231 CD151 glycosylation mutant (CD151 GLY) cell line in this study since

glycosylation mutation of CD151 retained all the biochemical properties of wild type CD151 but exihibited CD151(-) phenotype in relation to glycosylation of α3 integrin subunit.

The migration potential of MDA-231 cells towards Lm332 is reduced by 91% upon CD151 depletion (Figure 3.29). Re-expression of wild type CD151 restored the migration potential of MDA-231 CD151(-) cell line by (129%) compared to the control [CD151(+) cell line]. However, CD151 glycosylation mutant was unable to restore the migration potential of these cells to wild type levels and remained reduced at 17.5%. Migration of α3β1(-) cells were also greatly affected: 25.5% compared to the parental line. The inability of CD151(GLY) to restore the migration potential of these cells towards Lm332 and the result obtained with α3β1 depleted cells shows that under these conditions, migration of MDA-231 cells towards Lm332 is predominantly through its interaction with α3 integrin and is dependent on the glycosylation of the integrin.

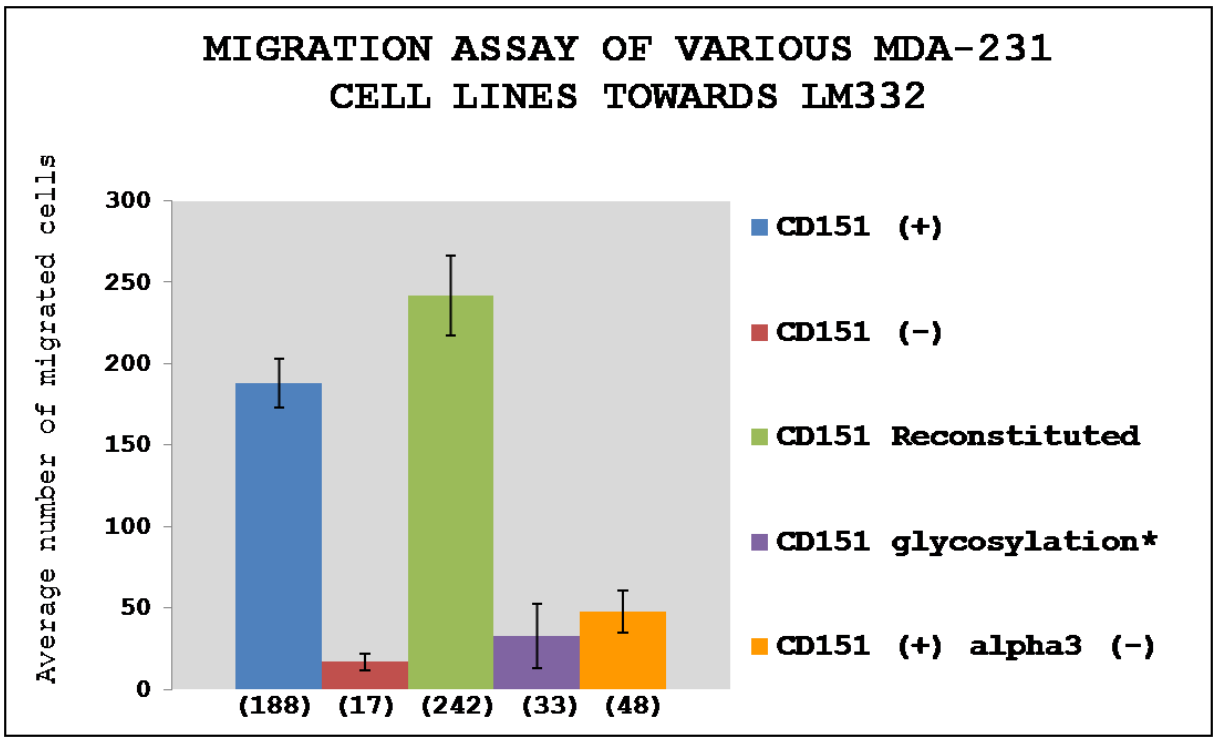

Figure 3.29 Migration potential of various MDA-231 derived cells lines towards 2µg/ml Lm332.

Haptotactic migration assay of various MDA-231 cell lines (wild type, CD151(-), CD151 reconstituted, CD151 glycosylation mutant and α3 integrin subunit knock-down) towards Lm332 was performed for 8hrs. Migrated cells were fixed, permiabilised, stained with Hoechst 33342 and counted. The data are presented as average number of cells per microscopic field (10X objective). Results are shown as mean $\pm$ SD calculated from two separate experiments, each performed in triplicates. The values at the base of the bar represent the average number of cells per viewing field. Raw data for this experiment is presented in Appendix 4.

To determine the extent to which CD151 influences the migration potential of MDA-231 cell, migration assay was performed under the same condition except the membrane was coated with 10μg/ml of fibronectin. Fibronectin is not a natural ligand for α3β1 integrin. No significant differences were observed in migration potential of MDA-231 CD151(+) and CD151(-) towards fibronectin under this condition (Figure 3.30). This result further emphasises the specificity of CD151/α3β1 interaction to Lm332 and the role played by α3β1 integrin glycosylation in migration towards Lm332.

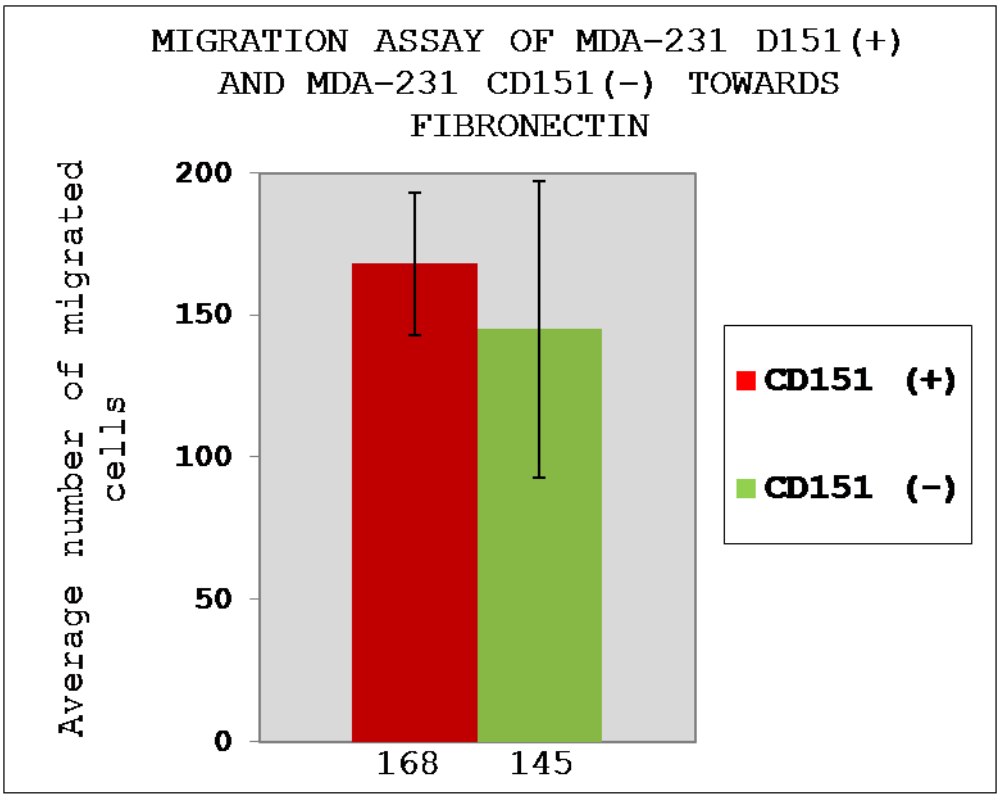

Figure 3.30Migration potential of various MDA-231 CD151(+) and CD151(-) cell lines towards 10µg/ml fibronectin.

Haptotactic migration assay towards fibronectin was performed and data are presented as average number of cells per microscopic field (10X objective). Results are shown as mean ± SD calculated from two separate experiments, each performed in quadruplicates. Depletion of CD151 did not have a significant impact on the migration potential of MDA-231 cells towards fibronectin. The values at the base of the bar represent the average number of cells per viewing field. Raw data for this experiment is presented in Appendix 5.

3.4.3 Adhesion assay

It has previously been reported that presence of CD151 stabilises the active conformation of α6 integrins and is important for adhesion strengthening in NIH 3T3 cell line (Lammerding et al., 2003). This characteristic was, however, attributed to CD151's interaction with cytoskeletal component. In this study we wanted to determine if CD151 and CD151 mediated glycosylation of α3β1 integrin contributes to direct ligand binding by performing a 30 minute static adhesion assay. For this purpose, adhesion assay was performed on 1μg/ml Lm332, 2μg/ml Lm332, 10μg/ml fibronectin and 10μg/ml BSA.

The results show no difference in attachment of MDA-231 CD151(+) and MDA-231 CD151(-) to Lm332 or fibronectin in 30 min static adhesion assay (Figure 3.31). Results from migration assay and adhesion assay taken together seem to indicate that CD151 mediated glycosylation changes to α3 integrin influences a specific type of interaction between the integrin and its ligand, Lm332.

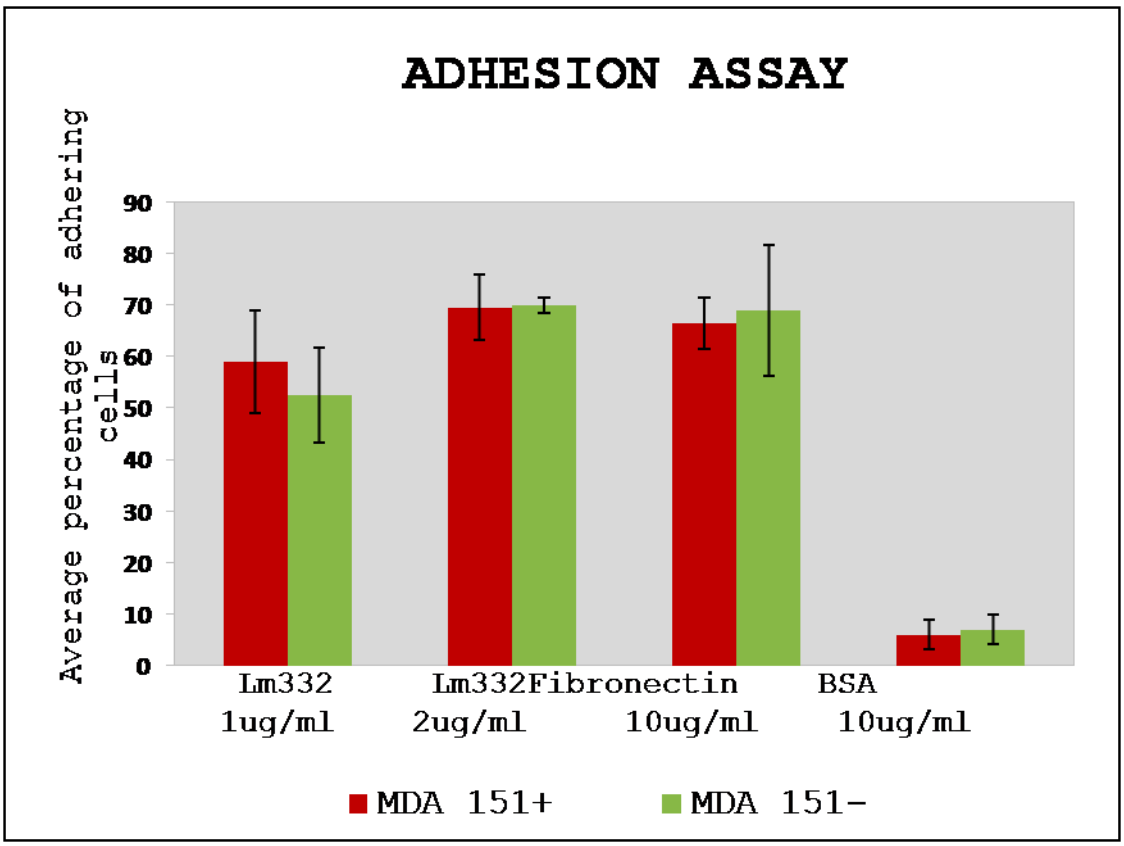

Figure 3.31 Adhesion assay of MDA-231 CD151(+) and CD151(-) to Lm332 and fibronectin.

30 minute adhesion assay was performed with BCECF-AM-labelled MDA 231 CD151(+) (red bar) and CD151(-) (green bar) cells on Lm332 (1µg/ml and 2µg/ml concentrations), Fibronectin (10µg/ml) and BSA (10µg/ml). No difference was observed in the binding capacity of the two cell lines towards the matrices. The experiment was performed in triplicate and the calculated percentage of adherent cells for each experiment is presented in Appendix 6.

3.4.4 Comparison of α3 integrin light chain that bind to GD6 peptide and to A3-IVA5 monoclonal antibody

It has previously been reported that a synthetic peptide corresponding to residues 3011-3032 of murine Laminin α1 chain is capable of binding to α3β1 integrin from detergent extracts of human melanoma cell line, C8161 (Gehlsen et al., 1992). This peptide sequence, KQNCLSSRASFRGCVRNLRLSR, also known as GD6 peptide, carries a 67% homology to human laminin α1 subunit, one of the components of Laminin111. Even though Lm111 is not a primary ligand for α3β1 integrin, it is still capable of binding to this integrin, albeit, with a lower affinity compared to Lm332. Consequently, I decided to compare the glycosylation profile of α3 integrin from MDA-231 CD151(+) and CD151(-) cell lines that interacts with this peptide, in order to determine if glycosylation of the integrin plays a role in binding to this ligand fragment.

GD6 peptides were coupled to activated CH-Sepharose and incubated with cell lysate prepared from MDA-231 CD151(+) and MDA-231 CD151(-) cell lines. Bound proteins were eluted, resolved on a 12 % SDS PAGE and analysed by Western blot for α3 integrin light chain fragment. As a control, cell lysate from both the cell lines were incubated with CH-Sepharose beads in the absence of GD6 peptide. α3 light chain fragments were also immunoprecipitated with anti-α3 antibody, A3-IVA5, and analysed by Western blot for comparison.

Western blot analysis of α3 integrin immunoprecipitated with anti-α3 antibody showed a difference in the mobility between α3 purified from CD151(+) and CD151(-) cells [(Figure 3.32A)]. The GD6 peptide pull down on the other hand strongly interacted with a distinct pool of glycoforms of the integrin, resulting in the loss of difference in the α3 integrin pulled down from the two cell lines [(Figure 3.32(B)]. This result seems to suggest a role played by glycosylation of α3 integrin in their binding capacity. Based on their Western blot profile, the GD6 peptide seems to prefer the two lower molecular weight glycoforms of α3 integrin which are highly expressed in CD151(+) cells but are reduced in the CD151(-) cells.

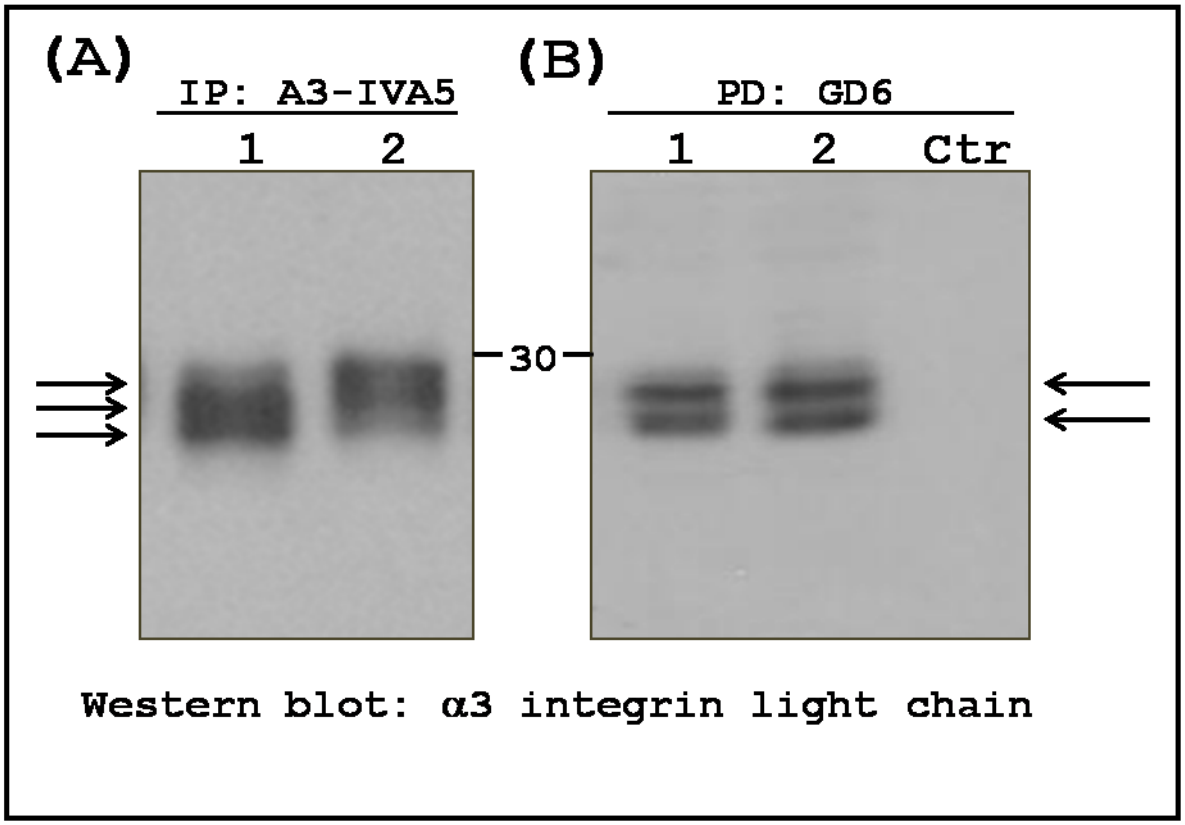

Figure 3.32 Western blot comparison of α3 integrin light chain from A3-IVA5 mAb IP and GD6 peptide pull down.

(A) A3-IVA5 Immunoprecipitation of α3β1 integrin from MDA-231 CD151(+) (lane 1) and MDA-231 CD151(-) (lane 2) Note the difference in the mobility of α3 subunit light chain fragment. (B) GD6 peptide purified α3β1 integrin from MDA-231 CD151(+) (lane 1) and MDA-231 CD151(-) (lane 2) shows no difference in their mobility on Western blot. As a control to eliminate non-specific binding of α3β1, lysate was incubated with beads without GD6 peptide (Ctr lane). The eluate was resolved by 12% SDS-PAGE and detected by Western blot with anti-α3 pAb. The Western blot data clearly shows that a peptide based on biological ligand seems to interact with a specific glycoforms of α3β1 integrin from both cell lines.

3.4.5 Laminar flow assay

Saccharides that form a lattice on the cell surface have been shown to slow down fast flowing leukocytes till they settle to a rolling motion on endothelial cell surface. Interactions between the Lewis antigen structures, presented on their cell surface glycoproteins such as PSGL-1 and CD44, with selectin molecules presented on the endothelial cell surface initiate this process. These interactions allows the leukocytes within the vasculature to adopt a rolling motion and tether to the cell surface before firmly anchoring to the endothelial cells through receptor-ligand interactions (Ley et al., 2007). Various studies have proposed that circulating tumour cells adopt the same mechanism when disseminating to secondary sites when it was found that P-Selectin deficiency and E-Selectin blocking attenuated metastasis (Kim et al., 1998; Kobayashi et al., 2000). In order to investigate the role of CD151 and CD151 mediated glycosylation in this rolling and tethering mechanism, I conducted a series of flow assays against various immobilised compounds/ligands.

MDA-231 cells were flown at three different rates (0.085ml/min 0.175ml/min and 0.35ml/min) into a flat micro slide tube precoated with E-Selectin, P-Selectin and Laminin 332 at saturating concentrations. The tumour cells did not appear to roll on these ligands; instead they steadily flew through the capillary tube. Following that, cell stream was halted mid flow for up to 5 minutes before resuming at the same flow rates. Upon restarting the flow, all the cells washed off from the coated surface. Since

firm interaction between the tumour cells and the matrix was not achieved within 5 minutes to withstand the subsequent shear force, a different approach was employed to study the interaction between tumour and endothelial cells. The flow assay was conducted on a monolayer of human umbilical vein endothelial cells (HUVEC), grown within microslides. The tumour cells were allowed to flow on the bed of HUVEC at different flow rates (0.085ml/min, 0.175ml/min and 0.35ml/min) to determine the best rate for them to roll like leukocytes on the endothelial layer. Again, no rolling was observed at these flow rates. Attempts at a lower flow rate clogged the tumour cells within the tubing network.

3.4.6 Endothelial rolling assay

It is generally thought that tumour cells escape through the vasculature to secondary sites by attaching itself to circulating leukocytes and thrombocytes or within a capillary bed. Both processes can clog and temporarily arrest tumour cell flow. In leukocytes, integrin function have been shown to become activated at slow rolling and tethering stage (McEver and Zhu, 2010). To explore this angle of tumour cell dissemination *in vitro*, endothelial monolayer was grown in a microslide and the flow of MDA-231 cells in these microslides was halted for 5 minutes, 2 minutes and 1 minute before resuming the flow. The number of tumour cells visible per a microscopic field upon initial flow suspension and the number of cells that remain

attached after 5 minute wash was scored for both MDA-231 CD151(+) and CD151(-) cells. During preliminary analysis, suspending the flow for either 2 minutes or 5 minutes did not produce significant difference in the ratio of cells that remained stuck after 1 minute of wash, between the two cell lines. Stopping the flow for 1 minute, however, showed a marked difference between MDA CD151 (+) and CD151 (-) cells. Up to 80% of the MDA 151(+) cells remained stuck to HUVEC after 5 minute wash while only 20% of the MDA 151 (-) cells remained (Figure 3.33, CORD 1). More interestingly, I found that when HUVEC from different sources were used, MDA CD151(+) and CD151(-) cells showed a varied interaction as presented in Figure 3.33. Since the adhesion assay was performed at a short interval of 1 minute, the endothelial-tumour cell interaction that's producing this variation is most likely a saccharide based interaction.

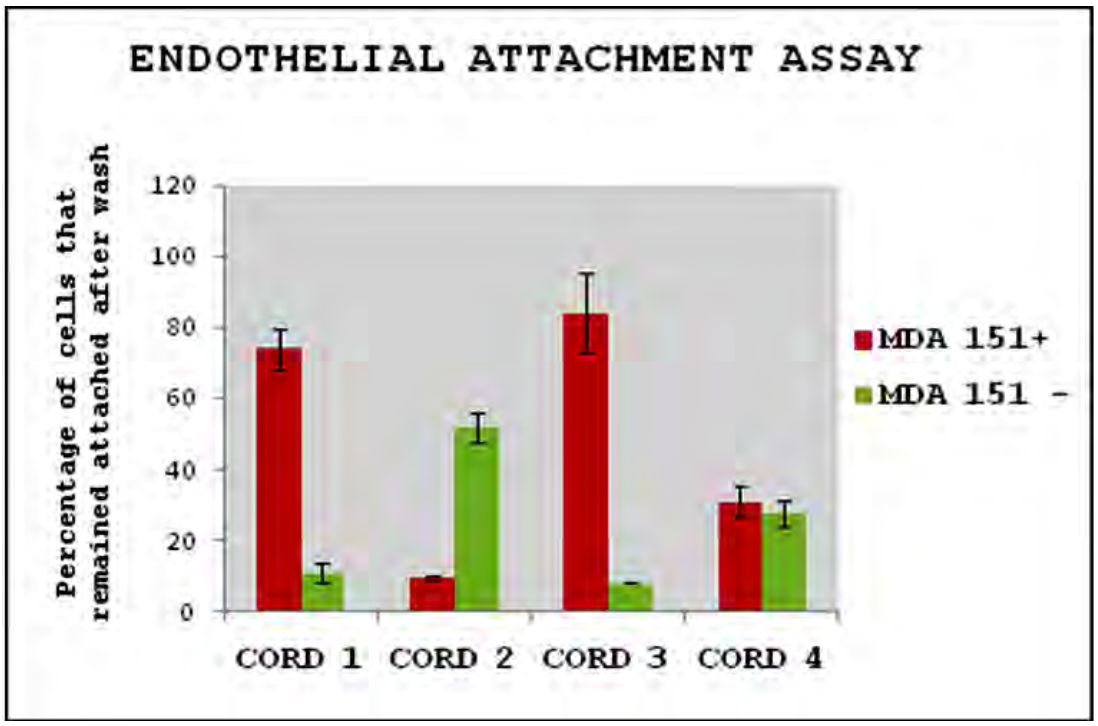

Figure 3.33 Endothelial attachment assay of MDA-231 CD151(+) and CD151(-) cells. HUVECs purified from 4 different umbilical cords were grown as a monolayer in a μ slide. The MDA-231 CD151(+) and CD151(-) cells were streamed into the μ slide at 0.35mlm/min and the ability of the cells to attach to HUVECS within 1 min was assayed by stopping and restarting the pump after 1 minute at the same shear rate (0.1Pa) as the flow rate. Cells that remained attached after 5 minutes wash was recorded and scored. A batch dependent difference was observed on how quickly the tumour cell lines interacted with HUVECs.

The results generated from 1 minute attachment assay of MDA-231 cells in HUVECs clearly shows that in three out of the four cases tested, the presence of CD151 effects how quickly the tumour cells bind to the endothelial layer. From the four HUVEC preparations collected from different individuals, two of them (Cord 1 and 3) showed a higher number of CD151(+) cells attaching to the endothelial layer compared to CD151(-) cells, one did not distinguish between CD151(+) and (-) cells

(Cord 4), while a final one had the opposite effect where CD151(-) cells adhered more readily than CD151(+) cells (Cord 2).

3.4.7 Tumour cell transendothelial migration assay

Albeit with some inconsistency, CD151 seems to play a role in the 'pre-extravasation' stages of metastasis. To establish whether CD151 is involved in extravasation during metastasis, I conducted transendothelial migration assay where the transendothelial migration potential of MDA-231 CD151(+) and CD151(-) cells across human brain microvascular endothelial cell line (HBMEC 1) was compared. The migration assays were performed for 4 hours, 6 hours and 8 hours.

The results from this study showed no significant difference in the transendothelial migration potential of MDA-231 CD151(+) and MDA-231 CD151(-) cells across the endothelial layer at any of the time points recorded (Figure 3.34).

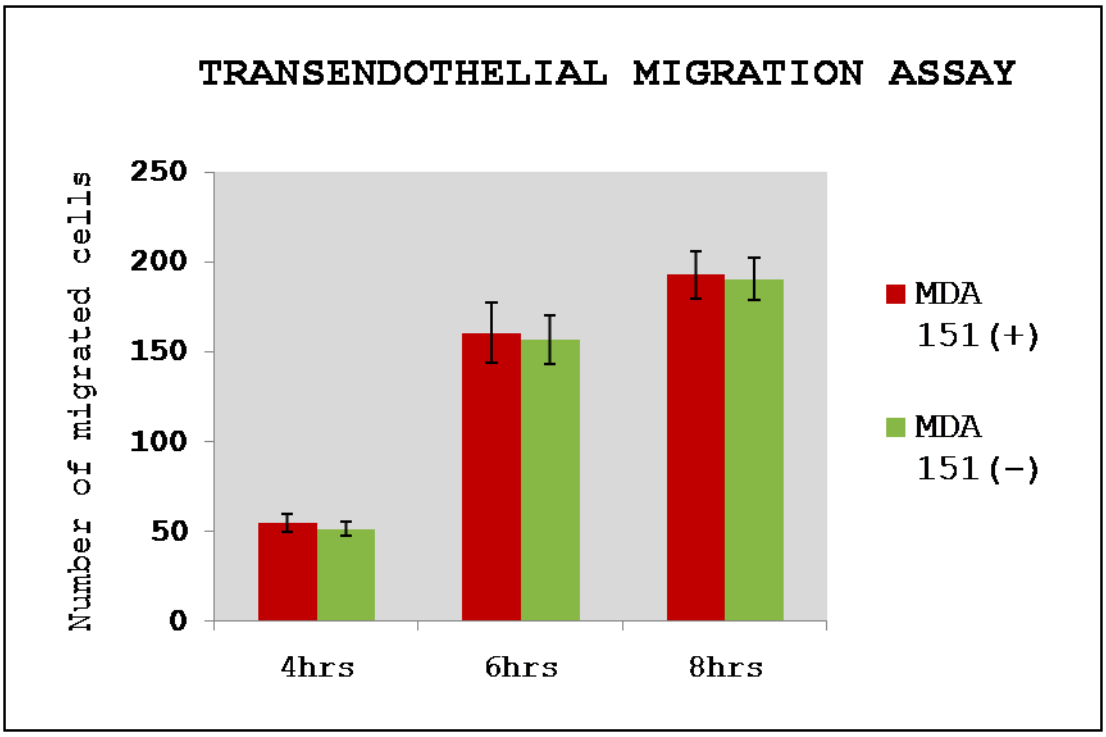

Figure 3.34 Transendothelial migration assay of MDA231-CD151(+) and CD151(-) cells across HBMEC 1 cells.

HBMEC-1 endothelial cells were grown as a tight monolayer within the internal chamber of tissue culture inserts. 500µl of 10% DMEM containing $2X10^5$ BCECF stained MDA-231 cells were introduced into the insert chamber and the transendothelial migration assay was performed for 4 hours, 6 hours and 8 hours. No difference was observed in the ability of the MDA-231 CD151 (+) / (-) cells to transmigrate across the endothelial layer at all three time points. Raw data for this experiment is presented in Appendix 7.

3.4.8 DISCUSSION

In this study, I showed that depletion of CD151 in MDA-231 cells had a dramatic impact on the ability of the cells to migrate towards Lm332 in a Boyden chamber migration assay. Furthermore, while reconstitution of wild type CD151 into the CD151(-) cells restored their migratory potential, reconstitution of the glycosylation-deficient mutant was unable to do so. CD151(GLY) cell line shared all the biochemical properties of wild type CD151, except for the ability to influence the glycosylation of α3 integrin. The inability of the CD151(GLY) cell line to restore the migration potential to the wild type CD151 level under the same conditions, strongly suggests the importance of α3β1 integrin glycosylation pattern in this particular type of cell migration. The migration potential of these MDA-231 cells was also reduced upon α3β1 integrin depletion. However, the migration potential of these cell were almost three times higher than in CD151(-) cells. This results probably reflects the trace level of α3β1 integrin expressed by the cells.

Blocking of α6β1/β4 integrin function had a mild inhibitory effect on migration of MDA-231 cells towards Lm332, a level comparable to the function blocking elicited by another α3β1 blocking antibody, A3-X8. I have earlier shown that depletion of CD151 increased the level of α6 clipped variant, α6p, in MDA-231 cells (Figure 3.11). Consequently, depletion of CD151 may inhibit migration of MDA-231 cells towards LM332 by collectively changing the glycosylation profile of α3β1

integrin and reducing the number of functional α6β1/β4 integrin at the cell surface through proteolitic cleavage. However, it should be reiterated here that α3β1 is the main receptor for Lm332. Consequently, while both integrins may play a role in migration towards Lm332, we predict that α3β1 integrin plays the dominant role in inhibiting the migration potential of MDA-231 cells.

It has previously been reported that overexpressing glycosyltransferase GnT-V stimulated while GnT-III inhibited α3β1 mediated cell migration in MNK45 human gastric cancer cell line (Zhao et al., 2006). In this study, the authors hypothesised that GnT-III overexpression introduced the bisecting β1-4 linkage which inhibits the addition of β1-6 branching by GnT-V and as a result, migration potential of these cells towards Lm332 was reduced. A concomitant decrease in GnT-V activity upon GnT-III expression and vice versa determines α3β1 migratory potential. However, in this study, the decrease in bisecting GlcNAc-β(1-4) presentation on α3β1 integrin upon CD151 depletion was followed by a corresponding decrease in their migration potential. Furthermore, the decrease in PHA-E lectin binding property of α3β1 integrin was not reciprocated by an increase in PHA-L binding indicating that CD151 did not affect the level of β1-6 branching on α3β1 integrin. Thus, it is possible that decreased β(1-4) GlcNAc branching must be accompanied by an increase in β(1-6) GlcNAc branching for it to have a promigratory effect. Furthermore, in this model system, depletion of CD151 also virtually removed all the α1-2 linked fucose from

α3β1 integrin. α1-2 linked fucosylation is a terminal modification usually attached to β(1-6) GlcNAc branching. These long 'broken wing' conformation serves as a 'backbone' which gives maximum exposure for the terminal α1-2 linked fucose to interact with its environment (as discussed in the Introduction chapter). I hypothesise that the promigratory effect of increased β(1-6) GlcNAc expression may indirectly be due to increased fucose residues being expressed on these branches. While in this study, depletion of CD151 did not change the level of β(1-6) GlcNAc branching, the presence of α1-2 linked fucose was almost completely lost. And this loss may have contributed to the decrease in migration towards Lm332.

Depletion of CD151 specifically effected α3β1(strongly) and α6β1/β4(mildly), mediated cell migration as I found no significant difference in the ability of MDA-231 CD151(+) and CD151(-) cells to migrate towards fibronectin, a ligand for α5β1 integrin. Furthermore, depletion of CD151 did not produce much difference in its ability to adhere directly on fibronectin or Lm332 in a 30 minute static adhesion assay indicating that only a specific type of α3β1 and α6β1/β4 integrin function is affected. Perhaps, the most convincing result we obtained on the contribution of α3β1 integrin glycosylation to ligand binding is from the pull-down assay performed with Lm111 based GD6 peptide (Figure 3.30). Western blot analysis of the α3β1 integrin pool pulled down with GD6 peptide showed no difference in α3 integrin light chain fragment between the CD151(+) and CD151(-) cell lines even though a difference was

detected in the subunit when immunoprecipitation was performed with anti α3 antibody (A3-IVA5).

The importance of integrin glycosylation in receptor-ligand interaction has previously been reported for α5β1 and α3β1 integrins. Strategically located N-linked glycosylation site have been shown to be crucial for the integrin's folding and dimer formation (Zheng et al., 1994; Isaji et al., 2006). More pertinently, it has been reported that enzymatic removal α2,8-linked polysialic acids from α5β1 integrin inhibited its binding to fibronectin (Nadanaka et al., 2001). Conversely, desialylation of purified α3β1 integrin increased their capacity to bind fibronectin (Pochec et al., 2003; Pochec et al., 2006). These findings imply that glycosylation not only effects integrin-ligand interaction, but it may also change the receptor's affinity towards non-conventional ligands.

In this study, I found that α1-2 linked fucosylation rather than sialylation was affected upon CD151 depletion in MDA-231 cell line. The α1-2 linked fucose structure is usually found on lewis b and lewis y antigens, a family of blood group antigens. Expression of other members of this blood group antigens such as the lewis a and lewis x have been shown to facilitates the rolling of leukocytes on endothelium by linking to selectins expressed on the endothelial cell surface (Fuhlbrigge et al., 1996). To investigate if α1-2 linked fucose is in anyway involved in selectin interaction, I performed laminar flow assay on selectin and Lm332 coated microslides with CD151(+) and CD151(-) MDA-231 cells. Additionally, I also simulated

'leukocyte like rolling' with these tumour cell lines on HUVEC. Neither of these approaches induced a leukocyte type rolling in MDA-231 cells. This may be due to the tumour cell size (10μm), deeming it unable to withstand the force generated by shear flow. A growing body of evidence suggests that tumour cells extravasate from vasculature via other mechanisms. One of the most common sites for tumour extravasation is while moving through the capillary bed where tumour cells are known to be temporarily trapped. In fact, experimental metastasis in mouse models show introduction of tumour cells via tail vein injection almost always resulted in lung metastasis since this is where the tumour cells encounter its first bed of capillaries (Elkin and Vlodavsky, 2001). Furthermore, interaction of tumour cells with other cells such as the leukocytes and platelets have also been shown to facilitate its exit from the blood vessel.

Building an experimental model to study this type of metastatic modes, our initial study showed presence of CD151 hastened the tumour cell attachment to the endothelial layer. A fourfold increase was observed in the percentage of MDA-231 CD151(+) cells able to attach to HUVEC compared to CD151(-) cells within one minute. However, the binding efficiency of the two cell lines differed when different batches of HUVEC were used. With some batches of HUVEC, CD151(+) cells bound more readily than CD151 (-) cells. In other batches, either the opposite or no difference was observed on how CD151(+) and CD151(-) cells interacted with HUVEC. It has previously been reported that cell surface glycans such as galectin 3

and galectin 9 plays an important role in immediate interaction (< 2minutes) with laminin 1 (Lm111) (Friedrichs et al., 2007). Since my experiments showed a difference between the two cell lines only at a short interval (1 minute), I hypothesise that this interaction too is most probably a glycan based interaction. Furthermore, the fact that there is a variation between different batches of HUVEC implies that this specific interaction may not be due to α3β1 adhesion strengthening characteristic which is typically attributed to CD151. No difference was however observed between the two cell lines upon longer incubation (> 2 minutes). This suggests that the removal of CD151 did not significantly contribute to the ability of tumour cells to attach to endothelial layer.

In order to determine if CD151 exerts its influence in these experiments by changing the surface glycosylation and not by affecting the α3β1 integrin's function as a cell surface receptor, transendothelial migration assay was performed. No difference was observed in the ability of MDA-231 CD151 (+) and CD151 (-) cells to migrate through / across the endothelial layer, confirmining that CD151 depletion does not affect the receptor-ligand interaction of α3β1 or α6β1/β4's during transendothelial migration. It is also interesting to note that increased cleavage of α6 integrins to form the α6p variant upon CD151 depletion did not seem to affect their ability to migrate across the endothelial layer. A possible explanation for this observation is that α6p variant formation occurs on both α6β1 and α6β4 integrins

which have opposing effects on cell migration. As a result, it may have negated each other's influence. Furthermore, the abundance of other functional receptors at the cell surface such as α3β1 integrin may have a more dominant role as well as sufficiently compensate α6p's influence during transendothelial migration.

Taken together, the observations made during both the endothelial rolling and transendothelial migration assay is reminiscent of Leukocyte Adhesion Defeciency, LAD I and LAD II syndromes. In both cases, a defect in leukocyte adhesion deficiency is observed. LAD I is due to a mutation in the β2 integrin molecule while LAD II arise from a genetic defect in Golgi GDP-fucose transporter which results in the loss of expression of selectin ligands on leukocytes. In the case of the former, leukocytes are able to roll on endothelial cells but are unable to transmigrate through the endothelial layer. LAD II on the other hand showed markedly reduced capacity for leukocytes to roll but they were able to transmigrate through the endothelial layer without any difficulty (Hirschberg, 2001). Depletion of CD151 in MDA-231 cells, in most cases, shows a 'LAD II like' symptom when it comes to interaction with endothelial cells. A milder and more arbitrary (observed when different batches of HUVEC were compared) influence of CD151 depletion compared to LAD II is most probably because it only affects the surface expression of α1,2 linked fucose. Other types of fucosylation (i.e α1,3 linked fucose, α1,4 linked fucose or core α1,6 linked

fucose) were not greatly affected since their capacity to bind AAL upon CD151 depletion was not duly altered (Figure 3.25).

3.5 Tetraspanin trafficking and function from glycosylation perspective

Almost all tetraspanins are N-link glycosylated, though the number of oligosaccharide branches they carry may differ from one tetraspanin to another. CD9 and CD151 for example, contain a single N-linked glycan, while CD63 and CD82 have three potential glycosylation sites. CD81 on the other hand is non-glycosylated. Despite glycosylation being a major post-translation modification, relatively little is known about the nature of their glycosylation and the physiological the role it may have in the tetraspanin molecule's cellular function. In this part of study, my main objective was to investigate the role that glycosylation of tetraspanins may play in the molecule's function. I also show how the glycosylation pathway can be exploited for cancer therapy from the integrin perspective.

3.5.1 Characterisation of tetraspanin glycosylation

Tetraspanins are characterised as N-linked glycoproteins. In this part of the study we looked into the glycosylation nature of CD9, CD63, CD82 and CD151. For this purpose, 1% Triton X-100 extracted total cell lysate was treated with glycosidases EndoH and PNGaseF. As previously mentioned, EndoH removes high mannose and hybrid N-linked oligosaccharides while PNGaseF cleaves off high mannose, hybrid

and complex oligosaccharides from the protein backbone. The lysate was then resolved on 12% SDS-PAGE and analysed by Western blotting for CD9 and CD151 (Figure 3.35) as well as CD63 and CD82 (Figure 3.36) under non reducing condition for their glycosylation status and profile.

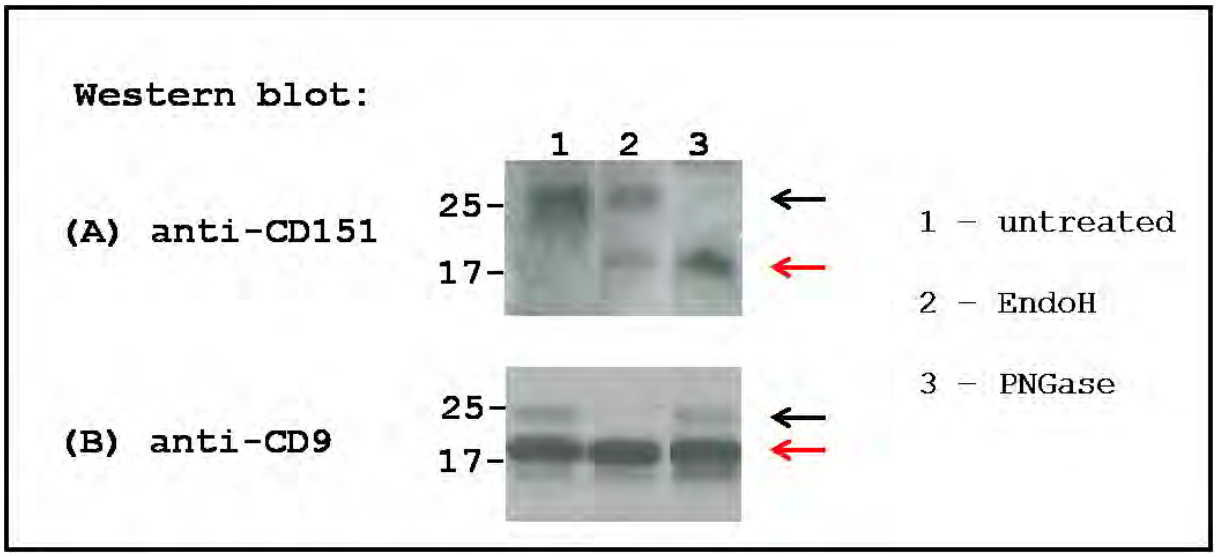

Figure 3.35 Western blot analysis of EndoH and PNGaseF treated MDA-231 cell lysate for CD9 and CD151.

(A): Western blot analysis of endogenous CD151 in MDA-231 gives a diffused glycosylated band at ~25kD (lane 1, black arrow). EndoH treated sample shows reduction in the intensity of the glycosylated band the appearance of a non-glycosylated low molecular weight band (lane 2, red arrow). The PNGaseF treated sample on the other hand produced only the deglycosylated form of CD151 (lane 3, red arrow). (B): Western blot analysis of endogenous CD9 (lane 1) shows the presence of a glycosylated (black arrow) and non-glycosylated (red arrow) form of CD9. EndoH treatment (lane 2) removes the glycan residues resulting in the detection of only the non-glycosylated form. Interestingly, CD9 is resistant to cleavage by PNGaseF (lane 3) (WB CD151: anti CD151 polyclonal; WB CD9: C9BB)

Analysis of CD9 and CD151 upon glycosidase treatment confirms that they are both N-linked glycosylated proteins. However, we also found that CD9, while resistant to PNGaseF treatment, was susceptible to cleavage by EndoH. This is a possible indication of phospho-mannosylation, a glyco-modification that commits the protein for lysosomal targeting via interaction with mannose-6-phosphate receptors. Susceptibility to PNGaseF can be restored upon phosphatase treatment (Zhao et al., 1997).

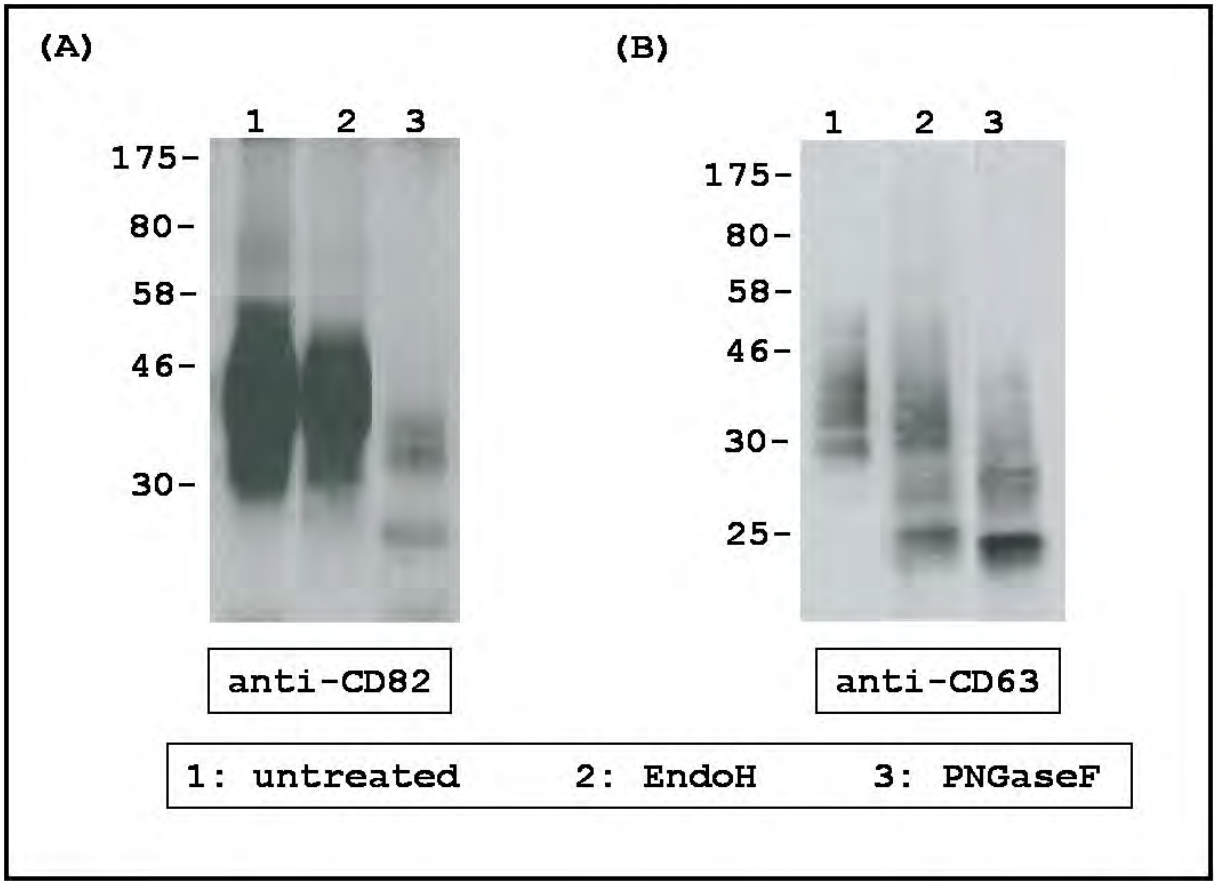

Figure 3.36 Western blot analysis of EndoH and PNGaseF treated MDA-231 cell for CD82 and CD63.

Western blot analysis of untreated (lane 1), EndoH treated (lane 2) and PNGaseF treated (lane 3) lysate for CD82 (A) and CD63 (B) shows the presence of glycosylated protein under all three conditions.

Analysis of CD63 and CD82 upon glycosidase treatment showed both tetraspanins responding only partially to EndoH and PNGaseF mediated deglycosylation. Partial resistance to EndoH indicates the presence of complex glycans. The presence of CD63 and CD82 glycoforms upon PNGaseF treatment suggests that, as with CD9 molecule, CD63 and CD82 too may be subjected to phospho-mannosylation.

3.5.2 Mapping the tetraspanin route within ER

The observation made on the glycosylation status of CD9 and CD151 indicates that even though they are both N-link glycosylated, the nature of their glycosylation commits them into different pathways within the ER and Golgi apparatus. Trafficking within the ER and Golgi determines the glycan constituent of a glycoprotein which, in turn, may contribute to its functional role. Inhibition of the glycosylation pathway, as I and others have shown, can be used to track the route that a glycoprotein takes during their ER to Golgi transit. In this study, I have identified CD9 to be phospho-mannosylated, a modification which will definitely contribute to one of its function as a lysosome targeting membrane protein. A simplified illustration of the multiple routes that exists within the N-linked

glycosylation pathway is presented in Figure 1.13. Molecules commited to the N-linked glycosylation process take a conventional glycosylation pathway, endomannosidase I pathway or phosphomannosylation pathway. In this study, the early routes taken by tetraspanins CD9, CD63, CD82 and CD151 is compared by inhibiting the glycosylation pathway with castanospermine, an inhibitor of glucosidase I and II. Inhibition with castanospermine allows for the distinction of proteins that take the conventional pathway and the endomannosidase pathway as illustrated in Figure 3.22.

Accordingly, MDA-231 cells were grown in medium supplemented with 1mg/ml castanospermine for 2 days. Harvested cells were lysed in 1% Triton X-100 and analysed by Western blotting. The glycosylation profile of CD9, CD63, CD82 and CD151 as well as a cell surface glycoprotein, emmprin, was compared to their counterpart from untreated cells. Western blot analysis showed all 4 tetraspanins and emmprin responding differently to castanospermine treatment (Figure 3.37). Emmprin, like CD63 and CD82, has 3 glycosylation sites. Upon castanospermine treatment, glycosylation of emmprin is abruptly terminated as seen from the appearance of tighter lower molecular weight bands. CD82 on the other hand responded very mildly to castanospermine. This may indicate that they are mainly committed to the endomannosidase pathway. CD63 too gave two distinct glyco-populations which were more or less, equally represented. In both CD63 and CD82,

the higher molecular weight group (black braket) shows similar profile as the untreated sample. A second lower molecular weight smear is also detected (red bracket) for these tetraspanins. The presence of two different populations may either mean that the upper population represents a 'leak' due to insufficient inhibition, similar to that seen in emmprin, or that they are committed to more than one pathway. Furthermore, the lower molecular weight population generated in response to castanospermine treatment did not share the abrupt termination in glycosylation seen in emmprin. This observation further suggests that CD63 and CD82 are not only committed to more than one pathway, but, inhibition of deglucosylation of these molecules did not terminate the glyco-modification of these tetraspanins.

CD9 on the other hand showed an increase in molecular mass of its glycosylated pool upon castanospermine treatment. This is probably due to the presence of uncleaved glucose residues. While the mobility of CD151 bands during Western blot analysis did not change upon castanospermine treatment, its total level was markedly reduced.

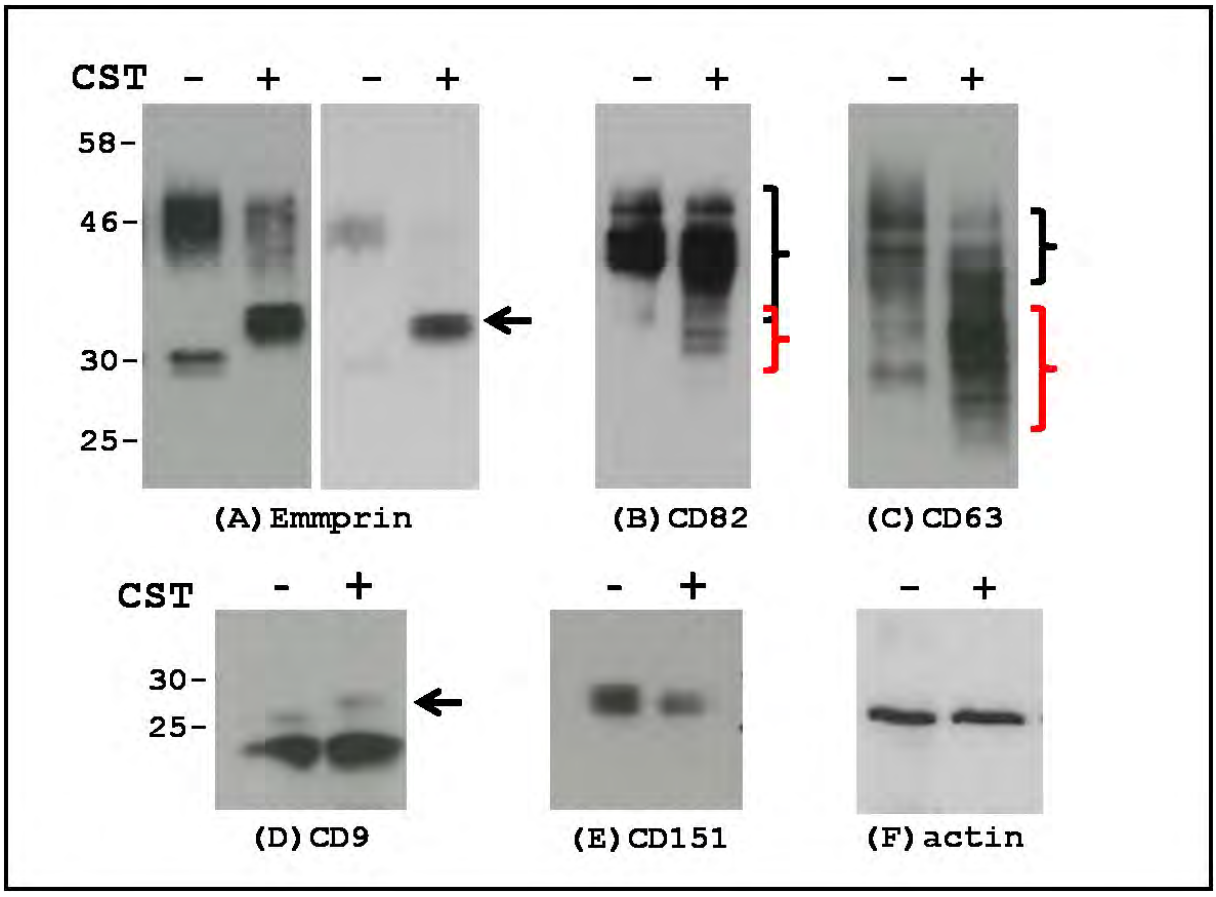

Figure 3.37 Castanospermine inhibition and Western blot analysis of various glycoproteins.

(A) Presence of castanospermine (Cst) arrests glycan diversification in emmprin and a tighter low molecular weight band is observed (+ lane, black arrow, right panel). Longer exposure of the blot (left panel) reveals incomplete blocking which 'leaks' a higher molecular weight smear corresponding to the mature glycosylated form detected in untreated sample (- lane,). (B) Glycosylation of CD82 remains mainly unaffected by Cst treatment. (C) Cst treatment effects glycosylation of CD63, however, there was no abrupt termination as seen with emmprin. Instead, upon Cst treatment, CD63 has two groups of glycosylated forms. One of them resembles the untreated CD63 profile (black bracket) while a second lower molecular weight group is also generated (red bracket). (D) Molecular weight of glycosylated CD9 population increased upon Cst treatment (black arrow) while the level of CD151 decreases in the presence of Cst (E). Equal loading of samples was determined from Western blot of actin level (F)

3.5.3 The effect of castanospermine on α3 and α6 integrin subunits

Castanospermine's effect on most of the glycoproteins tested seems to rest squarely on their glycosylation except for CD151 where the level of the protein was affected. Since CD151 associates tightly with laminin binding α3 and α6 integrins, I investigated the effect castanospermine may have on these integrins. Lysate was prepared from MDA-231 cells cultured for 2 days with or without 1mg/ml castanospermine. Proteins were resolved by 12% SDS PAGE and analysed by Western blot for α3 and α6 integrin light chain under reducing condition. Remarkably, I found that the level of α3 and α6 integrins was diminished upon castanospermine treatment (Figure 3.38). In order to determine if this is a cell line specific response, I analysed for α3 integrin level in two other cell lines, U87MG (human neuronal glioblastoma/ astrocytoma cell line) and BT474 (breast cancer cell line established from human invasive ductal carcinoma) upon castanospermine treatment. Both the cell lines exhibited similar response whereby the level of α3 integrin was reduced upon castanospermine treatment. However, the level of reduction differed between cell lines. This observation indicates that, while castanospermine may broadly affects α3β1 integrin level, the level of down-regulation differed from one cell line to another (Figure 3.39).

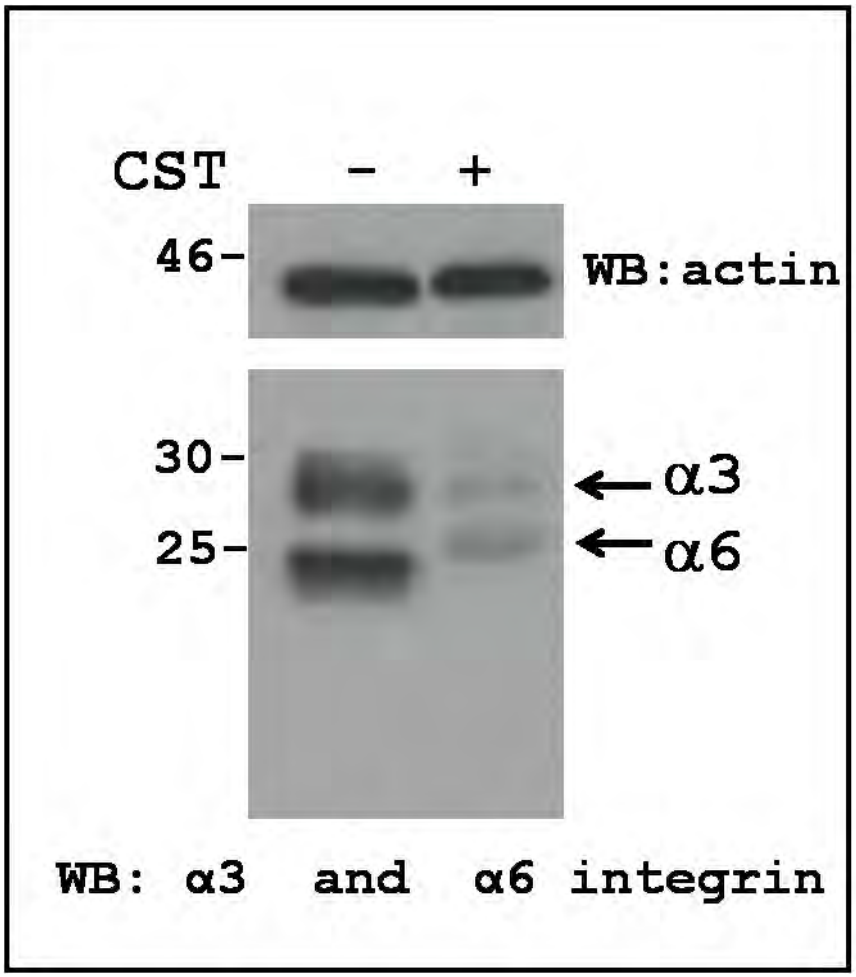

Figure 3.38 Western blot analyses of α3 and α6 integrins upon castanospermine treatment of MDA-231 cell line.

MDA-231 cells were grown in the absence or presence of 1mg/ml castanospermine for 2-3 days, harvest and lysed in 1% Triton X-100. The level of α3 and α6 integrins in treated and untreated samples were analysed by Western blot (lower panel). Actin level was detected for loading control (upper panel).

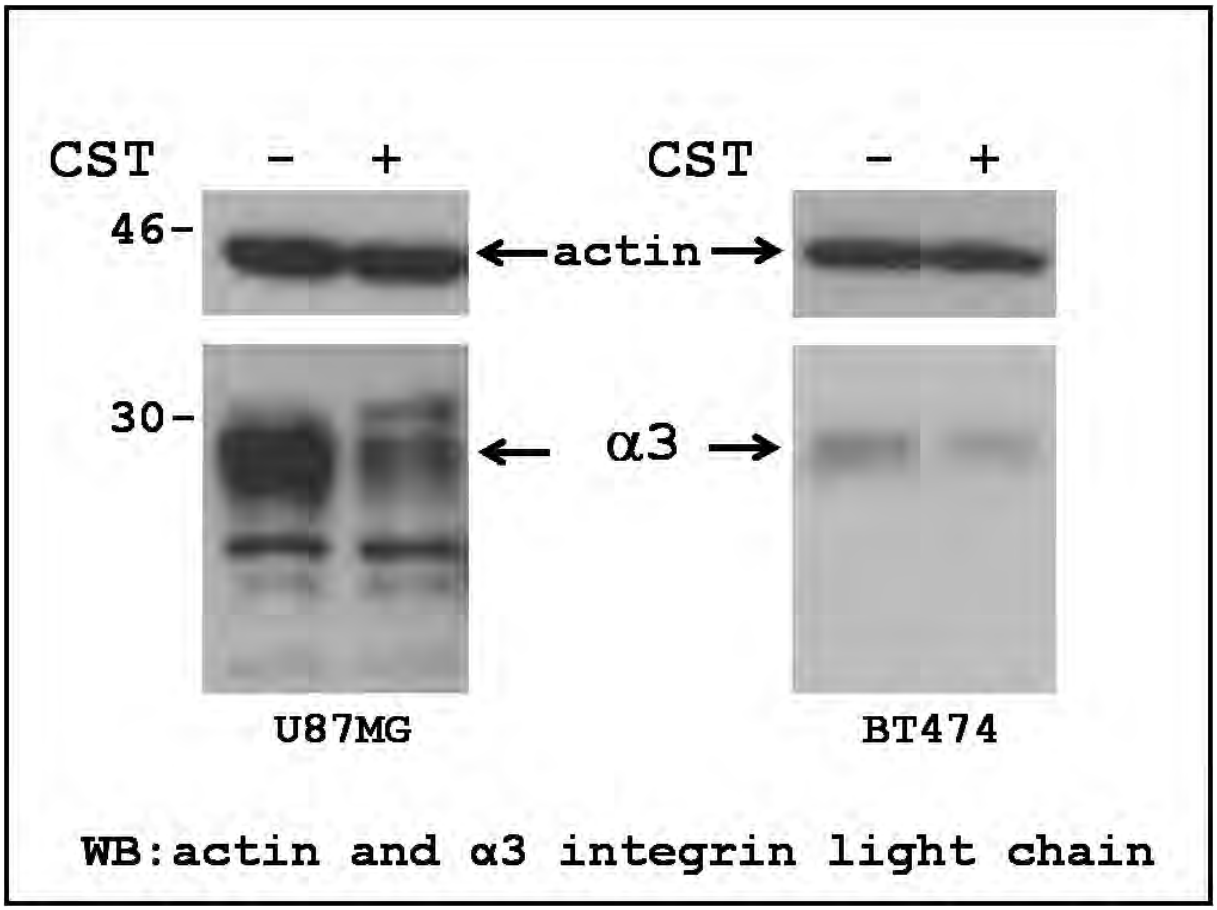

Figure 3.39 Western blot analyses of α3 integrin in U87MG and BT474 cell lines upon castanospermine treatment.

U87MG (left panel) and BT474 (right panel) cell lines were grown in the presence of 1mg/ml castanospermine for 3 days. The level of α3 integrin light chain reduced upon castanospermine treatment in U87MG cell line (left panels). The α3 integrin subunit level was mildly affected upon castanospermine treatment in BT474 cell lines (right panels).

3.5.4 The effect of castanospermine on other integrins and integrin associated proteins

Integrins, a major cell surface receptor family, play an important role in cell adhesion, migration and survival. During tumorigenesis, the expression levels of various members of this family have been shown to be upregulated. The pronounced effect of castanospermine on the level α3 and α6 integrins would clearly affect the potency of cancer cells. Consequently, I investigated the effect castanospermine might have on the level of other integrins such as α2, α5 and β1 in MDA-231 cells. Furthermore, I also compared the levels of integrin associated proteins such as epidermal growth factor receptor (EGFR), Talin and Src.

The level of α2 integrin was reduced after incubating the cells in the presence of castanospermine for 3 days. α5 integrin, β1 integrins and EGFR on the other hand showed a difference in glycosylation but not the levels of the protein based on the band shift. The level of talin and Src, two integrin associated cytoplasmic proteins, were not affected upon castanospermine treatment (Figure 3.40).

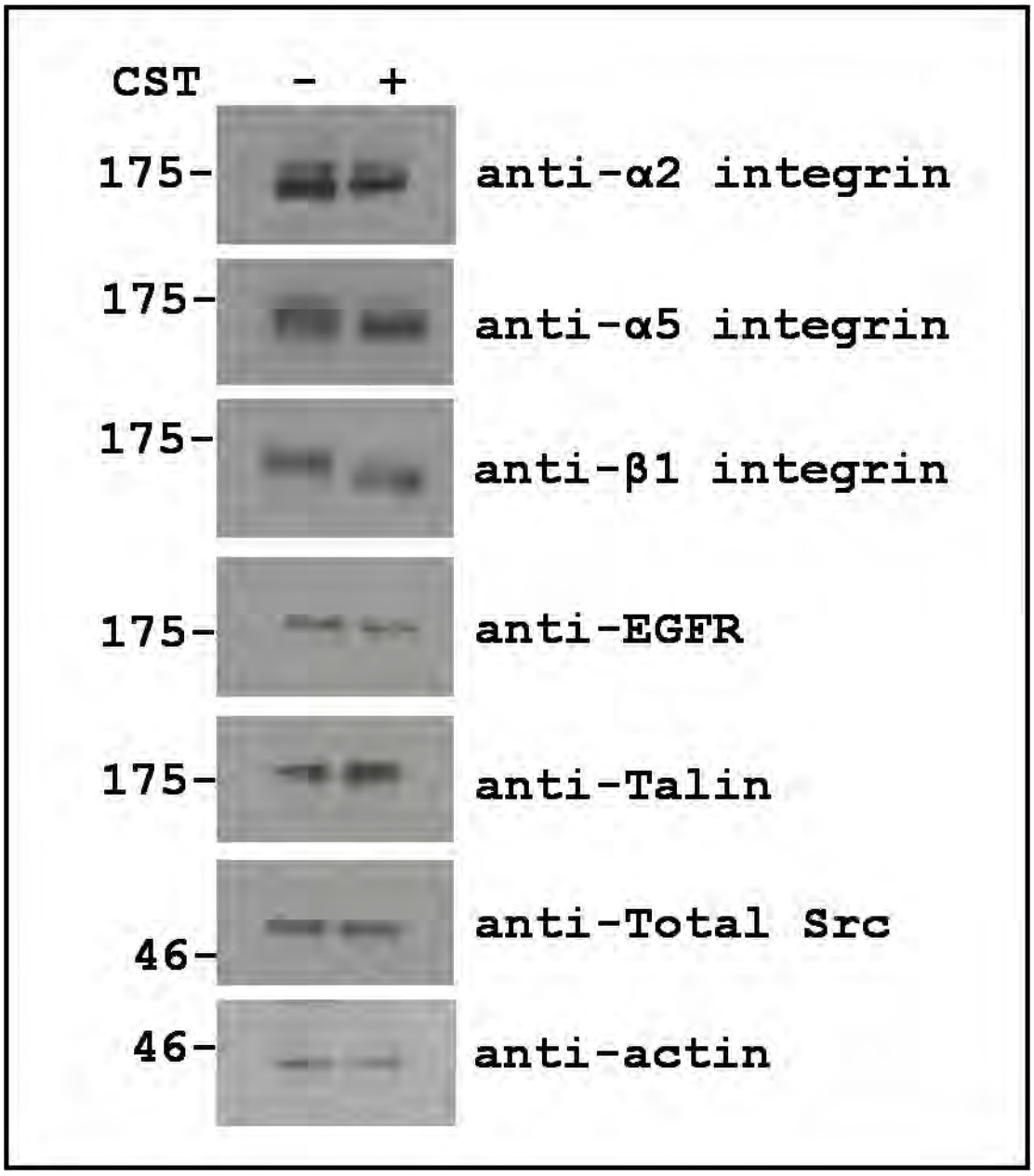

Figure 3.40 Western blot analysis of various proteins upon castanospermine treatment.

MDA-231 cells were grown in the presence of 1mg/ml castanospermine for 3 days, harvested, resolved by 10% SDS PAGE and detected for various proteins.

3.5.5 Castanospermine dosage effect on the level of α3 and α6 integrin subunits

Castanopermine's ability to affect the levels of α2, α3 and α6 integrins besides inhibiting the glycosylation of α5, β1 and EGFR indicates a potential use for this drug in cancer treatment. This previously undescribed effect of castanospermine on the integrins was further investigated by looking at the affect dosage had on the efficacy of this drug. For this purpose, MDA-231 cells were grown in DMEM medium or DMEM supplement with 0.1mg/ml and 0.5mg/ml castanospermine for 2 days. Cells were then lysed in 1% Triton X-100 and analysed by Western blot for α3 and α6 integrin levels.

The reduction in the α3 and α6 integrin levels was higher at 0.5mg/ml compared to 0.1mg/ml indicating castanospermine inhibition affects the level of α3 and α6 integrins in a dose dependent manner (Figure 3.41). However, no difference was observed in the level of the integrin when treated with 0.5mg/ml or 1.0mg/ml implying a saturation effect.

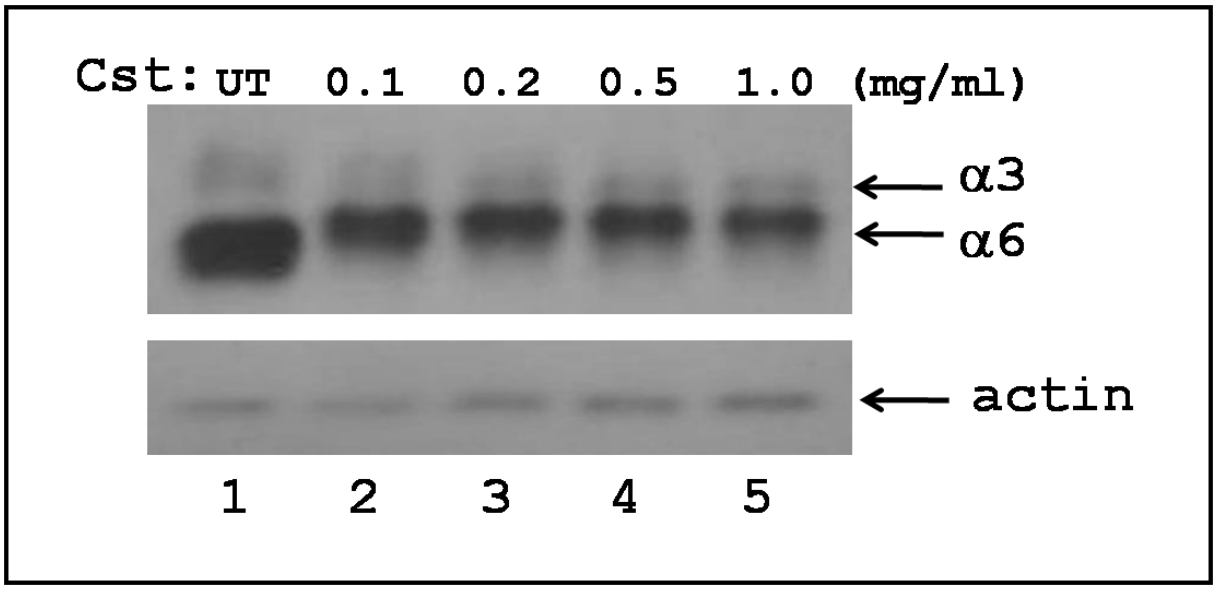

Figure 3.41 The effect of castanopermine dose on the level α3 and α6 integrins.

Cells were grown in the presence of castanospermine at various concentrations for 2 days. Western blot analysis of α3 and α6 integrins resolved on 12% SDS PAGE clearly shows that suppression of the integrin level is dependent on the concentration of castanospermine. The level of the integrins in untreated (UT) (lane 1) sample is higher compared to 0.1mg/ml castanospermine (CST) (lane 2) treated sample. The level is reduced further when incubated with 0.2mg/ml (lane 3) and 0.5mg/ml (lane 4) CST. Comparison of 0.5mg/ml and 1.0mg/ml (lane 5) CST treatment however does not show a much difference in the suppression levels indicating under these conditions, CST inhibition is saturated at around 0.5mg/ml.

3.5.6 DISCUSSION

Generally, there are three established pathways that a glycoprotein can follow within the ER. Firstly, the conventional pathway when their deglucosylation occurs prior to ER mannosidase trimming. Another type of glyco-modification involves phosphorylation of mannose residue which directs the glycoprotein to specific locations such as the late endosome and lysosomal compartments. A third pathway involves the exit of glycosylated protein into the Golgi apparatus where both glucose and mannose residues are removed by Golgi endo-mannosidase. These various pathways that a glycoprotein may take can be determined by treating with specific glycosidases and glycosylation pathway inhibitors. Phospho-mannosylated glycoproteins are deglucosylated by EndoH treatment but not PNGaseF treatment (Sahagian et al., 1981; Sahagian et al., 1982; Zhao et al., 1997). Western blot analysis to determine EndoH and PNGaseF susceptibility for CD9, CD151, CD63 and CD82 revealed novel characterics for some of these tetraspanins. CD151's susceptibility to PNGaseF cleavage but not to EndoH illustrates that this tetraspanin carries a complex oligosaccharide residue (Figure 3.35). CD9's response to deglycosylated treatment by EndoH but not by PNGaseF characterises it as a phosphomannosylated glycoprotein. CD63 and CD82 on the other hand, were only partially deglycosylated by PNGaseF, suggesting the possibility that these two tetraspanins may carry both complex and phosphomannosylated glycans (Figure 3.36). Phosphorylation of

mannose residue by GlcNAc phosphotransferase on N-linked glycans prepares the glycoprotein for mannose-6-phosphate receptor mediated lysosomal targeting. Both CD63 (Metzelaar et al., 1991) and CD82 (He et al., 2005) have been previously been described to carry lysosomal targeting motif on their C-tail domain. The presence of mannose-6-phosphate receptor ligand on their glycan structure may further augment this function. The association of CD9 with MHCII on the other hand, have been specifically attributed to the its recruitment into exosomes and not lysosomal compartment during CD4+ T cell mediated dendritic cells activation (Buschow et al., 2009). This inconsistency may be due to the fact that only a small fraction of CD9 is glycosylated compared to the total CD9 expression levels (Figure3.35). Alternatively, it may also reflect multifunctional nature of CD9 where it associates and targets molecules to different compartments.

Glycoproteins recruited into the endomannosidase pathway can be distinguished by treating the cells with a plant alkaloid, castanospermine, which inhibits the glucosidase I and glucosidase II activity. Glycoproteins that follow the endo mannosidase route are unaffected by this inhibition since they can be effectively trimmed by endomannosidase I and they go ahead with glyco-maturation. Western blot analysis of CD9 and emmprin showed a sudden change in their glycoprofile, identifying them to the conventional pathway. CD82 on the other hand was only mildly affected by castanospermine treatment. This indicates that

CD82 predominatly follows the endomannosidase I pathway. CD151 on the other hand showed a decrease in its level upon castanospermine treatment. It has previously been shown that castanospermine inhibited calnexin binding during protein folding which resulted in proteosomal degradation of nicotinic acetylcholine receptor (Keller et al., 1998). Since the level of CD151 reduced upon castanospermine treatment, I hypothesised that CD151 may be subjected to a similar fate. In earlier chapters, I have shown that CD151 forms primary, and predominatly secondary association with α3β1 and α6β1/β4 integrins respectively (Figures 3.13 and 3.14). Consequently, I analysed the responses of these integrin to castanospermine inhibition. Interestingly, I found the levels of both integrins to be markedly reduced upon castanospermine treatment (Figure 3.38). While castanospermine may have a direct role in down regulating the CD151, this result may also suggest that CD151's instability is due to its association α3/α6 integrins.

Further analysis of other integrins and integrin associated protein revealed only α2β1 level to be affected by castanospermine treatment. α5β1 and EGFR levels were not affected though their glycosylation was altered (Figure 3.40). Furthermore, we also found that castanospermine effect can be modulated by their dosage (Figure 3.41). This 'semi-specific' effect of castanospermine on cell surface receptors as well as their dosage dependent activity makes them an ideal candidate for therapeutic

intervention, especially since these integrins have been identified as one of the major cell surface receptor involved in cancer and its progression.

4. CONSPECTUS AND FUTURE WORK

The primary focus of this study was to investigate the significance of CD151/α3β1 association using an *in vitro* model system. Several novel observations were made during the course of the investigation, on the role of CD151/α3β1 axis as well as other associated molecules such as CD9, CD63, CD81, CD82 and α6β1/β4 integrins. These observations are summarised below:

1) CD151 regulates glycosylation of α3β1 integrin and this alteration has physiological consequences (Sections 3.1 & 3.4). In the MDA-231 cell line, presence of CD151 increases the level of α1,2 linked fucose presented on α3β1 integrin. CD151's influence on the glycosylation of α3β1 integrin seems to be a specific effect stemming from very early glycosylation events within the ER. Whereas CD9, which also influences glycosylation of α3β1 integrin, exerts its influence at the later stages of the glycosylation pathway (Section 3.3).

2) CD151's influence on the glycosylation of α3β1 integrin is only realised by maintaining several diverse but interdependent characteristics, namely, glycosylation, palmitoylation and tight association with the integrin. CD9, on the other hand, is able to influence glycosylation of the integrin through secondary association. Furthermore, a difference in the glyco-profile of CD9 or CD81 associated

α3β1 integrin indicates the presence of CD151/α3β1 in different type of TERMs (Sections 3.1 and 3.2).

3) CD151 appears to preferentially form tight association with α3β1 over α6β1/β4 integrins in MDA-231 cells. This observation may explain why CD151 did not alter the glycosylation profile of α6β1/β4 integrins, as tight association is one of the required criteria for glyco-modification of α3β1 integrin (Section 3.1).

4) CD151 recruited α3β1 integrin into the light fractions of Brij 96 SDG as part of a TERM, as well as a separate entity, highlighting the presence of multiple types of CD151/α3β1 associated microdomains (Section 3.2).

5) CD151 and CD9 were observed to have opposing effects on their ability to induce α6 integrin subunit cleavage, which results in α6p variant production (Section 3.1).

6) Analysis of glycans on various tetraspanins revealed the glycosylated CD9 to be phospho-mannosylated. Based on their resistance to PNGaseF cleavage and their localisation to late endosome and lysosomal compartments, CD63 and CD82 may also be phospho-mannosylated (Section 3.5).

7) Inhibition of glucosidase I/II by castanospermine treatment reduced the levels of CD151 as well as α3β1, α6β1/β4 and α2β1 integrins making this compound a possible candidate for clinical therapy (Section 3.5).

These observations suggest a fundamental role played by CD151 in cellular function which will certainly have some implication *in vivo*. Most of CD151's influence on α3β1 integrin seems have its roots in the early stages of it biosynthesis within the ER. Firstly, even before the association occurs, a selective pressure ensures that CD151 preferentially associates with α3β1 and not the α6β1/β4 integrins in MDA-231 cell line. This begs the question, *what facilitates the facilitators*? Are there other components within the ER that determine this preferential association? Does the tertiary folded structure of the integrin molecule determine this event? Does the association with OST complex result in an enrichment of a structurally favourable environment which selects for CD151-α3β1 association over α6β1/β4? Or is it simply due to abundance of the α3 subunit within the ER in our model system?

Interestingly, preferential association between αIIbβ3 integrin and the non-glycosylated fraction of CD151 has been reported in human platelets when immunoprecipitation of the integrin was performed under Triton X-100 condition (Lau et al., 2004). The significance of these selective associations has yet to be properly addressed. However, in this study, I found that glycosylation of CD151 is pivotal for the molecule to influence the glycosylation of α3β1 integrin (Section 3.2). CD151 (GLY) mutant MDA-231 cells showed similar glycosylation profile for α3β1 integrin as CD151 depleted cells. In this study, I also found that depletion of CD151 effected how tumour cells interact with HUVEC (Section 3.4). It would have been

interesting to determine the role played by α3β1 and α6β1/β4 integrin as well as the glycosylation of α3β1 during the tumour cells interaction with HUVEC. This could have been achieved by testing the integrin knock down and CD151 reconstituted cell lines under the same settings. Unfortunately, this study was terminated at this juncture. However, by drawing parallels between the two studies, the preferential association between non-glycosylated CD151 and αIIbβ3 may imply that a specific glycoform of αIIbβ3 is being generated to dictate which molecules/cells it can interact with *in vivo*. However, this model relies on the whether CD151 or glycosylation of CD151 has a role in glycosylation of αIIbβ3 integrin which we did not establish in this study. While the significance of this selective pairing between CD151 and various laminin binding integrins *in vivo* is still unknown, Sonnenberg's group (Sterk et al, 2002) reported that Ts151r reactive epitope of CD151 (which requires the QRD epitope / unligated CD151 molecule for recognition) was increased in the glomeruli of HIV positive patients. Based on their observation, the authors suggested a pathophysiological relevance to the expression of paired and unpaired CD151 molecules. This hypothesis is currently being explored in various cancers.

The Brij 96 SDG assay showed that both the QRD mutant of CD151 (which is capable of forming TERM) and the palmitoylation deficient of CD151 (which is not capable of doing so), are able to recruit α3β1 integrin into the light fractions. However, even though both CD151 (QRD) and CD151 (PLM) are capable of

recruiting α3β1 integrin and α6β1/β4 integrins (supplementary data) into the light fractions of the Brij96 SDG, various studies have shown that they respond differently to TGFβ1 stimulation (Sadej et al., 2010) and in adhesion and migration assays (Zevian et al., 2011). This is probably due to the difference in their lateral interaction formation whereby each CD151 mutant may be recruiting overlapping as well as unique sets of cytoskeletal and signalling molecules. Consequently, different signalling pathways will be activated upon stimulation resulting in diverse cellular responses. For example, MDA-231 cell lines expressing CD151 (QRD) and CD151 (PLM) respond differently to TGFβ1 stimulation despite the fact that both mutants retain their ability to recruit α3β1 and α6β1/β4 integrins to light fractions (Sadej et al., 2010). This result may also indicate that only a certain population of CD151 in the cell (in this case, the population belonging to the fraction that forms tight association with CD151) is involved in the TGFβ1 response. Similarly, the CD151 QRD mutant of HB2 was unable to emulate the organised acini-like structures of the wild type HB2 cells when grown in matrigel; indicating TERM containing tightly associated CD151 and α3β1 integrin is a prerequisite for this role. Depletion of α3β1 integrin resulted in severe growth retardation; while α6β1/β4 depleted cells displayed a similar phenotype to wild type HB2 (Novitskaya et al., 2010). It will be interesting to know if α3β1 preferentially associates with CD151 over α6β1/β4 in this cell line as well.

In contrast, migration and adhesion of the A431 cell on Lm332 was reduced in CD151 silenced and CD151 palmitoylation deficient cell lines, but not in QRD mutant CD151 (Zevian et al., 2011). The authors also reported that while α3β1 is required for initial attachment, α6β4 integrin is important for subsequent stable attachment and this process does not require palmitoylation of CD151. Interestingly, my result shows that despite not forming tight association with CD151, α6 integrins are recruited into the light fractions of Brij 96 SDG by CD151 (PLM). This result may as well indicate a completely different relationship between CD151 and α6 integrins compared to α3β1 integrin. It will be interesting to discover the factors attributing to CD151's association with the α6 integrins.

While the exact nature and composition of the CD151-associated microdomains was not addressed in this study, data generated during this study as well as other published work seem to indicate the presence of heterogeneous CD151 containing microdomains. During the course of my study, it became clear that CD151 recruits α3β1 integrin into the light fractions as part of the TERM as well as a 'separate entity'. The exact nature of the 'separate entity' remains to be established. It is tempting to speculate that this entity is a lipid raft component. Lipid rafts (LR) are a dynamic liquid-ordered phase of plasma membrane consisting of tightly packed saturated phospholipids, enriched in cholesterol and sphingolipid. Consequently, they are resistant to disruption by Triton X-100 at 4^0C, but are disrupted following

cholesterol depletion. LR components include GPI anchored proteins attached to the outer leaflet, signalling molecules (i.e. Src and Ras) attached to the inner leaflet as well as transmembrane proteins (Simons and van, 1988; Brown and London, 2000; London and Brown, 2000).

In agreement with previous reports, I found that CD151 was incapable of recruiting $\alpha 3\beta 1$ into the light fractions when SDG was performed under Triton X-100 conditions. This should effectively eliminate lipid raft's involvement in this process. However, the existence of more than one type of cholesterol rich domains has been suggested previously (Claas et al., 2001) and this view was augmented by the observation that CD9-CD81 interaction was disrupted upon cholesterol depletion with saponin, but not with methyl-β-cyclodextrin (MβCD) treatment (Charrin et al., 2003c). Furthermore, Brij97 SDG performed at 4^0C and 37^0C showed that in the presence of CD151, $\alpha 3\beta 1$ accumulated in the light fractions while cholesterol depletion with MβCD redistributed $\alpha 3\beta 1$ into the high density fraction (Charrin et al., 2003b). Whether cholesterol depletion specifically affects cholesterol enriched microdomains or the general stability of plasma membrane is unclear. While recruitment of $\alpha 3\beta 1$ integrin into the light fractions at 37^0C may suggest a non-LR component, this result may also indicate the presence of two distinct types of microdomains. In this study, Western blot comparison of CD9- and CD81- associated

pools of α3β1 integrin showed a difference in their glycosylation profiles possibly indicating distinct microdomains.

Heterogeneity of LRs and their components, and the need to address LRs in a wider rather than its traditional definition has been proposed in order for it to have a functional relevance (Pike, 2004). To this end, various models describing transmembrane proteins that tether at the periphery of LR and form protein-protein interaction with LR components have been presented. The possible existence of such interactions may explain how α3β1/CD151 complexes might coalesce with LR to form distinctive domains which buoy into the light fractions of Brij 96 SDG, but are lost under Triton X-100 conditions. Glycosylation which predominantly occurs in the ER, and Golgi apparatus precedes cholesterol enrichment and LR formation which occurs in the trans Golgi network (TGN) (Klemm et al., 2009). It will be interesting to determine if the clustering that occurs in the earlier stages of ER-Golgi transit contributes to the heterogeneity of LRs.

The role of tetraspanins in modulating the post-translational modification of their integrin partners is perhaps not surprising considering their capacity to recruit various components into their microdomain. As shown in this study, 'facilitation' starts at a very early stage in the ER. In the presence of CD151, the CD151/α3β1 complex seems to prefer an early exit from ER into the Golgi while in the absence of CD151, the integrin is trimmed within the ER prior to exit. From an evolutionary

point of view, N-linked glycosylation in yeast, which involves a simple mannose trimming step by MnsI prior to exit from ER, is replaced in the higher organism by a more complex system involving multiple α-mannosidases localised in the ER and the Golgi apparatus (Jelinek-Kelly and Herscovics, 1988; Puccia et al., 1993; Weng and Spiro, 1993b; Weng and Spiro, 1996). Parallel to this event, emergence of integrins and tetraspanins in metazoans may reflect how the higher organisms adapted to fully benefit from this evolutionary explosion. For example, the presence of CD151 seems to facilitate the early exit of the α3β1 integrin from the ER. While in yeast, the untrimmed Man_9NAc_2 high mannose precursor exiting ER is more susceptible to degradation compared to a Man_8NAc_2 structure (Jakob et al., 1998a), in higher organisms, evolutionary adaptation seems to not only rescue these molecules, but also confers them with functionally relevant glycan diversity. Additionally, the selective association between αIIbβ3 and non-glycosylated CD151 populations may also suggest an evolutionary adaptation.

Why is the glyco-modification important? In a multicellular organism, cell fate is determined from its response to stimulation from extracellular matrix (ECM) and ECM associated growth factors. This includes maintenance of stem cell niches, tissue patterning and differentiation during development, immunological and inflammatory response as well as cancer and other diseases. The ECM proteins are large and complex molecules consisting of multiple and distinct conserved domains

capable of simultaneous interaction with various cell surface receptors and soluble molecules. The fate or response of a cell to its environment is determined by the sum effect of the ECM-receptor interaction. R.O. Hynes beautifully compared the effect of this multifaceted interaction to music played as 'chords' and 'melodies', rather than 'single notes' (Hynes, 2009). One such family of receptors which interacts with the ECM is the ubiquitous integrin family. Glyco-modification on both the ECM and integrins have been suggested to be involved in exposing cryptic binding sites simultaneously changing the affinity of their interaction (Bellis, 2004).

Inhibition of glucosidase I/II (GI/GII) with castanospermine (CST) reduced the expression level of CD151 as well as the levels of α2β1, α3β1 and α6β1/β4 integrins. While the glycosylation of tetraspanins CD9, CD63, CD82 and α5β1 integrin was altered upon CST treatment, their levels remained relatively unchanged. Presence of GI/GII inhibitors has previously been shown to prevent lectin-glycoprotein interaction, in some cases resulting in proteosomal degradation of the affected glycoprotein (Peterson et al., 1995; Keller et al., 1998). A possible explanation for the differences in molecular response to castanospermine treatment may be due to the type and strength of the interaction that exist between the glycoprotein and CNX/CRT. It has previously been shown that the ER lectins are capable of associating with both oligosaccharide and polypeptide segments of nascent proteins (Danilczyk and Williams, 2001). This variation in lectin interaction may explain the differences in

CST's effect on various tetraspanins and integrins. However, the difference in the fate of the affected glycoproteins upon CST treatment remains to be determined.

5. APPENDICES

Appendix 1 - Flow cytometry analysis of MDA-231 cells

mAb	epitope	MDA-231 151(+) 50% CONFLUENCE	MDA-231 151(+) 90% CONFLUENCE	MDA-231 151(-) 50% CONFLUENCE	MDA-231 151(-) 90% CONFLUENCE
VIIC6	α 3 subunit	55.3	54.8	52.6	51.9
IVA5	α 2 subunit	35.1	32.7	42.1	41.8
A6 ELE	α 6 subunit	7.52	7.7	9.64	9.57
TS 2/16	β 1 subunit	79.2	75.4	81.2	89.2
C9BB	CD9	14.2	15.6	13.8	14.4
6H1	CD63	7.2	7.2	7.5	7.63
M38	CD81	22.9	23.1	21	20
M104	CD82	7.86	8.51	6.69	7.01
5C11	CD151	22.2	21.9	0.698	0.698

MDA-231 cells were plated at 50% and 90% confluence and analysed for cell surface expression of various membrane proteins by flow cytometry analysis. (The values represent mean fluorescence intensity).

Appendix - 2 Flow cytometry analysis of lectin binding property

(Values represent mean fluorescent intensity)

EXPERIMENT 1

LECTIN		PARENTAL	CD151(-)	CD9(-)	CD63(-)	CD81(-)
Aleuria aurantia Lectin	AAL	40.6	36.1	36.5	49.8	46.8
Concanavalin A	CON-A	14.9	12	13.6	13.8	10.4
Dolichos biflorus agglutinin	DBA	0.394	0.348	0.494	0.338	0.305
Peanut Agglutinin	PNA	6.15	5.66	5.75	16	5.28
Phaseolus vulgaris Erythroagglutinin	PHA-E	87.5	82.7	76.1	89.9	90.8
Phaseolus vulgaris Leucoagglutinin	PHA-L	90.7	88.6	66.5	99.7	92.3
Ricinus communis agglutinin	RCA	127.6	125.1	124.4	171.8	132.7
Sambucus nigra agglutinin	SNA	0.799	0.798	1.72	1.5	1.55
Soybean Agglutinin	SBA	2.41	1.43	1.71	3.8	2.41
Ulex europaeus Agglutinin	UEA	3.65	1.85	2.63	7.46	8.94
Wheat Germ Agglutinin	WGA	372	367.5	371.5	419.4	334

EXPERIMENT 2

LECTIN		PARENTAL	CD151(-)	CD9(-)	CD63(-)	CD81(-)
Aleuria aurantia Lectin	AAL	40.2	37.6	43.3	60.2	50.1
Concanavalin A	CON-A	17	13.8	17.9	17.9	14.9
Dolichos biflorus agglutinin	DBA	0.447	0.491	0.637	0.682	0.549
Peanut Agglutinin	PNA	9.28	8.22	7.38	20.4	8.34
Phaseolus vulgaris Erythroagglutinin	PHA-E	108.8	110.2	115.3	142.8	116.2
Phaseolus vulgaris Leucoagglutinin	PHA-L	96.4	114.4	101.2	149	112.5
Ricinus communis agglutinin	RCA	120.6	107.2	127.3	190.2	107.6
Sambucus nigra agglutinin	SNA	1.73	1.7	3.63	2.85	2.04
Soybean Agglutinin	SBA	3.8	2.12	3.56	5.96	2.87
Ulex europaeus Agglutinin	UEA	5.5	2.63	4.37	14.1	10.6
Wheat Germ Agglutinin	WGA	207.5	230	244.3	359.9	244.2

EXPERIMENT 3

LECTIN		PARENTAL	CD151(-)	CD9(-)	CD63(-)	CD81(-)
Aleuria aurantia Lectin	AAL	76.5	71.8	69.6	95.6	78.5
Concanavalin A	CON-A	40	37.2	42.6	42.6	35.5
Dolichos biflorus agglutinin	DBA	1.93	2.24	2.6	2.09	0.922
Peanut Agglutinin	PNA	23.8	19.6	16.8	33.6	13.7
Phaseolus vulgaris Erythroagglutinin	PHA-E	333.7	310.1	265.1	318.1	250.7
Phaseolus vulgaris Leucoagglutinin	PHA-L	195.5	185.9	134.8	188.9	145.7
Ricinus communis agglutinin	RCA	327.6	241.3	294.3	400.9	242
Sambucus nigra agglutinin	SNA	6.07	5.43	11	7.03	5.67
Soybean Agglutinin	SBA	7.43	4.13	5.25	10.2	4.32
Ulex europaeus Agglutinin	UEA	10.4	4.67	6.38	14.2	14.5
Wheat Germ Agglutinin	WGA	611	554.7	551.2	621.9	476.9

Appendix 3 - Migration assay of MDA-231 cells towards Lm332 after antibody blocking

EXPERIMENT 1

ANTIBODY	INSERT	NUMBER OF MIGRATED CELLS PER FIELD			
PKC	1	206	144	165	209
	2	97	132	181	122
X8	1	71	59	60	59
	2	83	68	83	73
GOH3	1	124	108	72	89
	2	199	78	170	101
IVA5	1	26	23	21	29
	2	24	22	19	20
IVA5+GOH3	1	4	4	3	3
	2	4	1	2	1

EXPERIMENT 2

ANTIBODY	INSERT	NUMBER OF MIGRATED CELLS PER FIELD			
PKC	1	155	203	146	198
	2	230	112	131	174
X8	1	95	140	98	100
	2	94	84	86	73
GOH3	1	87	108	42	55
	2	69	68	70	92
IVA5	1	13	12	12	4
	2	20	29	33	6
IVA5+GOH3	1	3	2	2	6
	2	16	8	11	6

Appendix 4 - Migration of various MDA-231 derived cells towards Lm332

EXPERIMENT 1

CELL LINE	INSERT	NUMBER OF MIGRATED CELL PER FIELD			
CD151(+)	1	236	343	203	210
	2	336	286	216	230
	3	393	344	348	295
CD151(-)	1	23	29	23	26
	2	26	17	13	35
	3	25	16	36	38
CD151 recon	1	114	111	77	90
	2	163	151	130	176
	3	232	134	273	151
CD151 glyco	1	25	16	15	16
	2	41	35	64	45
	3	87	68	100	92
CD151 sh alpha3	1	57	66	48	58
	2	35	44	54	38
	3	28	40	55	53

EXPERIMENT 2

CELL LINE	INSERT	NUMBER OF MIGRATED CELL PER FIELD			
CD151(+)	1	216	270	364	379
	2	265	348	283	290
	3	304	401	402	331
CD151(-)	1	46	52	46	54
	2	77	95	66	59
	3	58	21	9	30
CD151 recon	1	169	196	52	54
	2	61	58	65	60
	3	73	54	62	58
CD151 glyco	1	99	151	63	57
	2	88	124	101	190
	3	99	67	148	86
CD151 sh alpha3	1	70	72	53	75
	2	32	40	26	57
	3	37	37	33	48

Appendix 5 - Migration assay of MDA-231 CD151(+) and CD151 (-) cells towards fibronectin

Data presented represents number of migrated cells per field averaged from 7 fields per insert.

		AVERAGE NUMBER OF MIGRATED CELL PER FIELD PER INSERT			
CELL LINE	EXP	INSERT 1	INSERT 2	INSERT 3	INSERT 4
CD151 (+)	1	166	179	166	157
	2	197	181.5	163.5	133.5
CD151 (-)	1	140.5	101.5	86	122
	2	162	155.5	197	197

Appendix 6 - Adhesion assay of MDA-231 CD151(+) and CD151(-) cells on Lm332 and fibronectin

Data presented represents percentage of cells that remained attached to the matrices after washing during a 30 min adhesion assay.

EXPERIMENT 1

	Percentage of adhereing cells after 30min at 37°C			
	Laminin 332		Fibronectin	BSA
	1µg/ml	2µg/ml	10µg/ml	10mg/ml
MDA 151+	52	65	63	4
MDA151-	46	71	60	5

EXPERIMENT 2

	Percentage of adhereing cells after 30min at 37°C			
	Laminin 332		Fibronectin	BSA
	1µg/ml	2µg/ml	10µg/ml	10mg/ml
MDA 151+	66	74	70	8
MDA151-	59	69	78	9

EXPERIMENT 3

	Percentage of adhereing cells after 30min at 37°C			
	Laminin 332		Fibronectin	BSA
	1µg/ml	2µg/ml	10µg/ml	10mg/ml
MDA 151+	59	69.5	66.5	6
MDA151-	52.5	70	69	7

Appendix 7 - Endothelial attachment assay

Data represents percentage of MDA-231 CD151(+) / (-) cells that remained attached to TNF◎ stimulated HUVEC after 1 minute. The experiment was performed in duplicate (2 μ slides each) using HUVECs purified from 4 different cords. No attachment was observed for this time point when non stimulated HUVEC was used.

μ slide 1

	CORD 1	CORD 2	CORD 3	CORD 4
MDA 151+	78	10	76	34
MDA 151 -	13	54	8	30

μ slide 2

μ slide2	CORD 1	CORD 2	CORD 3	CORD 4
MDA 151+	70	9	92	28
MDA 151 -	9	48	8	25

Appendix 8 - Transendothelial migration assay of MDA-231 CD151 (+)/(-) cells across a monolayer of HBMEC at various time points

4hrs Migration	Number of migrated cells per field								
INSERT	1			2			3		
MDA 151(+)	48	55	51	60	55	49	55	61	60
MDA 151(-)	54	49	59	52	49	45	51	53	50

6hrs Migration	Number of migrated cells per field								
INSERT	1			2			3		
MDA 151(+)	160	153	148	170	155	173	190	132	164
MDA 151(-)	176	149	151	148	180	165	149	150	141

8hrs Migration	Number of migrated cells per field								
INSERT	1			2			3		
MDA 151(+)	201	190	182	222	186	179	194	194	186
MDA 151(-)	197	184	207	188	169	188	181	199	201

6. SUPPLEMENTARY DATA

Western blot analysis of sucrose density gradient fraction of MDA-231 (PLM)- and (QRD)- cell lines performed under 1% Brij 96 conditions, detected for CD151, α3 integrin light chain fragment and α6 integrin light chain fragment.

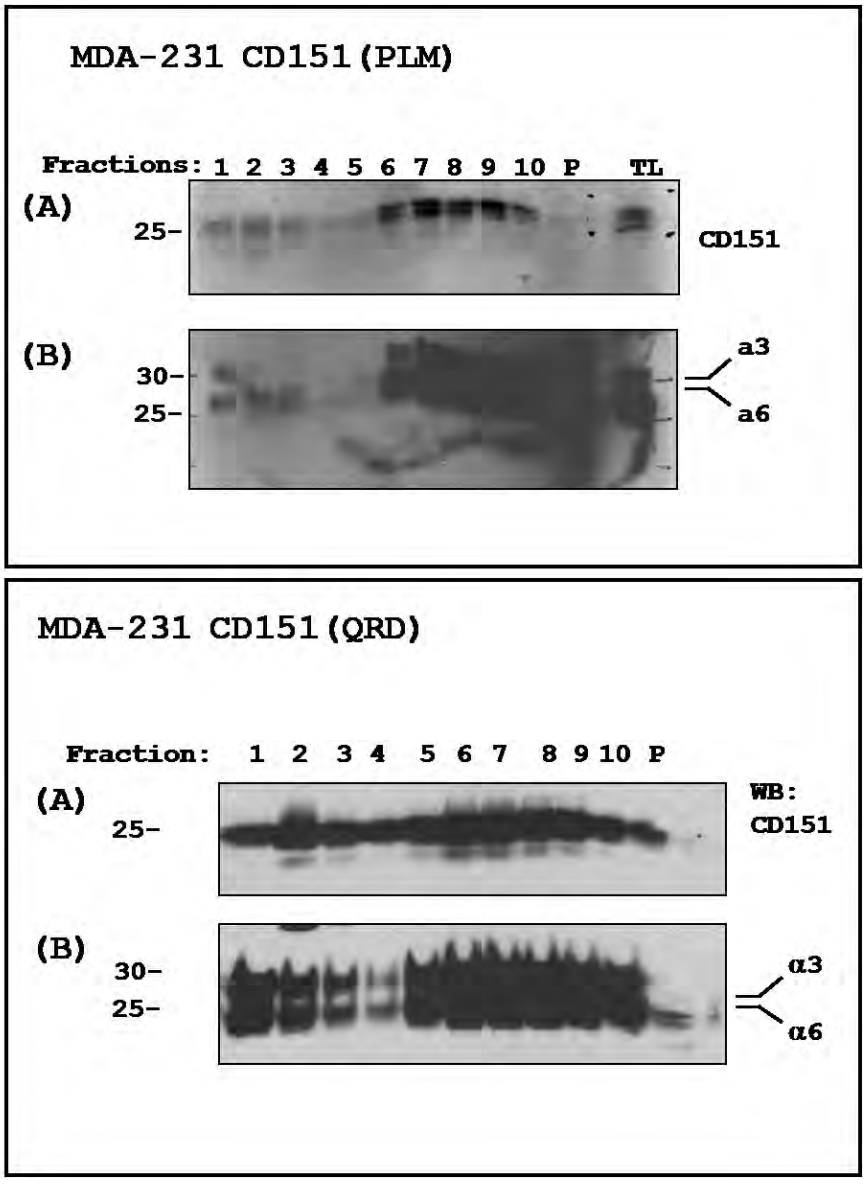

References

Adair, B.D., Xiong, J.P., Maddock, C., Goodman, S.L., Arnaout, M.A., & Yeager, M. 2005. Three-dimensional EM structure of the ectodomain of integrin {alpha}V{beta}3 in a complex with fibronectin. ***J.Cell Biol.*****, 168, (7) 1109-1118 available from: PM:15795319**

Ang, J., Fang, B.L., Ashman, L.K., & Frauman, A.G. 2010. The migration and invasion of human prostate cancer cell lines involves CD151 expression. ***Oncol.Rep.*****, 24, (6) 1593-1597 available from: PM:21042756**

Ang, J., Lijovic, M., Ashman, L.K., Kan, K., & Frauman, A.G. 2004. CD151 protein expression predicts the clinical outcome of low-grade primary prostate cancer better than histologic grading: a new prognostic indicator? ***Cancer Epidemiol.Biomarkers Prev.*****, 13, (11 Pt 1) 1717-1721 available from: PM:15533898**

Armulik, A. 2002. Splice variants of human beta 1 integrins: origin, biosynthesis and functions. ***Front Biosci.*****, 7, d219-d227 available from: PM:11779688**

Armulik, A., Nilsson, I., von, H.G., & Johansson, S. 1999. Determination of the border between the transmembrane and cytoplasmic domains of human integrin subunits. ***J.Biol.Chem.*****, 274, (52) 37030-37034 available from: PM:10601259**

Arnaout, M.A., Mahalingam, B., & Xiong, J.P. 2005. Integrin structure, allostery, and bidirectional signaling. ***Annu.Rev.Cell Dev.Biol.*****, 21, 381-410 available from: PM:16212500**

Arnold, M., Cavalcanti-Adam, E.A., Glass, R., Blummel, J., Eck, W., Kantlehner, M., Kessler, H., & Spatz, J.P. 2004. Activation of integrin function by nanopatterned adhesive interfaces. ***Chemphyschem.*****, 5, (3) 383-388 available from: PM:15067875**

Ashman, L.K., Aylett, G.W., Mehrabani, P.A., Bendall, L.J., Niutta, S., Cambareri, A.C., Cole, S.R., & Berndt, M.C. 1991. The murine monoclonal antibody, 14A2.H1, identifies a novel platelet surface antigen. ***Br.J.Haematol.*****, 79, (2) 263-270 available from: PM:1958484**

Aumailley, M., Bruckner-Tuderman, L., Carter, W.G., Deutzmann, R., Edgar, D., Ekblom, P., Engel, J., Engvall, E., Hohenester, E., Jones, J.C., Kleinman, H.K., Marinkovich, M.P., Martin, G.R., Mayer, U., Meneguzzi, G., Miner, J.H., Miyazaki, K., Patarroyo, M., Paulsson, M., Quaranta, V., Sanes, J.R., Sasaki, T., Sekiguchi, K., Sorokin, L.M., Talts, J.F., Tryggvason, K., Uitto, J., Virtanen, I., von der, M.K.,

Wewer, U.M., Yamada, Y., & Yurchenco, P.D. 2005. A simplified laminin nomenclature. ***Matrix Biol.*****, 24, (5) 326-332 available from: PM:15979864**

Baldwin, G., Novitskaya, V., Sadej, R., Pochec, E., Litynska, A., Hartmann, C., Williams, J., Ashman, L., Eble, J.A., & Berditchevski, F. 2008. Tetraspanin CD151 regulates glycosylation of (alpha)3(beta)1 integrin. ***J.Biol.Chem.*****, 283, (51) 35445-35454 available from: PM:18852263**

Baleato, R.M., Guthrie, P.L., Gubler, M.C., Ashman, L.K., & Roselli, S. 2008. Deletion of CD151 results in a strain-dependent glomerular disease due to severe alterations of the glomerular basement membrane. ***Am.J.Pathol.*****, 173, (4) 927-937 available from: PM:18787104**

Bandyopadhyay, S., Zhan, R., Chaudhuri, A., Watabe, M., Pai, S.K., Hirota, S., Hosobe, S., Tsukada, T., Miura, K., Takano, Y., Saito, K., Pauza, M.E., Hayashi, S., Wang, Y., Mohinta, S., Mashimo, T., Iiizumi, M., Furuta, E., & Watabe, K. 2006. Interaction of KAI1 on tumor cells with DARC on vascular endothelium leads to metastasis suppression. ***Nat.Med.*****, 12, (8) 933-938 available from: PM:16862154**

Barreiro, O., Yanez-Mo, M., Sala-Valdes, M., Gutierrez-Lopez, M.D., Ovalle, S., Higginbottom, A., Monk, P.N., Cabanas, C., & Sanchez-Madrid, F. 2005. Endothelial tetraspanin microdomains regulate leukocyte firm adhesion during extravasation. ***Blood*****, 105, (7) 2852-2861 available from: PM:15591117**

Beglova, N., Blacklow, S.C., Takagi, J., & Springer, T.A. 2002. Cysteine-rich module structure reveals a fulcrum for integrin rearrangement upon activation. ***Nat.Struct.Biol.*****, 9, (4) 282-287 available from: PM:11896403**

Bellis, S.L. 2004. Variant glycosylation: an underappreciated regulatory mechanism for beta1 integrins. ***Biochim.Biophys.Acta*****, 1663, (1-2) 52-60 available from: PM:15157607**

Berditchevski, F., Bazzoni, G., & Hemler, M.E. 1995. Specific association of CD63 with the VLA-3 and VLA-6 integrins. ***J.Biol.Chem.*****, 270, (30) 17784-17790 available from: PM:7629079**

Berditchevski, F., Chang, S., Bodorova, J., & Hemler, M.E. 1997. Generation of monoclonal antibodies to integrin-associated proteins. Evidence that alpha3beta1 complexes with EMMPRIN/basigin/OX47/M6. ***J.Biol.Chem.*****, 272, (46) 29174-29180 available from: PM:9360995**

Berditchevski, F., Gilbert, E., Griffiths, M.R., Fitter, S., Ashman, L., & Jenner, S.J. 2001. Analysis of the CD151-alpha3beta1 integrin and CD151-tetraspanin

interactions by mutagenesis. *J.Biol.Chem.*, 276, (44) 41165-41174 available from: PM:11479292

Berditchevski, F., Odintsova, E., Sawada, S., & Gilbert, E. 2002. Expression of the palmitoylation-deficient CD151 weakens the association of alpha 3 beta 1 integrin with the tetraspanin-enriched microdomains and affects integrin-dependent signaling. *J.Biol.Chem.*, 277, (40) 36991-37000 available from: PM:12110679

Berrier, A.L. & Yamada, K.M. 2007. Cell-matrix adhesion. *J.Cell Physiol*, 213, (3) 565-573 available from: PM:17680633

Bischoff, J. & Kornfeld, R. 1984. The effect of 1-deoxymannojirimycin on rat liver alpha-mannosidases. *Biochem.Biophys.Res.Commun.*, 125, (1) 324-331 available from: PM:6239623

Bischoff, J., Liscum, L., & Kornfeld, R. 1986. The use of 1-deoxymannojirimycin to evaluate the role of various alpha-mannosidases in oligosaccharide processing in intact cells. *J.Biol.Chem.*, 261, (10) 4766-4774 available from: PM:2937779

Blobel, G. & Sabatini, D.D. 1970. Controlled proteolysis of nascent polypeptides in rat liver cell fractions. I. Location of the polypeptides within ribosomes. *J.Cell Biol.*, 45, (1) 130-145 available from: PM:5458992

Bos, P.D., Zhang, X.H., Nadal, C., Shu, W., Gomis, R.R., Nguyen, D.X., Minn, A.J., van de Vijver, M.J., Gerald, W.L., Foekens, J.A., & Massague, J. 2009. Genes that mediate breast cancer metastasis to the brain. *Nature*, 459, (7249) 1005-1009 available from: PM:19421193

Brown, D.A. & London, E. 2000. Structure and function of sphingolipid- and cholesterol-rich membrane rafts. *J.Biol.Chem.*, 275, (23) 17221-17224 available from: PM:10770957

Buschow, S.I., Nolte-'t Hoen, E.N., van, N.G., Pols, M.S., ten, B.T., Lauwen, M., Ossendorp, F., Melief, C.J., Raposo, G., Wubbolts, R., Wauben, M.H., & Stoorvogel, W. 2009. MHC II in dendritic cells is targeted to lysosomes or T cell-induced exosomes via distinct multivesicular body pathways. *Traffic.*, 10, (10) 1528-1542 available from: PM:19682328

Cai, H., Wang, C.C., & Tsou, C.L. 1994. Chaperone-like activity of protein disulfide isomerase in the refolding of a protein with no disulfide bonds. *J.Biol.Chem.*, 269, (40) 24550-24552 available from: PM:7929125

Cailleau, R., Olive, M., & Cruciger, Q.V. 1978. Long-term human breast carcinoma cell lines of metastatic origin: preliminary characterization. *In Vitro*, 14, (11) 911-915 available from: PM:730202

Caplan, M.J., Kamsteeg, E.J., & Duffield, A. 2007. Tetraspan proteins: regulators of renal structure and function. *Curr.Opin.Nephrol.Hypertens.*, 16, (4) 353-358 available from: PM:17565278

Cavalcanti-Adam, E.A., Volberg, T., Micoulet, A., Kessler, H., Geiger, B., & Spatz, J.P. 2007. Cell spreading and focal adhesion dynamics are regulated by spacing of integrin ligands. *Biophys.J.*, 92, (8) 2964-2974 available from: PM:17277192

Chambrion, C. & Le, N.F. 2010. The tetraspanins CD9 and CD81 regulate CD9P1-induced effects on cell migration. *PLoS.One.*, 5, (6) e11219 available from: PM:20574531

Charrin, S., Le, N.F., Labas, V., Billard, M., Le Caer, J.P., Emile, J.F., Petit, M.A., Boucheix, C., & Rubinstein, E. 2003a. EWI-2 is a new component of the tetraspanin web in hepatocytes and lymphoid cells. *Biochem.J.*, 373, (Pt 2) 409-421 available from: PM:12708969

Charrin, S., Le, N.F., Silvie, O., Milhiet, P.E., Boucheix, C., & Rubinstein, E. 2009. Lateral organization of membrane proteins: tetraspanins spin their web. *Biochem.J.*, 420, (2) 133-154 available from: PM:19426143

Charrin, S., Manie, S., Billard, M., Ashman, L., Gerlier, D., Boucheix, C., & Rubinstein, E. 2003b. Multiple levels of interactions within the tetraspanin web. *Biochem.Biophys.Res.Commun.*, 304, (1) 107-112 available from: PM:12705892

Charrin, S., Manie, S., Oualid, M., Billard, M., Boucheix, C., & Rubinstein, E. 2002. Differential stability of tetraspanin/tetraspanin interactions: role of palmitoylation. *FEBS Lett.*, 516, (1-3) 139-144 available from: PM:11959120

Charrin, S., Manie, S., Thiele, C., Billard, M., Gerlier, D., Boucheix, C., & Rubinstein, E. 2003c. A physical and functional link between cholesterol and tetraspanins. *Eur.J.Immunol.*, 33, (9) 2479-2489 available from: PM:12938224

Chen, X., Jen, A., Warley, A., Lawrence, M.J., Quinn, P.J., & Morris, R.J. 2009. Isolation at physiological temperature of detergent-resistant membranes with properties expected of lipid rafts: the influence of buffer composition. *Biochem.J.*, 417, (2) 525-533 available from: PM:18831713

Chien, C.W., Lin, S.C., Lai, Y.Y., Lin, B.W., Lin, S.C., Lee, J.C., & Tsai, S.J. 2008. Regulation of CD151 by hypoxia controls cell adhesion and metastasis in colorectal cancer. *Clin.Cancer Res.*, 14, (24) 8043-8051 available from: PM:19073968

Chometon, G., Zhang, Z.G., Rubinstein, E., Boucheix, C., Mauch, C., & Aumailley, M. 2006. Dissociation of the complex between CD151 and laminin-binding integrins permits migration of epithelial cells. *Exp.Cell Res.*, 312, (7) 983-995 available from: PM:16490193

Claas, C., Stipp, C.S., & Hemler, M.E. 2001. Evaluation of prototype transmembrane 4 superfamily protein complexes and their relation to lipid rafts. *J.Biol.Chem.*, 276, (11) 7974-7984 available from: PM:11113129

Cowin, A.J., Adams, D., Geary, S.M., Wright, M.D., Jones, J.C., & Ashman, L.K. 2006. Wound healing is defective in mice lacking tetraspanin CD151. *J.Invest Dermatol.*, 126, (3) 680-689 available from: PM:16410781

Dall'Olio, F., Malagolini, N., Di, S.G., Minni, F., Marrano, D., & Serafini-Cessi, F. 1989. Increased CMP-NeuAc:Gal beta 1,4GlcNAc-R alpha 2,6 sialyltransferase activity in human colorectal cancer tissues. *Int.J.Cancer*, 44, (3) 434-439 available from: PM:2476402

Danilczyk, U.G. & Williams, D.B. 2001. The lectin chaperone calnexin utilizes polypeptide-based interactions to associate with many of its substrates in vivo. *J.Biol.Chem.*, 276, (27) 25532-25540 available from: PM:11337494

Davis, T.L., Buerger, F., & Cress, A.E. 2002. Differential regulation of a novel variant of the alpha(6) integrin, alpha(6p). *Cell Growth Differ.*, 13, (3) 107-113 available from: PM:11959811

Davis, T.L., Rabinovitz, I., Futscher, B.W., Schnolzer, M., Burger, F., Liu, Y., Kulesz-Martin, M., & Cress, A.E. 2001. Identification of a novel structural variant of the alpha 6 integrin. *J.Biol.Chem.*, 276, (28) 26099-26106 available from: PM:11359780

de Melker, A.A., Sterk, L.M., Delwel, G.O., Fles, D.L., Daams, H., Weening, J.J., & Sonnenberg, A. 1997. The A and B variants of the alpha 3 integrin subunit: tissue distribution and functional characterization. *Lab Invest*, 76, (4) 547-563 available from: PM:9111516

Demetriou, M.C. & Cress, A.E. 2004. Integrin clipping: a novel adhesion switch? *J.Cell Biochem.*, 91, (1) 26-35 available from: PM:14689578

Demetriou, M.C., Pennington, M.E., Nagle, R.B., & Cress, A.E. 2004. Extracellular alpha 6 integrin cleavage by urokinase-type plasminogen activator in human prostate cancer. ***Exp.Cell Res.*****, 294, (2) 550-558 available from: PM:15023541**

Dennis, J.W., Laferte, S., Waghorne, C., Breitman, M.L., & Kerbel, R.S. 1987. Beta 1-6 branching of Asn-linked oligosaccharides is directly associated with metastasis. ***Science*****, 236, (4801) 582-585 available from: PM:2953071**

Dennis, J.W., Nabi, I.R., & Demetriou, M. 2009. Metabolism, cell surface organization, and disease. ***Cell*****, 139, (7) 1229-1241 available from: PM:20064370**

Duffield, A., Kamsteeg, E.J., Brown, A.N., Pagel, P., & Caplan, M.J. 2003. The tetraspanin CD63 enhances the internalization of the H,K-ATPase beta-subunit. ***Proc.Natl.Acad.Sci.U.S.A*****, 100, (26) 15560-15565 available from: PM:14660791**

Elbein, A.D. 1987. Inhibitors of the biosynthesis and processing of N-linked oligosaccharide chains. ***Annu.Rev.Biochem.*****, 56, 497-534 available from: PM:3304143**

Elbein, A.D., Tropea, J.E., Mitchell, M., & Kaushal, G.P. 1990. Kifunensine, a potent inhibitor of the glycoprotein processing mannosidase I. ***J.Biol.Chem.*****, 265, (26) 15599-15605 available from: PM:2144287**

Elkin, M. & Vlodavsky, I. 2001. Tail vein assay of cancer metastasis. ***Curr.Protoc.Cell Biol.*****, Chapter 19, Unit available from: PM:18228345**

Ellerman, D.A., Ha, C., Primakoff, P., Myles, D.G., & Dveksler, G.S. 2003. Direct binding of the ligand PSG17 to CD9 requires a CD9 site essential for sperm-egg fusion. ***Mol.Biol.Cell*****, 14, (12) 5098-5103 available from: PM:14528020**

Ellgaard, L. & Frickel, E.M. 2003. Calnexin, calreticulin, and ERp57: teammates in glycoprotein folding. ***Cell Biochem.Biophys.*****, 39, (3) 223-247 available from: PM:14716078**

Ellgaard, L., Molinari, M., & Helenius, A. 1999. Setting the standards: quality control in the secretory pathway. ***Science*****, 286, (5446) 1882-1888 available from: PM:10583943**

Ellgaard, L. & Ruddock, L.W. 2005. The human protein disulphide isomerase family: substrate interactions and functional properties. ***EMBO Rep.*****, 6, (1) 28-32 available from: PM:15643448**

Ermonval, M., Kitzmuller, C., Mir, A.M., Cacan, R., & Ivessa, N.E. 2001. N-glycan structure of a short-lived variant of ribophorin I expressed in the MadIA214 glycosylation-defective cell line reveals the role of a mannosidase that is not ER

mannosidase I in the process of glycoprotein degradation. *Glycobiology*, 11, (7) 565-576 available from: PM:11447136

Feizi, T. 1985. Demonstration by monoclonal antibodies that carbohydrate structures of glycoproteins and glycolipids are onco-developmental antigens. *Nature*, 314, (6006) 53-57 available from: PM:2579340

Fitter, S., Tetaz, T.J., Berndt, M.C., & Ashman, L.K. 1995. Molecular cloning of cDNA encoding a novel platelet-endothelial cell tetra-span antigen, PETA-3. *Blood*, 86, (4) 1348-1355 available from: PM:7632941

Fiuza, C., Salcedo, M., Clemente, G., & Tellado, J.M. 2002. Granulocyte colony-stimulating factor improves deficient in vitro neutrophil transendothelial migration in patients with advanced liver disease. *Clin.Diagn.Lab Immunol.*, 9, (2) 433-439 available from: PM:11874890

Fradet, Y., Cordon-Cardo, C., Thomson, T., Daly, M.E., Whitmore, W.F., Jr., Lloyd, K.O., Melamed, M.R., & Old, L.J. 1984. Cell surface antigens of human bladder cancer defined by mouse monoclonal antibodies. *Proc.Natl.Acad.Sci.U.S.A*, 81, (1) 224-228 available from: PM:6364135

Frenette, G.P., Carey, T.E., Varani, J., Schwartz, D.R., Fligiel, S.E., Ruddon, R.W., & Peters, B.P. 1988. Biosynthesis and secretion of laminin and laminin-associated glycoproteins by nonmalignant and malignant human keratinocytes: comparison of cell lines from primary and secondary tumors in the same patient. *Cancer Res.*, 48, (18) 5193-5202 available from: PM:2457436

Frenette, G.P., Ruddon, R.W., Krzesicki, R.F., Naser, J.A., & Peters, B.P. 1989. Biosynthesis and deposition of a noncovalent laminin-heparan sulfate proteoglycan complex and other basal lamina components by a human malignant cell line. *J.Biol.Chem.*, 264, (6) 3078-3088 available from: PM:2492529

Friedrichs, J., Torkko, J.M., Helenius, J., Teravainen, T.P., Fullekrug, J., Muller, D.J., Simons, K., & Manninen, A. 2007. Contributions of galectin-3 and -9 to epithelial cell adhesion analyzed by single cell force spectroscopy. *J.Biol.Chem.*, 282, (40) 29375-29383 available from: PM:17675292

Fuhlbrigge, R.C., Alon, R., Puri, K.D., Lowe, J.B., & Springer, T.A. 1996. Sialylated, fucosylated ligands for L-selectin expressed on leukocytes mediate tethering and rolling adhesions in physiologic flow conditions. *J.Cell Biol.*, 135, (3) 837-848 available from: PM:8909555

Fukudome, K., Furuse, M., Imai, T., Nishimura, M., Takagi, S., Hinuma, Y., & Yoshie, O. 1992. Identification of membrane antigen C33 recognized by monoclonal antibodies inhibitory to human T-cell leukemia virus type 1 (HTLV-1)-induced syncytium formation: altered glycosylation of C33 antigen in HTLV-1-positive T cells. ***J.Virol.*****, 66, (3) 1394-1401 available from: PM:1738199**

Garcia-Alvarez, B., de Pereda, J.M., Calderwood, D.A., Ulmer, T.S., Critchley, D., Campbell, I.D., Ginsberg, M.H., & Liddington, R.C. 2003. Structural determinants of integrin recognition by talin. ***Mol.Cell*****, 11, (1) 49-58 available from: PM:12535520**

Garcia-Espana, A., Chung, P.J., Sarkar, I.N., Stiner, E., Sun, T.T., & Desalle, R. 2008. Appearance of new tetraspanin genes during vertebrate evolution. ***Genomics*****, 91, (4) 326-334 available from: PM:18291621**

Geary, S.M., Cowin, A.J., Copeland, B., Baleato, R.M., Miyazaki, K., & Ashman, L.K. 2008. The role of the tetraspanin CD151 in primary keratinocyte and fibroblast functions: implications for wound healing. ***Exp.Cell Res.*****, 314, (11-12) 2165-2175 available from: PM:18534576**

Gehlsen, K.R., Sriramarao, P., Furcht, L.T., & Skubitz, A.P. 1992. A synthetic peptide derived from the carboxy terminus of the laminin A chain represents a binding site for the alpha 3 beta 1 integrin. ***J.Cell Biol.*****, 117, (2) 449-459 available from: PM:1560034**

Gidwitz, S., Temple, B., & White, G.C. 2004. Mutations in and near the second calcium-binding domain of integrin alphaIIb affect the structure and function of integrin alphaIIbbeta3. ***Biochem.J.*****, 379, (Pt 2) 449-459 available from: PM:14670082**

Goldstein, I.J. 2002. Lectin structure-activity: the story is never over. ***J.Agric.Food Chem.*****, 50, (22) 6583-6585 available from: PM:12381155**

Hakomori, S. 2002. Glycosylation defining cancer malignancy: new wine in an old bottle. ***Proc.Natl.Acad.Sci.U.S.A*****, 99, (16) 10231-10233 available from: PM:12149519**

Hammond, C., Braakman, I., & Helenius, A. 1994. Role of N-linked oligosaccharide recognition, glucose trimming, and calnexin in glycoprotein folding and quality control. ***Proc.Natl.Acad.Sci.U.S.A*****, 91, (3) 913-917 available from: PM:8302866**

Hao, J., Yang, Y., McDaniel, K.M., Dalkin, B.L., Cress, A.E., & Nagle, R.B. 1996. Differential expression of laminin 5 (alpha 3 beta 3 gamma 2) by human malignant and normal prostate. ***Am.J.Pathol.*****, 149, (4) 1341-1349 available from: PM:8863681**

He, B., Liu, L., Cook, G.A., Grgurevich, S., Jennings, L.K., & Zhang, X.A. 2005. Tetraspanin CD82 attenuates cellular morphogenesis through down-regulating

integrin alpha6-mediated cell adhesion. *J.Biol.Chem.*, 280, (5) 3346-3354 available from: PM:15557282

Hebert, D.N. & Molinari, M. 2007. In and out of the ER: protein folding, quality control, degradation, and related human diseases. *Physiol Rev.*, 87, (4) 1377-1408 available from: PM:17928587

Hemler, M.E. 2005. Tetraspanin functions and associated microdomains. *Nat.Rev.Mol.Cell Biol.*, 6, (10) 801-811 available from: PM:16314869

Hemler, M.E., Huang, C., & Schwarz, L. 1987. The VLA protein family. Characterization of five distinct cell surface heterodimers each with a common 130,000 molecular weight beta subunit. *J.Biol.Chem.*, 262, (7) 3300-3309 available from: PM:3546305

Hemler, M.E., Sanchez-Madrid, F., Flotte, T.J., Krensky, A.M., Burakoff, S.J., Bhan, A.K., Springer, T.A., & Strominger, J.L. 1984. Glycoproteins of 210,000 and 130,000 m.w. on activated T cells: cell distribution and antigenic relation to components on resting cells and T cell lines. *J.Immunol.*, 132, (6) 3011-3018 available from: PM:6327814

Herscovics, A., Schneikert, J., Athanassiadis, A., & Moremen, K.W. 1994. Isolation of a mouse Golgi mannosidase cDNA, a member of a gene family conserved from yeast to mammals. *J.Biol.Chem.*, 269, (13) 9864-9871 available from: PM:8144579

Higashiyama, S., Iwamoto, R., Goishi, K., Raab, G., Taniguchi, N., Klagsbrun, M., & Mekada, E. 1995. The membrane protein CD9/DRAP 27 potentiates the juxtacrine growth factor activity of the membrane-anchored heparin-binding EGF-like growth factor. *J.Cell Biol.*, 128, (5) 929-938 available from: PM:7876316

Hintermann, E., Bilban, M., Sharabi, A., & Quaranta, V. 2001. Inhibitory role of alpha 6 beta 4-associated erbB-2 and phosphoinositide 3-kinase in keratinocyte haptotactic migration dependent on alpha 3 beta 1 integrin. *J.Cell Biol.*, 153, (3) 465-478 available from: PM:11331299

Hirsch, C., Blom, D., & Ploegh, H.L. 2003. A role for N-glycanase in the cytosolic turnover of glycoproteins. *EMBO J.*, 22, (5) 1036-1046 available from: PM:12606569

Hirschberg, C.B. 2001. Golgi nucleotide sugar transport and leukocyte adhesion deficiency II. *J.Clin.Invest*, 108, (1) 3-6 available from: PM:11435449

Hosokawa, N., Wada, I., Hasegawa, K., Yorihuzi, T., Tremblay, L.O., Herscovics, A., & Nagata, K. 2001. A novel ER alpha-mannosidase-like protein accelerates ER-associated degradation. *EMBO Rep.*, 2, (5) 415-422 available from: PM:11375934

Hosomi, A., Tanabe, K., Hirayama, H., Kim, I., Rao, H., & Suzuki, T. 2010. Identification of an Htm1 (EDEM)-dependent, Mns1-independent Endoplasmic Reticulum-associated Degradation (ERAD) pathway in Saccharomyces cerevisiae: application of a novel assay for glycoprotein ERAD. ***J.Biol.Chem.*****, 285, (32) 24324-24334 available from: PM:20511219**

Hu, M., Yao, J., Carroll, D.K., Weremowicz, S., Chen, H., Carrasco, D., Richardson, A., Violette, S., Nikolskaya, T., Nikolsky, Y., Bauerlein, E.L., Hahn, W.C., Gelman, R.S., Allred, C., Bissell, M.J., Schnitt, S., & Polyak, K. 2008. Regulation of in situ to invasive breast carcinoma transition. ***Cancer Cell*****, 13, (5) 394-406 available from: PM:18455123**

Huang, S., Yuan, S., Dong, M., Su, J., Yu, C., Shen, Y., Xie, X., Yu, Y., Yu, X., Chen, S., Zhang, S., Pontarotti, P., & Xu, A. 2005. The phylogenetic analysis of tetraspanins projects the evolution of cell-cell interactions from unicellular to multicellular organisms. ***Genomics*****, 86, (6) 674-684 available from: PM:16242907**

Hughes, A.L. 1992. Coevolution of the vertebrate integrin alpha- and beta-chain genes. ***Mol.Biol.Evol.*****, 9, (2) 216-234 available from: PM:1560759**

Humphries, J.D., Byron, A., & Humphries, M.J. 2006. Integrin ligands at a glance. ***J.Cell Sci.*****, 119, (Pt 19) 3901-3903 available from: PM:16988024**

Hynes, R.O. 1987. Integrins: a family of cell surface receptors. ***Cell*****, 48, (4) 549-554 available from: PM:3028640**

Hynes, R.O. 2009. The extracellular matrix: not just pretty fibrils. ***Science*****, 326, (5957) 1216-1219 available from: PM:19965464**

Igdoura, S.A., Herscovics, A., Lal, A., Moremen, K.W., Morales, C.R., & Hermo, L. 1999. Alpha-mannosidases involved in N-glycan processing show cell specificity and distinct subcompartmentalization within the Golgi apparatus of cells in the testis and epididymis. ***Eur.J.Cell Biol.*****, 78, (7) 441-452 available from: PM:10472797**

Isaji, T., Sato, Y., Zhao, Y., Miyoshi, E., Wada, Y., Taniguchi, N., & Gu, J. 2006. N-glycosylation of the beta-propeller domain of the integrin alpha5 subunit is essential for alpha5beta1 heterodimerization, expression on the cell surface, and its biological function. ***J.Biol.Chem.*****, 281, (44) 33258-33267 available from: PM:16959765**

Iwamoto, R., Higashiyama, S., Mitamura, T., Taniguchi, N., Klagsbrun, M., & Mekada, E. 1994. Heparin-binding EGF-like growth factor, which acts as the diphtheria toxin receptor, forms a complex with membrane protein DRAP27/CD9,

which up-regulates functional receptors and diphtheria toxin sensitivity. *EMBO J.*, 13, (10) 2322-2330 available from: PM:8194524

Jakob, C.A., Burda, P., Roth, J., & Aebi, M. 1998a. Degradation of misfolded endoplasmic reticulum glycoproteins in Saccharomyces cerevisiae is determined by a specific oligosaccharide structure. *J.Cell Biol.*, 142, (5) 1223-1233 available from: PM:9732283

Jakob, C.A., Burda, P., te, H.S., Aebi, M., & Roth, J. 1998b. Genetic tailoring of N-linked oligosaccharides: the role of glucose residues in glycoprotein processing of Saccharomyces cerevisiae in vivo. *Glycobiology*, 8, (2) 155-164 available from: PM:9451025

Jelinek-Kelly, S. & Herscovics, A. 1988. Glycoprotein biosynthesis in Saccharomyces cerevisiae. Purification of the alpha-mannosidase which removes one specific mannose residue from Man9GlcNAc. *J.Biol.Chem.*, 263, (29) 14757-14763 available from: PM:3049586

Johnson, J.L., Winterwood, N., DeMali, K.A., & Stipp, C.S. 2009. Tetraspanin CD151 regulates RhoA activation and the dynamic stability of carcinoma cell-cell contacts. *J.Cell Sci.*, 122, (Pt 13) 2263-2273 available from: PM:19509057

Jones, P.A. & DeClerck, Y.A. 1980. Destruction of extracellular matrices containing glycoproteins, elastin, and collagen by metastatic human tumor cells. *Cancer Res.*, 40, (9) 3222-3227 available from: PM:7000340

Kahn, H.J., Brodt, P., & Baumal, R. 1988. Lectin binding by liver and lung metastasizing variants of the murine Lewis lung carcinoma. *Am.J.Pathol.*, 132, (1) 180-185 available from: PM:3394799

Kang, S.J. & Cresswell, P. 2002. Calnexin, calreticulin, and ERp57 cooperate in disulfide bond formation in human CD1d heavy chain. *J.Biol.Chem.*, 277, (47) 44838-44844 available from: PM:12239218

Katayama, M., Sanzen, N., Funakoshi, A., & Sekiguchi, K. 2003. Laminin gamma2-chain fragment in the circulation: a prognostic indicator of epithelial tumor invasion. *Cancer Res.*, 63, (1) 222-229 available from: PM:12517801

Kazarov, A.R., Yang, X., Stipp, C.S., Sehgal, B., & Hemler, M.E. 2002. An extracellular site on tetraspanin CD151 determines alpha 3 and alpha 6 integrin-dependent cellular morphology. *J.Cell Biol.*, 158, (7) 1299-1309 available from: PM:12356873

Keith, N., Parodi, A.J., & Caramelo, J.J. 2005. Glycoprotein tertiary and quaternary structures are monitored by the same quality control mechanism. *J.Biol.Chem.*, 280, (18) 18138-18141 available from: PM:15746090

Keller, S.H., Lindstrom, J., & Taylor, P. 1998. Inhibition of glucose trimming with castanospermine reduces calnexin association and promotes proteasome degradation of the alpha-subunit of the nicotinic acetylcholine receptor. *J.Biol.Chem.*, 273, (27) 17064-17072 available from: PM:9642271

Kiema, T., Lad, Y., Jiang, P., Oxley, C.L., Baldassarre, M., Wegener, K.L., Campbell, I.D., Ylanne, J., & Calderwood, D.A. 2006. The molecular basis of filamin binding to integrins and competition with talin. *Mol.Cell*, 21, (3) 337-347 available from: PM:16455489

Kim, Y.J., Borsig, L., Varki, N.M., & Varki, A. 1998. P-selectin deficiency attenuates tumor growth and metastasis. *Proc.Natl.Acad.Sci.U.S.A*, 95, (16) 9325-9330 available from: PM:9689079

Klemm, R.W., Ejsing, C.S., Surma, M.A., Kaiser, H.J., Gerl, M.J., Sampaio, J.L., de, R.Q., Ferguson, C., Proszynski, T.J., Shevchenko, A., & Simons, K. 2009. Segregation of sphingolipids and sterols during formation of secretory vesicles at the trans-Golgi network. *J.Cell Biol.*, 185, (4) 601-612 available from: PM:19433450

Kobayashi, K., Matsumoto, S., Morishima, T., Kawabe, T., & Okamoto, T. 2000. Cimetidine inhibits cancer cell adhesion to endothelial cells and prevents metastasis by blocking E-selectin expression. *Cancer Res.*, 60, (14) 3978-3984 available from: PM:10919677

Kohl, S., Giddings, I., Besch, D., Apfelstedt-Sylla, E., Zrenner, E., & Wissinger, B. 1998. The role of the peripherin/RDS gene in retinal dystrophies. *Acta Anat.(Basel)*, 162, (2-3) 75-84 available from: PM:9831753

Kohno, M., Hasegawa, H., Miyake, M., Yamamoto, T., & Fujita, S. 2002. CD151 enhances cell motility and metastasis of cancer cells in the presence of focal adhesion kinase. *Int.J.Cancer*, 97, (3) 336-343 available from: PM:11774285

Kong, X.T., Deng, F.M., Hu, P., Liang, F.X., Zhou, G., Auerbach, A.B., Genieser, N., Nelson, P.K., Robbins, E.S., Shapiro, E., Kachar, B., & Sun, T.T. 2004. Roles of uroplakins in plaque formation, umbrella cell enlargement, and urinary tract diseases. *J.Cell Biol.*, 167, (6) 1195-1204 available from: PM:15611339

Kornfeld, R. & Kornfeld, S. 1985. Assembly of asparagine-linked oligosaccharides. *Annu.Rev.Biochem.*, 54, 631-664 available from: PM:3896128

Krokhin, O.V., Cheng, K., Sousa, S.L., Ens, W., Standing, K.G., & Wilkins, J.A. 2003. Mass spectrometric based mapping of the disulfide bonding patterns of integrin alpha chains. ***Biochemistry*****, 42, (44) 12950-12959 available from: PM:14596610**

Laferte, S. & Dennis, J.W. 1989. Purification of two glycoproteins expressing beta 1-6 branched Asn-linked oligosaccharides from metastatic tumour cells. ***Biochem.J.*****, 259, (2) 569-576 available from: PM:2719668**

Lajoie, P., Goetz, J.G., Dennis, J.W., & Nabi, I.R. 2009. Lattices, rafts, and scaffolds: domain regulation of receptor signaling at the plasma membrane. ***J.Cell Biol.*****, 185, (3) 381-385 available from: PM:19398762**

Lal, A., Pang, P., Kalelkar, S., Romero, P.A., Herscovics, A., & Moremen, K.W. 1998. Substrate specificities of recombinant murine Golgi alpha1, 2-mannosidases IA and IB and comparison with endoplasmic reticulum and Golgi processing alpha1,2-mannosidases. ***Glycobiology*****, 8, (10) 981-995 available from: PM:9719679**

Lammerding, J., Kazarov, A.R., Huang, H., Lee, R.T., & Hemler, M.E. 2003. Tetraspanin CD151 regulates alpha6beta1 integrin adhesion strengthening. ***Proc.Natl.Acad.Sci.U.S.A*****, 100, (13) 7616-7621 available from: PM:12805567**

Lasfargues, E.Y., Coutinho, W.G., & Redfield, E.S. 1978. Isolation of two human tumor epithelial cell lines from solid breast carcinomas. ***J.Natl.Cancer Inst.*****, 61, (4) 967-978 available from: PM:212572**

Lau, K.S., Partridge, E.A., Grigorian, A., Silvescu, C.I., Reinhold, V.N., Demetriou, M., & Dennis, J.W. 2007. Complex N-glycan number and degree of branching cooperate to regulate cell proliferation and differentiation. ***Cell*****, 129, (1) 123-134 available from: PM:17418791**

Lau, L.M., Wee, J.L., Wright, M.D., Moseley, G.W., Hogarth, P.M., Ashman, L.K., & Jackson, D.E. 2004. The tetraspanin superfamily member CD151 regulates outside-in integrin alphaIIbbeta3 signaling and platelet function. ***Blood*****, 104, (8) 2368-2375 available from: PM:15226180**

Lee, R.T., Berditchevski, F., Cheng, G.C., & Hemler, M.E. 1995. Integrin-mediated collagen matrix reorganization by cultured human vascular smooth muscle cells. ***Circ.Res.*****, 76, (2) 209-214 available from: PM:7834831**

Ley, K., Laudanna, C., Cybulsky, M.I., & Nourshargh, S. 2007. Getting to the site of inflammation: the leukocyte adhesion cascade updated. ***Nat.Rev.Immunol.*****, 7, (9) 678-689 available from: PM:17717539**

Liotta, L.A., Kleinerman, J., Catanzaro, P., & Rynbrandt, D. 1977. Degradation of basement membrane by murine tumor cells. ***J.Natl.Cancer Inst.*****, 58, (5) 1427-1431 available from: PM:192901**

Livingston, B.D., Jacobs, J.L., Glick, M.C., & Troy, F.A. 1988. Extended polysialic acid chains (n greater than 55) in glycoproteins from human neuroblastoma cells. ***J.Biol.Chem.*****, 263, (19) 9443-9448 available from: PM:3288635**

London, E. & Brown, D.A. 2000. Insolubility of lipids in triton X-100: physical origin and relationship to sphingolipid/cholesterol membrane domains (rafts). ***Biochim.Biophys.Acta*****, 1508, (1-2) 182-195 available from: PM:11090825**

Luo, B.H., Carman, C.V., & Springer, T.A. 2007. Structural basis of integrin regulation and signaling. ***Annu.Rev.Immunol.*****, 25, 619-647 available from: PM:17201681**

Ma, Y.Q., Qin, J., Wu, C., & Plow, E.F. 2008. Kindlin-2 (Mig-2): a co-activator of beta3 integrins. ***J.Cell Biol.*****, 181, (3) 439-446 available from: PM:18458155**

Madjd, Z., Parsons, T., Watson, N.F., Spendlove, I., Ellis, I., & Durrant, L.G. 2005. High expression of Lewis y/b antigens is associated with decreased survival in lymph node negative breast carcinomas. ***Breast Cancer Res.*****, 7, (5) R780-R787 available from: PM:16168124**

Maecker, H.T. & Levy, S. 1997. Normal lymphocyte development but delayed humoral immune response in CD81-null mice. ***J.Exp.Med.*****, 185, (8) 1505-1510 available from: PM:9126932**

Mast, S.W., Diekman, K., Karaveg, K., Davis, A., Sifers, R.N., & Moremen, K.W. 2005. Human EDEM2, a novel homolog of family 47 glycosidases, is involved in ER-associated degradation of glycoproteins. ***Glycobiology*****, 15, (4) 421-436 available from: PM:15537790**

Mathieu, S., Prorok, M., Benoliel, A.M., Uch, R., Langlet, C., Bongrand, P., Gerolami, R., & El-Battari, A. 2004. Transgene expression of alpha(1,2)-fucosyltransferase-I (FUT1) in tumor cells selectively inhibits sialyl-Lewis x expression and binding to E-selectin without affecting synthesis of sialyl-Lewis a or binding to P-selectin. ***Am.J.Pathol.*****, 164, (2) 371-383 available from: PM:14742243**

McEver, R.P. & Zhu, C. 2010. Rolling cell adhesion. ***Annu.Rev.Cell Dev.Biol.*****, 26, 363-396 available from: PM:19575676**

Mendelsohn, R., Cheung, P., Berger, L., Partridge, E., Lau, K., Datti, A., Pawling, J., & Dennis, J.W. 2007. Complex N-glycan and metabolic control in tumor cells. ***Cancer Res.*****, 67, (20) 9771-9780 available from: PM:17942907**

Metzelaar, M.J., Wijngaard, P.L., Peters, P.J., Sixma, J.J., Nieuwenhuis, H.K., & Clevers, H.C. 1991. CD63 antigen. A novel lysosomal membrane glycoprotein, cloned by a screening procedure for intracellular antigens in eukaryotic cells. ***J.Biol.Chem.*****, 266, (5) 3239-3245 available from: PM:1993697**

Millon-Fremillon, A., Bouvard, D., Grichine, A., Manet-Dupe, S., Block, M.R., & Albiges-Rizo, C. 2008. Cell adaptive response to extracellular matrix density is controlled by ICAP-1-dependent beta1-integrin affinity. ***J.Cell Biol.*****, 180, (2) 427-441 available from: PM:18227284**

Miranti, C.K. & Brugge, J.S. 2002. Sensing the environment: a historical perspective on integrin signal transduction. ***Nat.Cell Biol.*****, 4, (4) E83-E90 available from: PM:11944041**

Misaghi, S., Pacold, M.E., Blom, D., Ploegh, H.L., & Korbel, G.A. 2004. Using a small molecule inhibitor of peptide: N-glycanase to probe its role in glycoprotein turnover. ***Chem.Biol.*****, 11, (12) 1677-1687 available from: PM:15610852**

Mitoma, J., Bao, X., Petryanik, B., Schaerli, P., Gauguet, J.M., Yu, S.Y., Kawashima, H., Saito, H., Ohtsubo, K., Marth, J.D., Khoo, K.H., von Andrian, U.H., Lowe, J.B., & Fukuda, M. 2007. Critical functions of N-glycans in L-selectin-mediated lymphocyte homing and recruitment. ***Nat.Immunol.*****, 8, (4) 409-418 available from: PM:17334369**

Miyazaki, T., Muller, U., & Campbell, K.S. 1997. Normal development but differentially altered proliferative responses of lymphocytes in mice lacking CD81. ***EMBO J.*****, 16, (14) 4217-4225 available from: PM:9250665**

Miyoshi, E., Nishikawa, A., Ihara, Y., Gu, J., Sugiyama, T., Hayashi, N., Fusamoto, H., Kamada, T., & Taniguchi, N. 1993. N-acetylglucosaminyltransferase III and V messenger RNA levels in LEC rats during hepatocarcinogenesis. ***Cancer Res.*****, 53, (17) 3899-3902 available from: PM:8240532**

Molinari, M. & Helenius, A. 2000. Chaperone selection during glycoprotein translocation into the endoplasmic reticulum. ***Science*****, 288, (5464) 331-333 available from: PM:10764645**

Montanez, E., Ussar, S., Schifferer, M., Bosl, M., Zent, R., Moser, M., & Fassler, R. 2008. Kindlin-2 controls bidirectional signaling of integrins. *Genes Dev.*, 22, (10) 1325-1330 available from: PM:18483218

Moolenaar, C.E., Muller, E.J., Schol, D.J., Figdor, C.G., Bock, E., Bitter-Suermann, D., & Michalides, R.J. 1990. Expression of neural cell adhesion molecule-related sialoglycoprotein in small cell lung cancer and neuroblastoma cell lines H69 and CHP-212. *Cancer Res.*, 50, (4) 1102-1106 available from: PM:2153450

Moremen, K.W., Trimble, R.B., & Herscovics, A. 1994. Glycosidases of the asparagine-linked oligosaccharide processing pathway. *Glycobiology*, 4, (2) 113-125 available from: PM:8054711

Moser, M., Nieswandt, B., Ussar, S., Pozgajova, M., & Fassler, R. 2008. Kindlin-3 is essential for integrin activation and platelet aggregation. *Nat.Med.*, 14, (3) 325-330 available from: PM:18278053

Munro, S. 2001. The MRH domain suggests a shared ancestry for the mannose 6-phosphate receptors and other N-glycan-recognising proteins. *Curr.Biol.*, 11, (13) R499-R501 available from: PM:11470418

Nadanaka, S., Sato, C., Kitajima, K., Katagiri, K., Irie, S., & Yamagata, T. 2001. Occurrence of oligosialic acids on integrin alpha 5 subunit and their involvement in cell adhesion to fibronectin. *J.Biol.Chem.*, 276, (36) 33657-33664 available from: PM:11418585

Nilsson, I., Kelleher, D.J., Miao, Y., Shao, Y., Kreibich, G., Gilmore, R., von, H.G., & Johnson, A.E. 2003. Photocross-linking of nascent chains to the STT3 subunit of the oligosaccharyltransferase complex. *J.Cell Biol.*, 161, (4) 715-725 available from: PM:12756234

Nilsson, I.M. & von, H.G. 1993. Determination of the distance between the oligosaccharyltransferase active site and the endoplasmic reticulum membrane. *J.Biol.Chem.*, 268, (8) 5798-5801 available from: PM:8449946

Nishiuchi, R., Murayama, O., Fujiwara, H., Gu, J., Kawakami, T., Aimoto, S., Wada, Y., & Sekiguchi, K. 2003. Characterization of the ligand-binding specificities of integrin alpha3beta1 and alpha6beta1 using a panel of purified laminin isoforms containing distinct alpha chains. *J.Biochem.*, 134, (4) 497-504 available from: PM:14607975

Nishiuchi, R., Sanzen, N., Nada, S., Sumida, Y., Wada, Y., Okada, M., Takagi, J., Hasegawa, H., & Sekiguchi, K. 2005. Potentiation of the ligand-binding activity of

integrin alpha3beta1 via association with tetraspanin CD151. ***Proc.Natl.Acad.Sci.U.S.A*****, 102, (6) 1939-1944 available from: PM:15677332**

Nishiuchi, R., Takagi, J., Hayashi, M., Ido, H., Yagi, Y., Sanzen, N., Tsuji, T., Yamada, M., & Sekiguchi, K. 2006. Ligand-binding specificities of laminin-binding integrins: a comprehensive survey of laminin-integrin interactions using recombinant alpha3beta1, alpha6beta1, alpha7beta1 and alpha6beta4 integrins. ***Matrix Biol.*****, 25, (3) 189-197 available from: PM:16413178**

Novitskaya, V., Romanska, H., Dawoud, M., Jones, J.L., & Berditchevski, F. 2010. Tetraspanin CD151 regulates growth of mammary epithelial cells in three-dimensional extracellular matrix: implication for mammary ductal carcinoma in situ. ***Cancer Res.*****, 70, (11) 4698-4708 available from: PM:20501858**

Okada, Y., Arima, T., Togawa, K., Nagashima, H., Jinno, K., Moriwaki, S., Kunitomo, T., Thurin, J., & Koprowski, H. 1987. Neoexpression of ABH and Lewis blood group antigens in human hepatocellular carcinomas. ***J.Natl.Cancer Inst.*****, 78, (1) 19-28 available from: PM:3025503**

Olivari, S., Galli, C., Alanen, H., Ruddock, L., & Molinari, M. 2005. A novel stress-induced EDEM variant regulating endoplasmic reticulum-associated glycoprotein degradation. ***J.Biol.Chem.*****, 280, (4) 2424-2428 available from: PM:15579471**

Ono, M., Handa, K., Sonnino, S., Withers, D.A., Nagai, H., & Hakomori, S. 2001. GM3 ganglioside inhibits CD9-facilitated haptotactic cell motility: coexpression of GM3 and CD9 is essential in the downregulation of tumor cell motility and malignancy. ***Biochemistry*****, 40, (21) 6414-6421 available from: PM:11371204**

Oxley, C.L., Anthis, N.J., Lowe, E.D., Vakonakis, I., Campbell, I.D., & Wegener, K.L. 2008. An integrin phosphorylation switch: the effect of beta3 integrin tail phosphorylation on Dok1 and talin binding. ***J.Biol.Chem.*****, 283, (9) 5420-5426 available from: PM:18156175**

Oz, O.K., Campbell, A., & Tao, T.W. 1989. Reduced cell adhesion to fibronectin and laminin is associated with altered glycosylation of beta 1 integrins in a weakly metastatic glycosylation mutant. ***Int.J.Cancer*****, 44, (2) 343-347 available from: PM:2788145**

Parodi, A.J., Mendelzon, D.H., Lederkremer, G.Z., & Martin-Barrientos, J. 1984. Evidence that transient glucosylation of protein-linked Man9GlcNAc2, Man8GlcNAc2, and Man7GlcNAc2 occurs in rat liver and Phaseolus vulgaris cells. ***J.Biol.Chem.*****, 259, (10) 6351-6357 available from: PM:6373756**

Partridge, A.W., Liu, S., Kim, S., Bowie, J.U., & Ginsberg, M.H. 2005. Transmembrane domain helix packing stabilizes integrin alphaIIbbeta3 in the low affinity state. ***J.Biol.Chem.*****, 280, (8) 7294-7300 available from: PM:15591321**

Partridge, E.A., Le, R.C., Di Guglielmo, G.M., Pawling, J., Cheung, P., Granovsky, M., Nabi, I.R., Wrana, J.L., & Dennis, J.W. 2004. Regulation of cytokine receptors by Golgi N-glycan processing and endocytosis. ***Science*****, 306, (5693) 120-124 available from: PM:15459394**

Paszek, M.J., Zahir, N., Johnson, K.R., Lakins, J.N., Rozenberg, G.I., Gefen, A., Reinhart-King, C.A., Margulies, S.S., Dembo, M., Boettiger, D., Hammer, D.A., & Weaver, V.M. 2005. Tensional homeostasis and the malignant phenotype. ***Cancer Cell*****, 8, (3) 241-254 available from: PM:16169468**

Pelham, R.J., Jr. & Wang, Y. 1997. Cell locomotion and focal adhesions are regulated by substrate flexibility. ***Proc.Natl.Acad.Sci.U.S.A*****, 94, (25) 13661-13665 available from: PM:9391082**

Peschon, J.J., Slack, J.L., Reddy, P., Stocking, K.L., Sunnarborg, S.W., Lee, D.C., Russell, W.E., Castner, B.J., Johnson, R.S., Fitzner, J.N., Boyce, R.W., Nelson, N., Kozlosky, C.J., Wolfson, M.F., Rauch, C.T., Cerretti, D.P., Paxton, R.J., March, C.J., & Black, R.A. 1998. An essential role for ectodomain shedding in mammalian development. ***Science*****, 282, (5392) 1281-1284 available from: PM:9812885**

Peterson, J.R., Ora, A., Van, P.N., & Helenius, A. 1995. Transient, lectin-like association of calreticulin with folding intermediates of cellular and viral glycoproteins. ***Mol.Biol.Cell*****, 6, (9) 1173-1184 available from: PM:8534914**

Phillips, M.L., Nudelman, E., Gaeta, F.C., Perez, M., Singhal, A.K., Hakomori, S., & Paulson, J.C. 1990. ELAM-1 mediates cell adhesion by recognition of a carbohydrate ligand, sialyl-Lex. ***Science*****, 250, (4984) 1130-1132 available from: PM:1701274**

Pike, L.J. 2004. Lipid rafts: heterogeneity on the high seas. ***Biochem.J.*****, 378, (Pt 2) 281-292 available from: PM:14662007**

Pileri, P., Uematsu, Y., Campagnoli, S., Galli, G., Falugi, F., Petracca, R., Weiner, A.J., Houghton, M., Rosa, D., Grandi, G., & Abrignani, S. 1998. Binding of hepatitis C virus to CD81. ***Science*****, 282, (5390) 938-941 available from: PM:9794763**

Pinho, S.S., Osorio, H., Nita-Lazar, M., Gomes, J., Lopes, C., Gartner, F., & Reis, C.A. 2009a. Role of E-cadherin N-glycosylation profile in a mammary tumor

model. ***Biochem.Biophys.Res.Commun.*****, 379, (4) 1091-1096 available from: PM:19159617**

Pinho, S.S., Reis, C.A., Paredes, J., Magalhaes, A.M., Ferreira, A.C., Figueiredo, J., Xiaogang, W., Carneiro, F., Gartner, F., & Seruca, R. 2009b. The role of N-acetylglucosaminyltransferase III and V in the post-transcriptional modifications of E-cadherin. ***Hum.Mol.Genet.*****, 18, (14) 2599-2608 available from: PM:19403558**

Piscatelli, J.J., Cohen, S.A., Berenson, C.S., & Lance, P. 1995. Determinants of differential liver-colonizing potential of variants of the MCA-38 murine colon cancer cell line. ***Clin.Exp.Metastasis*****, 13, (2) 141-150 available from: PM:7882616**

Plow, E.F., Haas, T.A., Zhang, L., Loftus, J., & Smith, J.W. 2000. Ligand binding to integrins. ***J.Biol.Chem.*****, 275, (29) 21785-21788 available from: PM:10801897**

Pochec, E., Litynska, A., Amoresano, A., & Casbarra, A. 2003. Glycosylation profile of integrin alpha 3 beta 1 changes with melanoma progression. ***Biochim.Biophys.Acta*****, 1643, (1-3) 113-123 available from: PM:14654234**

Pochec, E., Litynska, A., Bubka, M., Amoresano, A., & Casbarra, A. 2006. Characterization of the oligosaccharide component of alpha3beta1 integrin from human bladder carcinoma cell line T24 and its role in adhesion and migration. ***Eur.J.Cell Biol.*****, 85, (1) 47-57 available from: PM:16373174**

Ponten, J. & Macintyre, E.H. 1968. Long term culture of normal and neoplastic human glia. ***Acta Pathol.Microbiol.Scand.*****, 74, (4) 465-486 available from: PM:4313504**

Puccia, R., Grondin, B., & Herscovics, A. 1993. Disruption of the processing alpha-mannosidase gene does not prevent outer chain synthesis in Saccharomyces cerevisiae. ***Biochem.J.*****, 290 (Pt 1), 21-26 available from: PM:8439291**

Pulukuri, S.M., Gondi, C.S., Lakka, S.S., Jutla, A., Estes, N., Gujrati, M., & Rao, J.S. 2005. RNA interference-directed knock-down of urokinase plasminogen activator and urokinase plasminogen activator receptor inhibits prostate cancer cell invasion, survival, and tumorigenicity in vivo. ***J.Biol.Chem.*****, 280, (43) 36529-36540 available from: PM:16127174**

Ruiz-Canada, C., Kelleher, D.J., & Gilmore, R. 2009. Cotranslational and posttranslational N-glycosylation of polypeptides by distinct mammalian OST isoforms. ***Cell*****, 136, (2) 272-283 available from: PM:19167329**

Sabatini, D.D. & Blobel, G. 1970. Controlled proteolysis of nascent polypeptides in rat liver cell fractions. II. Location of the polypeptides in rough microsomes. ***J.Cell Biol.*****, 45, (1) 146-157 available from: PM:5458993**

Sachs, N., Kreft, M., van den Bergh Weerman MA, Beynon, A.J., Peters, T.A., Weening, J.J., & Sonnenberg, A. 2006. Kidney failure in mice lacking the tetraspanin CD151. ***J.Cell Biol.*****, 175, (1) 33-39 available from: PM:17015618**

Sadej, R., Romanska, H., Baldwin, G., Gkirtzimanaki, K., Novitskaya, V., Filer, A.D., Krcova, Z., Kusinska, R., Ehrmann, J., Buckley, C.D., Kordek, R., Potemski, P., Eliopoulos, A.G., Lalani, e., & Berditchevski, F. 2009. CD151 regulates tumorigenesis by modulating the communication between tumor cells and endothelium. ***Mol.Cancer Res.*****, 7, (6) 787-798 available from: PM:19531562**

Sadej, R., Romanska, H., Kavanagh, D., Baldwin, G., Takahashi, T., Kalia, N., & Berditchevski, F. 2010. Tetraspanin CD151 regulates transforming growth factor beta signaling: implication in tumor metastasis. ***Cancer Res.*****, 70, (14) 6059-6070 available from: PM:20570898**

Sahagian, G.G., Distler, J., & Jourdian, G.W. 1981. Characterization of a membrane-associated receptor from bovine liver that binds phosphomannosyl residues of bovine testicular beta-galactosidase. ***Proc.Natl.Acad.Sci.U.S.A*****, 78, (7) 4289-4293 available from: PM:6270668**

Sahagian, G.G., Distler, J.J., & Jourdian, G.W. 1982. Membrane receptor for phosphomannosyl residues. ***Methods Enzymol.*****, 83, 392-396 available from: PM:6285135**

Sanyal, S., Frank, C.G., & Menon, A.K. 2008. Distinct flippases translocate glycerophospholipids and oligosaccharide diphosphate dolichols across the endoplasmic reticulum. ***Biochemistry*****, 47, (30) 7937-7946 available from: PM:18597486**

Sanyal, S. & Menon, A.K. 2009. Specific transbilayer translocation of dolichol-linked oligosaccharides by an endoplasmic reticulum flippase. ***Proc.Natl.Acad.Sci.U.S.A*****, 106, (3) 767-772 available from: PM:19129492**

Saul, R., Molyneux, R.J., & Elbein, A.D. 1984. Studies on the mechanism of castanospermine inhibition of alpha- and beta-glucosidases. ***Arch.Biochem.Biophys.*****, 230, (2) 668-675 available from: PM:6424575**

Sawada, S., Yoshimoto, M., Odintsova, E., Hotchin, N.A., & Berditchevski, F. 2003. The tetraspanin CD151 functions as a negative regulator in the adhesion-

dependent activation of Ras. *J.Biol.Chem.*, 278, (29) 26323-26326 available from: PM:12782641

Scherer, W.F., Syverton, J.T., & Gey, G.O. 1953. Studies on the propagation in vitro of poliomyelitis viruses. IV. Viral multiplication in a stable strain of human malignant epithelial cells (strain HeLa) derived from an epidermoid carcinoma of the cervix. *J.Exp.Med.*, 97, (5) 695-710 available from: PM:13052828

Serru, V., Le, N.F., Billard, M., Azorsa, D.O., Lanza, F., Boucheix, C., & Rubinstein, E. 1999. Selective tetraspan-integrin complexes (CD81/alpha4beta1, CD151/alpha3beta1, CD151/alpha6beta1) under conditions disrupting tetraspan interactions. *Biochem.J.*, 340 (Pt 1), 103-111 available from: PM:10229664

Shailubhai, K., Pukazhenthi, B.S., Saxena, E.S., Varma, G.M., & Vijay, I.K. 1991. Glucosidase I, a transmembrane endoplasmic reticular glycoprotein with a luminal catalytic domain. *J.Biol.Chem.*, 266, (25) 16587-16593 available from: PM:1885588

Shang, M., Koshikawa, N., Schenk, S., & Quaranta, V. 2001. The LG3 module of laminin-5 harbors a binding site for integrin alpha3beta1 that promotes cell adhesion, spreading, and migration. *J.Biol.Chem.*, 276, (35) 33045-33053 available from: PM:11395486

Sharma, C., Yang, X.H., & Hemler, M.E. 2008. DHHC2 affects palmitoylation, stability, and functions of tetraspanins CD9 and CD151. *Mol.Biol.Cell*, 19, (8) 3415-3425 available from: PM:18508921

Shattil, S.J., Kim, C., & Ginsberg, M.H. 2010. The final steps of integrin activation: the end game. *Nat.Rev.Mol.Cell Biol.*, 11, (4) 288-300 available from: PM:20308986

Shi, G.M., Ke, A.W., Zhou, J., Wang, X.Y., Xu, Y., Ding, Z.B., Devbhandari, R.P., Huang, X.Y., Qiu, S.J., Shi, Y.H., Dai, Z., Yang, X.R., Yang, G.H., & Fan, J. 2010. CD151 modulates expression of matrix metalloproteinase 9 and promotes neoangiogenesis and progression of hepatocellular carcinoma. *Hepatology*, 52, (1) 183-196 available from: PM:20578262

Shoham, T., Rajapaksa, R., Kuo, C.C., Haimovich, J., & Levy, S. 2006. Building of the tetraspanin web: distinct structural domains of CD81 function in different cellular compartments. *Mol.Cell Biol.*, 26, (4) 1373-1385 available from: PM:16449649

Simons, K. & van, M.G. 1988. Lipid sorting in epithelial cells. *Biochemistry*, 27, (17) 6197-6202 available from: PM:3064805

Singh, J., Itahana, Y., Knight-Krajewski, S., Kanagawa, M., Campbell, K.P., Bissell, M.J., & Muschler, J. 2004. Proteolytic enzymes and altered glycosylation modulate dystroglycan function in carcinoma cells. *Cancer Res.*, 64, (17) 6152-6159 available from: PM:15342399

Soule, H.D., Vazguez, J., Long, A., Albert, S., & Brennan, M. 1973. A human cell line from a pleural effusion derived from a breast carcinoma. *J.Natl.Cancer Inst.*, 51, (5) 1409-1416 available from: PM:4357757

Spiro, R.G. 2002. Protein glycosylation: nature, distribution, enzymatic formation, and disease implications of glycopeptide bonds. *Glycobiology*, 12, (4) 43R-56R available from: PM:12042244

Stanley, P. 2002. Biological consequences of overexpressing or eliminating N-acetylglucosaminyltransferase-TIII in the mouse. *Biochim.Biophys.Acta*, 1573, (3) 363-368 available from: PM:12417419

Stanley, P., Schachter, H., & Taniguchi, N. 2009. N-Glycans. In: Varki A, Cummings RD, Esko JD, Freeze HH, Stanley P, Bertozzi CR, Hart GW, Etzler ME, editors. Essentials of Glycobiology. 2nd edition. Cold Spring Harbor (NY): Cold Spring Harbor Laboratory Press; 2009. Chapter 8 available from: PM:20301244

Sterk, L.M., Geuijen, C.A., Oomen, L.C., Calafat, J., Janssen, H., & Sonnenberg, A. 2000. The tetraspan molecule CD151, a novel constituent of hemidesmosomes, associates with the integrin alpha6beta4 and may regulate the spatial organization of hemidesmosomes. *J.Cell Biol.*, 149, (4) 969-982 available from: PM:10811835

Sterk, L.M., Geuijen, C.A., van den Berg, J.G., Claessen, N., Weening, J.J., & Sonnenberg, A. 2002a. Association of the tetraspanin CD151 with the laminin-binding integrins alpha3beta1, alpha6beta1, alpha6beta4 and alpha7beta1 in cells in culture and in vivo. *J.Cell Sci.*, 115, (Pt 6) 1161-1173 available from: PM:11884516

Sterk, L.M., Geuijen, C.A., van den Berg, J.G., Claessen, N., Weening, J.J., & Sonnenberg, A. 2002b. Association of the tetraspanin CD151 with the laminin-binding integrins alpha3beta1, alpha6beta1, alpha6beta4 and alpha7beta1 in cells in culture and in vivo. *J.Cell Sci.*, 115, (Pt 6) 1161-1173 available from: PM:11884516

Stipp, C.S. 2010. Laminin-binding integrins and their tetraspanin partners as potential antimetastatic targets. *Expert.Rev.Mol.Med.*, 12, e3 available from: PM:20078909

Stipp, C.S., Kolesnikova, T.V., & Hemler, M.E. 2001a. EWI-2 is a major CD9 and CD81 partner and member of a novel Ig protein subfamily. *J.Biol.Chem.*, 276, (44) 40545-40554 available from: PM:11504738

Stipp, C.S., Kolesnikova, T.V., & Hemler, M.E. 2003. Functional domains in tetraspanin proteins. *Trends Biochem.Sci.*, 28, (2) 106-112 available from: PM:12575999

Stipp, C.S., Orlicky, D., & Hemler, M.E. 2001b. FPRP, a major, highly stoichiometric, highly specific. *J.Biol.Chem.*, 276, (7) 4853-4862 available from: PM:11087758

Stupack, D.G., Puente, X.S., Boutsaboualoy, S., Storgard, C.M., & Cheresh, D.A. 2001. Apoptosis of adherent cells by recruitment of caspase-8 to unligated integrins. *J.Cell Biol.*, 155, (3) 459-470 available from: PM:11684710

Tachibana, I., Bodorova, J., Berditchevski, F., Zutter, M.M., & Hemler, M.E. 1997. NAG-2, a novel transmembrane-4 superfamily (TM4SF) protein that complexes with integrins and other TM4SF proteins. *J.Biol.Chem.*, 272, (46) 29181-29189 available from: PM:9360996

Tadokoro, S., Shattil, S.J., Eto, K., Tai, V., Liddington, R.C., de Pereda, J.M., Ginsberg, M.H., & Calderwood, D.A. 2003. Talin binding to integrin beta tails: a final common step in integrin activation. *Science*, 302, (5642) 103-106 available from: PM:14526080

Takagi, J., Petre, B.M., Walz, T., & Springer, T.A. 2002. Global conformational rearrangements in integrin extracellular domains in outside-in and inside-out signaling. *Cell*, 110, (5) 599-11 available from: PM:12230977

Takagi, J. & Springer, T.A. 2002. Integrin activation and structural rearrangement. *Immunol.Rev.*, 186, 141-163 available from: PM:12234369

Takala, H., Nurminen, E., Nurmi, S.M., Aatonen, M., Strandin, T., Takatalo, M., Kiema, T., Gahmberg, C.G., Ylanne, J., & Fagerholm, S.C. 2008. Beta2 integrin phosphorylation on Thr758 acts as a molecular switch to regulate 14-3-3 and filamin binding. *Blood*, 112, (5) 1853-1862 available from: PM:18550856

Tector, M., Zhang, Q., & Salter, R.D. 1997. Beta 2-microglobulin and calnexin can independently promote folding and disulfide bond formation in class I histocompatibility proteins. *Mol.Immunol.*, 34, (5) 401-408 available from: PM:9293773

Tempel, W., Karaveg, K., Liu, Z.J., Rose, J., Wang, B.C., & Moremen, K.W. 2004. Structure of mouse Golgi alpha-mannosidase IA reveals the molecular basis for substrate specificity among class 1 (family 47 glycosylhydrolase) alpha1,2-mannosidases. *J.Biol.Chem.*, 279, (28) 29774-29786 available from: PM:15102839

Tokuhara, T., Hasegawa, H., Hattori, N., Ishida, H., Taki, T., Tachibana, S., Sasaki, S., & Miyake, M. 2001. Clinical significance of CD151 gene expression in non-small cell lung cancer. *Clin.Cancer Res.*, 7, (12) 4109-4114 available from: PM:11751509

Tremblay, L.O. & Herscovics, A. 2000. Characterization of a cDNA encoding a novel human Golgi alpha 1, 2-mannosidase (IC) involved in N-glycan biosynthesis. *J.Biol.Chem.*, 275, (41) 31655-31660 available from: PM:10915796

Trombetta, E.S. 2003. The contribution of N-glycans and their processing in the endoplasmic reticulum to glycoprotein biosynthesis. *Glycobiology*, 13, (9) 77R-91R available from: PM:12736198

Trombetta, E.S. & Helenius, A. 1998. Lectins as chaperones in glycoprotein folding. *Curr.Opin.Struct.Biol.*, 8, (5) 587-592 available from: PM:9818262

Trombetta, E.S. & Helenius, A. 1999. Glycoprotein reglucosylation and nucleotide sugar utilization in the secretory pathway: identification of a nucleoside diphosphatase in the endoplasmic reticulum. *EMBO J.*, 18, (12) 3282-3292 available from: PM:10369669

Trombetta, E.S. & Helenius, A. 2000. Conformational requirements for glycoprotein reglucosylation in the endoplasmic reticulum. *J.Cell Biol.*, 148, (6) 1123-1129 available from: PM:10725325

Trombetta, E.S., Simons, J.F., & Helenius, A. 1996. Endoplasmic reticulum glucosidase II is composed of a catalytic subunit, conserved from yeast to mammals, and a tightly bound noncatalytic HDEL-containing subunit. *J.Biol.Chem.*, 271, (44) 27509-27516 available from: PM:8910335

Tsitsikov, E.N., Gutierrez-Ramos, J.C., & Geha, R.S. 1997. Impaired CD19 expression and signaling, enhanced antibody response to type II T independent antigen and reduction of B-1 cells in CD81-deficient mice. *Proc.Natl.Acad.Sci.U.S.A*, 94, (20) 10844-10849 available from: PM:9380722

Vagin, O., Turdikulova, S., & Sachs, G. 2004. The H,K-ATPase beta subunit as a model to study the role of N-glycosylation in membrane trafficking and apical sorting. *J.Biol.Chem.*, 279, (37) 39026-39034 available from: PM:15247221

Wang, J.C., Begin, L.R., Berube, N.G., Chevalier, S., Aprikian, A.G., Gourdeau, H., & Chevrette, M. 2007. Down-regulation of CD9 expression during prostate carcinoma progression is associated with CD9 mRNA modifications. ***Clin.Cancer Res.*****, 13, (8) 2354-2361 available from: PM:17406028**

Weerapana, E. & Imperiali, B. 2006. Asparagine-linked protein glycosylation: from eukaryotic to prokaryotic systems. ***Glycobiology*****, 16, (6) 91R-101R available from: PM:16510493**

Wegener, K.L., Partridge, A.W., Han, J., Pickford, A.R., Liddington, R.C., Ginsberg, M.H., & Campbell, I.D. 2007. Structural basis of integrin activation by talin. ***Cell*****, 128, (1) 171-182 available from: PM:17218263**

Weitzman, J.B., Pasqualini, R., Takada, Y., & Hemler, M.E. 1993. The function and distinctive regulation of the integrin VLA-3 in cell adhesion, spreading, and homotypic cell aggregation. ***J.Biol.Chem.*****, 268, (12) 8651-8657 available from: PM:8473308**

Weng, S. & Spiro, R.G. 1993a. Demonstration that a kifunensine-resistant alpha-mannosidase with a unique processing action on N-linked oligosaccharides occurs in rat liver endoplasmic reticulum and various cultured cells. ***J.Biol.Chem.*****, 268, (34) 25656-25663 available from: PM:8245001**

Weng, S. & Spiro, R.G. 1993b. Demonstration that a kifunensine-resistant alpha-mannosidase with a unique processing action on N-linked oligosaccharides occurs in rat liver endoplasmic reticulum and various cultured cells. ***J.Biol.Chem.*****, 268, (34) 25656-25663 available from: PM:8245001**

Weng, S. & Spiro, R.G. 1996. Evaluation of the early processing routes of N-linked oligosaccharides of glycoproteins through the characterization of Man8GlcNAc2 isomers: evidence that endomannosidase functions in vivo in the absence of a glucosidase blockade. ***Glycobiology*****, 6, (8) 861-868 available from: PM:9023549**

Whitley, P., Nilsson, I.M., & von, H.G. 1996. A nascent secretory protein may traverse the ribosome/endoplasmic reticulum translocase complex as an extended chain. ***J.Biol.Chem.*****, 271, (11) 6241-6244 available from: PM:8626416**

Wilson, C.M., Roebuck, Q., & High, S. 2008. Ribophorin I regulates substrate delivery to the oligosaccharyltransferase core. ***Proc.Natl.Acad.Sci.U.S.A*****, 105, (28) 9534-9539 available from: PM:18607003**

Winterwood, N.E., Varzavand, A., Meland, M.N., Ashman, L.K., & Stipp, C.S. 2006. A critical role for tetraspanin CD151 in alpha3beta1 and alpha6beta4 integrin-

dependent tumor cell functions on laminin-5. *Mol.Biol.Cell*, 17, (6) 2707-2721 available from: PM:16571677

Xia, L., McDaniel, J.M., Yago, T., Doeden, A., & McEver, R.P. 2004. Surface fucosylation of human cord blood cells augments binding to P-selectin and E-selectin and enhances engraftment in bone marrow. *Blood*, 104, (10) 3091-3096 available from: PM:15280192

Xiong, J.P., Stehle, T., Diefenbach, B., Zhang, R., Dunker, R., Scott, D.L., Joachimiak, A., Goodman, S.L., & Arnaout, M.A. 2001. Crystal structure of the extracellular segment of integrin alpha Vbeta3. *Science*, 294, (5541) 339-345 available from: PM:11546839

Xiong, J.P., Stehle, T., Goodman, S.L., & Arnaout, M.A. 2003. New insights into the structural basis of integrin activation. *Blood*, 102, (4) 1155-1159 available from: PM:12714499

Yamada, M., Tamura, Y., Sanzen, N., Sato-Nishiuchi, R., Hasegawa, H., Ashman, L.K., Rubinstein, E., Yanez-Mo, M., Sanchez-Madrid, F., & Sekiguchi, K. 2008. Probing the interaction of tetraspanin CD151 with integrin alpha 3 beta 1 using a panel of monoclonal antibodies with distinct reactivities toward the CD151-integrin alpha 3 beta 1 complex. *Biochem.J.*, 415, (3) 417-427 available from: PM:18601653

Yan, Q. & Lennarz, W.J. 2002. Studies on the function of oligosaccharyl transferase subunits. Stt3p is directly involved in the glycosylation process. *J.Biol.Chem.*, 277, (49) 47692-47700 available from: PM:12359722

Yanez-Mo, M., Alfranca, A., Cabanas, C., Marazuela, M., Tejedor, R., Ursa, M.A., Ashman, L.K., de Landazuri, M.O., & Sanchez-Madrid, F. 1998. Regulation of endothelial cell motility by complexes of tetraspan molecules CD81/TAPA-1 and CD151/PETA-3 with alpha3 beta1 integrin localized at endothelial lateral junctions. *J.Cell Biol.*, 141, (3) 791-804 available from: PM:9566977

Yang, X., Claas, C., Kraeft, S.K., Chen, L.B., Wang, Z., Kreidberg, J.A., & Hemler, M.E. 2002. Palmitoylation of tetraspanin proteins: modulation of CD151 lateral interactions, subcellular distribution, and integrin-dependent cell morphology. *Mol.Biol.Cell*, 13, (3) 767-781 available from: PM:11907260

Yang, X.H., Richardson, A.L., Torres-Arzayus, M.I., Zhou, P., Sharma, C., Kazarov, A.R., Andzelm, M.M., Strominger, J.L., Brown, M., & Hemler, M.E. 2008. CD151 accelerates breast cancer by regulating alpha 6 integrin function, signaling, and molecular organization. *Cancer Res.*, 68, (9) 3204-3213 available from: PM:18451146

Yashiro-Ohtani, Y., Zhou, X.Y., Toyo-Oka, K., Tai, X.G., Park, C.S., Hamaoka, T., Abe, R., Miyake, K., & Fujiwara, H. 2000. Non-CD28 costimulatory molecules present in T cell rafts induce T cell costimulation by enhancing the association of TCR with rafts. ***J.Immunol.*****, 164, (3) 1251-1259 available from: PM:10640738**

Yauch, R.L., Berditchevski, F., Harler, M.B., Reichner, J., & Hemler, M.E. 1998. Highly stoichiometric, stable, and specific association of integrin alpha3beta1 with CD151 provides a major link to phosphatidylinositol 4-kinase, and may regulate cell migration. ***Mol.Biol.Cell*****, 9, (10) 2751-2765 available from: PM:9763442**

Yauch, R.L., Kazarov, A.R., Desai, B., Lee, R.T., & Hemler, M.E. 2000. Direct extracellular contact between integrin alpha(3)beta(1) and TM4SF protein CD151. ***J.Biol.Chem.*****, 275, (13) 9230-9238 available from: PM:10734060**

Yoshida, Y. 2005. Expression and assay of glycoprotein-specific ubiquitin ligases. ***Methods Enzymol.*****, 398, 159-169 available from: PM:16275327**

Yoshida, Y., Adachi, E., Fukiya, K., Iwai, K., & Tanaka, K. 2005. Glycoprotein-specific ubiquitin ligases recognize N-glycans in unfolded substrates. ***EMBO Rep.*****, 6, (3) 239-244 available from: PM:15723043**

Yoshida, Y. & Tanaka, K. 2010. Lectin-like ERAD players in ER and cytosol. ***Biochim.Biophys.Acta*****, 1800, (2) 172-180 available from: PM:19665047**

Yoshimura, M., Ihara, Y., Matsuzawa, Y., & Taniguchi, N. 1996. Aberrant glycosylation of E-cadherin enhances cell-cell binding to suppress metastasis. ***J.Biol.Chem.*****, 271, (23) 13811-13815 available from: PM:8662832**

Yoshimura, M., Nishikawa, A., Ihara, Y., Taniguchi, S., & Taniguchi, N. 1995. Suppression of lung metastasis of B16 mouse melanoma by N-acetylglucosaminyltransferase III gene transfection. ***Proc.Natl.Acad.Sci.U.S.A*****, 92, (19) 8754-8758 available from: PM:7568011**

Yuan, M., Itzkowitz, S.H., Palekar, A., Shamsuddin, A.M., Phelps, P.C., Trump, B.F., & Kim, Y.S. 1985. Distribution of blood group antigens A, B, H, Lewisa, and Lewisb in human normal, fetal, and malignant colonic tissue. ***Cancer Res.*****, 45, (9) 4499-4511 available from: PM:4028031**

Zevian, S., Winterwood, N.E., & Stipp, C.S. 2011. Structure-function analysis of tetraspanin CD151 reveals distinct requirements for tumor cell behaviors mediated by alpha3beta1 versus alpha6beta4 integrin. ***J.Biol.Chem.*****, 286, (9) 7496-7506 available from: PM:21193415**

Zhang, Q., Tector, M., & Salter, R.D. 1995. Calnexin recognizes carbohydrate and protein determinants of class I major histocompatibility complex molecules. *J.Biol.Chem.*, 270, (8) 3944-3948 available from: PM:7876141

Zhang, Y., Zhang, X.Y., Liu, F., Qi, H.L., & Chen, H.L. 2002. The roles of terminal sugar residues of surface glycans in the metastatic potential of human hepatocarcinoma. *J.Cancer Res.Clin.Oncol.*, 128, (11) 617-620 available from: PM:12458342

Zhao, J., Chen, H., Peschon, J.J., Shi, W., Zhang, Y., Frank, S.J., & Warburton, D. 2001. Pulmonary hypoplasia in mice lacking tumor necrosis factor-alpha converting enzyme indicates an indispensable role for cell surface protein shedding during embryonic lung branching morphogenesis. *Dev.Biol.*, 232, (1) 204-218 available from: PM:11254358

Zhao, K.W., Faull, K.F., Kakkis, E.D., & Neufeld, E.F. 1997. Carbohydrate structures of recombinant human alpha-L-iduronidase secreted by Chinese hamster ovary cells. *J.Biol.Chem.*, 272, (36) 22758-22765 available from: PM:9278435

Zhao, Y., Nakagawa, T., Itoh, S., Inamori, K., Isaji, T., Kariya, Y., Kondo, A., Miyoshi, E., Miyazaki, K., Kawasaki, N., Taniguchi, N., & Gu, J. 2006. N-acetylglucosaminyltransferase III antagonizes the effect of N-acetylglucosaminyltransferase V on alpha3beta1 integrin-mediated cell migration. *J.Biol.Chem.*, 281, (43) 32122-32130 available from: PM:16940045

Zheng, M., Fang, H., & Hakomori, S. 1994. Functional role of N-glycosylation in alpha 5 beta 1 integrin receptor. De-N-glycosylation induces dissociation or altered association of alpha 5 and beta 1 subunits and concomitant loss of fibronectin binding activity. *J.Biol.Chem.*, 269, (16) 12325-12331 available from: PM:7512965